

**South Dakota
Department of Transportation
Office of Research**



**U.S. Department
of Transportation
Federal Highway
Administration**

SD2001-05-F

Mechanical and Corrosion Properties of a High-Strength, High Chromium Reinforcing Steel for Concrete

**Study SD2001-05
Final Report**

**Prepared by
University of Kansas Center for Research, Inc.
2385 Irving Hill Road
Lawrence, Kansas 66044-7552**

March 2002

DISCLAIMER

The contents of this report reflect the views of the authors who are responsible for the facts and accuracy of the data presented herein. The contents do not necessarily reflect the official views or policies of the South Dakota Department of Transportation, the State Transportation Commission, or the Federal Highway Administration. This report does not constitute a standard, specification, or regulation.

ACKNOWLEDGEMENTS

This work was performed under the supervision of the SD2001-05 Technical Panel:

Mark Clausen	FHWA	David Huft	Research
Tom Gilsrud	Bridge Design	Dan Johnston	Research
Todd Hertel	Aberdeen Region	Darin Larson.....	Operations Support
Darin Hodges	Materials & Surfacing	Paul Nelson	Pierre Region

The work was performed in cooperation with the United States Department of Transportation Federal Highway Administration, the Kansas Department of Transportation under Contracts 1131 and 1281, and the National Science Foundation under Research Grant No. CMS-98122716. Javier Balma, Jianxin Ji, Lien Gong, and Keith Johnson made significant contributions to the research described in this report.

TECHNICAL REPORT STANDARD TITLE PAGE

1. Report No. SD2001-05-F	2. Government Accession No.	3. Recipient's Catalog No.	
4. Title and Subtitle Mechanical and Corrosion Properties of a High-Strength, High Chromium Reinforcing Steel for Concrete		5. Report Date March 31,2002	
		6. Performing Organization Code	
7. Author(s) David Darwin, JoAnn Browning, Trung Van Nguyen, Carl Locke, Jr.		8. Performing Organization Report No. SM Report No. 66	
9. Performing Organization Name and Address University of Kansas Center for Research, Inc. 2385 Irving Hill Road Lawrence, Kansas 66044-7552		10. Work Unit No.	
		11. Contract or Grant No. 310741	
12. Sponsoring Agency Name and Address South Dakota Department of Transportation Office of Research 700 East Broadway Avenue Pierre, SD 57501-2586		13. Type of Report and Period Covered Final Report March 2001 to March 2002	
		14. Sponsoring Agency Code	
15. Supplementary Notes An executive summary is published separately as SD2001-05-X.			
16. Abstract <p>The corrosion of reinforcing steel in highway structures results in maintenance and replacement costs in the United States that are measured in billions of dollars. The use of deicing salts has resulted in the steady deterioration of roadway bridge decks due to corrosion. One method to reduce corrosion is the use of corrosion-resistant alloys. A high-strength, high chromium reinforcing steel, MMFX Microcomposite steel, is evaluated for corrosion resistance, mechanical properties, applicability for structural applications, life expectancy and cost effectiveness. The steel is compared with conventional mild steel reinforcement, and epoxy-coated reinforcement. Principal emphasis is placed on corrosion performance of the steel, which is evaluated using rapid macrocell tests of bare and mortar-wrapped reinforcement and initial test results for Southern Exposure and cracked beam tests. Life expectancy and cost effectiveness are evaluated based on experience and costs in South Dakota, combined with laboratory results for the chloride content required for corrosion initiation and the rate of corrosion in cracked concrete.</p> <p>MMFX microcomposite steel has average yield strengths between 120 and 140 ksi. Most of the specimens tested satisfy the requirements for high-strength steel bars for prestressing concrete, as specified under ASTM A 722. In most cases, the steel also satisfies the requirements for conventional reinforcement under ASTM A 615, although some samples do not meet the requirements for elongation. MMFX steel bars satisfy the ASTM requirements for bar geometry and will provide satisfactory bond strength with concrete. Depending on bridge deck design, the use of MMFX Microcomposite steel provides few or no alternatives that satisfy all AASHTO bridge design criteria. The corrosion threshold of MMFX Microcomposite steel is approximately four times higher than that of conventional reinforcement. It has a corrosion rate between one-third and two-thirds that of uncoated conventional reinforcing steel. Epoxy-coated steel provides superior corrosion performance to MMFX Microcomposite steel. Bridge decks containing MMFX Microcomposite reinforcing steel will require repair approximately 30 years after construction, compared to 10 to 25 years for conventional steel and 40 years for epoxy-coated reinforcement under typical conditions in South Dakota. Bridge decks containing MMFX Microcomposite steel do not appear to be cost effective when compared to bridge decks containing epoxy-coated reinforcement. MMFX Microcomposite steel is not recommended for use in bridge decks without the use of a supplementary corrosion protection system.</p>			
17. Keywords bridge decks, costs, corrosion, design life, reinforcing steel, strength		18. Distribution Statement No restrictions. This document is available to the public from the sponsoring agency.	
19. Security Classification (of this report) Unclassified	20. Security Classification (of this page) Unclassified	21. No. of Pages 142	22. Price

TABLE OF CONTENTS

LIST OF FIGURES	v
LIST OF TABLES.....	xiv
CHAPTER 1 EXECUTIVE SUMMARY	1
1.1 PROBLEM DESCRIPTION	1
1.2 OBJECTIVES.....	2
1.3 FINDINGS	2
1.3.1 Literature Search	2
1.3.2 Physical and Mechanical Tests	3
1.3.3 Corrosion Tests	4
1.3.4 Life Expectancy and Economic Analysis	7
1.4 CONCLUSIONS	8
1.5 IMPLEMENTATION RECOMMENDATIONS	9
CHAPTER 2 PROBLEM DESCRIPTION.....	11
CHAPTER 3 OBJECTIVES	13
CHAPTER 4 TASK DESCRIPTION.....	15
4.1 LITERATURE SEARCH	15
4.2 PHYSICAL AND MECHANICAL TESTS	15
4.2.1 Mechanical Tests and Bar Geometry.....	15
4.2.2 X-Ray Microanalysis	18
4.2.3 Structural Analysis	18
4.3 CORROSION TESTS.....	22
4.3.1 Rapid Macrocell Tests	22
4.3.2 Bench-Scale Tests	26
4.4 CORROSION EFFECTS	30
4.5 LIFE EXPECTANCY AND COST EFFECTIVENESS	31

4.5.1 Life Expectancy	31
4.5.2 Cost Effectiveness	31
CHAPTER 5 FINDINGS AND CONCLUSIONS.....	37
5.1 LITERATURE SEARCH	37
5.1.1 Mechanical Properties	37
5.1.2 Corrosion Tests	38
5.2 PHYSICAL AND MECHANICAL TESTS	38
5.2.1 Mechanical Tests and Bar Geometry.....	38
5.2.2 X-Ray Microanalysis	41
5.2.3 Structural Analysis of Three Bridge Decks Using MMFX Steel.....	41
5.3 CORROSION TESTS.....	50
5.3.1 Rapid Macrocell Tests	50
5.3.2 Bench-Scale Tests	60
5.4 CORROSION EFFECTS	71
5.5 LIFE EXPECTANCY AND COST EFFECTIVENESS	76
5.5.1 Life Expectancy.....	76
5.5.2 Cost Effectiveness	78
5.6 CONCLUSIONS	80
CHAPTER 6 IMPLEMENTATION RECOMMENDATIONS	83
REFERENCES	85
APPENDIX A DETAILS OF STRUCTURAL ANALYSES	89
APPENDIX B CORROSION TEST RESULTS FOR INDIVIDUAL SPECIMENS	97

LIST OF FIGURES

Figure 1.1 – Macrocell Test. Average corrosion rate. Bare specimens in 1.6 m ion NaCl and simulated concrete pore solution	5
Figure 1.2 - Macrocell Tests. Average corrosion rate. Mortar-wrapped specimens with w/c=0.50 in 1.6 m ion NaCl and simulated concrete pore solution	5
Figure 1.3 – Southern Exposure Test. Average total corrosion loss, specimens with w/c=0.45, ponded with a 15% NaCl solution	6
Figure 1.4 - Cracked Beam Test. Average total corrosion loss, specimens with w/c=0.45, ponded with a 15% NaCl solution	7
Figure 4.1 - Cross-Section of Mortar-wrapped Test Specimen Used for Rapid Corrosion Macrocell Test.....	23
Figure 4.2 - Schematic of Macrocell Test.....	23
Figure 4.3 - Test Specimen for Southern Exposure Test	27
Figure 4.4 - Test Specimen for Cracked Beam Test.....	29
Figure 5.1 - Macrocell Test. Average corrosion rate. Bare specimens in 1.6 m ion NaCl and simulated concrete pore solution	50
Figure 5.2a - Macrocell Test. Average corrosion potential vs. saturated calomel electrode, anode. Bare specimens in 1.6 m ion NaCl and simulated concrete pore solution.....	53
Figure 5.2b - Macrocell Test. Average corrosion potential vs. saturated calomel electrode, cathode. Bare specimens in 1.6 m ion NaCl and simulated concrete pore solution.....	53
Figure 5.3 - Bare conventional N3 anode bar, at 15 weeks	54
Figure 5.4 – Bare MMFX anode bar from group MMFX(1), at 15 weeks, showing corrosion products that formed above the surface of the solution.....	54
Figure 5.5 – Bare MMFX anode bar from group MMFX(2), at 15 weeks, showing corrosion products that formed below the surface of the solution.	54
Figure 5.6 - Macrocell Test. Average corrosion rate. Bare specimens in 6.04 m ion (15%) NaCl and simulated concrete pore solution.....	55

Figure 5.7a - Macrocell Test. Average corrosion potential vs. saturated calomel electrode, anode. Bare specimens in 6.04 m ion (15%) NaCl and simulated concrete pore solution.....	56
Figure 5.7b - Macrocell Test. Average corrosion potential vs. saturated calomel electrode, cathode. Bare specimens in 6.04 m ion (15%) NaCl and simulated concrete pore solution.....	56
Figure 5.8a - Macrocell Tests. Average corrosion rate. Mortar-wrapped specimens with w/c=0.50 in 1.6 m ion NaCl and simulated concrete pore solution.....	57
Figure 5.8b - Macrocell Tests. Average corrosion rate. Mortar-wrapped specimens with w/c=0.50 in 1.6 m ion NaCl and simulated concrete pore solution.....	57
Figure 5.9a - Macrocell Test. Average corrosion potential vs. saturated calomel electrode, anode. Mortar-wrapped specimens with w/c=0.50 in 1.6 m ion NaCl and simulated concrete pore solution.	59
Figure 5.9b - Macrocell Test. Average corrosion potential vs. saturated calomel electrode, cathode. Mortar-wrapped specimens with w/c=0.50 in 1.6 m ion NaCl and simulated concrete pore solution.	59
Figure 5.10 - Conventional N3 anode bar after removal of mortar, at 15 weeks.....	60
Figure 5.11 - MMFX anode bar after removal of mortar, at 15 weeks	60
Figure 5.12 - Southern Exposure Test. Average corrosion rate, specimens with w/c=0.45, ponded with a 15% NaCl solution.....	62
Figure 5.13 - Southern Exposure Test. Average total corrosion loss, specimens with w/c=0.45, ponded with a 15% NaCl solution.....	62
Figure 5.14 - Southern Exposure Test. Average corrosion rate, epoxy-coated bars, specimens with w/c=0.45, ponded with a 15% NaCl solution.....	64
Figure 5.15 - Southern Exposure Test. Average total corrosion loss, epoxy-coated bars, specimens with w/c=0.45, ponded with a 15% NaCl solution.....	64
Figure 5.16a - Southern Exposure Test. Average corrosion potential vs. CSE, top mat. Specimens with w/c=0.45, ponded with a 15% NaCl solution.	65
Figure 5.16b - Southern Exposure Test. Average corrosion potential vs. CSE, bottom mat. Specimens with w/c=0.45, ponded with a 15% NaCl solution.	65

Figure 5.17 - Cracked Beam Test. Average corrosion rate, specimens with w/c=0.45, ponded with a 15% NaCl solution.....	67
Figure 5.18 - Cracked Beam Test. Average total corrosion loss, specimens with w/c=0.45, ponded with a 15% NaCl solution.....	67
Figure 5.19 - Cracked Beam Test. Average corrosion rate, epoxy-coated bars, specimens with w/c=0.45, ponded with a 15% NaCl solution.....	68
Figure 5.20 - Cracked Beam Test. Average total corrosion loss, epoxy-coated bars, specimens with w/c=0.45, ponded with a 15% NaCl solution.....	69
Figure 5.21a - Cracked Beam Test. Average corrosion potential vs. CSE, top mat. Specimens with w/c=0.45, ponded with a 15% NaCl solution.....	70
Figure 5.21b - Cracked Beam Test. Average corrosion potential vs. CSE, bottom mat. Specimens with w/c=0.45, ponded with a 15% NaCl solution.....	70
Figure 5.22 - Nodular corrosion products with fibers on bare bar anodes for (a) MMFX and (b) conventional steel. 680X.....	72
Figure 5.23 - Amorphous corrosion products with small crystal-like features on bare bar anodes for (a) MMFX and (b) conventional steel. 680X.....	72
Figure 5.24 - Amorphous corrosion products with small crystal-like features on bare bar anodes for (a) MMFX and (b) conventional steel. 680X.....	73
Figure 5.25 - Amorphous corrosion products on bare bar anodes for (a) MMFX and (b) conventional steel. 680X.....	73
Figure 5.26 - Corrosion products on bare bar anodes for (a) MMFX and (b) conventional steel. 85X.....	74
Figure 5.27 - Nodular corrosion products on anode bars in mortar-wrapped specimens for (a) MMFX and b) conventional steel. 680X.....	74
Figure 5.28 - Corrosion products on anode bars in mortar-wrapped specimens showing differing structure for (a) MMFX and b) conventional steel. 680X.....	75
Figure 5.29 - Amorphous, rock-like corrosion products for anode bars in mortar-wrapped specimens for (a) MMFX and b) conventional steel. 680X	75
Figure 5.30 - Corrosion products with fine structure for anode bars in mortar-wrapped specimens for (a) MMFX and b) conventional steel. 680X.....	76
Figure 5.31 - Increase in water-soluble chloride content over background chloride content versus age for 40 bridge decks in Kansas [data from Miller and Darwin (2000)]...	78

Figure B.1 - Macrocell Test. Corrosion rate. Bare conventional, normalized steel in 1.6 m ion NaCl and simulated concrete pore solution.....	97
Figure B.2a - Macrocell Test. Corrosion potential vs. saturated calomel electrode, anode. Bare conventional, normalized steel in 1.6 m ion NaCl and simulated concrete pore solution.	98
Figure B.2b - Macrocell Test. Corrosion potential vs. saturated calomel electrode, cathode. Bare conventional, normalized steel in 1.6 m ion NaCl and simulated concrete pore solution.	98
Figure B.3 - Macrocell Test. Corrosion rate. Bare MMFX steel in 1.6 m ion NaCl and simulated concrete pore solution.	99
Figure B.4a - Macrocell Test. Corrosion potential vs. saturated calomel electrode, anode. Bare MMFX steel in 1.6 m ion NaCl and simulated concrete pore solution.	100
Figure B.4b - Macrocell Test. Corrosion potential vs. saturated calomel electrode, cathode. Bare MMFX steel in 1.6 m ion NaCl and simulated concrete pore solution.	100
Figure B.5 - Macrocell Test. Corrosion rate. Bare MMFX steel in 1.6 m ion NaCl and simulated concrete pore solution.	101
Figure B.6a - Macrocell Test. Corrosion potential vs. saturated calomel electrode, anode. Bare MMFX steel in 1.6 m ion NaCl and simulated concrete pore solution.	102
Figure B.6b - Macrocell Test. Corrosion potential vs. saturated calomel electrode, cathode. Bare MMFX steel in 1.6 m ion NaCl and simulated concrete pore solution.	102
Figure B.7 - Macrocell Test. Corrosion rate. Bare, sandblasted MMFX steel in 1.6 m ion NaCl and simulated concrete pore solution.	103
Figure B.8a - Macrocell Test. Corrosion potential vs. saturated calomel electrode, anode. Bare, sandblasted MMFX steel in 1.6 m ion NaCl and simulated concrete pore solution.	104
Figure B.8b - Macrocell Test. Corrosion potential vs. saturated calomel electrode, cathode. Bare, sandblasted MMFX steel in 1.6 m ion NaCl and simulated concrete pore solution.	105
Figure B.9 - Macrocell Test. Corrosion rate. Bare MMFX steel, bent bar at the anode, in 1.6 m ion NaCl and simulated concrete pore solution.	105
Figure B.10a - Macrocell Test. Corrosion potential vs. saturated calomel electrode, anode. Bare MMFX steel, bent bar at the anode, in 1.6 m ion NaCl and simulated concrete pore solution.	106

Figure B.10b - Macrocell Test. Corrosion potential vs. saturated calomel electrode, cathode. Bare MMFX steel, bent bar at the anode, in 1.6 m ion NaCl and simulated concrete pore solution.	106
Figure B.11 - Macrocell Test. Corrosion rate. Bare #6 MMFX steel in 1.6 m ion and simulated concrete pore solution.	107
Figure B.12a - Macrocell Test. Corrosion potential vs. saturated calomel electrode, anode. Bare #6 MMFX steel in 1.6 m ion NaCl and simulated concrete pore solution	108
Figure B.12b - Macrocell Test. Corrosion potential vs. saturated calomel electrode, cathode. Bare #6 MMFX steel in 1.6 m ion NaCl and simulated concrete pore solution. ..	108
Figure B.13 - Macrocell Test. Corrosion rate. Bare #6 MMFX steel in 1.6 m ion NaCl and simulated concrete pore solution.....	109
Figure B.14a - Macrocell Test. Corrosion potential vs. saturated calomel electrode, anode. Bare #6 MMFX steel in 1.6 m ion NaCl and simulated concrete pore solution.	110
Figure B.14b - Macrocell Test. Corrosion potential vs. saturated calomel electrode, cathode. Bare #6 MMFX steel in 1.6 m ion NaCl and simulated concrete pore solution. ..	110
Figure B.15 - Macrocell Test. Corrosion rate. Bare conventional, normalized steel in 6.04 m ion (15%) NaCl and simulated concrete pore solution.	111
Figure B.16a - Macrocell Test. Corrosion potential vs. saturated calomel electrode, anode. Bare conventional, normalized steel in 6.04 m ion (15%) NaCl and simulated concrete pore solution.	112
Figure B.16b - Macrocell Test. Corrosion potential vs. saturated calomel electrode, cathode. Bare conventional, normalized steel in 6.04 m ion (15%) NaCl and simulated concrete pore solution.	112
Figure B.17 - Macrocell Test. Corrosion rate. Bare sandblasted MMFX steel in 6.04 m ion (15%) NaCl and simulated concrete pore solution.	113
Figure B.18a - Macrocell Test. Corrosion potential vs. saturated calomel electrode, anode. Bare sandblasted MMFX steel in 6.04 m ion (15%) NaCl and simulated concrete pore solution	114
Figure B.18b - Macrocell Test. Corrosion potential vs. saturated calomel electrode, cathode. Bare sandblasted MMFX steel in 6.04 m ion (15%) NaCl and simulated concrete pore solution.	114

Figure B.19 - Macrocell Test. Corrosion rate. Mortar-wrapped conventional, normalized steel in 1.6 m ion NaCl and simulated concrete pore solution.....	115
Figure B.20a - Macrocell Test. Corrosion potential vs. saturated calomel electrode, anode. Mortar-wrapped conventional, normalized steel in 1.6 m ion NaCl and simulated concrete pore solution.	116
Figure B.20b - Macrocell Test. Corrosion potential vs. saturated calomel electrode, cathode. Mortar-wrapped conventional, normalized steel in 1.6 m ion NaCl and simulated concrete pore solution.	116
Figure B.21 - Macrocell Test. Corrosion rate. Mortar-wrapped MMFX steel in 1.6 m ion NaCl and simulated concrete pore solution.....	117
Figure B.22a - Macrocell Test. Corrosion potential vs. saturated calomel electrode, anode. Mortar-wrapped MMFX steel in 1.6 m ion NaCl and simulated concrete pore solution.....	118
Figure B.22b - Macrocell Test. Corrosion potential vs. saturated calomel electrode, anode. Mortar-wrapped MMFX steel in 1.6 m ion NaCl and simulated concrete pore solution.....	118
Figure B.23 - Macrocell Test. Corrosion rate. Cathode = mortar-wrapped conventional, normalized steel. Anode = mortar-wrapped MMFX steel in 1.6 m ion NaCl and simulated concrete pore solution.	119
Figure B.24a - Macrocell Test. Corrosion potential vs. saturated calomel electrode, anode. Cathode = mortar-wrapped conventional, normalized steel. Anode = mortar-wrapped MMFX steel in 1.6 m ion NaCl and simulated concrete pore solution.....	120
Figure B.24b - Macrocell Test. Corrosion potential vs. saturated calomel electrode, cathode. Cathode = mortar-wrapped conventional, normalized steel. Anode = mortar-wrapped MMFX steel in 1.6 m ion NaCl and simulated concrete pore solution.....	120
Figure B.25 - Macrocell Test. Corrosion rate. Cathode = mortar-wrapped MMFX steel. Anode = mortar-wrapped conventional, normalized steel in 1.6 m ion NaCl and simulated concrete pore solution.....	121
Figure B.26a - Macrocell Test. Corrosion potential vs. saturated calomel electrode, anode. Cathode = mortar-wrapped MMFX steel. Anode = mortar-wrapped conventional, normalized steel in 1.6 m ion NaCl and simulated concrete pore solution....	122
Figure B.26b - Macrocell Test. Corrosion potential vs. saturated calomel electrode, cathode. Cathode = mortar-wrapped MMFX steel. Anode = mortar-wrapped conventional, normalized steel in 1.6 m ion NaCl and simulated concrete pore solution....	122

Figure B.27 - Macrocell Test. Corrosion rate based on exposed area of steel (four $\frac{1}{8}$ -in. holes in epoxy). Epoxy-coated steel in 1.6 m ion NaCl and simulated concrete pore solution.....	123
Figure B.28 - Macrocell Test. Corrosion rate based on total area of bar exposed to solution. Epoxy-coated steel in 1.6 m ion NaCl and simulated concrete pore solution.	123
Figure B.29a - Macrocell Test. Corrosion potential vs. saturated calomel electrode, anode. Epoxy-coated steel in 1.6 m ion NaCl and simulated concrete pore solution.	124
Figure B.29b - Macrocell Test. Corrosion potential vs. saturated calomel electrode, cathode. Epoxy-coated steel in 1.6 m ion NaCl and simulated concrete pore solution.....	124
Figure B.30 - Southern Exposure Test. Corrosion rate. Conventional, normalized steel, w/c=0.45, ponded with 15% NaCl solution.	125
Figure B.31a - Southern Exposure Test. Corrosion potential vs. CSE, top mat. Conventional, normalized steel, w/c=0.45, ponded with 15% NaCl solution.	126
Figure B.31b - Southern Exposure Test. Corrosion potential vs. CSE, bottom mat. Conventional, normalized steel, w/c=0.45, ponded with 15% NaCl solution.	126
Figure B.32 - Southern Exposure Test. Corrosion rate. MMFX steel, w/c=0.45, ponded with 15% NaCl solution.....	127
Figure B.33a - Southern Exposure Test. Corrosion potential vs. CSE, top mat. MMFX steel, w/c=0.45, ponded with 15% NaCl solution.	128
Figure B.33b - Southern Exposure Test. Corrosion potential vs. CSE, bottom mat. MMFX steel, w/c=0.45, ponded with 15% NaCl solution.	128
Figure B.34 - Southern Exposure Test. Corrosion rate. Top mat = conventional, normalized steel, bottom mat = MMFX steel, w/c=0.45, ponded with 15% NaCl solution.....	129
Figure B.35a - Southern Exposure Test. Corrosion potential vs. CSE, top mat. Top mat = conventional, normalized steel, bottom mat = MMFX steel, w/c=0.45, ponded with 15% NaCl solution.....	130
Figure B.35b - Southern Exposure Test. Corrosion potential vs. CSE, bottom mat. Top mat = conventional, normalized steel. Bottom mat = MMFX steel, w/c=0.45, ponded with 15% NaCl solution.....	130
Figure B.36 - Southern Exposure Test. Corrosion rate. Top mat = MMFX steel, bottom mat = conventional steel, normalized, w/c=0.45, ponded with 15% NaCl solution.....	131

Figure B.37a - Southern Exposure Test. Corrosion potential vs. CSE, top mat. Top mat = MMFX steel, bottom mat = conventional, normalized steel, w/c=0.45, ponded with 15% NaCl solution.....	132
Figure B.37b - Southern Exposure Test – Corrosion potential vs. CSE, bottom mat. Top mat = MMFX steel, bottom mat = conventional, normalized steel, w/c=0.45, ponded with 15% NaCl solution.....	132
Figure B.38 - Southern Exposure Test. Corrosion rate. MMFX steel, bent bar at anode, w/c=0.45, ponded with 15% NaCl solution.	133
Figure B.39a - Southern Exposure Test – Corrosion potential vs. CSE, top mat. MMFX steel, bent bar at anode, w/c=0.45, ponded with 15% NaCl solution.	134
Figure B.39b - Southern Exposure Test – Corrosion potential vs. CSE, bottom mat. MMFX steel, bent bar at anode, w/c=0.45, ponded with 15% NaCl solution.	134
Figure B.40 - Southern Exposure Test. Corrosion rate based on total bar area exposed to solution. Epoxy-coated bars, w/c=0.45, ponded with 15% NaCl solution.	135
Figure B.41 - Southern Exposure Test. Corrosion rate based on exposed area of steel (four $\frac{1}{8}$ -in. diameter holes in epoxy). Epoxy-coated steel, w/c=0.45, ponded with 15% NaCl solution.....	135
Figure B.42a - Southern Exposure Test. Corrosion potential vs. CSE, top mat. Epoxy-coated steel, w/c=0.45, ponded with 15% NaCl solution.	136
Figure B.42b - Southern Exposure Test. Corrosion potential vs. CSE, bottom mat. Epoxy-coated steel, w/c=0.45, ponded with 15% NaCl solution.....	136
Figure B.43 - Cracked Beam Test. Corrosion rate. Conventional, normalized steel, w/c=0.45, ponded with 15% NaCl solution.	137
Figure B.44a - Cracked Beam Test. Corrosion potential vs. CSE, top mat. Conventional, normalized steel, w/c=0.45, ponded with 15% NaCl solution.	138
Figure B.44b - Cracked Beam Test. Corrosion potential vs. CSE, top mat. Conventional, normalized steel, w/c=0.45, ponded with 15% NaCl solution.	138
Figure B.45 - Cracked Beam Test. Corrosion rate. MMFX steel, w/c=0.45, ponded with 15% NaCl solution.....	139
Figure B.46a - Cracked Beam Test. Corrosion potential vs. CSE, top mat. MMFX steel, w/c=0.45, ponded with 15% NaCl solution.	140
Figure B.46b - Cracked Beam Test. Corrosion potential vs. CSE, bottom mat. MMFX steel, w/c=0.45, ponded with 15% NaCl solution.	140

Figure B.47 - Cracked Beam Test. Corrosion rate based on total area of bar exposed to solution. Epoxy-coated steel, w/c=0.45, ponded with 15% NaCl solution.....	141
Figure B.48 - Cracked Beam Test. Corrosion rate based on exposed area of steel (four 1/8-in. diameter holes in epoxy). Epoxy-coated steel, w/c=0.45, ponded with 15% NaCl solution.....	141
Figure B.49a - Cracked Beam Test. Corrosion potential vs. CSE, top mat. Epoxy-coated steel, w/c=0.45, ponded with 15% NaCl solution.	142
Figure B.49b - Cracked Beam Test. Corrosion potential vs. CSE, bottom mat. Epoxy-coated steel, w/c=0.45, ponded with 15% NaCl solution.	142

LIST OF TABLES

Table 4.1a - Mechanical properties of reinforcing steel as reported by producing mills	16
Table 4.1b - Chemical composition of reinforcing steel as reported by producing mills....	17
Table 4.2 - Rapid macrocell test program	26
Table 4.3 - Concrete properties and mix proportions, cubic yard basis.....	28
Table 4.4 - Bench-scale test program.....	30
Table 4.5 - Repair costs for bridge decks in South Dakota (Gilsrud 2000)	32
Table 4.6 – Bridge deck construction costs in South Dakota (Gilsrud 2000)	33
Table 5.1 – Mechanical test results.....	39
Table 5.2 – Geometrical properties of MMFX reinforcing bars	40
Table 5.3 - Results of X-Ray Microanalysis of MMFX Microcomposite Steel.....	42
Table 5.4 – Prestressed Girder Bridge – Negative Moment Region.....	43
Table 5.5 – Prestressed Girder Bridge – Positive Moment Region	44
Table 5.6 – Continuous Composite (Steel) Girder Bridge – Negative Moment Region	45
Table 5.7 – Continuous Composite (Steel) Girder Bridge – Positive Moment Region.....	46
Table 5.8 – Continuous Concrete Bridge – Negative Moment Region	47
Table 5.9 – Continuous Concrete Bridge – Positive Moment Region.....	48
Table 5.10 – Average corrosion rates and corrosion losses as measured in the macrocell tests	52
Table 5.11 – Average corrosion rates and corrosion losses as measured in the bench-scale tests.....	61
Table 5-12 – Cost estimates and repair schedules for bridge decks containing conventional, epoxy-coated and MMFX Microcomposite steel	79

Table A.1 - Prestressed Girder Bridge - Negative Moment Region.....	89
Table A.2 - Prestressed Girder Bridge - Positive Moment Region	90
Table A.3 - Continuous Composite (Steel) Girder Bridge - Negative Moment Region.....	91
Table A.4 - Continuous Composite (Steel) Girder Bridge - Positive Moment Region	92
Table A.5 - Continuous Concrete Bridge - Negative Moment Region.....	93
Table A.6 - Continuous Concrete Bridge - Positive Moment Region	94

CHAPTER 1

EXECUTIVE SUMMARY

1.1 PROBLEM DESCRIPTION

The corrosion of reinforcing steel in highway structures results in maintenance and replacement costs in the United States that are measured in billions of dollars. The use of deicing salts has resulted in the steady deterioration of roadway bridge decks. The deicers penetrate the decks and attack the reinforcing steel, causing corrosion and a continued increase in the cost of maintaining highway structures. As a result, methods that can significantly reduce or halt chloride-induced corrosion have been pursued aggressively for well over 30 years.

The methods used to reduce corrosion of reinforcing steel may be divided into two categories. The first includes methods that slow the initiation of corrosion. The second includes methods that lengthen the corrosion period, the time between initiation of corrosion and the end of service life. Since the middle 1970s, the principal corrosion protection techniques for bridges have involved the use of epoxy-coated reinforcement and increased cover over the reinforcing bars. The combination of the two systems has greatly lengthened the life of bridge decks, but does not represent a perfect solution. Increased cover, which is not required for structural purposes, increases bridge dead load and the cost of construction. The use of epoxy-coated reinforcement adds only slightly to the cost of bridge construction. However, there are a number of well-documented cases in both the field and laboratory in which poorly adhering epoxy coatings have actually increased corrosion problems. There is clear evidence that, given enough time, even well applied coatings lose adhesion, and the concern of many is that by the time chlorides have reached the level of the reinforcing steel, the coatings will have deteriorated to the point that the epoxy will not protect the reinforcement effectively.

As a result of these concerns, a number of other protective measures have been developed or are under development. These include corrosion-resistant steel alloys, one of which, MMFX Microcomposite steel, a high-strength, high chromium (9%) alloy is evaluated in this study. Initial runs of this steel produced a material with a yield strength of 126 ksi, more than twice that required of conventional ASTM A 615 reinforcing bars. The results of an anodic polarization test, commissioned by MMFX Steel Corporation of America, indicate that the steel has significantly improved corrosion resistance. It involves both a delay in corrosion initiation and slower corrosion after initiation. While the steel appears to offer significant advantages, such as lower construction costs and a longer life for reinforced concrete bridge decks, concerns exist since none of the corrosion tests reported involve corrosion of the new reinforcing steel in which a *macrocell* formed and the tests were not performed in highly alkaline environments, such as exist in concrete. In addition, questions have been raised about material uniformity and the

effective use of such a high-strength material as reinforcement. These concerns are addressed by the research described in this report.

1.2 OBJECTIVES

The research program has three objectives. They are to:

- 1) Determine the corrosion resistance of MMFX Microcomposite steel compared to epoxy-coated reinforcement (ECR).
- 2) Determine the mechanical properties, quality, and suitability of MMFX Microcomposite steel for use in bridge decks.
- 3) Estimate life expectancy and cost effectiveness of MMFX Microcomposite, ECR, and mild steel reinforcement in South Dakota.

The principal reason for selecting a new reinforcing material for concrete bridge decks is to improve the life expectancy and cost effectiveness of the structural system. A prerequisite for selection is the requirement that the material must provide a significant improvement in corrosion resistance compared to the current material of choice, epoxy-coated reinforcement. To this end, MMFX Microcomposite steel, conventional mild steel reinforcement, and ECR are evaluated using rapid macrocell tests and the initial results from longer term Southern Exposure and cracked beam tests.

MMFX Microcomposite steel has significantly higher yield and tensile strengths than conventional ASTM A 615 reinforcing bars. Thus, it is important to understand the mechanical properties of the steel and how these properties will affect the structural performance of bridge decks. To this end, the reinforcing steel is tested, bar deformations are measured, the material is analyzed to evaluate uniformity of composition, and the impact of bar properties on the structural performance of bridge decks is evaluated.

Finally, the results of the corrosion evaluation are combined with construction and maintenance experience in South Dakota and other states to evaluate the impact of the new reinforcing steel on the life expectancy and cost effectiveness of reinforced concrete bridge decks.

1.3 FINDINGS

A series of tasks were completed to evaluate the performance of MMFX Microcomposite steel. The principal results of that research are summarized in this section.

1.3.1 Literature Search

MMFX Microcomposite steel is a proprietary material. No published papers are available on its mechanical or corrosion-resistant properties. However, the MMFX Steel Corporation of America made test results available during the course of the study. Those results dealt primarily with the mechanical properties of the steel. The tests indicate that the steel produces yield strengths based on a 0.2% offset method between 119 and 133 ksi, with tensile strengths between 180 and 186 ksi. High elongations are measured when short gauge lengths are

used, while elongations in the range of 7 to 9% are more typical when an 8-in. gauge length, the gauge length required when testing conventional reinforcing steel, is used. Charpy V-notch tests indicate that the steel has significantly higher fracture toughness than conventional reinforcing steel and therefore may be useful for other applications.

Corrosion data is limited to that provided by an anodic polarization test, which is not indicative of the type of corrosion to which reinforcing steel is exposed in highway structures.

1.3.2 Physical and Mechanical Tests

Samples of conventional and MMFX Microcomposite steel were evaluated based on tensile and bend properties, bar geometry, uniformity of chemical analysis, and structural performance as reflected in reinforced concrete bridge deck designs.

The results of the mechanical tests indicate that the steel provides tensile strengths in the range of 160 to 175 ksi. Measured values of yield strength depend on the definition used. Based on the 0.2% offset method, yield strengths of approximately 110 and 120 ksi are obtained for the No. 5 and No. 6 MMFX bars, respectively, considerably above the minimum value required for Grade 60 reinforcement. Based on a total strain of 0.35%, the value specified in ASTM A 615 for cases in which yield strength is selected based on strain value, produced similar strengths. The values change significantly, however, if a strain of 0.7% is used, a value that may be used in place of the 0.2% offset method in ASTM A 772 for high-strength steel bars for prestressing concrete. At 0.7% strain, the yield strengths increase to values near 130 ksi for No. 5 bars and in excess of 130 ksi for No. 6 bars, allowing the bars to meet the requirements for prestressing steel under ASTM A 722. Elongations average 7%, the minimum required for Grade 75 ASTM A 615 reinforcement, but range from 6.3 to 7.8% based on an 8-in. gauge length. All MMFX bars passed the bend test.

Measurements of bar geometry indicated that the bars will provide bond strengths equal to or exceeding those provided by conventional reinforcing steel.

An x-ray microanalysis performed on multiple samples demonstrates that the chemistry of MMFX steel is consistent for bars within the same heat and very close for the two heats analyzed.

The bars were used in trial designs for three SDDOT bridge decks. The results of the designs indicate that under current AASHTO design procedures, MMFX Microcomposite steel provides few satisfactory options for replacing conventional reinforcing steel. Shortcomings in designs that incorporate MMFX reinforcing steel include exceeding maximum allowable steel and concrete stresses, violating crack control and fatigue provisions, and exceeding the maximum allowable percentage of reinforcement. These drawbacks potentially could be overcome if design standards were modified to allow the incorporation of steel with a yield stress of 120 ksi.

1.3.3 Corrosion Tests

Major emphasis in the study was placed on the comparison of corrosion performance of MMFX Microcomposite steel, conventional mild steel reinforcement, and epoxy-coated reinforcement. The principal test used for the evaluation is the rapid macrocell test. The test involves placing either a bare or mortar-covered (wrapped) reinforcing bar in a container containing simulated concrete pore solution and a preselected concentration of sodium chloride. Two similar specimens are placed in a second container containing simulated pore solution. The specimens are electrically connected across a 10-ohm resistor and the solutions are connected with a salt bridge. The specimen subjected to chlorides (the anode) represents the top layer of a bridge deck, while the specimens in the other container (cathode) represent the bars in the bottom layer of a bridge deck. Air is supplied to the liquid surrounding the cathode to ensure an adequate supply of oxygen. The corrosion rate, measured in micrometers per year ($\mu\text{m}/\text{yr}$), is determined based on the current in the system, which can be determined based on the voltage drop across the resistor. The results for bare and mortar-wrapped bars are shown in Figs. 1.1 and 1.2, respectively.

The tests shown in Fig. 1.1 involve one series of conventional (N3) specimens, two series of straight MMFX steel [MMFX(1) and (2)] in an “as delivered” condition, one series of MMFX sand-blasted bars (MMFXs), and one series of MMFX bent bars (MMFXb), all of which involve No. 5 bars. In addition, two series of No. 6 bar specimens are also tested [MMFX#6(1) and (2)]. For the No. 5 bars shown in Fig. 1.1, at 15 weeks, the MMFX steel corrodes at an average rate equal to 37% of that exhibited by the conventional bars. An inspection of the test specimens indicates that in some cases MMFX steel will corrode when the surface is exposed to moist air and chlorides. A microscopic evaluation shows that similar corrosion products are deposited on the surfaces of MMFX and conventional reinforcing steel.

For mortar-wrapped bars, which provide a closer match to reinforcing steel under service conditions, conventional N3 steel is compared with MMFX steel and epoxy-coated reinforcement. In the latter case, the epoxy coating is penetrated by four $\frac{1}{8}$ -in. diameter holes to represent flaws in the coating. In addition, two series of macrocells are evaluated in which MMFX and N3 steel are combined — in one case with MMFX serving as the anode and in one case with N3 steel serving as the anode. The mortar has a water-cement ratio of 0.5 and a sand-cement ratio of 2.0.

The results for mortar-wrapped bars indicate that MMFX steel corrodes at a rate equal to 60% of that observed for conventional N3 steel, while, based on total bar surface area, epoxy-coated reinforcement corrodes at a rate equal to less than half that of MMFX steel. Mixing MMFX with conventional reinforcement improves the performance of the conventional steel and reduces the performance of the MMFX steel.

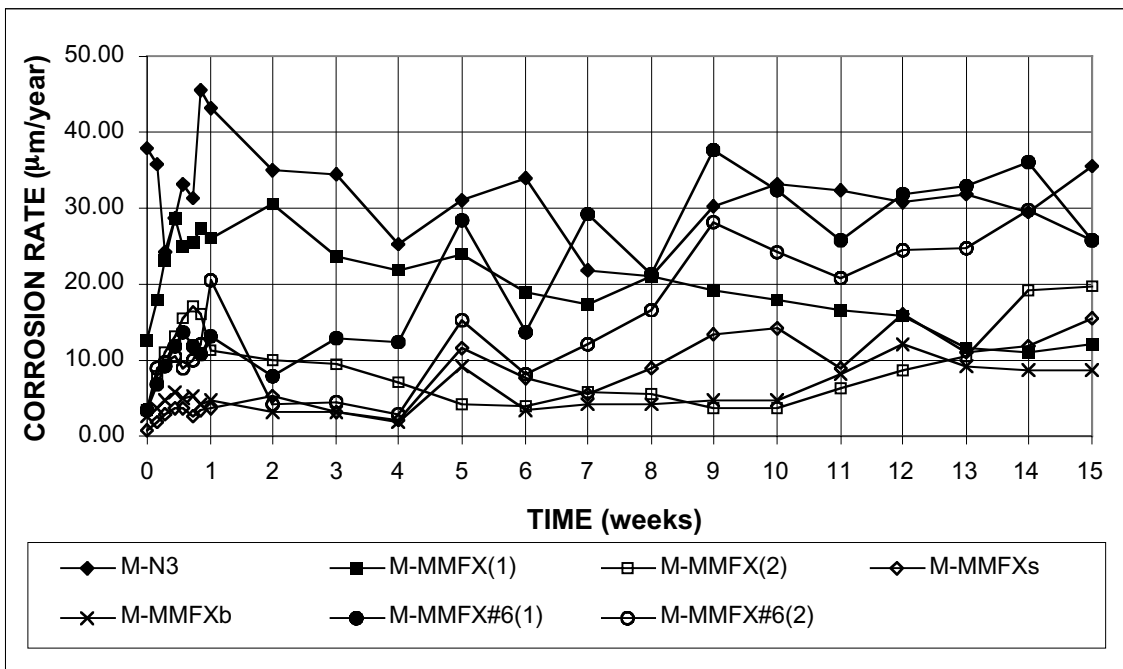


Figure 1.1 - Macrocell Test. Average corrosion rate. Bare specimens in 1.6 m ion NaCl and simulated concrete pore solution.

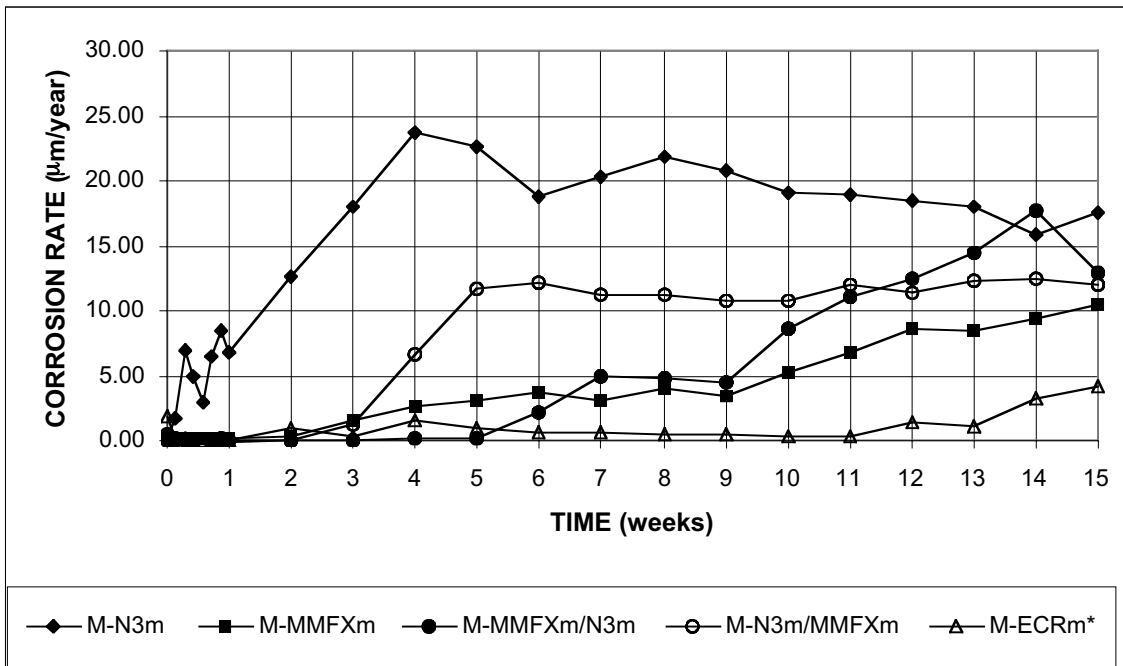


Figure 1.2 - Macrocell Tests. Average corrosion rate. Mortar-wrapped specimens with w/c=0.50 in 1.6 m ion NaCl and simulated concrete pore solution.

* Based on total area of bar exposed to solution

The longer-term corrosion performance of reinforcing steel is measured using Southern Exposure and cracked beam tests. The specimens used in these tests are 7-in. deep slabs with two layers of steel that represent portions of bridge decks. The Southern Exposure specimen represents deck regions with intact concrete and the cracked beam specimen represents regions in which the top layer of steel is exposed due to settlement cracks. A 15% sodium chloride solution is ponded on the surface of the slabs, and the specimens are subjected to cycles of wetting and drying, which raises the chloride concentration within the concrete. These 96-week tests are nearly 25% complete at this writing. In addition to evaluating corrosion performance, the results of the tests are used in the economic analysis.

The key results for the Southern Exposure and cracked beam tests are summarized in terms of total corrosion loss, in micrometers, in Figs. 1.3 and 1.4, respectively. Figure 1.3 demonstrates that the corrosion of MMFX steel is delayed, requiring a higher chloride content for initiation, and proceeds at a lower rate than it does for conventional steel. Epoxy-coated steel corrodes at an even lower rate. Without the holes in the epoxy, it is expected that corrosion would not have been measurable in these tests. Similar results are observed for the cracked beam tests (Fig. 1.4), with the principal difference being the rapid initiation of corrosion in all specimens due to direct access of the chlorides to the reinforcing steel through the simulated crack that is placed in the specimen at the time of fabrication.

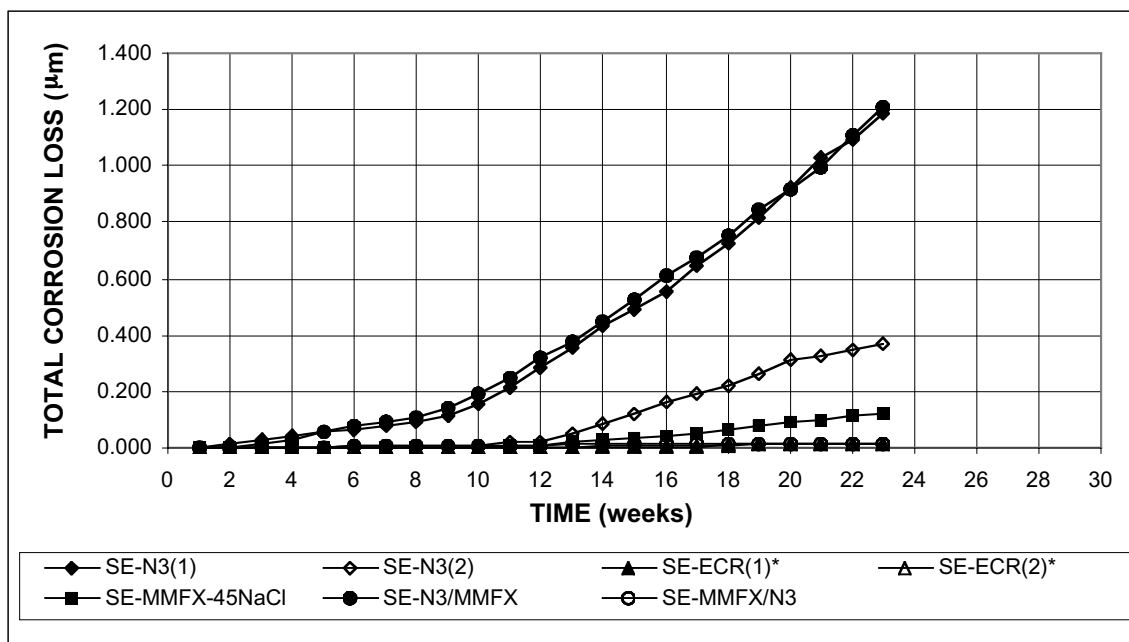


Figure 1.3 – Southern Exposure Test. Average total corrosion loss, specimens with w/c=0.45, ponded with a 15% NaCl solution.

* Based on total area of bar exposed to solution

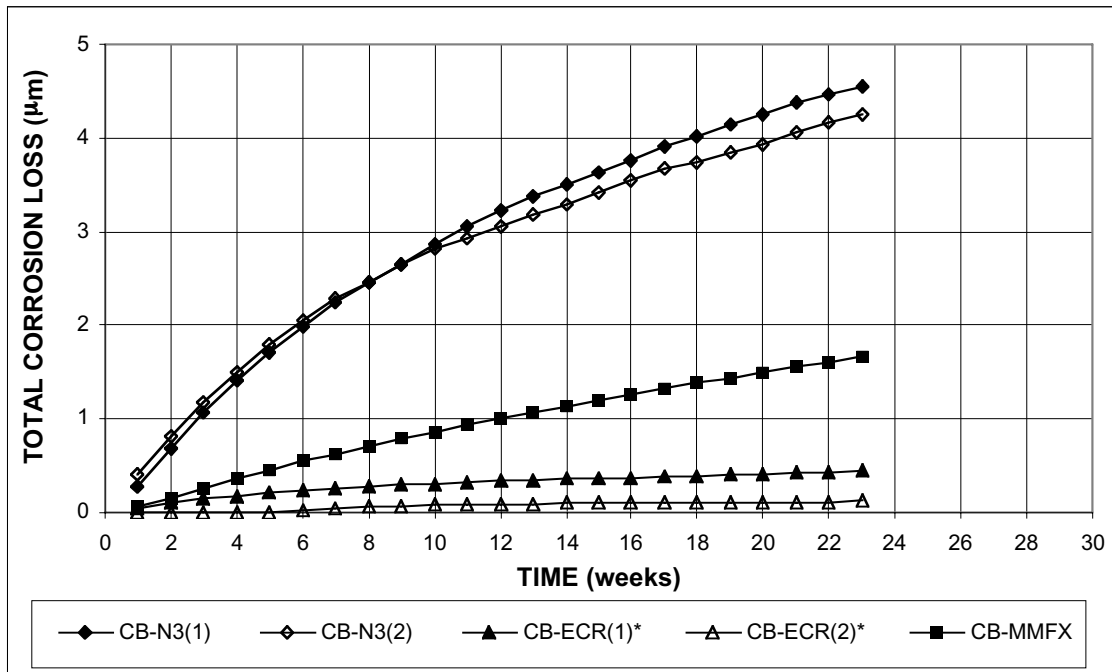


Figure 1.4 - Cracked Beam Test. Average total corrosion loss, specimens with w/c=0.45, ponded with a 15% NaCl solution.

* Based on total area of bar exposed to solution

1.3.4 Life Expectancy and Economic Analysis

The life expectancy and cost effectiveness of bridges containing MMFX Microcomposite, ECR, and conventional reinforcement is determined based on the experience of the South Dakota Department of Transportation, in conjunction with the laboratory results obtained in this study. Estimates of times to first repair for conventional reinforcement are 10 years under harsh conditions and 25 years under arid conditions. Time to first repair for epoxy-coated reinforcement is estimated to be 40 years based on the observation that no bridges built with epoxy coating in South Dakota have required repair. Laboratory results, supported by prior research, indicate that conventional reinforcement or exposed epoxy-coated reinforcement will begin corroding at a chloride concentration of approximately 1 lb/yd³, whereas the MMFX Microcomposite steel will begin corroding at a value of approximately 3½ lb/yd³. These values are used to estimate time-to-corrosion-initiation, based on observed chloride contents in cracked bridge decks. Results from the cracked beam tests, which provide estimates of long-term corrosion rates of approximately 2.2 and 1.2 μm/yr for conventional and MMFX steel, respectively, are then used to determine the time, after corrosion initiation, to reach a total thickness loss of 25 μm (0.00098 in.), the expected value that will result in concrete cracking due to the deposition of corrosion products adjacent to the bar.

Based on the combined laboratory results and analyses, times to first repair of 13 and 27 years are obtained for conventional and MMFX steel.

Using the time to first repair and a standard 25-year period for subsequent repairs, the cost effectiveness of conventional, epoxy-coated, and MMFX reinforcement is evaluated using a typical 8.5-in bridge deck with an economic life of 75 years at discount rates of 2, 4, and 6%. The analysis indicates that, at a discount rate of 2%, epoxy-coated reinforcement, with either a 35 or a 40-year time to first repair, has the lowest present value cost, \$276 or \$261/yd², compared to \$316/yd² for MMFX steel with a time to first repair of 27 years, and \$444/yd² for conventional steel with a time to first repair of 10 years and a cost of \$312/yd² for time to first repair of 25 years. The present value cost for MMFX steel drops to \$305 and \$288/yd³ for assumed times to first repair of 30 and 35 years, respectively, but is still more expensive than either value for epoxy-coated steel.

1.4 CONCLUSIONS

The following conclusions are based on the test results and analyses presented in this report.

1. MMFX Microcomposite steel reinforcing bars exhibit yield strengths equal to approximately twice that required of conventional Grade 60 reinforcing steel. Average values range from 110 to 122 ksi, based on the 0.2% offset method and from 128 to 138 ksi, based on 0.7% strain. Tensile strengths range from 161 to 174 ksi. Elongations average approximately 7%, the minimum requirement for ASTM A 615 Grade 75 reinforcement; some individual samples fail to meet this criterion. MMFX reinforcement satisfies ASTM A 615 bend requirements.

2. MMFX Microcomposite steel bars satisfy the mechanical property requirements of high-strength steel bars for prestressing concrete, as specified in ASTM A 722, if the yield strength is based on 0.7% strain.

3. The MMFX Microcomposite steel bars satisfy the requirements for bar geometry specified in ASTM A 615 and provide relative rib areas within or above the normal range in U.S. practice. The bars will provide satisfactory bond strength with concrete.

4. X-ray microanalysis indicates that the chemistry of MMFX steel is consistent for bars within the same heat and very close for the two heats analyzed.

5. Depending on the bridge deck design, use of MMFX Microcomposite steel provides few or no alternative designs that will satisfy all AASHTO bridge design criteria.

6. The corrosion threshold chloride content for MMFX Microcomposite steel is approximately four times higher than the corrosion threshold for conventional reinforcement. The corrosion rate for MMFX Microcomposite steel is between one-third and two-thirds that of conventional reinforcing steel. In all evaluations, epoxy-coated steel meeting the requirements of ASTM A 775 provides superior corrosion performance to MMFX Microcomposite steel. MMFX Microcomposite steel appears to corrode when the surface is exposed to moist air and chlorides but not in contact with concrete or submerged in water.

7. Similar corrosion products are deposited on the surfaces of MMFX Microcomposite steel and conventional reinforcing steel.

8. Bridge decks containing MMFX Microcomposite reinforcing steel will require repair due to corrosion-induced concrete cracking approximately 30 years after construction, compared to conventional bridge decks which require repair in 10 to 25 years, depending on exposure conditions. Bridge decks containing epoxy-coated reinforcement will require repair 30 to 40 years after construction.

9. Bridge decks containing MMFX Microcomposite steel do not appear to be cost effective when compared to bridge decks containing epoxy-coated reinforcement.

1.5 IMPLEMENTATION RECOMMENDATIONS

The evaluations and test results presented in this report lead to the following implementation recommendations.

1. MMFX Microcomposite reinforcing steel should not be used as a direct replacement for epoxy-coated reinforcement without the use of a supplementary corrosion protection system. Use of the material in its current form is not recommended for reinforced concrete bridge decks in South Dakota.

This recommendation is based on the observations that, while MMFX reinforcing steel requires a higher corrosion threshold and corrodes at a lower rate than conventional reinforcement, (1) its corrosion-resistant properties are not superior to that of epoxy-coated reinforcement and (2) bridge decks constructed with MMFX Microcomposite steel will have a shorter life expectancy, a higher first cost, and a higher lifetime cost than bridge decks constructed with epoxy-coated reinforcement. The cost effectiveness of bridges constructed with MMFX reinforcement would be improved if the total reinforcement in the bridge deck were reduced, taking advantage of the material's higher strength. However, concerns of serviceability, especially bridge deck cracking, mitigate against this.

2. MMFX Microcomposite steel meets or comes close to meeting the requirements for high-strength steel bars for prestressing concrete as specified in ASTM A 722. Specifications for reinforcing materials should be modified to allow its use in post-tensioned prestressed concrete construction.

MMFX Microcomposite steel is a high-strength material with properties similar to those specified under ASTM A 722. With a price of approximately \$0.40/lb, MMFX steel should be competitive with other steels that satisfy this standard. Its high fracture toughness, shown in tests run for the MMFX Steel Corporation of America indicates that the steel provides other, desirable mechanical properties that are not available in more traditional reinforcing materials.

3. SDDOT should continue to use epoxy-coated reinforcement to provide corrosion protection in bridge decks until such time as a superior corrosion protection system becomes available.

This recommendation is based on superior corrosion performance of epoxy-coated steel compared to MMFX steel (Section 5.3) and the superior life expectancy and cost effectiveness of bridge decks containing epoxy-coated reinforcement compared to the alternatives evaluated in this study.

CHAPTER 2

PROBLEM DESCRIPTION

The corrosion of reinforcing steel in highway structures results in maintenance and replacement costs in the United States that are measured in billions of dollars. The use of deicing salts has resulted in the steady deterioration of roadway bridge decks. The deicers penetrate the decks and attack the reinforcing steel, causing corrosion. As a result, the cost of maintaining highway structures in the U.S. has continued to increase. In 1979, the cost of bridge repairs in the federal-aid system due to corrosion damage was estimated to be \$6.3 billion (Locke 1986). By 1986, the estimated cost was \$20 billion and was forecast to increase at the rate of \$500 million per year (Cady and Gannon 1992). By 1992, the estimated repair cost had risen to \$51 billion (Fliz et al. 1992). As a result, methods that can significantly reduce or halt chloride-induced corrosion have been pursued aggressively for well over 30 years.

The methods used to reduce corrosion of reinforcing steel may be divided into two categories. The first includes methods that slow the initiation of corrosion, that is lengthen the time it takes the chlorides to reach the reinforcing steel in the concrete. The second includes methods that lengthen the corrosion period, the time between initiation of corrosion and the end of service life. Since the middle 1970s, the principal corrosion protection techniques for bridge decks have involved the use of epoxy-coated reinforcement and increased cover over the reinforcing bars. Both techniques slow the initiation of corrosion and lengthen the corrosion period. Increased cover increases the time required for chlorides to reach the reinforcing steel and lowers the rate at which oxygen and moisture are available to participate in the corrosion process. The epoxy coating also limits access of chlorides, oxygen, and moisture to the surface of the reinforcing steel. In regions where the chlorides have access to the steel at breaks in the coating, corrosion is slowed because the coated reinforcement still limits access of oxygen and moisture, required for active corrosion.

The combination of the two systems has greatly lengthened the life of bridge decks, but does not represent a perfect solution. Increased cover, which is not required for structural purposes, increases bridge dead load and the cost of construction. The use of epoxy-coated reinforcement adds only slightly to the cost of bridge construction. However, there are a number of well-documented cases in both the field and laboratory in which poorly adhering epoxy coatings have actually increased corrosion problems, and there is some indication that all epoxy coatings will be susceptible to those shortcomings eventually. The problem involves small breaks in the coating that allow the bond between the coating and the steel to be lost. The coating remains generally intact, but the chloride concentration increases in the solution underneath the coating in an environment that is low in oxygen. The result is crevice corrosion, which essentially involves hydrochloric acid attack of the steel. This happened for poorly applied coatings in substructures in Florida (Sagues et al. 1994). There is clear evidence that,

given enough time, even well applied coatings lose adhesion (Manning 1996, Smith and Virmani 1996), and the concern of many is that, by the time chlorides have reached the level of the reinforcing steel, the coatings will have deteriorated to the point that the epoxy will not protect the reinforcement effectively.

As a result of these concerns, a number of other protective measures have been developed or are under development. These include the use of denser concretes, corrosion inhibitors, and corrosion-resistant steel alloys. Two alloys identified as MMFX steel have been developed. One type, described as “dual phase” steel, involves an alloy that is quenched after rolling. The quenching process causes the formation of a ferritic-martensitic low carbon steel that has improved corrosion resistance and produces strength properties that are equal or exceed those of conventional ASTM A 615 reinforcing bars. The lack of a general availability of facilities to quench reinforcing steel has led the developers to formulate MMFX “microcomposite” steel that can be manufactured without the quenching operation. Initial runs of the MMFX Microcomposite steel produced a material with a yield strength of 126 ksi, more than twice that required of A 615 steel. Based on an anodic polarization test (data available on website of MMFX Steel Corporation of America), the steel appears to have significantly improved corrosion resistance. That corrosion resistance appears to both delay corrosion initiation and slow corrosion after initiation. While the microcomposite steel appears to offer significant advantages, it could lead to lower construction costs and longer life for reinforced concrete bridge decks, a number of questions remain. In particular, none of the corrosion tests reported has involved corrosion of the new reinforcing steel in which a *macrocell* has formed. The tests reported by the developers have involved accelerated testing in noncementitious environments. Since corrosion in highly alkaline environments is significantly different from corrosion in the atmosphere, testing the reinforcing steel in cementitious systems is mandatory, as is testing the steel within a macrocell, such as will form between the top and bottom layers of reinforcement in a bridge deck. In addition, questions have been raised about material uniformity and the effective use of such a high-strength material as reinforcement. These concerns are addressed by the research presented in this report.

CHAPTER 3

OBJECTIVES

This research program has three objectives. They are: to determine if MMFX Microcomposite steel has superior corrosion-resistance properties compared to epoxy-coated reinforcement, to determine if MMFX steel will serve as a suitable reinforcement for concrete, and to compare the life expectancy and cost effectiveness of the new material with epoxy-coated reinforcement and conventional mild steel reinforcement.

OBJECTIVE 1

Determine the corrosion-resistance of MMFX Microcomposite steel compared to ECR reinforcement.

The principal reason for selecting a new reinforcing material for concrete bridge decks is to improve the life expectancy and cost effectiveness of the structural system. A prerequisite for such a selection is the requirement that the material, which presumably is more expensive than the current system, provides a significant improvement in corrosion resistance compared to the current material of choice, epoxy-coated reinforcement (ECR) meeting the requirements of ASTM A 775. The corrosion-resistance of MMFX Microcomposite steel, conventional mild steel reinforcement, and ECR are evaluated using rapid macrocell tests and the initial results from longer term Southern Exposure and cracked beam tests. Additional measures of corrosion resistance are also used to compare the performance of the three materials. Rapid macrocell tests in which both bare and mortar-clad reinforcing bars are subjected to elevated chloride levels represent the principal procedure for gauging corrosion resistance. Longer term bench-scale tests with fully intact concrete (Southern Exposure tests) and precracked concrete (cracked beam tests) are also used, with the first 23 weeks of data available for evaluation. Results for the balance of these 96-week tests will be provided to SDDOT at six-month intervals. The nature of the corrosion products on the steels is also evaluated using a scanning electron microscope.

OBJECTIVE 2

Determine the mechanical properties, quality, and suitability of MMFX Microcomposite steel for use in bridge decks.

MMFX Microcomposite steel has significantly higher yield and tensile strengths than conventional ASTM A 615 reinforcing bars. Thus, it is important to understand the mechanical properties of the steel and how those properties will affect the structural performance of bridge decks. To this end, the reinforcing steel is evaluated for yield and tensile strength, elongation, and bendability. Bar deformations are measured and used to calculate the relative rib area, the principal controller of bond strength (Darwin and Graham 1993, Darwin et al. 1996a, 1996b, Zuo

and Darwin 2000). X-ray microanalysis is used to evaluate the bars for consistency and uniformity in composition. Finally, the high strength of the bars affects the ductility, strength, and potentially the serviceability of reinforced concrete bridge decks. The impact of these properties on deck performance is evaluated using three design examples.

OBJECTIVE 3

Estimate life expectancy and cost effectiveness of MMFX Microcomposite, ECR, and mild steel reinforcement in South Dakota.

Given that MMFX Microcomposite steel has superior corrosion resistance compared to uncoated *mild steel* reinforcement, it is necessary to determine if incorporation of MMFX Microcomposite steel will increase the life expectancy and/or improve the cost effectiveness of reinforced concrete bridge decks. The results of the corrosion evaluation are incorporated in an economic analysis using techniques described by Kepler, Darwin, and Locke (2000). The procedures involve estimating the costs of construction and repair for each type of reinforcing material, and the time periods between construction and first repair and between subsequent repairs. The costs are then used at selected discount rates to compare the present value of construction and maintenance costs for bridge decks containing each form of reinforcement over a 75-year economic life.

The following chapters cover the specific tasks, findings, conclusions, and implementation recommendations on the use and desirability of incorporating MMFX Microcomposite steel in reinforced concrete bridge decks.

CHAPTER 4

TASK DESCRIPTION

4.1 LITERATURE SEARCH

Perform a literature search on MMFX Microcomposite steel and its use as reinforcement.

MMFX Microcomposite steel is a proprietary material. No papers have been published describing the steel, and the information available is limited to that released by the MMFX Steel Corporation of America. A request was made to the company for full disclosure of the properties and research performed on the steel to date, including a request for disclosure of any identified users. During the course of the study, the company made test results available. That information is summarized in Section 5.1.

4.2 PHYSICAL AND MECHANICAL TESTS

Conduct a series of laboratory tests consisting, at a minimum, of elongation, yield strength, tensile strength, uniformity, thickness, variability, development lengths, effects due to deformation profile, composition, and corrosion rate on No. 4, No. 5, and No. 6 MMFX Microcomposite steel, ECR, and mild steel randomly obtained.

Steel samples were obtained in coordination with the South Dakota Department of Transportation. The samples consisted of two heats of No. 5 and three heats each of No. 4 and No. 6 conventional steel, and one heat of No. 5 and two heats of No. 6 MMFX steel (one of the heats of No. 6 MMFX bars was the same heat as the No. 5 bars). The results of mill tests and chemistries are presented in Table 4.1. An additional heat of conventional steel, designated N2, is also used for corrosion testing. The conventional and matching epoxy-coated reinforcement were obtained from the same heats of steel.

This section addresses mechanical properties and bar geometry, x-ray microanalysis to evaluate material uniformity, and analyses to evaluate the performance of MMFX steel as a structural reinforcing material in bridge decks.

4.2.1 Mechanical Tests and Bar Geometry

Full stress-strain curves are used to determine yield strength, tensile strength, and elongation. Bend tests are conducted in accordance with ASTM A 615. Five and three specimens for each property were used to determine the mechanical properties of MMFX and conventional reinforcing steel, respectively.

Table 4.1a - Mechanical properties of reinforcing steel as reported by producing mills

Steel Type	Heat No.	Mark	Size	Yield Strength (ksi)	Tensile Strength (ksi)	Elongation % in 8 in.	Bending
	K0-C696	-	No. 5	67.7	106.1	15.00	Pass
N3 ¹	S46753	Heat 1	No. 4	69.5	107.5	14.69	Pass
N3	S46757	Heat 2	No. 4	70.5	108.0	13.13	Pass
N3	S46760	Heat 3	No. 4	69.0	108.0	14.38	Pass
N3	S44420	Heat 1	No. 5	68.1	106.5	15.00	Pass
N3	S44407	Heats 2 & 3	No. 5	68.1	107.4	12.50	Pass
N3	S47695	Heat 1	No. 6	74.5	116.4	11.88	Pass
N3	S47790	Heat 2	No. 6	72.0	116.1	15.00	Pass
N3	S47814	Heat 3	No. 6	71.8	111.8	12.50	Pass
MMFX ²	810737	-	No. 5	-	164.1	6.00	-
MMFX	810737	-	No. 6	-	168.6	6.00	-
MMFX	710788	-	No. 6	-	171.4	5.00	-

¹ N2 and N3: Conventional, normalized A 615 reinforcing steel

² MMFX: MMFX Microcomposite steel

Bar deformation geometry is measured and the relative rib area of the bars is calculated. The relative rib area (R_r) of a reinforcing bar is the ratio of the bearing area of the ribs to the perimeter area of the bar between the ribs. Following the procedures of ACI Committee 408 (ACI 408.3), it may be calculated as

$$R_r = \frac{h_r}{s_r} \left(1 \pm \frac{\Sigma \text{gaps}}{p} \right) \quad (4.1)$$

where h_r = average height of deformations, s_r = average spacing of deformations, Σgaps = sum of the gaps between ends of transverse deformations, plus the width of any continuous longitudinal lines used to represent the grade of the bar multiplied by the ratio of the height of the line to h_r , and p = nominal perimeter of bar. When transverse deformations tie into longitudinal ribs, the gap may be measured across the longitudinal rib at the midheight of the transverse deformation. The average height of the deformations, or ribs, (h_r) is determined based on measurements made on at least two deformations on each side of a bar. Determinations are based on five measurements per deformation, one at the center of the overall length, two at the ends of the overall length, and two located halfway between the center and the ends. The measurement at the ends of the overall length are averaged to obtain a single value, and that value is combined

with the other three values to obtain the average rib height R_r . Deformation measurements are made with a depth gauge with a knife-edge support that spans not more than two adjacent ribs.

Table 4.1b - Chemical composition of reinforcing steel as reported by producing mills

Steel Type	Heat No.	Mark	Size	C	Mn	P	S	Si	Cr	Cu	Ni
N2 ¹	K0-C696	-	No. 5	0.420	0.960	0.014	0.040	0.020	0.140	0.300	0.100
N3 ¹	S46753	Heat 1	No. 4	0.420	1.140	0.017	0.033	0.240	0.160	0.260	0.080
N3	S46757	Heat 2	No. 4	0.430	1.140	0.022	0.023	0.220	0.170	0.270	0.080
N3	S46760	Heat 3	No. 4	0.430	1.050	0.012	0.043	0.210	0.220	0.310	0.120
N3	S44420	Heat 1	No. 5	0.430	1.150	0.013	0.020	0.240	0.100	0.380	0.080
N3	S44407	Heats 2 & 3	No. 5	0.450	1.150	0.012	0.024	0.260	0.120	0.380	0.120
N3	S47695	Heat 1	No. 6	0.420	1.150	0.014	0.017	0.220	0.230	0.480	0.130
N3	S47790	Heat 2	No. 6	0.440	1.090	0.014	0.018	0.240	0.180	0.300	0.100
N3	S47814	Heat 3	No. 6	0.430	1.130	0.021	0.025	0.230	0.170	0.330	0.110
MMFX ²	810737	-	No. 5	0.060	0.460	0.010	0.011	0.230	9.130	0.100	0.090
MMFX	810737	-	No. 6	0.060	0.460	0.010	0.011	0.230	9.130	0.100	0.090
MMFX	710788	-	No. 6	0.060	0.460	0.010	0.012	0.250	9.170	0.070	0.070

Steel Type	Heat No.	Mark	Size	Sn	Mo	V	Nb	N2	Al	Cb	Ca
N2 ¹	K0-C696	-	No. 5	0.009	0.019	0.002	-	-	0.001	-	-
N3 ¹	S46753	Heat 1	No. 4	0.019	0.020	0.001	-	-	0.002	0.002	8 ppm
N3	S46757	Heat 2	No. 4	0.018	0.020	0.002	-	-	0.002	0.001	10 ppm
N3	S46760	Heat 3	No. 4	0.012	0.040	0.001	-	-	0.002	0.001	9 ppm
N3	S44420	Heat 1	No. 5	0.015	0.020	0.001	-	-	-	0.002	12 ppm
N3	S44407	Heats 2 & 3	No. 5	0.017	0.030	0.001	-	-	-	0.002	14 ppm
N3	S47695	Heat 1	No. 6	0.012	0.050	0.001	-	-	0.002	0.002	9 ppm
N3	S47790	Heat 2	No. 6	0.009	0.030	0.001	-	-	0.003	0.001	12 ppm
N3	S47814	Heat 3	No. 6	0.013	0.030	0.003	-	-	0.003	0.002	11 ppm
MMFX ²	810737	-	No. 5	-	0.020	0.018	0.007	118 ppm	-	-	-
MMFX	810737	-	No. 6	-	0.020	0.018	0.007	118 ppm	-	-	-
MMFX	710788	-	No. 6	-	0.010	0.018	0.007	108 ppm	-	-	-

¹ N2 and N3: Conventional, normalized A 615 reinforcing steel

² MMFX: MMFX Microcomposite steel

R_r has been demonstrated to be the key parameter in the development and splice strength of reinforcing bars (Darwin and Graham 1993, Darwin et al. 1996a, 1996b, Zuo and Darwin 2000). The relative rib area for most conventional reinforcing bars in the U.S. ranges between 0.06 and 0.085. Changes in R_r have no measurable effect on the bond strength of reinforcing bars that are not confined by transverse reinforcement. Changes in relative rib area do have an effect on the bond strength of bars that are confined by transverse reinforcement, but the change is relatively small for the usual values of R_r . Values of R_r within the typical range will ensure adequate development and splice strength for the bars.

The mechanical and geometrical evaluation of the bars is presented in Section 5.2.1.

4.2.2 X-Ray Microanalysis

The chemical composition of the bars from point to point in a cross section and for different heats is measured using a scanning electron microscope (SEM) and energy dispersive spectrometer (EDS). Three points on each of two samples from each heat of MMFX steel and one heat No. 5 conventional steel are analyzed to determine uniformity in chemical composition.

Specimens used for the EDS analysis are prepared by cutting transverse sections from the reinforcing bars using a band saw. The specimens are cleaned in an acetone bath to remove grease, dirt, and hydraulic fluid. The faces of the specimens are then cleaned with soft soap and water. The cut surfaces are polished using, in sequential order, 150, 300, 600, and 2000 grit carborundum paper. The specimens are cleaned with soft soap and 100% ethyl alcohol between polishes. Finally, the specimens are mounted on aluminum stubs using carbon-coated tape. The specimens are placed in a humidity-controlled storage container prior to viewing in the SEM.

The analysis is performed using an EDAX PV 9900 EDS mounted on a Philips 515 SEM at an accelerating voltage of 20 kV, working distance between 0.906 and 1.102 in. (23 and 28 mm), tilt of 40°, and take-off angle between 55 and 60°. Specimens are analyzed for iron, silicon, chromium, and magnesium using standardless quantitative analysis (Superquant program 1989).

4.2.3 Structural Analysis

Three bridges designed by the South Dakota Department of Transportation are evaluated for the benefits of using MMFX reinforcing steel in concrete bridge decks in lieu of conventional Grade 60 reinforcing steel. The bridge decks are from the following bridges:

1. Str. No. 52-500-250, ***Prestressed Girder Bridge*** with 8.25-in. deck and girders spaced 8'0" on center.
2. Str. No. 68-120-077, ***Continuous Composite (steel) Girder Bridge*** with 8.25-in. deck and girders spaced 8'11" on center.
3. Str. No. 06-141-150, ***Continuous Concrete Bridge*** with 11-in. deck and 15-in. haunch over bents

The bridges are analyzed according to the design procedures used by the South Dakota Department of Transportation with the 16th edition of AASHTO Standard Specification for

Highway Bridges (1996). Calculation data sheets for the bridge decks that are provided by the South Dakota Department of Transportation (SDDOT) are used to ensure compliance with typical design procedures. The bridge decks on girders are analyzed using working stress design procedures, and the continuous concrete bridge is analyzed using strength design procedures.

Prestressed Girder and Continuous Composite (steel) Girder Bridges—The first two bridge decks are analyzed principally using working stress design procedures with MMFX steel having $f_y = 120$ ksi and $E_s = 29,000$ ksi. The allowable stress in the steel is kept at the code specified 24 ksi (AASHTO 16th ed. 8.15.2.2). Variations of bar sizes and spacings are used to determine if a more economical design could be obtained using MMFX steel.

Seven failure criteria are evaluated for each bridge to determine the adequacy of a selected distribution of reinforcement.

- 1) Maximum allowable stress in the steel (AASHTO 16th ed. 8.15.2.2),
- 2) Maximum allowable stress in the concrete (AASHTO 16th ed. 8.15.2.1.1),
- 3) Maximum allowable spacing of reinforcement (AASHTO 16th ed. 8.21.6),
- 4) Minimum required reinforcement (AASHTO 16th ed. 8.17.1.1),
- 5) Distribution of reinforcement for crack control (AASHTO 16th ed. 8.16.8.4),
- 6) Maximum allowable reinforcement ratio (AASHTO 16th ed. 8.16.3.1.1), and
- 7) Modified flexural strength at least equal to original strength of deck.

Fatigue provisions are not checked because SDDOT does not perform fatigue checks for decks designed using working stress procedures (Gilsrud 2002). Specific calculation procedures are described next. The results of this analysis are presented in Section 5.2.3.

Maximum Allowable Stresses. The allowable stresses in the concrete and steel are calculated for each selected reinforcement configuration as defined by AASHTO 16th ed. 8.15.2.2 and 8.15.2.1.1. For the steel, a maximum allowable tensile stress ($f_{s,max}$) of 24,000 psi is used. For the concrete, the maximum allowable compressive stress ($f_{c,max}$) is defined as

$$f_{c,max} = 0.40 f_c^{\text{c}} \quad (4.2)$$

For a concrete compressive strength (f_c^{c}) of 4500 psi, the maximum compressive stress used in the SDDOT design was reported to be 1450 psi for both bridges. The reduction in allowable concrete compressive stress is based on historical practice at SDDOT and is used to anticipate deterioration in the compression block area due to the use of deicing chemicals (Gilsrud 2002). The maximum allowable compressive stress in the concrete used in the structural analysis is 1450 psi.

Maximum Allowable Spacing. The maximum allowable spacing (s_{max}) as defined by AASHTO 16th ed. 8.21.6 is

$$s_{max} \leq \begin{matrix} 1.5 \times \text{thickness} \\ \text{or} \\ 18 \text{ in.} \end{matrix} \quad (4.3)$$

where the thickness is the total depth of the slab. The maximum allowable spacing is 12 in. for both bridges.

Minimum Required Reinforcement. For any section requiring tensile reinforcement, there is a minimum required amount of reinforcement so that the moment capacity at the section (ϕM_n) must equal or exceed 1.2 times the cracking moment (M_{cr}) calculated for that section [AASHTO 16th ed. 8.17.1.1, Eq. (8-62)].

$$\phi M_n \geq 1.2 M_{cr} \quad (4.4)$$

with ϕ defined to be 0.9 for flexure (AASHTO 16th ed. 8.16.1.2.2). The cracking moment is calculated to be 69 k-in. for both bridge decks using a modulus of rupture of $7.5\sqrt{f'_c}$ (AASHTO 16th ed. 8.15.2.1).

Distribution of Reinforcement for Crack Control. The tension reinforcement must be well-distributed in the bridge decks to control the crack widths. For reinforcement with a yield strength exceeding 40 ksi, bar sizes and spacings must be selected so that the service load stress in the reinforcement (f_s) does not exceed the value computed by [AASHTO 16th ed. 8.16.8.4, Eq. (8-61)]

$$f_s = \frac{z}{(d_c A)^{1/3}} \leq 0.6 f_y \quad (4.5)$$

where A is the effective area in inches of concrete surrounding the flexural tension reinforcement, d_c is the distance from the extreme tension fiber to the center of the closest bar, and z is 130 kips/in. for negative moment steel and 170 kips/in. for positive moment steel. The cover used in the calculation is 2 in. for the negative moment reinforcement (maximum allowable for crack control provisions) and 1 in. for the positive moment reinforcement. The maximum service load moments were provided in the SDDOT calculations.

Maximum Allowable Reinforcement. For each reinforcement configuration, the maximum allowable reinforcement ratio is calculated based on the provisions in AASHTO 16th ed. 8.16.8.4s. The criterion is satisfied with the following condition:

$$\rho \leq \rho_{max} \quad (4.6)$$

where ρ is the reinforcement ratio for the selected configuration, and ρ_{max} is the maximum allowable reinforcement ratio. The maximum allowable reinforcement ratio is defined as three-quarters of the reinforcement ratio that produces a balanced failure condition for the section.

Flexural Strength. For all selected combinations of reinforcement size and spacing, the flexural strengths (strength design) of the new configurations are compared with the original flexural strengths of the decks. The criterion is satisfied if the flexural strength of the new configuration is equal to or greater than the flexural strength of the original configuration. This is never the controlling criterion for determining the adequacy of the design, but indicated the relative effectiveness of the selected reinforcement configuration for strength.

Continuous Concrete Bridge—The continuous concrete bridge is analyzed using strength design. The reinforcement in the bridge deck is replaced with MMFX reinforcing steel having $f_y = 120$ ksi and $E_s = 29,000$ ksi. Variations of bar sizes and spacing are used to determine if a more economical design can be obtained using MMFX steel.

The bridge decks are analyzed using different combinations of MMFX reinforcement and spacing. The designs are checked using six failure criteria.

- 1) Maximum allowable spacing of reinforcement (AASHTO 16th ed. 8.21.6),
- 2) Minimum required reinforcement (AASHTO 16th ed. 8.17.1.1),
- 3) Maximum allowable reinforcement (AASHTO 16th ed. 8.16.3.1.1),
- 4) Distribution of reinforcement for crack control (AASHTO 16th ed. 8.16.8.4)
- 5) Fatigue limits (AASHTO 16th ed. 8.16.8.3), and
- 6) Modified flexural strength at least equal to original strength of deck.

Specific calculation procedures are described next, and results from the analysis are presented in Section 5.2.3.

Maximum Allowable Spacing. The calculation for maximum allowable spacing (s_{max}) is the same as described for the girder bridges [Eq. (4.3)]. The deeper deck sections for the continuous concrete bridge result in larger allowable spacings, 18 in. in the negative moment region and 16 in. in the positive moment region.

Minimum Required Reinforcement. The calculation for minimum required reinforcement at any section is identical to that described above using Eq. (4.4). The cracking moment calculated for the negative moment region with a 15-in. haunch was 226 kip-in. and for the positive moment region with an 11-in. slab was 122 kip-in.

Maximum Allowable Reinforcement. For each reinforcement configuration, the maximum allowable reinforcement ratio is calculated based on the provisions in AASHTO 16th ed. 8.16.8.4. The criterion is identical to the procedure described above using Eq. (4.6).

Distribution of Reinforcement for Crack Control. The calculations for the required distribution of reinforcement for crack control are the same as described above using Eq. (4.5); z is 130 kip/in. for the negative moment steel and 170 kip/in. for the positive moment steel. The cover used in the calculations is 2 in. for the negative moment reinforcement and 1 in. for the positive moment reinforcement. The maximum service load moments were provided in the SDDOT calculations.

Fatigue Limits. Fatigue stress limits in steel are satisfied by limiting the range between the maximum tensile stress and minimum stress in the reinforcement caused by live load plus

impact at service load conditions. This limit is defined in AASHTO 16th ed. 8.16.8.3 by Eq. (8-60) as

$$f_r = 21 - 0.33f_{\min} + 8(r/h) \quad (4.7)$$

where f_r is the stress range in ksi, f_{\min} is the algebraic minimum stress level in ksi (tension positive), and r/h is the ratio of base radius to height of rolled-on transverse deformations (assumed to be 0.3 as allowed by AASHTO). The maximum tensile stress and minimum stress caused by live load plus impact are determined from the SDDOT design calculations. The fatigue limits should not be affected by the change in yield strength of the steel (ACI Committee 215 1992).

Flexural Strength. As described for the previous bridge deck analyses, the flexural strength for the new configurations are compared with the original flexural strength of the deck for all selected combinations of reinforcement size and spacing. The criterion is satisfied if the flexural strength of the new configuration is equal to or greater than the flexural strength of the original configuration. This is never the controlling criterion for determining the adequacy of the design, but indicates the relative effectiveness of the selected reinforcement configuration for strength.

4.3 CORROSION TESTS

Conduct a series of statistically valid comparative tests of corrosion resistance of MMFX Microcomposite steel, ECR, and mild steel reinforcement to determine general corrosion properties both inside and outside concrete, stress, and pitting corrosion properties.

The corrosion resistance of MMFX Microcomposite steel is compared to that of epoxy-coated reinforcement and conventional mild steel reinforcement using rapid macrocell and bench-scale tests. These tests have been shown to provide valid comparisons using realistic exposure conditions. Corrosion performance is evaluated based on relative corrosion rates, changes in corrosion potential, and chloride concentrations needed for corrosion initiation. Pitting corrosion is the dominant form of corrosion in the field and in the current tests.

4.3.1 Rapid Macrocell Tests

The principal comparisons of corrosion response are made using the *rapid macrocell* test, a test originally developed at the University of Kansas under the SHRP program (Martinez et al. 1990, Chappelow et al. 1992) and updated under the NCHRP-IDEA program (Smith et al. 1995, Darwin 1995, Senecal et al. 1995, Darwin et al. 1996) and in the current study. The goal of the technique is to obtain a realistic measure of the performance of corrosion protection systems in a short period of time. The basic test specimen consists of either a bare reinforcing bar or a mortar-wrapped specimen, illustrated in Fig. 4.1. The contact surface between the mortar and the bar simulates the concrete-reinforcing bar interface in actual structures. When epoxy-coated bars are tested, the ends of the bars are protected with a plastic cap filled with epoxy.

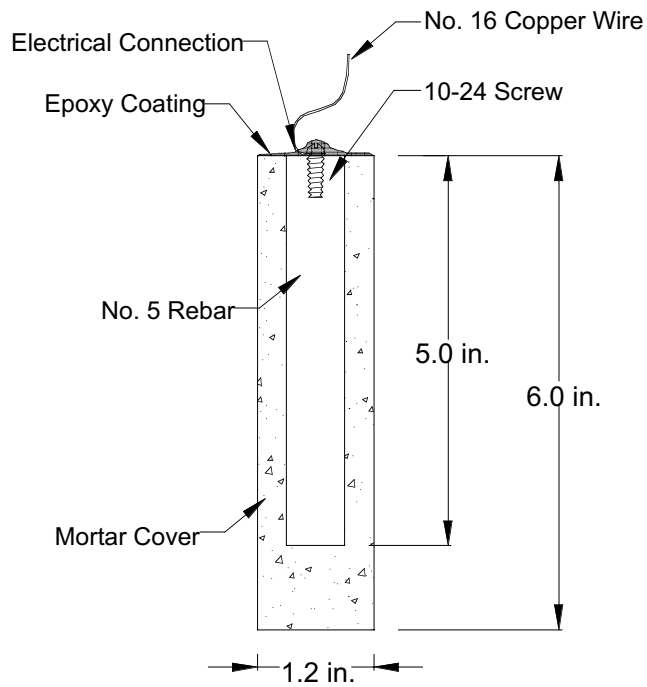


Figure 4.1 - Cross-Section of Mortar-wrapped Test Specimen Used for Rapid Corrosion Macrocell Test

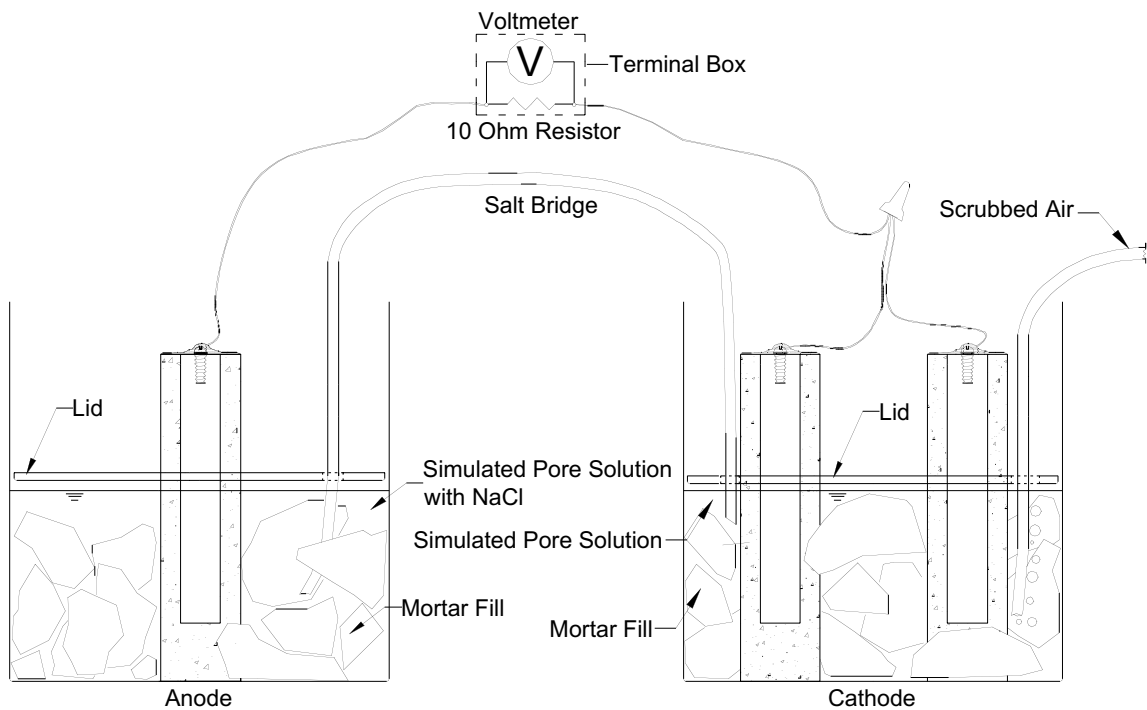


Figure 4.2 - Schematic of Macrocell Test

The macrocell test (Fig. 4.2) requires two containers. The test specimen, either a bare bar or a mortar-wrapped specimen, is placed in a four-quart container, along with simulated pore solution containing a preselected concentration of sodium chloride. Two specimens are placed in a second container and immersed in simulated pore solution (with no chlorides added). Crushed mortar fill is added to containers with mortar-wrapped specimens to more closely simulate the concrete environment. The solution depth places 3 in. of a bar below surface of the liquid. The solutions in the two containers are connected by a salt bridge and the test specimen in the pore solution containing sodium chloride (anode) is electrically connected through a single 10-ohm resistor to the two specimens in the simulated pore solution (cathode). The resistors are mounted in a terminal box to consolidate the specimen wires.

Air (scrubbed to remove CO₂) is bubbled into the liquid surrounding the cathode to ensure an adequate supply of oxygen. The air causes some evaporation, which is countered by adding deionized water to the container to maintain a constant volume of the solution. The corrosion current and the rate of corrosion can be determined by measuring the voltage drop across the resistor. The corrosion rate is calculated by first determining the corrosion current, which is equal to the voltage divided by the resistance. The actual resistance of each 10-ohm resistor is measured separately. Once the current is measured, the corrosion rate, in terms of metal loss, is calculated using Faraday's law.

$$r = \frac{ia}{nFD} \quad (4.8)$$

where r = corrosion rate (thickness loss per unit time), i = current density (amperes/cm² or coulombs/cm² · sec), a = atomic weight (weight of a gram-mole, = 55.84 g for iron), n = number of equivalents exchanged (number of electrons transferred; for Fe⁺⁺ = 2), F = Faraday's Constant = 96500 coulombs/equivalent, and D = density of metal (7.87 g/cm³ for steel).

In terms of current density (i) in $\mu\text{mA}/\text{cm}^2$, r in $\mu\text{m}/\text{yr}$ is

$$r = 11.59i \quad (4.9)$$

The open circuit corrosion potential of the cathode and anode are also measured, using a saturated calomel electrode (SCE). The open circuit is maintained for two hours prior to taking potential readings. Corrosion potential is also used to establish the chloride-to-hydroxyl ion ratios (Cl⁻/OH⁻) at which corrosion is initiated. Corrosion potentials more negative than approximately -275 mV indicate that the metal is corroding. Chloride and hydroxyl ion ratios are obtained using titration procedures.

The simulated pore solution, consisting of sodium hydroxide and potassium hydroxide is based on pore solution analysis (Farzammehr 1985, Farzammehr, Dehghanian and Locke 1987). One quart of the solution contains 0.034 lb of potassium hydroxide (KOH) and 0.037 lb of sodium hydroxide (NaOH). The pH of the solution is 13.4. Most tests in the study use a 1.6 molal (m) ion NaCl solution at the anode. The solution is made using 0.095 lb of NaCl in one quart of simulated concrete pore solution. A limited number of tests use a 6.04 m ion (15%) solution of NaCl to evaluate the performance of the metals at a higher chloride concentration. Epoxy-coated steel is evaluated using specimens in which the coating is breeched by four $\frac{1}{8}$ -inch diameter holes to simulate defects in the epoxy coating.

Specimen Fabrication—No. 5 reinforcing bars are cut with a band saw to a length of five inches. One end of the bar is then drilled and tapped $\frac{1}{2}$ inch to accommodate a No. 10-24 machine screw and the edges of both ends of the bar are belt sanded to grind off sharp edges. Bars are then soaked in acetone to remove grease, dirt, and hydraulic fluid from the surface, and dried at room temperature. The ends of epoxy-coated bars that will be submerged in the macrocell are protected using a plastic cap filled with Herberts O'Brien Rebar Patch Kit epoxy. Some bars in the study are sand blasted, in which case they are cleaned a second time following the sand-blasting operation. Twenty-in. bars are used to evaluate the corrosion performance of bent MMFX bars. After cutting, the bars are bent around a 2 in. diameter pin and then cleaned with acetone. The bars, bend down, are immersed to a depth of 4 in. in the anode solution.

Mortar-wrapped bars are cast in a mold consisting of PVC pipe. The bars are centered using rubber stoppers. As shown in Fig. 4.1, the mortar sheathing covers the exterior surface of the bar and projects one inch past one end of the bar. The mortar has a water-cement ratio of 0.5 and sand-cement ratio of 2.0, and is fabricated using Type I portland cement, distilled water, and ASTM C 778 graded Ottawa sand. The mix proportions represent the mortar constituent of concrete. The mortar is mixed following the procedures outlined in ASTM C 305. Mortar is placed in the cylindrical mold in four layers. Each layer is rodded 25 times using a $\frac{1}{8}$ -inch diameter rod, followed by external vibration for 30 seconds using a vibration table with an amplitude of 0.006 in. and a frequency of 60 Hz.

Specimens are cured in the molds for 24 hours. Specimens are then removed from the molds and cured in lime $[\text{Ca}(\text{OH})_2]$ saturated water (pH = 12.5) for 13 days. After 14 days of curing, the specimens are vacuum dried for one day. For both bare and mortar-wrapped bars, a 16-gauge copper electrical wire is secured to the tapped end of each specimen with a 10-24 steel screw. The top of the screw wire and mortar are then coated with two layers of Herberts O'Brien epoxy for bare bars and two layers of Ceilgard 615 epoxy, produced by Ceilcote, for mortar-wrapped bars.

Test Program—The rapid macrocell test program, summarized in Table 4.2, consists of a total of 68 individual tests in 14 series. The tests evaluate both bare and mortar-wrapped specimens. Most bar specimens and all mortar-wrapped specimens were subjected to a 1.6 m ion NaCl solution. The bare specimen tests consisted of conventional steel, MMFX as delivered (2 series), MMFX sand blasted, and MMFX bent. In addition, one series of bare conventional bars

and one series of MMFX sand-blasted bars were subjected to a 6.04 (15%) m ion NaCl solution. Two series of bare No. 6 MMFX bars were subjected to a 1.6 m ion solution. Mortar-wrapped tests were used to evaluate conventional, MMFX, and epoxy-coated reinforcing steel. In addition, two series of three tests each were used to evaluate the performance of MMFX when combined with conventional steel, one series with MMFX steel as the anode and one series with MMFX as the cathode. Macrocell tests continue for a minimum of 15 weeks, with readings obtained daily for the first week and weekly thereafter. The results of the tests are presented in Section 5.3.1.

Table 4.2 - Rapid macrocell test program

Steel Designation	Heat No.	NaCl concentration	# of tests	Notes
Bare specimens				
N3 ¹	S44407	1.6 m	6	
MMFX(1) ²	810737	1.6 m	6	Lid above bars
MMFX(2)	810737	1.6 m	6	
MMFXs	810737	1.6 m	6	Sandblasted bars
MMFXb	810737	1.6 m	3	Bent bars at anode
MMFX#6(1)	810737	1.6 m	3	
MMFX#6(2)	710788	1.6 m	3	
N2h ¹	K0-C696	6.04 m	5	
MMFXsh	810737	6.04 m	6	Sandblasted bars
Mortar-wrapped specimens				
N3m	S44407	1.6 m	6	
MMFXm	810737	1.6 m	6	
ECRm ³	S44407	1.6 m	6	
MMFX/N3	810737/S44407	1.6 m	3	
N3/MMFX	S44407/810737	1.6 m	3	

¹ N2 and N3: Conventional, normalized A 615 reinforcing steel

² MMFX: MMFX Microcomposite steel

³ ECR: Epoxy coated N3 steel

4.3.2 Bench-Scale Tests

During the past two decades, bench-scale tests, such as the Southern Exposure, ASTM G 109, and cracked beam tests, have been used most often to evaluate the corrosion performance of reinforcing steel. Although these tests typically require one to two years for completion, they qualify as accelerated tests, considering that the service life of actual structures should be 30+

times as long. Of these tests, the Southern Exposure and cracked beam tests have proven to give the most useful data and are used in this study.

Southern Exposure Test — The specimen used for the *Southern Exposure*, or SE, test (Pfeifer and Scali 1981) consists of a small slab containing two mats of reinforcing steel (Fig. 4.3). A dam is cast integrally with the slab to retain liquid on the upper surface. The top mat of reinforcement consists of two bars; the bottom mat consists of four bars. The mats are connected electrically across a 10-ohm resistor and the sides of the concrete are sealed with epoxy (Ceilgard 615). A 15% sodium chloride solution is placed inside the dam, allowing chlorides to penetrate into the concrete. The slabs are subjected to a seven day alternate ponding and drying regime, with ponding at 68-84°F for four days and drying at 100°F for three days. The ponding and drying regime is continued for 12 weeks. The specimens are then subjected to continuous ponding for 12 weeks, at which time the alternating ponding and drying regime begins again. The two regimes are continued for 96 weeks. Corrosion current and the corresponding corrosion rates are determined by measuring the voltage drop across the resistor. The corrosion potential for top and bottom mats and mat-to-mat resistance are also measured. The test provides a very severe corrosion environment that is believed to simulate 30 to 40 years of exposure for bridges within a 48-week period (Perenchio 1992). To obtain an estimate of the chloride concentration required for corrosion initiation, chloride samples are taken at the level of the top reinforcing bars (1 in. below the top surface) at the initiation of corrosion.

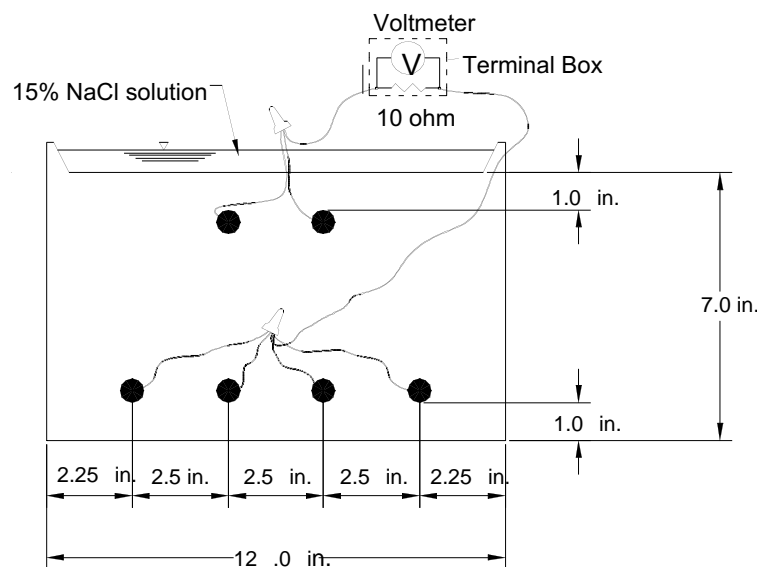


Figure 4.3 - Test Specimen for Southern Exposure Test

The Southern Exposure specimens are fabricated in an inverted position. The concrete is consolidated in two layers. Each layer is vibrated for 30 seconds on a vibrating table with an amplitude of 0.006 in. and a frequency of 60 Hz. The concrete mix proportions (Table 4.3) match those used in on-going studies at the University of Kansas and are selected to provide an objective comparison between the different systems. The concrete has a water-cement ratio of 0.45 and an air content of 6%. The specimens are wet cured for three days (one day in the form and two days in a plastic bag with deionized water) and then air cured until the test begins at 28 days. The top surface of the concrete is sanded lightly prior to initiation of the tests.

Table 4.3 - Concrete properties and mix proportions, cubic yard basis

Cement	599 lb
Water	269 lb
Fine aggregate ¹	1436 lb
Coarse aggregate ²	1473 lb
Air-entraining agent	70 mL
Slump	3.0 in.
Air content	6.0 %
Unit weight	139.9 lb/ft ³ (3777 lb/yd ³)

¹ S.G.(SSD) = 2.60, absorption = 0.78%, fineness modulus = 2.51

² S.G.(SSD) = 2.58, absorption = 2.27%, unit weight = 95.9 lb/ft³,
3/4 in. nominal maximum size

Cracked Beam Test — The *cracked beam* specimen (Fig. 4.4) is used to model the corrosion of reinforcing steel in concrete where cracks directly expose the steel to deicing chemicals. The specimen is half the width of the SE specimen, with one bar on top and two bars on the bottom. A crack is simulated parallel to and above the top reinforcing bar through the insertion of a 0.012 in. (0.3mm) stainless steel shim when the specimen is fabricated. The shim is removed within 24 hours of placement, leaving a direct path for chlorides to the reinforcing steel and simulating the effects of a settlement crack over the bar. Like the SE specimen, the cracked beam specimen is subjected to cycles of wetting and drying with a 15% sodium chloride solution, continuing up to 96 weeks. For conventional steel, the SE and cracked beam specimens typically exhibit corrosion initiation during the first eight weeks.

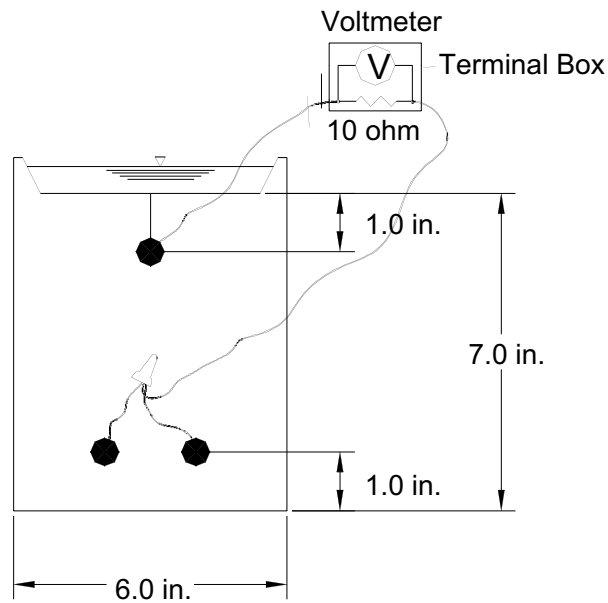


Figure 4.4 - Test Specimen for Cracked Beam Test

Test Program — The bench-scale test program, summarized in Table 4.4, consists of 27 Southern Exposure and 18 cracked beam tests. Six each Southern Exposure and cracked beam tests are used to evaluate straight MMFX, conventional, and epoxy-coated reinforcing steel. Three Southern Exposure tests were used to evaluate bent MMFX bars (pin diameter = $1\frac{7}{8}$ in.). Three additional Southern Exposure tests are used for each of two configurations combining MMFX Microcomposite steel and conventional steel to evaluate galvanic effect. For three of the specimens, conventional steel is used as the top mat, with MMFX steel as the bottom mat; in the other three specimens, the position of the steels is reversed.

For tests of epoxy-coated bars, the coating is breached by four $\frac{1}{8}$ -inch diameter holes on each bar, to simulate defects in the epoxy coating. The bottom mat of bars in these tests consists of uncoated steel from the same heat as used for the epoxy-coated bars.

The results for the first 23 weeks of the bench-scale tests are presented in Section 5.3.2. The results for the full duration of the tests will be provided in separate reports.

Table 4.4 - Bench-scale test program

Steel Designation	Heat No.	# of tests	Notes
Southern Exposure (SE) Tests			
N3(1) ¹	S44407	4	
N3(2)	S44420	2	
MMFX ²	810737	6	
MMFXb	810737	3	Bent bars at anode
MMFX/N3	810737/S44420	3	MMFX top bars
N3/MMFX	S44420/810737	3	N3 top bars
ECR(1) ³	S44407	4	
ECR(2) ³	S44420	2	
Cracked Beam (CB) Tests			
N3(1) ¹	S44407	4	
N3(2)	S44420	2	
MMFX	810737	6	
ECR(1)	S44407	4	
ECR(2)	S44420	2	

¹ N2 and N3: Conventional, normalized A 615 reinforcing steel

² MMFX: MMFX Microcomposite steel

³ ECR: Epoxy coated N3 steel

4.4 CORROSION EFFECTS

Analyze corrosion effects on MMFX Microcomposite steel and ECR using scanning electron microscopy.

The nature of the steel surface on both bare and mortar-embedded bars after completion of the macrocell tests is evaluated using a Phillips 515 scanning electron microscope (SEM). The technique used follows that developed by Axelsson, Darwin, and Locke (1999).

As the macrocell tests are discontinued, specimens are tagged for identification purposes. A visual inspection is made of the steel surface, epoxy coating, and the mortar cover. For wrapped specimens, the mortar is removed following an evaluation of the intact specimen and mortar pieces are examined for voids. The nature of surface damage and corrosion products are evaluated. The bar surface is examined with a light microscope, providing information for the selection of areas on the specimen to be examined further using the SEM. A hacksaw is used to obtain reinforcing bar slices of the proper size for SEM imaging.

Prior to SEM analysis, cut pieces of steel are mounted with conductive double-sided sticky carbon tabs on aluminum stubs. Conductive carbon paint is used to provide a good

conductive path from the top of the specimen to the stub. An Anatech Hummer X sputter coater is used to coat the specimens with a 10-20 nm thick layer of gold palladium to prevent charging.

Specimens are examined using secondary electron imaging to record surface morphology. Images were recorded using an ELMDAS digital image acquisition system at an accelerating voltage of 20 kV with a spot size of 20 nm at a pixel density of 512 in both the vertical and horizontal directions.

The results of the analysis are presented in Section 5.4.

4.5 LIFE EXPECTANCY AND COST EFFECTIVENESS

Estimate life expectancy and cost effectiveness of MMFX Microcomposite steel, ECR, and mild steel reinforcement in South Dakota.

The life expectancy and cost effectiveness of bridges containing MMFX Microcomposite, ECR, and conventional steel reinforcement are determined based on the experience of the Department of Transportation in South Dakota (Gilsrud 2002) and other states (Kepler, Darwin, and Locke 2000) in conjunction with the laboratory results obtained in this study.

4.5.1. Life Expectancy

The life expectancy of bridges constructed with different steel reinforcing systems is estimated based on both experience and analysis. In South Dakota, bridges containing epoxy-coated reinforcement, dating to the late 1970s, have never required repair due to corrosion-induced damaged (Gilsrud 2002). This is similar to the experience in Kansas (Kepler et al. 2000). Engineers in the two states estimate time to first repair for epoxy-coated reinforcement as 40 and 30 years, respectively. Both figures are used in the current study for comparison. An analytical estimate of life expectancy is obtained based on estimates of the time required for corrosion initiation and subsequent period required to cause delamination cracking due to corrosion. The time to corrosion initiation is estimated using chloride concentrations measured at crack locations on bridge decks (Miller and Darwin 2000) and chloride concentrations at corrosion initiation, as measured in the current study. Prior research has demonstrated that chloride concentrations between 1.0 and 1.4 lb/yd³ will result in corrosion initiation for conventional uncoated reinforcement and epoxy-coated reinforcement for which the coating has been damaged. In contrast, stainless steel exhibits values on the order of 18 to 30 lb/yd³ (McDonald, Pfeifer, and Sherman 1998). Time to delamination cracking induced by corrosion is estimated based on the rate of corrosion measured in the current study and an estimate that a thickness loss of 0.025 mm (0.00098 in.) will result in a volume of corrosion products that will crack concrete (Pfeifer 2000).

4.5.2 Cost Effectiveness

Life Cycle Cost Analysis — A 75-year economic life is used to compare the current costs associated with using conventional, epoxy-coated, and MMFX reinforcement in South Dakota

bridge decks. An 8.5-in. bridge deck is used in the analysis including the costs associated with a new bridge deck and repair costs over the 75-year life of the bridge. Initial construction and repair costs were obtained from SDDOT (Gilsrud 2002). The cost of MMFX steel was obtained from the MMFX Steel Corporation of America (Cano 2002).

Repair Costs — Repair costs for a “typical” 8.5-in. bridge deck were obtained from SDDOT. Current data includes repair of bridge decks with conventional reinforcement only because the bridge decks constructed since the late 1970s have been constructed using epoxy-coated reinforcement and have not needed repair as of the date of this report. It is estimated that repair costs of bridge decks with epoxy-coated reinforcement and MMFX reinforcement will be similar to those for decks with conventional reinforcement.

The repair costs are based on an average of costs for previous bridge deck repair projects through the end of the year 2001. A “typical” repair project includes costs for removing deleterious concrete and replacing with a low-slump dense concrete overlay, bridge rail modifications, approach guard rail replacement, approach pavement work, mobilization, traffic control and other miscellaneous costs. Costs were determined per square yard considering a typical bridge deck as described by SDDOT (Gilsrud 2002) with a width of 36 ft and a total length of 150 ft. A summary of the repair costs and conversion to \$/yd² are shown in Table 4.5 and described in Eqs. (4.10)-(4.15). User costs are difficult to quantify and are not included in this analysis.

Table 4.5 - Repair costs for bridge decks in South Dakota (Gilsrud 2000)

Item	Unit	Cost	Cost/yd ²
Low Slump Dense Concrete Overlay	Per yd ²	\$80.00	\$80
Bridge Rail Modification	Per linear ft	\$45.25	\$23
Approach Guard Rail	Lump sum	\$16,000.00	\$27
Approach Pavement Work	Lump sum	\$16,500.00	\$28
Mobilization	Lump sum	\$18,600.00	\$31
Traffic Control and Misc.	Lump sum	\$9,000.00	\$15
Total Repair Costs			\$204

Bridge Rail Modification

$$\frac{\$45.25}{\text{ft}} \times \frac{2 \text{ sides}}{\text{bridge}} \times \frac{1}{36 - \text{ft deck width}} \times \frac{9 \text{ ft}^2}{\text{yd}^2} = \$23/\text{yd}^2 \quad (4.10)$$

Approach Guard Rail

$$\frac{\$16,000}{\text{project}} \times \frac{\text{typical bridge}}{5,400 \text{ ft}^2} \times \frac{9 \text{ ft}^2}{\text{yd}^2} = \$27/\text{yd}^2 \quad (4.11)$$

Approach Pavement Work

$$\frac{\$16,500}{\text{project}} \times \frac{\text{typical bridge}}{5,400 \text{ ft}^2} \times \frac{9 \text{ ft}^2}{\text{yd}^2} = \$28/\text{yd}^2 \quad (4.12)$$

Mobilization

$$\frac{\$18,600}{\text{project}} \times \frac{\text{typical bridge}}{5,400 \text{ ft}^2} \times \frac{9 \text{ ft}^2}{\text{yd}^2} = \$31/\text{yd}^2 \quad (4.13)$$

Traffic Control and Misc.

$$\frac{\$9,000}{\text{project}} \times \frac{\text{typical bridge}}{5,400 \text{ ft}^2} \times \frac{9 \text{ ft}^2}{\text{yd}^2} = \$15/\text{yd}^2 \quad (4.14)$$

Total repair costs = Total overlay deck + bridge rail modification + approach guard rail + mobilization + traffic control and misc.

$$\begin{aligned} &= \$80/\text{yd}^2 + \$23/\text{yd}^2 + \$27/\text{yd}^2 + \$28/\text{yd}^2 + \$31/\text{yd}^2 + \$15/\text{yd}^2 \\ &= \$204/\text{yd}^2 \end{aligned} \quad (4.15)$$

New Bridge Deck Costs — Current costs for new bridge decks were calculated considering the in-place costs of concrete and the various types of reinforcing steel. The costs were calculated for a “typical” 8.5-in. bridge deck using conventional, epoxy-coated, and MMFX reinforcement. The in-place costs for the concrete, conventional and epoxy-coated reinforcement were obtained from SDDOT. In-place costs for MMFX reinforcement were estimated considering a base cost of \$0.40/lb and placement costs of \$0.44/lb.

All in-place costs considered in the analysis are listed in Table 4.6. The calculations for cost/yd² are shown in Eqs. (4.16)-(4.20). The reinforcement costs were calculated considering an average amount of reinforcement of 210 lb/yd³ (Gilsrud 2002).

Table 4.6 – Bridge deck construction costs in South Dakota (Gilsrud 2000)

Item	In-place Cost	Cost/yd ²
Concrete	\$350/yd ³	\$82.6
Conventional steel	\$0.59/lb	\$29.3
Epoxy-coated steel	\$0.60/lb	\$29.8
MMFX steel	\$0.84/lb	\$41.7

Concrete

$$\frac{\$350}{\text{yd}^3} \times \frac{8.5 \text{ in.}}{\text{typical deck}} \times \frac{\text{yd}}{36 \text{ in.}} = \$82.6/\text{yd}^2 \quad (4.16)$$

Typical Amount of Reinforcement

$$\frac{210 \text{ lb}}{\text{yd}^3} \times \frac{8.5 \text{ in.}}{\text{typical deck}} \times \frac{\text{yd}}{36 \text{ in.}} = 49.6 \text{ lb}/\text{yd}^2 \quad (4.17)$$

Conventional Steel

$$\frac{\$0.59}{\text{lb}} \times \frac{49.6 \text{ lb}}{\text{yd}^2} = \$29.3/\text{yd}^2 \quad (4.18)$$

Epoxy-Coated Steel

$$\frac{\$0.60}{\text{lb}} \times \frac{49.6 \text{ lb}}{\text{yd}^2} = \$29.8/\text{yd}^2 \quad (4.19)$$

MMFX Steel

$$\frac{\$0.84}{\text{lb}} \times \frac{49.6 \text{ lb}}{\text{yd}^2} = \$41.7/\text{yd}^2 \quad (4.20)$$

Calculations for current costs for a new deck using the various options of reinforcement are shown in Eqs. (4.21)-(4.23).

Conventional Steel

$$8.5\text{-in. Concrete Deck} + \text{Conventional Steel} = \$82.6/\text{yd}^2 + \$29.3/\text{yd}^2 = \$111.9/\text{yd}^2 \quad (4.21)$$

Epoxy-Coated Steel

$$8.5\text{-in. Concrete Deck} + \text{Epoxy-Coated Steel} = \$82.6/\text{yd}^2 + \$29.8/\text{yd}^2 = \$112.4/\text{yd}^2 \quad (4.22)$$

MMFX Steel

$$8.5\text{-in. Concrete Deck} + \text{MMFX Steel} = \$82.6/\text{yd}^2 + \$41.7/\text{yd}^2 = \$124.3/\text{yd}^2 \quad (4.23)$$

Comparisons with KDOT Cost Analysis — Results from a cost-analysis of various corrosion-protection systems for the Kansas Department of Transportation (Kepler et al. 2000) are presented for the purpose of comparison with the SDDOT cost-analysis.

Repair costs were tabulated considering data from 27 bridge deck repair projects in Kansas for 1999. From the records it was determined that 22% of the bridge decks received

partial-depth repairs and 6% received full-depth repairs. Standard repair practice for KDOT is to place a silica fume overlay over the deck as part of the repair procedure.

The repair costs are separated into material and incidental costs. The incidental costs represented a large portion of the total cost and included mobilization, traffic control, and repairs and improvements to other part of the bridge including drains, barrier rails, and approaches. Average costs were calculated for the study from the bid tabulations of the 27 repair projects. The calculation of the average repair cost used for comparison is shown with Eq. (4.24). User costs are not included in the analysis.

$$\begin{aligned}
 \text{Deck repair} &= 22\% \text{ partial depth} + 6\% \text{ full depth} + \text{machine} \\
 \text{(no overlay on original deck)} &\text{ preparation} + \text{silica fume overlay} + \text{incidental costs} \\
 &= \$159/\text{yd}^2 \times 0.22 + \$223/\text{yd}^2 \times 0.06 + \$18/\text{yd}^2 + \\
 &\quad \$45/\text{yd}^2 + \$105/\text{yd}^2 \\
 &= \$216/\text{yd}^2
 \end{aligned} \tag{4.24}$$

Current costs for the KDOT study were calculated for a number of corrosion protection systems. For the purposes of comparison with this study, and 8.5-in. bridge deck using conventional steel and epoxy-coated steel were considered. In-place costs for concrete, conventional and epoxy-coated steel used in the analysis were \$355/yd³, \$0.59/lb, and \$0.66/lb respectively. An average of 241 lb/yd³ of reinforcement was used to calculate the current cost for the typical bridge decks. Calculations are shown in Eqs. (4.25)-(4.28).

Concrete

$$\frac{\$325}{\text{yd}^3} \times \frac{8.5 \text{ in.}}{\text{typical deck}} \times \frac{\text{yd}}{36 \text{ in.}} = \$76.7/\text{yd}^2 \tag{4.25}$$

Typical Amount of Reinforcement

$$\frac{241 \text{ lb}}{\text{yd}^3} \times \frac{8.5 \text{ in.}}{\text{typical deck}} \times \frac{\text{yd}}{36 \text{ in.}} = 56.9 \text{ lb}/\text{yd}^2 \tag{4.26}$$

Conventional Steel

$$\frac{\$0.59}{\text{lb}} \times \frac{56.9 \text{ lb}}{\text{yd}^2} = \$33.6/\text{yd}^2 \tag{4.27}$$

Epoxy-Coated Steel

$$\frac{\$0.66}{\text{lb}} \times \frac{56.9 \text{ lb}}{\text{yd}^2} = \$37.6/\text{yd}^2 \quad (4.28)$$

Calculations for current costs for a new deck using the various options of reinforcement are shown in Eqs. (4.29) and (4.30).

Conventional Steel

$$8.5\text{-in. Concrete Deck} + \text{Conventional Steel} = \$76.7/\text{yd}^2 + \$33.6/\text{yd}^2 = \$110.3/\text{yd}^2 \quad (4.29)$$

Epoxy-Coated Steel

$$8.5\text{-in. Concrete Deck} + \text{Epoxy-Coated Steel} = \$76.7/\text{yd}^2 + \$37.6/\text{yd}^2 = \$114.3/\text{yd}^2 \quad (4.30)$$

The costs for new deck construction for Kansas, \$110.30/yd² and \$114.30/yd² for bridge decks containing conventional and epoxy-coated steel, respectively, based on KDOT figures, match closely with the respective values obtained by SDDOT \$111.90/yd² and \$112.40/yd².

CHAPTER 5

FINDINGS AND CONCLUSIONS

5.1 LITERATURE SEARCH

There are no published papers on MMFX Microcomposite steel describing its mechanical or corrosion-resistant properties. However, the MMFX Steel Corporation of America has had tests performed at laboratories throughout the U.S. and has made those test results available to the University of Kansas and, more recently, to the members of ASTM Subcommittee A01.05. Most of the results pertain to the mechanical properties of the steel and only very limited information has been provided on its corrosion properties. This information is summarized next.

5.1.1 Mechanical Properties

Yield strength, tensile strength, and elongation at failure of both reduced section and as-delivered reinforcing bars have been measured. Bars have been subjected to the ASTM A 615 bend test. Material toughness has been measured using a Charpy V-notch bend test and the fatigue properties of reduced section bars have been measured.

Most of the mechanical tests were tensile tests on specimens with reduced cross sections. Elongations were measured over 1 or 1.4 in. gauge lengths. The lack of a well-defined yield plateau required that the yield strengths be obtained based on the 0.2% offset method. The reported yield strengths range from 119 to 133 ksi, while the tensile strengths range from 180 to 186 ksi. Elongations range from 13 to 18% based on the short gauge lengths. This is in contrast to the requirement in ASTM A 615 to use an 8 in. gauge length to measure elongation. Eight tests of full-sized No. 6 bars produced tensile strengths between 181 and 184 ksi (yield strengths were not reported) and elongations between 7.6 and 10.6% over an 8 in. gauge length. Tests of full-sized No. 5, No. 8, and No. 9 bars were run by a second laboratory. The No. 5 bars had yield strengths of 120 to 139 ksi, tensile strengths between 177 and 181 ksi, and elongations between 12 and 15%; the No. 8 bars had yield strengths between 126 and 129 ksi, tensile strengths of about 183 ksi, and elongations between 8 and 9%; and the No. 9 bars had yield strengths between 125 and 129 ksi, tensile strengths between 179 and 184 ksi, and elongations between 2.3 and 9.6%. In the latter case, however, only one bar exhibited the 2.3% elongation, with the next lowest value equal to 5.6% (two test results). With the exception of the three tests with elongations below 7% for the No. 9 bars, the test results of the full-sized bars met the elongation criteria for ASTM A 615 Grade 75 reinforcement (7% for No. 6-No. 8 bars and 6% for No. 9-No. 18 bars — ASTM A 615 has no criteria for No. 5 and smaller bars in Grade 75).

The Charpy V-notch test (ASTM E 23) was performed for MMFX Microcomposite steel and A 615 steel. The MMFX bars were subjected to temperatures between -140 and 120°F, while the ASTM A 615 bars were subjected to temperatures between 0 and 120°F. The MMFX steel exhibited significantly higher toughness than the A 615 steel; at -60°F the MMFX steel was tougher than the A 615 steel was at 120°F. These values demonstrate that MMFX steel is a

superior material where impact resistance is required. Such a property is not particularly important for concrete reinforcement, but may prove to be highly useful if the steel is used for attaching sections of precast concrete.

Tests of reduced section bars demonstrated that MMFX steel is better than A 615 steel in fatigue. The tests, however, are not useful in evaluating the fatigue life of reinforcing bars, which depends more on bar geometry than on tensile strength and is not well correlated to the fatigue behavior of smooth specimens (ACI Committee 215 1992).

5.1.2 Corrosion Tests

The information provided by MMFX Steel Corporation of America on the corrosion properties of MMFX Microcomposite steel is limited to a single comparison test between A 615 and MMFX steel in an anodic polarization test. In the 20-day test, one sample of each steel was subjected to an electrical current. The MMFX steel exhibited virtually no corrosion after 20 days, while the A 615 steel exhibited extensive corrosion. This accelerated test has proven to be useful as an indication of the corrosion performance of some metals. However, it does not represent the type of corrosion to which reinforcing steel is exposed in highway structures.

5.2 PHYSICAL AND MECHANICAL TESTS

The work reported in this section demonstrates that MMFX Microcomposite steel has considerably higher tensile and yield strengths, but lower elongations than conventional reinforcement. Measurements of reinforcing bar geometry indicate that MMFX steel will provide bond strengths similar to that of conventional reinforcement, and structural analyses performed on three bridges indicate that MMFX Microcomposite steel is less than an ideal replacement for conventional steel if current design criteria (AASHTO 1996) are followed.

5.2.1 Mechanical Tests and Bar Geometry

Mechanical Tests — The results of the mechanical tests are presented in Table 5.1 and include yield strength, tensile strength, elongation, and bend test results. Yield strengths are measured based on a well-defined yield point for conventional steel and based on the 0.2% offset method and 0.7% total strain for MMFX steel. Data is reported for No. 4, No. 5, and No. 6 conventional bars and No. 5 and No. 6 MMFX Microcomposite steel bars. As pointed out in Chapter 4, one of the two groups of No. 6 MMFX bars was manufactured from the same heat as the single group of No. 5 bars.

The results for the conventional steel are as expected. Average yield strengths for individual heats range from a low of 66.7 ksi for a heat of No. 4 bars to a high of 74.1 ksi for a heat of No. 6 bars. Average tensile strengths range from 108.7 to 118.4 ksi. Average elongations range from 13.6 to 16.8%, with a low value of 10.9%.

Table 5.1 – Mechanical test results

Steel	Heat No.	Size	Sample Number	Yield Strength		Tensile Strength (ksi)	Elongation % in 8 in.	Bending
N3 ¹	S46753	No. 4	1	65.5		106.4	14.1	Pass
			2	66.0		108.4	12.5	
			3	68.7		111.4	12.5	
			Average	66.7		108.7	13.0	
N3	S46757	No. 4	1	72.7		114.7	12.5	Pass
			2	69.1		111.3	12.9	
			3	69.0		111.5	15.6	
			Average	70.3		112.5	13.7	
N3	S46760	No. 4	1	71.9		111.5	12.5	Pass
			2	70.0		110.9	10.9	
			3	69.3		110.3	13.3	
			Average	70.4		110.9	12.2	
N3	S44407	No. 5	1	68.2		110.5	16.4	Pass
			2	67.0		108.5	15.6	
			3	66.8		108.3	14.8	
			Average	67.3		109.1	15.6	
N3	S44420	No. 5	1	68.1		113.1	12.5	Pass
			2	68.2		110.9	15.6	
			3	69.8		114.7	14.1	
			Average	68.7		112.9	14.1	
N3	S47695	No. 6	1	74.2		118.8	14.1	Pass
			2	74.7		119.2	12.5	
			3	73.2		117.2	14.1	
			Average	74.0		118.4	13.6	
N3	S47790	No. 6	1	73.7		115.6	12.9	Pass
			2	74.9		117.6	14.1	
			3	73.9		115.8	18.8	
			Average	74.1		116.3	15.3	
N3	S47814	No. 6	1	68.6		110.1	18.4	Pass
			2	69.5		111.1	16.4	
			3	68.9		110.2	15.6	
			Average	69.0		110.5	16.8	
				0.2% offset	0.7% total strain			
MMFX ¹	810737	No. 5	1	113.9	118.8	158.7	7.0	Pass
			2	124.6	125.6	161.5	6.6	
			3	116.4	126.0	161.5	7.8	
			4	114.0	119.3	157.8	8.5	
			5	128.9	114.8	161.3	6.3	
			Average	119.6	120.9	160.2	7.2	
MMFX	810737	No. 6	1	150.4	149.1	174.1	6.3	Pass
			2	134.0	136.6	173.5	7.8	
			3	125.7	131.6	173.5	7.0	
			4	149.1	148.0	171.5	6.6	
			5	149.0	148.0	172.6	7.0	
			Average	141.6	142.7	173.1	7.0	
MMFX	710788	No. 6	1	131.3	134.1	163.5	7.8	Pass
			2	132.9	134.1	166.5	7.8	
			3	131.9	133.5	163.8	6.3	
			4	121.2	127.4	162.6	7.0	
			5	145.0	146.3	166.6	6.6	
			Average	132.5	135.1	164.6	7.1	

The No. 5 MMFX bars had an average yield strength (based on the 0.2% offset method) of 119.5 ksi, compared to values of 141.6 and 132.5 ksi for the two No. 6 bar heats. If a strain of 0.7% is used, a value that is specified as an alternative to that obtained using the 0.2% offset method in ASTM A 722 for high-strength steel bars for prestressing steel, yield strengths increase slightly, to 120.9, 142.7, and 135.1 ksi. Tensile strengths for the three groups were 160.2, 173.1, and 164.6 ksi, respectively. Average elongations for an 8-in. gauge length vary within a narrow range. Average values for the three groups are 7.2, 7.0, and 7.1%, respectively, with a low value of 6.3% for an individual test. A minimum elongation of 7% is required for Grade 75 ASTM A 615 No. 6 bars, the smallest size specified for Grade 75. All conventional and MMFX bars passed the bend test.

The lower elongations obtained with MMFX steel are expected for high-strength steels. The tensile and yield strengths of MMFX steel are closer to those specified for high-strength steel bars for prestressing concrete (ASTM A 722) than they are to conventional reinforcement (ASTM A 615). The tensile strengths exceed the 150 ksi minimum required for A 722 bars. The yield strengths, based on 0.7% total strain, of the individual No. 6 bars meet the minimum requirements for both Type I and Type II bars, which are set at 85% (127.5 ksi) and 80% (120 ksi), respectively, of the minimum tensile strength. The average value for No. 5 bars (120.9 ksi) meets the criterion for Type II bars. Some individual No. 5 bar tests, however, fall below the requirements for Type II bars. ASTM A 722 also allows the use of the 0.2% offset method. Values obtained with this procedure, however, consistently satisfy only the Type II bar criteria, and only for the No. 6 bars. Values as low as 113.9 ksi for No. 5 bars would not be acceptable. The test results indicate that, with careful quality control, the bars could be used under the provisions of ASTM A 722.

Bar Geometry — Table 5.2 summarizes the geometric properties of the bars. The bars satisfy the criteria in ASTM A 615. Rib heights exceed the minimums of 0.028 and 0.038 in. for No. 5 and No. 6 bars, respectively. Average rib spacings are below the maximum allowable values of 0.437 and 0.525, respectively. As shown in Table 5.2, the relative rib areas, calculated using Eq. (4.1), are within or above the range obtained for most U.S. reinforcing bars. The values 0.063, 0.066, and 0.088 compare favorably to typical values (between 0.06 and 0.085). Bars with relative rib areas within and above the normal range will provide fully satisfactory bond strengths with concrete (Darwin and Graham 1993, Darwin et al. 1996a, 1996b, Zuo and Darwin 2000).

Table 5.2 – Geometrical properties of MMFX reinforcing bars

Bar Size	Heat No.	Average Rib Height (in.)	Average Rib Spacing (in.)	Relative Rib Area
No. 5	810737	0.032	0.450	0.063
No. 6	810737	0.038	0.514	0.066
No. 6	710788	0.051	0.520	0.088

5.2.2 X-Ray Microanalysis

X-ray microanalyses were performed on one heat of conventional steel and all three groups of MMFX Microcomposite steel. The results for Fe, Cr, Si, and Mn are shown in Table 5.3. The variations in the individual constituents are fully within the scatter expected for a high quality x-ray microanalysis. The differences between the chemistry reported by the mill (Table 4.1b) and that obtained by x-ray microanalysis is expected because of differences in the analysis techniques. The results shown in Table 5.3 demonstrate that the chemistry of MMFX steel is consistent for bars within the same heat and very close for the two heats analyzed.

5.2.3 Structural Analysis of Three Typical SDDOT Bridge Decks Using MMFX Steel

The structural analyses of the three bridge decks described in Section 4.2.3 are summarized in Tables 5.4-5.9. The results are presented as either “ok,” indicating that all design criteria are satisfied, or “NG” indicating that at least one design criterion was not met. The results for the individual criteria are also presented in the table. Separate tables are provided for the negative and positive moment regions for each bridge deck. The original design provided by SDDOT is listed as the first entry in each table. As pointed out in Section 4.2.3, working stress design was used for the first two decks and strength design was used for the third deck. Tabulated calculations for each selection of MMFX reinforcement configuration are presented in Tables A.1–A.6 in Appendix A.

Prestressed Girder Bridge Results — The results for the prestressed girder bridge structural analysis are shown in Tables 5.4 and 5.5. Using No. 5 MMFX reinforcement spaced at 7 in. in the top mat of steel is the only viable option in the negative moment region. The bottom mat can be reinforced using No. 5 MMFX reinforcement spaced at 6, 7, or 8 in.

Negative moment region. Table 5.4 presents the analysis for the negative moment region using primarily working stress design criteria. The original design used No. 5 Grade 60 steel at 6-in. spacing. Substituting No. 5 MMFX steel at the same spacing produces an over-reinforced section. Using No. 5 MMFX at 7-in. spacing is the only viable alternative for this grade of steel. As the spacing is increased to 8 in. with No. 5 MMFX, the maximum allowable stress for the steel is exceeded. The specifications for crack control are violated at 9-in. spacing, and maximum allowable compressive stress in the concrete at 10-in. spacing. The decks with No. 5 MMFX steel have strength at least equal to that of the original design, except when the maximum allowable spacing criterion (12 in.) is exceeded.

Using No. 4 MMFX at spacings ranging from 6 to 13 in. produces no viable design options. Six-in. spacing results in tensile stresses in the steel that exceed the allowable tensile stress of 24 ksi. Further increases in spacing lead to failures in terms of maximum compressive stress in the concrete and the crack-control criterion. Similarly, no viable options are available using No. 3 MMFX reinforcement spaced at 6 to 13 in.

Table 5.3 - Results of X-Ray Microanalysis of MMFX Microcomposite Steel

Steel	Bar Size	Heat No.	Sample	Location	Fe	Cr	Si	Mn
N3 ¹	No. 5	S44420	1	1	98.26	0.22	0.45	1.07
				2	98.04	0.27	0.52	1.17
				3	98.17	0.23	0.45	1.15
				average	98.16	0.24	0.47	1.13
			2	1	98.16	0.28	0.42	1.14
				2	98.18	0.22	0.39	1.21
				3	98.11	0.25	0.45	1.19
				average	98.15	0.25	0.42	1.18
			average for this heat		98.15	0.25	0.45	1.16
MMFX ²	No. 5	810737	1	1	89.54	9.67	0.40	0.38
				2	89.37	9.78	0.44	0.40
				3	89.36	9.86	0.45	0.34
				average	89.42	9.77	0.43	0.37
			2	1	89.39	9.59	0.34	0.68
				2	89.56	9.72	0.41	0.31
				3	90.06	9.24	0.35	0.35
				average	89.67	9.52	0.37	0.45
			average for this heat		89.55	9.64	0.40	0.41
MMFX	No. 6	810737	1	1	89.58	9.37	0.66	0.38
				2	89.65	9.39	0.49	0.47
				3	90.01	9.31	0.25	0.43
				average	89.75	9.36	0.47	0.43
			2	1	89.54	9.72	0.25	0.49
				2	89.54	9.64	0.43	0.39
				3	89.38	9.69	0.49	0.44
				average	89.49	9.68	0.39	0.44
			average for this heat		89.62	9.52	0.43	0.43
MMFX	No. 6	710788	1	1	89.62	9.41	0.66	0.32
				2	89.76	9.40	0.29	0.54
				3	89.56	9.31	0.61	0.52
				average	89.65	9.37	0.52	0.46
			2	1	89.54	9.70	0.44	0.33
				2	89.55	9.71	0.50	0.25
				3	89.58	9.54	0.49	0.39
				average	89.56	9.65	0.48	0.32
			average for this heat		89.60	9.51	0.50	0.39

¹ N2 and N3: Conventional, normalized A 615 reinforcing steel² MMFX: MMFX Microcomposite steel

Table 5.4 – Prestressed Girder Bridge – Negative Moment Region

Steel	Spacing (in)	Overall Rating	Failure Criteria						
			Max. allowable steel stress*	Max. allowable concrete stress	Max. allowable spacing	Min. required steel	Crack- control provisions	Max. allowable steel	Strength ≥ original
Given Design: Grade 60 No.5	6	ok	ok	ok	ok	ok	ok	ok	-
MMFX No.5	6	NG	ok	ok	ok	ok	ok	NG	ok
MMFX No.5	7	ok	ok	ok	ok	ok	ok	ok	ok
MMFX No.5	8	NG**	NG	ok	ok	ok	ok	ok	ok
MMFX No.5	9	NG	NG	ok	ok	ok	NG	ok	ok
MMFX No.5	10	NG	NG	NG	ok	ok	NG	ok	ok
MMFX No.5	11	NG	NG	NG	ok	ok	NG	ok	ok
MMFX No.5	12	NG	NG	NG	ok	ok	NG	ok	ok
MMFX No.5	13	NG	NG	NG	NG	ok	NG	ok	NG
MMFX No.4	6	NG**	NG	ok	ok	ok	ok	ok	ok
MMFX No.4	7	NG	NG	NG	ok	ok	NG	ok	ok
MMFX No.4	8	NG	NG	NG	ok	ok	NG	ok	ok
MMFX No.4	9	NG	NG	NG	ok	ok	NG	ok	NG
MMFX No.4	10	NG	NG	NG	ok	ok	NG	ok	NG
MMFX No.4	11	NG	NG	NG	ok	ok	NG	ok	NG
MMFX No.4	12	NG	NG	NG	ok	ok	NG	ok	NG
MMFX No.4	13	NG	NG	NG	NG	ok	NG	ok	NG
MMFX No.3	6	NG	NG	NG	ok	ok	NG	ok	NG
MMFX No.3	7	NG	NG	NG	ok	ok	NG	ok	NG
MMFX No.3	8	NG	NG	NG	ok	ok	NG	ok	NG
MMFX No.3	9	NG	NG	NG	ok	ok	NG	ok	NG
MMFX No.3	10	NG	NG	NG	ok	NG	NG	ok	NG
MMFX No.3	11	NG	NG	NG	ok	NG	NG	ok	NG
MMFX No.3	12	NG	NG	NG	ok	NG	NG	ok	NG
MMFX No.3	13	NG	NG	NG	NG	NG	NG	ok	NG

* based on maximum allowable tensile stress of 24000 psi

** design limited only by maximum allowable tensile stress in steel

Positive moment region. Table 5.5 presents the analysis results for the positive moment region of the prestressed girder bridge. The original design used No. 5 and No. 4 Grade 60 bars alternating at 6-in. spacing. There are several viable options for using MMFX steel. No. 5 MMFX bars spaced at 6, 7, and 8 in. satisfy all criteria. At spacings greater than 8 in., the maximum tensile stress in the steel exceeds the allowable limit of 24 ksi. The maximum allowable spacing for the bridge deck is 12 in. and all options exceeding that value are not valid.

Configurations using No. 4 and No. 3 MMFX steel fail to satisfy one or more design criteria. The maximum allowable steel stress criterion is violated using spacings ranging from 6 to 13 in. Provisions for crack control are not satisfied for No. 4 MMFX steel spaced at 13 in. and for No. 3 MMFX spaced at 9 in. The strength provided by the No. 4 MMFX steel spaced at 10 in. and No. 3 MMFX spaced at 6 in. do not equal the strength of the original design.

Table 5.5 – Prestressed Girder Bridge – Positive Moment Region

Steel	Spacing (in)	Overall Rating	Failure Criteria						
			Max. allowable steel stress*	Max. allowable concrete stress	Max. allowable spacing	Min. required steel	Crack- control provisions	Max. allowable steel	Strength ≥ original
Given Design: Gr60 No. 5/ No. 4 alt.	6	ok	ok	ok	ok	ok	ok	ok	ok
MMFX No.5	6	ok	ok	ok	ok	ok	ok	ok	ok
MMFX No.5	7	ok	ok	ok	ok	ok	ok	ok	ok
MMFX No.5	8	ok	ok	ok	ok	ok	ok	ok	ok
MMFX No.5	9	NG**	NG	ok	ok	ok	ok	ok	ok
MMFX No.5	10	NG**	NG	ok	ok	ok	ok	ok	ok
MMFX No.5	11	NG**	NG	ok	ok	ok	ok	ok	ok
MMFX No.5	12	NG**	NG	ok	ok	ok	ok	ok	ok
MMFX No.5	13	NG	NG	ok	NG	ok	ok	ok	ok
MMFX No.4	6	NG**	NG	ok	ok	ok	ok	ok	ok
MMFX No.4	7	NG**	NG	ok	ok	ok	ok	ok	ok
MMFX No.4	8	NG**	NG	ok	ok	ok	ok	ok	ok
MMFX No.4	9	NG**	NG	ok	ok	ok	ok	ok	ok
MMFX No.4	10	NG	NG	ok	ok	ok	ok	ok	NG
MMFX No.4	11	NG	NG	ok	ok	ok	ok	ok	NG
MMFX No.4	12	NG	NG	ok	ok	ok	ok	ok	NG
MMFX No.4	13	NG	NG	ok	NG	ok	NG	ok	NG
MMFX No.3	6	NG	NG	ok	ok	ok	ok	ok	NG
MMFX No.3	7	NG	NG	ok	ok	ok	ok	ok	NG
MMFX No.3	8	NG	NG	NG	ok	ok	ok	ok	NG
MMFX No.3	9	NG	NG	NG	ok	ok	NG	ok	NG
MMFX No.3	10	NG	NG	NG	ok	ok	NG	ok	NG
MMFX No.3	11	NG	NG	NG	ok	ok	NG	ok	NG
MMFX No.3	12	NG	NG	NG	ok	NG	NG	ok	NG
MMFX No.3	13	NG	NG	NG	NG	NG	NG	ok	NG

* based on maximum allowable tensile stress of 24000 psi

** design limited only by maximum allowable tensile stress in steel

Continuous Composite (steel) Girder Bridge — Results for the structural analysis of the continuous composite steel girder bridge are shown in Tables 5.6 and 5.7. There are no viable options for using MMFX reinforcing steel in the continuous composite steel girder bridge. Although the bottom mat could be reinforced using No. 5 MMFX steel at 5.5-in., 6-in., 6.5-in., or 7-in. spacing (Table 5.7), there are no options available for using MMFX steel in the top mat. Mixing MMFX steel with Grade 60 steel in the same bridge deck is not recommended.

Negative moment region. The original design for the continuous composite steel girder bridge in the negative moment region used No. 5 Grade 60 steel with 5.5-in. spacing (Table 5.6). As shown in Table 5.6, the criterion used by SDDOT for a maximum allowable concrete compressive stress ($f_{c\text{-allowable}} = 1450$ psi) was not satisfied with the original design ($f_{c\text{-calculated}} = 1469$ psi). This was noted in the design calculation sheet and marked as “ok.” Replacing the Grade 60 steel with equal amounts of MMFX steel results in an over-reinforced section with

maximum compressive stresses in the concrete exceeding the allowable stresses. Increasing the spacing increases the discrepancy in the maximum allowable compressive stresses, followed by failure of the maximum allowable steel stress criterion, and finally the crack-control provision.

Table 5.6 – Continuous Composite (Steel) Girder Bridge – Negative Moment Region

Steel	Spacing (in)	Overall Rating	Failure Criteria						
			Max. allowable steel stress*	Max. allowable concrete stress	Max. allowable spacing	Min. required steel	Crack-control provisions	Max. allowable steel	Strength \geq original
Given Design: Grade 60 No.5	5.5	ok	ok	NG**	ok	ok	ok	ok	-
MMFX No.5	5.5	NG	ok	NG	ok	ok	ok	NG	ok
MMFX No.5	6	NG	NG	NG	ok	ok	ok	NG	ok
MMFX No.5	6.5	NG	NG	NG	ok	ok	ok	NG	ok
MMFX No.5	7	NG	NG	NG	ok	ok	ok	ok	ok
MMFX No.5	7.5	NG	NG	NG	ok	ok	NG	ok	ok
MMFX No.5	8	NG	NG	NG	ok	ok	NG	ok	ok
MMFX No.5	8.5	NG	NG	NG	ok	ok	NG	ok	ok
MMFX No.5	9	NG	NG	NG	ok	ok	NG	ok	ok
MMFX No.5	9.5	NG	NG	NG	ok	ok	NG	ok	ok
MMFX No.5	10	NG	NG	NG	ok	ok	NG	ok	ok
MMFX No.5	10.5	NG	NG	NG	ok	ok	NG	ok	ok
MMFX No.5	11	NG	NG	NG	ok	ok	NG	ok	ok
MMFX No.4	5.5	NG	NG	NG	ok	ok	NG	ok	ok
MMFX No.4	6	NG	NG	NG	ok	ok	NG	ok	ok
MMFX No.4	6.5	NG	NG	NG	ok	ok	NG	ok	ok
MMFX No.4	7	NG	NG	NG	ok	ok	NG	ok	ok
MMFX No.4	7.5	NG	NG	NG	ok	ok	NG	ok	NG
MMFX No.4	8	NG	NG	NG	ok	ok	NG	ok	NG
MMFX No.4	8.5	NG	NG	NG	ok	ok	NG	ok	NG
MMFX No.4	9	NG	NG	NG	ok	ok	NG	ok	NG
MMFX No.3	5.5	NG	NG	NG	ok	ok	NG	ok	NG
MMFX No.3	6	NG	NG	NG	ok	ok	NG	ok	NG
MMFX No.3	6.5	NG	NG	NG	ok	ok	NG	ok	NG
MMFX No.3	7	NG	NG	NG	ok	ok	NG	ok	NG
MMFX No.3	7.5	NG	NG	NG	ok	ok	NG	ok	NG
MMFX No.3	8	NG	NG	NG	ok	ok	NG	ok	NG
MMFX No.3	8.5	NG	NG	NG	ok	ok	NG	ok	NG
MMFX No.3	9	NG	NG	NG	ok	ok	NG	ok	NG

* based on maximum allowable tensile stress of 24000 psi

** marked "o.k." on SDDOT data tables

Using No. 4 or No. 3 MMFX steel at all investigated spacings (5.5 to 9 in.) results in failure of the maximum allowable stress criteria for steel and concrete as well as the crack-control provision. The strengths of the MMFX designs do not equal the original strength once the spacing exceeds 7 in. for the No. 4 MMFX steel and beginning with 5.5-in. spacing for the No. 3 MMFX steel.

Positive moment region. The original positive moment region designed by SDDOT uses alternating No. 4 and No. 5 Grade 60 steel at a 5.5-in. spacing (Table 5.7). Using No. 5 MMFX steel spaced at 5.5 in., 6 in., 6.5 in., and 7 in. provides viable alternatives for the bottom mat of steel. The maximum steel stress exceeds 24 ksi using spacings of 7.5 in. and greater.

Table 5.7 – Continuous Composite (Steel) Girder Bridge – Positive Moment Region

Steel	Spacing (in)	Overall Rating	Failure Criteria						
			Max. allowable steel stress*	Max. allowable concrete stress	Max. allowable spacing	Min. required steel	Crack-control provisions	Max. allowable steel	Strength \geq original
Given Design: Gr60 No. 5/ No. 4 alt.	5.5	ok	ok	ok	ok	ok	ok	ok	-
MMFX No.5	5.5	ok	ok	ok	ok	ok	ok	ok	ok
MMFX No.5	6	ok	ok	ok	ok	ok	ok	ok	ok
MMFX No.5	6.5	ok	ok	ok	ok	ok	ok	ok	ok
MMFX No.5	7	ok	ok	ok	ok	ok	ok	ok	ok
MMFX No.5	7.5	NG**	NG	ok	ok	ok	ok	ok	ok
MMFX No.5	8	NG**	NG	ok	ok	ok	ok	ok	ok
MMFX No.5	8.5	NG**	NG	ok	ok	ok	ok	ok	ok
MMFX No.5	9	NG**	NG	ok	ok	ok	ok	ok	ok
MMFX No.5	9.5	NG**	NG	ok	ok	ok	ok	ok	ok
MMFX No.5	10	NG**	NG	ok	ok	ok	ok	ok	ok
MMFX No.5	10.5	NG**	NG	ok	ok	ok	ok	ok	ok
MMFX No.5	11	NG	NG	ok	ok	ok	ok	ok	ok
MMFX No.5	11.5	NG	NG	ok	ok	ok	ok	ok	ok
MMFX No.5	12	NG	NG	ok	ok	ok	ok	ok	ok
MMFX No.5	12.5	NG	NG	ok	NG	ok	ok	ok	ok
MMFX No.4	5.5	NG**	NG	ok	ok	ok	ok	ok	ok
MMFX No.4	6	NG**	NG	ok	ok	ok	ok	ok	ok
MMFX No.4	6.5	NG**	NG	ok	ok	ok	ok	ok	ok
MMFX No.4	7	NG**	NG	ok	ok	ok	ok	ok	ok
MMFX No.4	7.5	NG**	NG	ok	ok	ok	ok	ok	ok
MMFX No.4	8	NG	NG	ok	ok	ok	ok	ok	ok
MMFX No.4	8.5	NG	NG	ok	ok	ok	ok	ok	ok
MMFX No.4	9	NG	NG	NG	ok	ok	ok	ok	ok
MMFX No.3	5.5	NG	NG	NG	ok	ok	ok	ok	NG
MMFX No.3	6	NG	NG	NG	ok	ok	ok	ok	NG
MMFX No.3	6.5	NG	NG	NG	ok	ok	ok	ok	NG
MMFX No.3	7	NG	NG	NG	ok	ok	ok	ok	NG
MMFX No.3	7.5	NG	NG	NG	ok	ok	NG	ok	NG
MMFX No.3	8	NG	NG	NG	ok	ok	NG	ok	NG
MMFX No.3	8.5	NG	NG	NG	ok	ok	NG	ok	NG
MMFX No.3	9	NG	NG	NG	ok	ok	NG	ok	NG

* based on maximum allowable tensile stress of 24000 psi

** design limited only by maximum allowable tensile stress in steel

Using the No. 4 MMFX steel at spacings ranging from 5.5 to 9 in. results in maximum steel stresses that exceed the allowable defined by AASHTO 16th ed. of 24 ksi. The options

investigated using No. 3 MMFX steel with spacings ranging from 5.5 to 9 in. violate criteria for maximum allowable stresses in the concrete and steel and the cracking provisions, and do not provide strength equal to the original design. Crack control provisions are violated with spacings exceeding 7 in.

Continuous Concrete Bridge — Results for the structural analysis of the continuous concrete bridge are shown in Tables 5.8 and 5.9. There are no viable options for using MMFX reinforcing steel in this deck.

Table 5.8 – Continuous Concrete Bridge – Negative Moment Region

Steel	Spacing (in)	Overall Rating	Failure Criteria					
			Max. allowable spacing	Min. required steel	Max. allowable steel	Crack-control provisions	Fatigue provisions	Strength \geq original
Given Design: Grade 60 No.8	6	ok	ok	ok	ok	ok	ok	-
MMFX No.8	6	NG	ok	ok	NG	ok	ok	ok
MMFX No.8	7	NG	ok	ok	NG	ok	ok	ok
MMFX No.8	8	NG	ok	ok	ok	NG	NG	ok
MMFX No.8	9	NG	ok	ok	ok	NG	NG	ok
MMFX No.8	10	NG	ok	ok	ok	NG	NG	ok
MMFX No.8	11	NG	ok	ok	ok	NG	NG	ok
MMFX No.8	12	NG	ok	ok	ok	NG	NG	ok
MMFX No.8	13	NG	ok	ok	ok	NG	NG	NG
MMFX No.8	14	NG	ok	ok	ok	NG	NG	NG
MMFX No.8	15	NG	ok	ok	ok	NG	NG	NG
MMFX No.8	16	NG	ok	ok	ok	NG	NG	NG
MMFX No.8	17	NG	ok	ok	ok	NG	NG	NG
MMFX No.7	6	NG	ok	ok	ok	ok	NG	ok
MMFX No.7	7	NG	ok	ok	ok	NG	NG	ok
MMFX No.7	8	NG	ok	ok	ok	NG	NG	ok
MMFX No.7	9	NG	ok	ok	ok	NG	NG	ok
MMFX No.7	10	NG	ok	ok	ok	NG	NG	NG
MMFX No.7	11	NG	ok	ok	ok	NG	NG	NG
MMFX No.7	12	NG	ok	ok	ok	NG	NG	NG
MMFX No.7	13	NG	ok	ok	ok	NG	NG	NG
MMFX No.7	14	NG	ok	ok	ok	NG	NG	NG
MMFX No.7	15	NG	ok	ok	ok	NG	NG	NG
MMFX No.7	16	NG	ok	ok	ok	NG	NG	NG
MMFX No.7	17	NG	ok	ok	ok	NG	NG	NG
MMFX No.6	6	NG	ok	ok	ok	NG	NG	NG
MMFX No.6	7	NG	ok	ok	ok	NG	NG	NG
MMFX No.6	8	NG	ok	ok	ok	NG	NG	NG
MMFX No.6	9	NG	ok	ok	ok	NG	NG	NG
MMFX No.6	10	NG	ok	ok	ok	NG	NG	NG
MMFX No.6	11	NG	ok	ok	ok	NG	NG	NG
MMFX No.6	12	NG	ok	ok	ok	NG	NG	NG
MMFX No.6	13	NG	ok	ok	ok	NG	NG	NG
MMFX No.6	14	NG	ok	ok	ok	NG	NG	NG

Negative moment region. The results for the analysis of the negative moment region are shown in Table 5.8. The original design specified No. 8 Grade 60 steel spaced at 6 in. Replacing this steel with No. 8 MMFX steel results in an over-reinforced section. The spacing must be increased to 8 in. to reach allowable reinforcement levels, but at that spacing the provisions for crack control and fatigue are not satisfied. The new designs with MMFX fail to provide strength equal to the original design once the spacing is increased to 13 in.

Using No. 7 MMFX steel also does not provide any viable options. At a spacing of 6 in. the fatigue criterion is not satisfied. Crack control provisions are violated with spacings greater than 7 in., and the design using MMFX steel fails to provide strength equal to the original design once the spacing exceeds 9 in. None of the options investigated using No. 6 MMFX steel satisfy the criteria for crack control or fatigue, providing strength equal to that of the original design.

Positive moment region. Table 5.9 lists the results of the structural analysis for the positive moment region of the continuous concrete bridge. The original design specified No. 8 Grade 60 reinforcement spaced at 6 in. Initially, No. 9 MMFX reinforcement is investigated. Spacings ranging from 6 to 12 in. produce an over-reinforced section, and spacings above 7 in. violate the fatigue provisions.

Table 5.9 – Continuous Concrete Bridge – Positive Moment Region

Steel	Spacing (in)	Overall Rating	Failure Criteria					
			Max. allowable spacing	Min. required steel	Max. allowable steel	Crack-control provisions	Fatigue provisions	Strength \geq original
Given Design: Grade 60 No.8	6	ok	ok	ok	ok	ok	ok	-
MMFX No.9	6	NG	ok	ok	NG	ok	ok	ok
MMFX No.9	7	NG	ok	ok	NG	ok	ok	ok
MMFX No.9	8	NG	ok	ok	NG	ok	NG	ok
MMFX No.9	9	NG	ok	ok	NG	ok	NG	ok
MMFX No.9	10	NG	ok	ok	NG	ok	NG	ok
MMFX No.9	11	NG	ok	ok	NG	ok	NG	ok
MMFX No.9	12	NG	ok	ok	NG	ok	NG	ok
MMFX No.9	13	NG	ok	ok	ok	ok	NG	ok
MMFX No.9	14	NG	ok	ok	ok	NG	NG	NG
MMFX No.9	15	NG	ok	ok	ok	NG	NG	NG
MMFX No.9	16	NG	ok	ok	ok	NG	NG	NG
MMFX No.9	17	NG	NG	ok	ok	NG	NG	NG
MMFX No.8	6	NG	ok	ok	NG	ok	NG	ok
MMFX No.8	7	NG	ok	ok	NG	ok	NG	ok
MMFX No.8	8	NG	ok	ok	NG	ok	NG	ok
MMFX No.8	9	NG	ok	ok	NG	ok	NG	ok
MMFX No.8	10	NG	ok	ok	ok	ok	NG	ok
MMFX No.8	11	NG	ok	ok	ok	ok	NG	ok
MMFX No.8	12	NG	ok	ok	ok	NG	NG	NG
MMFX No.8	13	NG	ok	ok	ok	NG	NG	NG
MMFX No.8	14	NG	ok	ok	ok	NG	NG	NG
MMFX No.8	15	NG	ok	ok	ok	NG	NG	NG
MMFX No.8	16	NG	ok	ok	ok	NG	NG	NG
MMFX No.8	17	NG	NG	ok	ok	NG	NG	NG

Table 5.9 – Continuous Concrete Bridge – Positive Moment Region (cont)

Steel	Spacing (in)	Overall Rating	Failure Criteria					
			Max. allowable spacing	Min. required steel	Max. allowable steel	Crack- control provisions	Fatigue provisions	Strength ≥ original
MMFX No.7	6	NG	ok	ok	NG	ok	NG	ok
MMFX No.7	7	NG	ok	ok	NG	ok	NG	ok
MMFX No.7	8	NG	ok	ok	ok	ok	NG	ok
MMFX No.7	9	NG	ok	ok	ok	ok	NG	NG
MMFX No.7	10	NG	ok	ok	ok	NG	NG	NG
MMFX No.7	11	NG	ok	ok	ok	NG	NG	NG
MMFX No.7	12	NG	ok	ok	ok	NG	NG	NG
MMFX No.7	13	NG	ok	ok	ok	NG	NG	NG
MMFX No.7	14	NG	ok	ok	ok	NG	NG	NG
MMFX No.7	15	NG	ok	ok	ok	NG	NG	NG
MMFX No.7	16	NG	ok	ok	ok	NG	NG	NG
MMFX No.7	17	NG	NG	ok	ok	NG	NG	NG
MMFX No.6	6	NG	ok	ok	ok	ok	NG	ok
MMFX No.6	7	NG	ok	ok	ok	ok	NG	NG
MMFX No.6	8	NG	ok	ok	ok	ok	NG	NG
MMFX No.6	9	NG	ok	ok	ok	NG	NG	NG
MMFX No.6	10	NG	ok	ok	ok	NG	NG	NG
MMFX No.6	11	NG	ok	ok	ok	NG	NG	NG
MMFX No.6	12	NG	ok	ok	ok	NG	NG	NG
MMFX No.6	13	NG	ok	ok	ok	NG	NG	NG
MMFX No.6	14	NG	ok	ok	ok	NG	NG	NG
MMFX No.6	15	NG	ok	ok	ok	NG	NG	NG
MMFX No.6	16	NG	ok	ok	ok	NG	NG	NG
MMFX No.6	17	NG	NG	ok	ok	NG	NG	NG
MMFX No.5	6	NG	ok	ok	ok	ok	NG	NG
MMFX No.5	7	NG	ok	ok	ok	NG	NG	NG
MMFX No.5	8	NG	ok	ok	ok	NG	NG	NG
MMFX No.5	9	NG	ok	ok	ok	NG	NG	NG
MMFX No.5	10	NG	ok	ok	ok	NG	NG	NG
MMFX No.5	11	NG	ok	ok	ok	NG	NG	NG
MMFX No.5	12	NG	ok	ok	ok	NG	NG	NG
MMFX No.5	13	NG	ok	ok	ok	NG	NG	NG
MMFX No.5	14	NG	ok	ok	ok	NG	NG	NG
MMFX No.5	15	NG	ok	ok	ok	NG	NG	NG
MMFX No.5	16	NG	ok	ok	ok	NG	NG	NG
MMFX No.5	17	NG	NG	ok	ok	NG	NG	NG

Replacing the original design with No. 8 MMFX steel also results in an over-reinforced section. Using spacings of 6 to 17 in. also violated the provisions for fatigue. All options for using No. 7, No. 6, and No. 5 MMFX steel with spacings ranging from 6 to 17 in. violate the provisions for fatigue.

Alternatives — Although the analyses described above do not provide many options for using MMFX in current bridge deck designs, it is important to note that the design standards were not written to incorporate steel with a yield stress of 120 ksi. For the decks proportioned using working stress design, the options considered in this study for which the maximum

allowable stress in the steel was the only criterion violated are indicated in Tables 5.4-5.7. It is important to note that if the maximum allowable stress criterion is increased for higher-strength steel, these designs could become viable options for using MMFX steel in SDDOT bridges.

5.3 CORROSION TESTS

The test results described in this section demonstrate that MMFX Microcomposite steel is more corrosion resistant than conventional mild steel reinforcement, but less corrosion resistant than epoxy-coated reinforcement meeting the requirements of ASTM A 775. Compared to conventional reinforcement, MMFX steel requires a higher chloride concentration for corrosion initiation. At lower chloride concentrations, it corrodes at a lower rate than conventional steel; at higher chloride concentrations, however, the two materials corrode at a similar rate. Specific findings, discussed next, are presented in terms of average values, at 15 weeks for the macrocell tests and 23 weeks for the bench-scale tests. Some macrocell tests were extended for as long as 18 weeks. Results for individual specimens are presented in Appendix B.

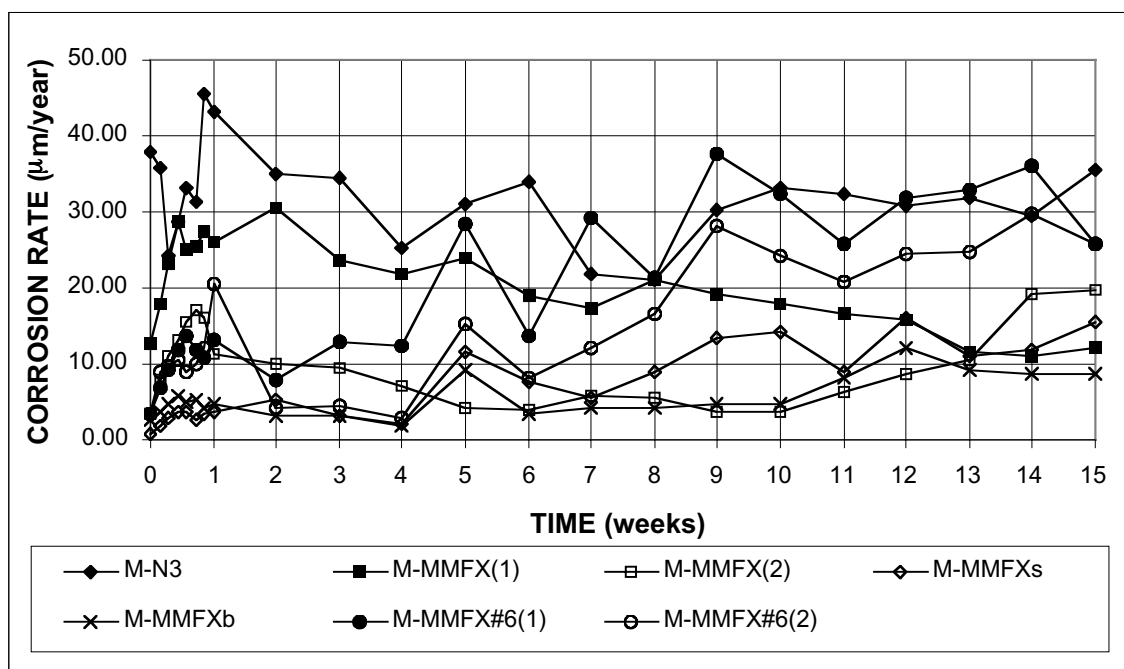


Figure 5.1 - Macrocell Test. Average corrosion rate. Bare specimens in 1.6 m ion NaCl and simulated concrete pore solution.

5.3.1 Rapid Macrocell Tests

Bare Bar Specimens — The average corrosion rates for bare specimens in the 1.6 m ion concentration NaCl solution are presented in Figure 5.1. The figure shows the average (in most cases of six specimens) corrosion rates for conventional (N3) reinforcement and six sets of MMFX steel. The MMFX(1) tests were carried out with the test configuration shown in Fig. 4.2 modified with the lid placed above the top of the bars. This maintained a high humidity

environment over the portion of the bars not submerged in the solution. All other tests were carried out using the test configuration shown in Fig. 4.2. The MMFX(1) and MMFX(2) tests evaluated No. 5 bars in the “as delivered” condition. Tests were also carried out on No. 5 sand-blasted bars (MMFXs) and bent bars (MMFXb). Two sets of three No. 6 bars each, MMFX#6(1) and MMFX #6(2), were tested in the “as delivered” condition.

As shown in Fig. 5.1, with the exception of MMFX#6(1) and (2), the MMFX bars corroded at a lower rate than the conventional, N3, bars. The average corrosion rates and average corrosion losses at 15 weeks are summarized in Table 5.10. At 15 weeks, the N3 bars are corroding at $35.6 \mu\text{m/yr}$. The corrosion rates for the No. 5 MMFX bars range from $8.8 \mu\text{m/yr}$ for the bent bars to $19.7 \mu\text{m/yr}$ for the MMFX(2) bars. On the average, the 24 No. 5 MMFX specimens corroded at a rate of $13.3 \mu\text{m/yr}$, equal to 37% of the corrosion rate exhibited by the conventional bars. The average total corrosion loss for the 24 No. 5 MMFX specimens was $3.1 \mu\text{m}$, equal to 34% of the average loss for the N3 bars ($9.0 \mu\text{m}$). In contrast to the No. 5 MMFX bars, the No. 6 MMFX bars corroded at a rate equal to 81% of that shown by the N3 No. 5 bars, finishing at almost $26 \mu\text{m/yr}$.

The average corrosion potentials of the bare bars in the 1.6 m ion NaCl solution are shown in Figs. 5.2a and 5.2b for the anode and cathode bars, respectively. The corrosion potentials are with respect to a saturated calomel electrode (SCE), and values more negative than -275 mV (-0.275V) indicate active corrosion. Figure 5.2a shows that, after the first week, all bars were undergoing active corrosion at the anode. At 15 weeks, the conventional N3 steel shows the most negative corrosion potential, with a value of -560 mV . The MMFX steel shows values between -410 and -495 mV . As shown in Fig. 5.2b, all of the average values for the cathode bars are more positive than -275 mV , indicating that the bars are passive.

Corrosion products were observed on the anode bars within the solution, with the exception of the bars in MMFX(1), for which the principal corrosion products occurred at and above the level of the solution. In some cases, corrosion products appeared on the bar at contact points with the plastic lid. Figure 5.3 shows a conventional N3 anode bar, at 15 weeks, with corrosion products that have formed on the bar both above and below the surface of the solution. Figures 5.4 and 5.5 show bars from groups MMFX(1) and MMFX(2), respectively, with corrosion products that have formed above (right of figure) and below (left of figure) the surface of the solution.

Table 5.10 – Average corrosion rates and corrosion losses as measured in the macrocell tests**CORROSION RATE AT WEEK 15**

Steel Designation	Heat No.	Specimen						Average	Std. Deviation
		1	2	3	4	5	6		
Bare specimens									
N3 ¹	S44407	52.23	0.26	67.30	39.89	32.20	21.93	35.64	23.44
MMFX(1) ²	810737	10.76	3.27	13.98	4.76	11.82	27.41	12.00	8.62
MMFX(2)	810737	12.25	7.98	22.90	18.08	32.03	24.85	19.68	8.77
MMFXs	810737	11.85	20.09	15.21	31.57	11.48	3.47	15.61	9.52
MMFXb	810737	7.58	17.84	6.70	6.73	7.08	6.63	8.76	4.46
MMFX#6(1)	810737	28.35	26.06	23.23	-	-	-	25.88	2.56
MMFX#6(2)	710788	23.21	25.89	28.39	-	-	-	25.83	2.59
N2h ¹	K0-C696	46.45	51.84	16.68	33.61	26.00	-	34.91	14.43
MMFXsh	810737	46.75	31.05	48.59	33.38	51.83	33.55	40.86	9.17
Mortar-wrapped specimens									
N3m	S44407	11.14	9.10	25.89	19.17	21.01	19.17	17.58	6.31
MMFXm	810737	8.81	17.25	10.05	9.47	11.59	5.94	10.52	3.79
ECRm ^{3,+}	S44407	3.65	1841.62	76.73	646.76	621.18	0.00	531.7	707.91
ECRm*	S44407	0.03	14.46	0.60	5.08	4.88	0.00	4.2	5.56
N3/MMFX	S44407/810737	14.92	10.50	10.48	-	-	-	12.0	2.56
MMFX/N3	810737/S44407	15.10	11.37	12.20	-	-	-	12.9	1.96

TOTAL CORROSION LOSS AFTER 15 WEEKS

Steel Designation	Heat No.	Specimen						Average	Std. Deviation
		1	2	3	4	5	6		
Bare specimens									
N3	S44407	12.98	4.81	13.12	11.02	6.92	5.27	9.02	3.81
MMFX(1)	810737	7.21	4.74	6.16	4.86	3.62	6.61	5.53	1.35
MMFX(2)	810737	3.08	2.09	3.23	1.12	1.62	3.81	2.49	1.04
MMFXs	810737	1.95	2.61	3.21	3.27	2.84	2.13	2.67	0.55
MMFXb	810737	1.51	2.76	1.20	1.46	1.51	1.99	1.74	0.56
MMFX#6(1)	810737	9.85	5.83	5.19	-	-	-	6.96	2.53
MMFX#6(2)	710788	3.60	6.17	5.36	-	-	-	5.04	1.32
N2h	K0-C696	16.67	14.73	8.38	11.51	11.75	-	12.61	3.19
MMFXsh	810737	15.32	8.39	12.66	6.20	9.84	13.16	10.93	3.38
Mortar-wrapped specimens									
N3m	S44407	5.13	4.74	6.69	5.17	4.75	5.08	5.26	0.72
MMFXm	810737	2.17	0.55	1.87	0.98	1.67	0.92	1.36	0.63
ECRm ⁺	S44407	1.26	130.00	9.06	63.10	28.18	1.26	38.8	50.44
ECRm [*]	S44407	0.01	1.02	0.07	0.50	0.22	0.01	0.3	0.40
N3/MMFX	S44407/810737	3.30	2.19	2.33	-	-	-	2.6	0.60
MMFX/N3	810737/S44407	1.59	1.74	2.10	-	-	-	1.8	0.26

¹ N2 and N3: Conventional, normalized A 615 reinforcing steel² MMFX: MMFX Microcomposite steel³ ECR: Epoxy coated N3 steel

+ Based on exposed area, four 1/8-in. diameter holes in epoxy * Based on total area of bar exposed to solution

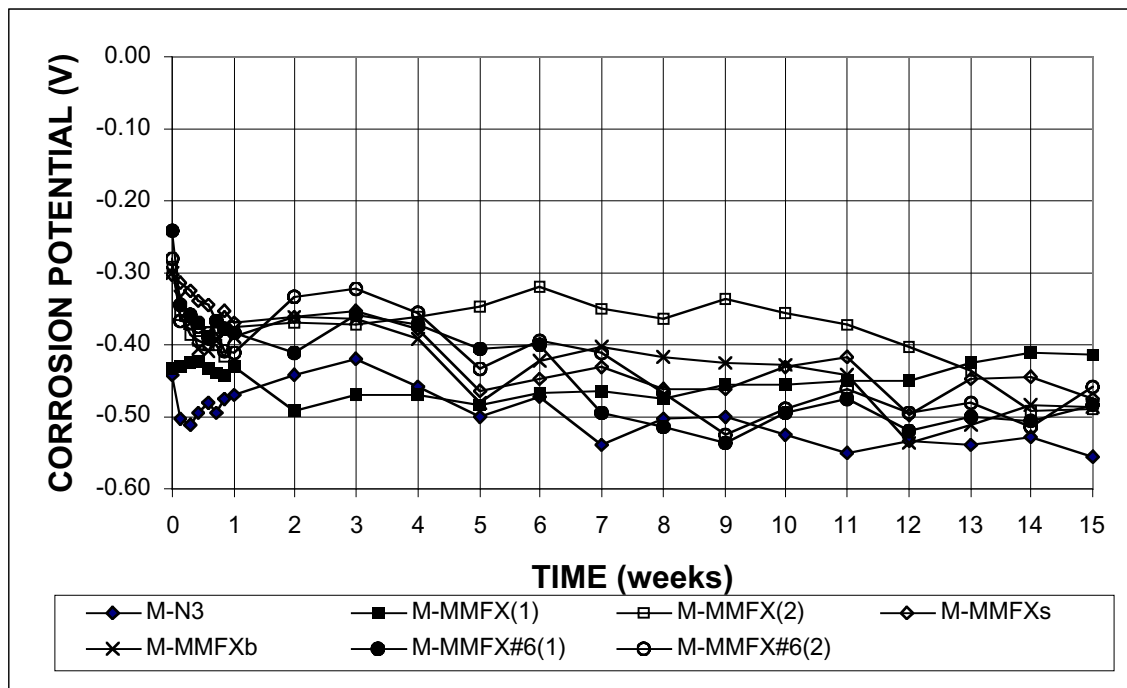


Figure 5.2a - Macrocell Test. Average corrosion potential vs. saturated calomel electrode, anode. Bare specimens in 1.6 m ion NaCl and simulated concrete pore solution.

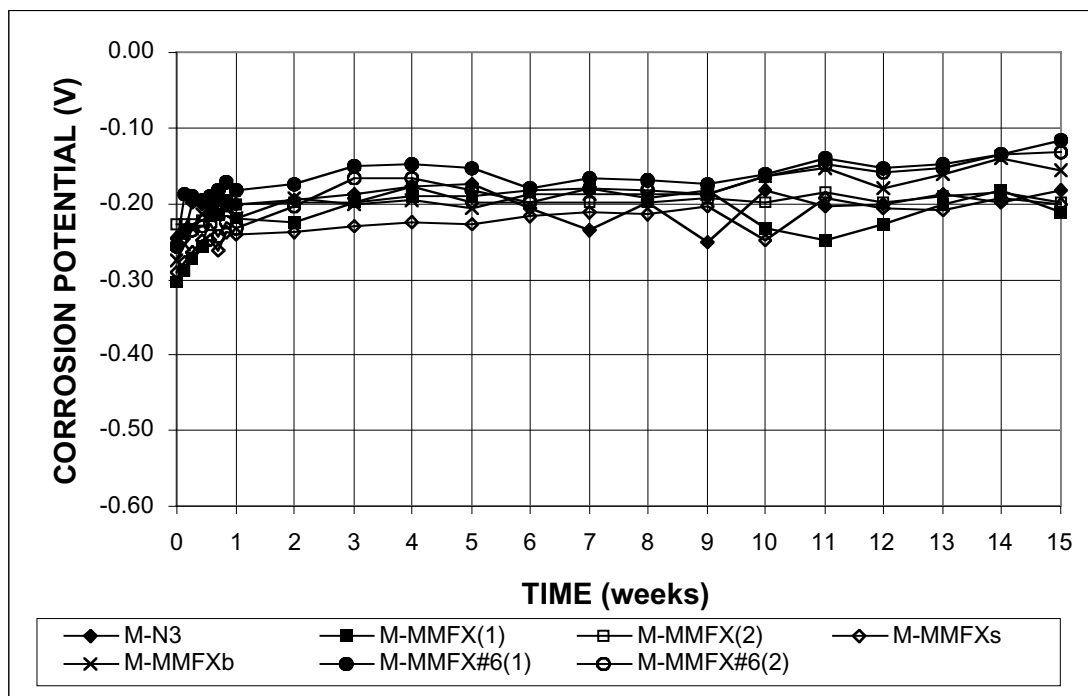


Figure 5.2b - Macrocell Test. Average corrosion potential vs. saturated calomel electrode, cathode. Bare specimens in 1.6 m ion NaCl and simulated concrete pore solution.



Figure 5.3 - Bare conventional N3 anode bar, at 15 weeks

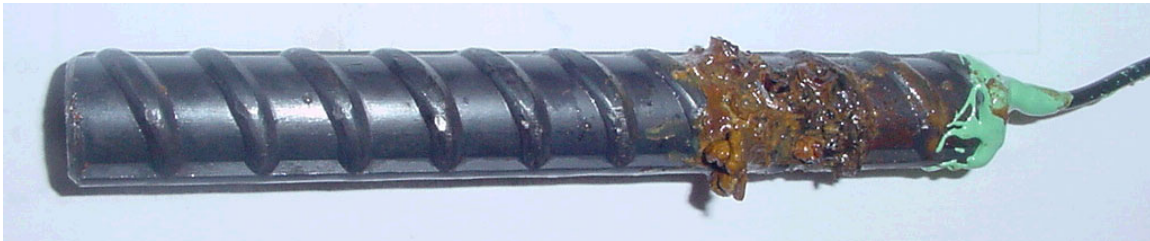


Figure 5.4 – Bare MMFX anode bar from group MMFX(1), at 15 weeks, showing corrosion products that formed above the surface of the solution.



Figure 5.5 – Bare MMFX anode bar from group MMFX(2), at 15 weeks, showing corrosion products that formed below the surface of the solution.

To evaluate the performance of the bars subjected to a high chloride concentration, two series of tests were performed on conventional and sand-blasted MMFX bars in a 6.04 m ion (15%) NaCl solution. The results are presented in Figs. 5.6 and 5.7. As shown in Fig. 5.6, initially the MMFX specimen corroded at about one-half the rate of the conventional N2 steel. However, after about seven weeks, the two steels corroded at approximately the same rate, with

both exhibiting a corrosion rate near $40 \mu\text{m}/\text{yr}$. At 15 weeks, the average corrosion loss (Table 5.10) of the MMFX specimens was $10.9 \mu\text{m}$, equal to 87 percent of the N2 specimens ($12.6 \mu\text{m}$). The standard deviations shown in Table 5.10 emphasize the high scatter inherent in these tests (Appendix B). As shown in Figs. 5.7a and 5.7b, the average corrosion potentials were quite similar for the two steels. The results in Figs. 5.1, 5.2, 5.6, and 5.7 indicate that MMFX steel will corrode at a lower rate than conventional steel at low chloride concentrations, but at a similar rate at high chloride concentrations.

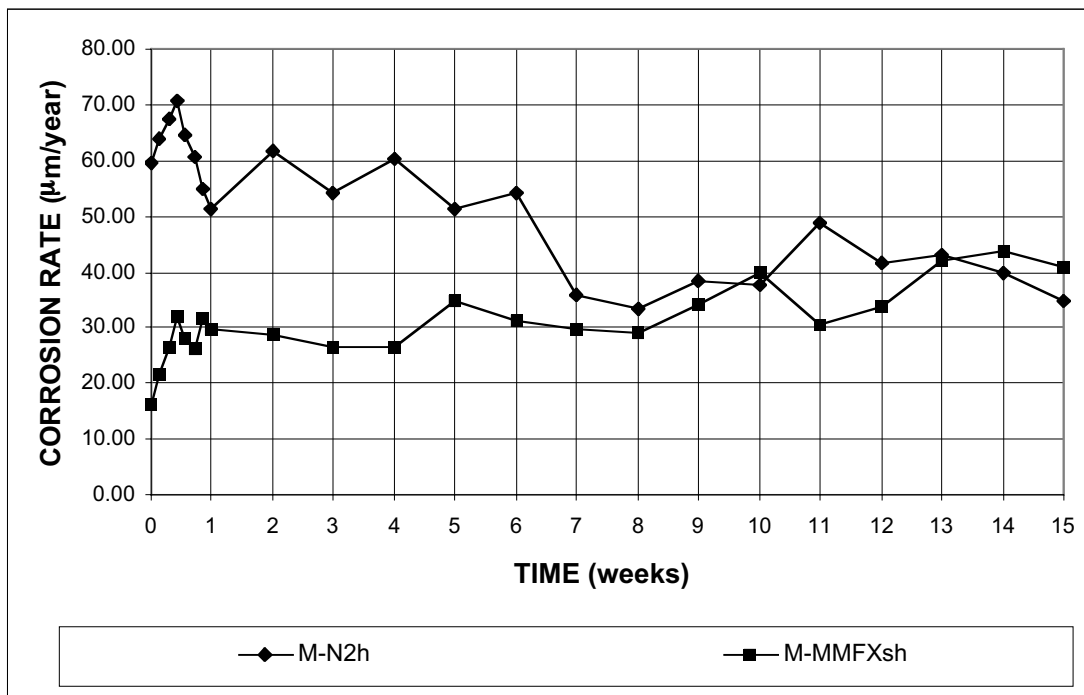


Figure 5.6 - Macrocell Test. Average corrosion rate. Bare specimens in 6.04 m ion (15%) NaCl and simulated concrete pore solution.

Mortar-Wrapped Specimens — Rapid macrocell tests of mortar-wrapped specimens included six tests each of conventional (N3), MMFX, and epoxy-coated (ECR) reinforcement. The coating on the ECR bars was penetrated by four $\frac{1}{8}$ -in. diameter holes. In addition, three specimens each were used for two combinations of MMFX and N3 steel, one combination with MMFX as the anode and one combination with N3 steel as the anode. The results are shown in Figs. 5.8 and 5.9 and summarized in Table 5.10.

Average corrosion rates are shown in Figs. 5.8a and 5.8b; the only difference in the two figures is the scale of the vertical axis. The results for the epoxy-coated reinforcement are shown in terms of both the exposed area (area of the four holes), ECRm^+ , and the total bar area exposed to the solution, ECRm^* .

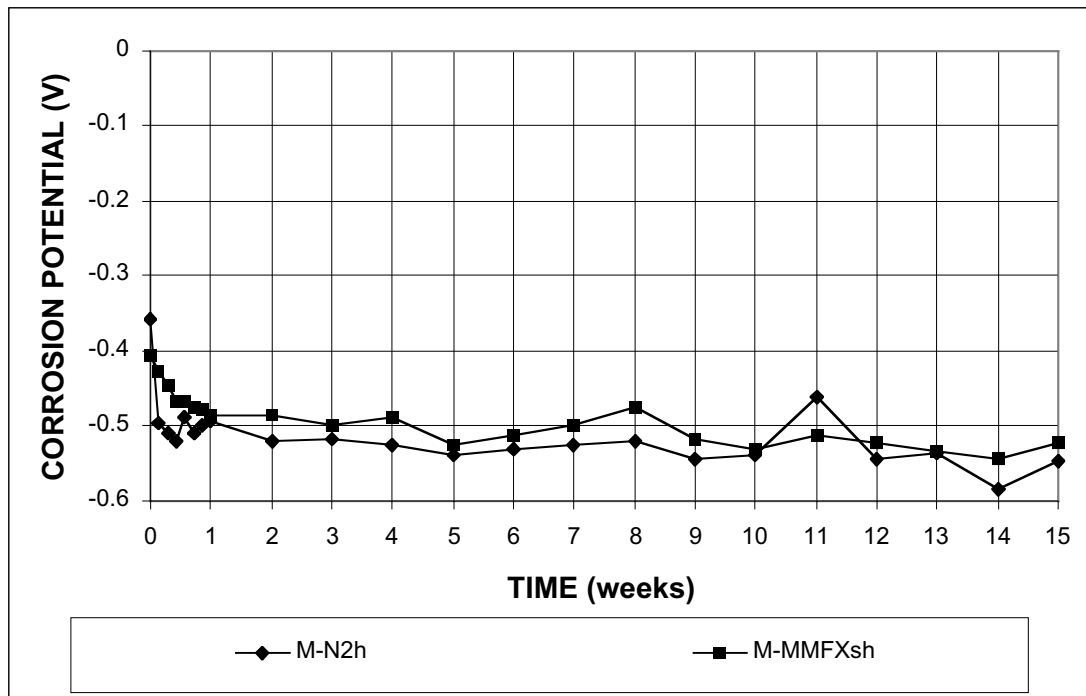


Figure 5.7a - Macrocell Test. Average corrosion potential vs. saturated calomel electrode, anode. Bare specimens in 6.04 m ion (15%) NaCl and simulated concrete pore solution.

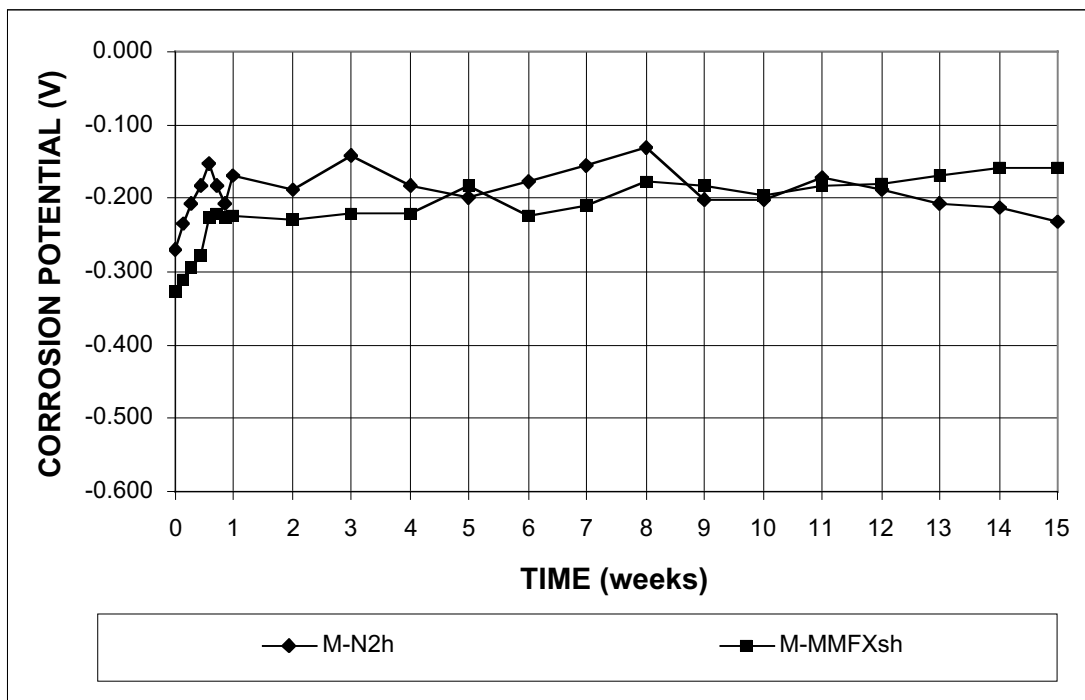


Figure 5.7b - Macrocell Test. Average corrosion potential vs. saturated calomel electrode, cathode. Bare specimens in 6.04 m ion (15%) NaCl and simulated concrete pore solution

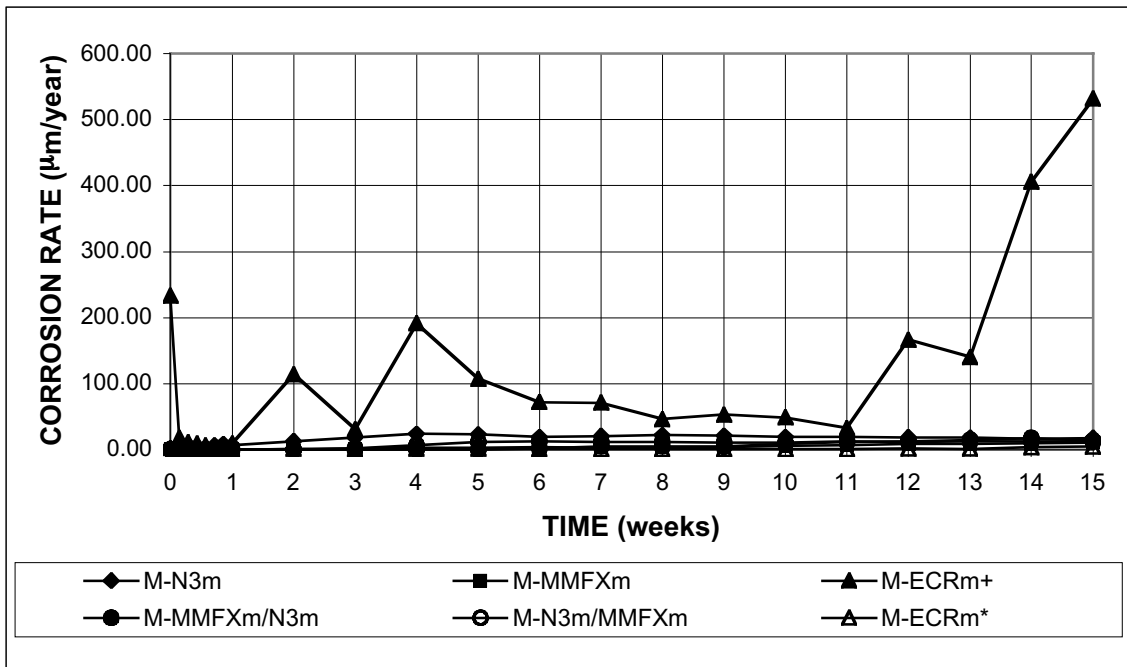


Figure 5.8a - Macrocell Tests. Average corrosion rate. Mortar-wrapped specimens with w/c=0.50 in 1.6 m ion NaCl and simulated concrete pore solution.

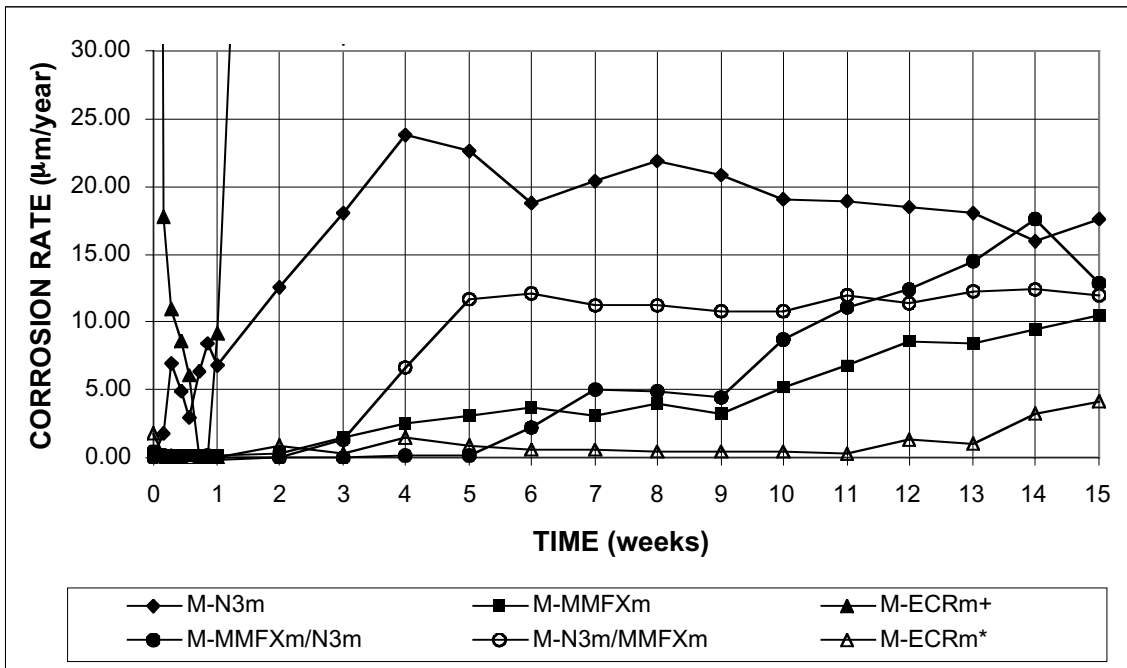


Figure 5.8b - Macrocell Tests. Average corrosion rate. Mortar-wrapped specimens with w/c=0.50 in 1.6 m ion NaCl and simulated concrete pore solution

⁺ Based on exposed area of steel, four 1/8-in diameter holes in epoxy

^{*} Based on total area of bar exposed to solution

As shown in Table 5.10 and Fig. 5.8a, the corrosion rate for the epoxy-coated reinforcement is very high based on exposed area, reaching a value of $532 \mu\text{m/yr}$ at 15 weeks. As pointed out in Section 4.3.1, uncoated bars were used as the cathode bars in these tests. The results demonstrate the importance of using all epoxy-coated reinforcement on bridge decks, not just the top layer of steel.

Figure 5.8b expands the vertical scale and shows the corrosion rates based on the total bar area. In this case, the epoxy-coated reinforcement exhibits the lowest total corrosion rate, peaking at $4.2 \mu\text{m/yr}$ at 15 weeks. Had the epoxy not been penetrated, it is expected that the corrosion rate would not have been measurable on these bars. For the other forms of reinforcement, the macrocells with all MMFX steel exhibited the next lowest corrosion rate, $10.5 \mu\text{m/yr}$ at 15 weeks. The highest corrosion rate was exhibited by the conventional N3 reinforcement, peaking at $23.5 \mu\text{m/yr}$ at 4 weeks and ending at $17.6 \mu\text{m/yr}$ at 15 weeks. At this point, MMFX steel was corroding at a rate equal to 60% of that observed for the N3 steel. In the same period, the total losses for MMFX steel averaged $1.4 \mu\text{m}$, equal to 26% of the total loss for the N3 bars ($5.3 \mu\text{m}$).

The macrocells containing both steels exhibited results that were generally intermediate between the other two sets of specimens. The mixed macrocells with N3 steel at the anode exhibited a corrosion rate of about $12 \mu\text{m/yr}$ beginning in week 5. The macrocells with MMFX steel at the anode exhibited lower corrosion rates until week 11, and actually ended the tests with slightly higher corrosion rates than the macrocells with the conventional steel at the anode. Combining the steel, independent of whether MMFX or conventional steel is the anode, reduced corrosion performance below that exhibited by MMFX steel alone.

The average corrosion potential of the test specimens is shown in Figs. 5.9a and 5.9b. The corrosion potentials at the anode (Fig. 5.9a) dropped most rapidly for the N3 bars, dropping below -275 mV by the second day. The ECR bars exhibited a low corrosion potential, -470 mV , at the initiation of the test, but this rose rapidly and remained near -300 mV through week 13, dropping to -480 mV at weeks 14 and 15. The other test specimens remained in a passive condition for a longer period of time. The mixed macrocell with the N3 bars at the anode exhibited passive behavior beginning in week 4, as did the macrocell containing all MMFX steel, although the corrosion potential in the latter test remained relatively high until week 11 when it dropped to -440 mV . Beginning in week 8, the average corrosion potentials of the MMFX bars, in both the all-MMFX macrocells and the mixed macrocells, exhibited nearly identical corrosion potentials, ending at -515 mV at 15 weeks.

The corrosion potentials at the cathode (Fig. 5.9b) indicate that the cathodes in the epoxy-coated bar test and in the all-MMFX macrocells remained passive for the duration of the test. The cathode potentials in the other tests dropped to values in the range of -250 to -295 mV , indicating that there may have been a slight tendency to corrode.

An evaluation of the test specimens after the test indicated some corrosion products under the mortar, as shown in Figs. 5.10 and 5.11 for conventional N3 and MMFX bars, respectively.

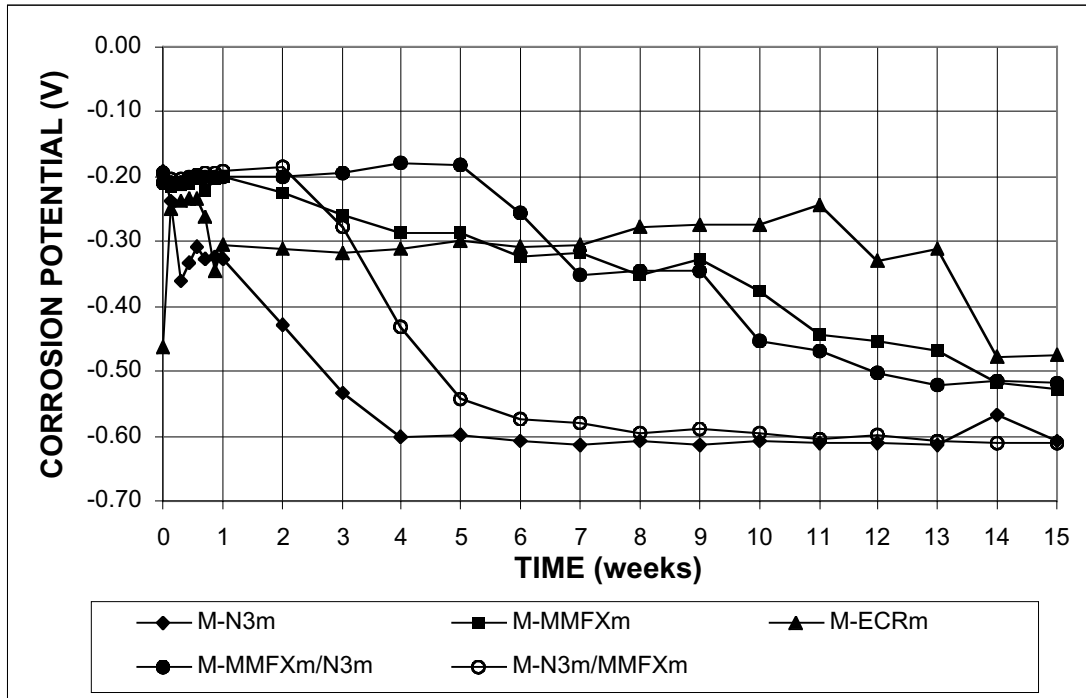


Figure 5.9a - Macrocell Test. Average corrosion potential vs. saturated calomel electrode, anode. Mortar-wrapped specimens with $w/c=0.50$ in 1.6 m ion NaCl and simulated concrete pore solution.

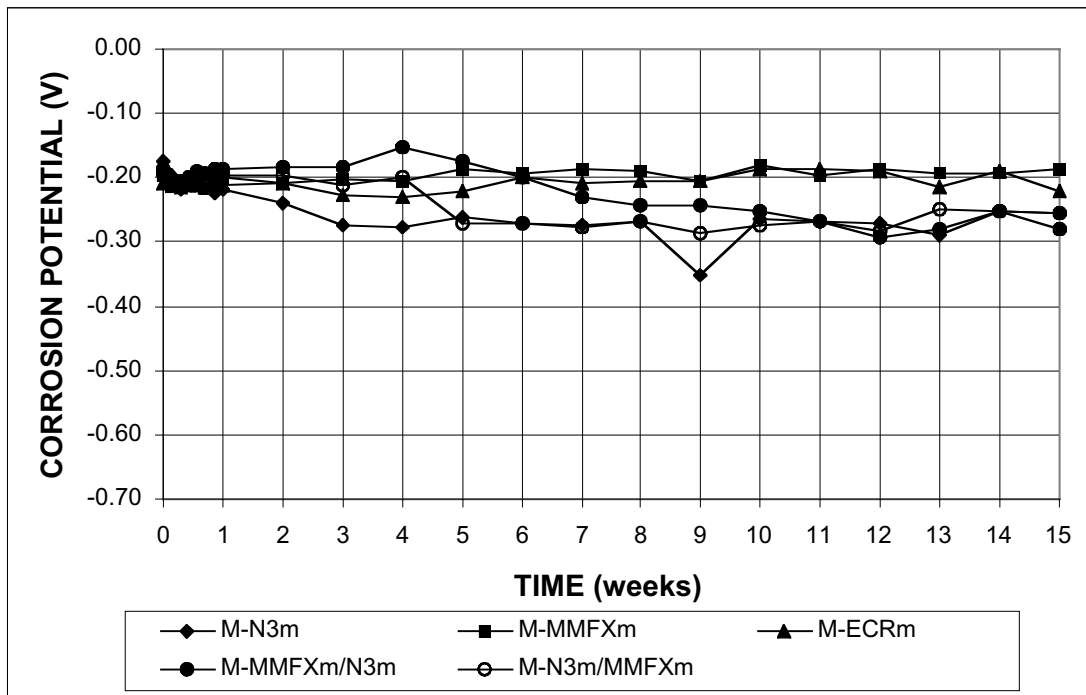


Figure 5.9b - Macrocell Test. Average corrosion potential vs. saturated calomel electrode, cathode. Mortar-wrapped specimens with $w/c=0.50$ in 1.6 m ion NaCl and simulated concrete pore solution.



Figure 5.10 - Conventional N3 anode bar after removal of mortar, at 15 weeks.



Figure 5.11 - MMFX anode bar after removal of mortar, at 15 weeks.

5.3.2 Bench-Scale Tests

The average corrosion rates and total corrosion losses at 23 weeks for the Southern Exposure and cracked beam tests are summarized in Table 5.11. Test results for the duration of these 96-week tests will be presented in follow-up reports. Findings to date are discussed next.

Southern Exposure Tests — Six Southern Exposure tests are underway for conventional (N3), MMFX, and epoxy-coated (ECR) reinforcement. In addition, three specimens are under test for each of two combinations of MMFX and conventional reinforcement, three specimens with MMFX as the top layer of steel and three with conventional steel as the top layer. Three Southern Exposure specimens with bent MMFX steel are also under test; however, these started at a later date and have been underway for only 10 weeks. Average corrosion rates and average total corrosion losses are shown in Figs. 5.12 and 5.13, respectively.

During the early stages of these 96-week tests, the three bent MMFX specimens exhibit the highest corrosion rate. At 23 weeks, the specimens with N3 steel in the upper layer show the highest average corrosion rates ($4.8 \mu\text{m/yr}$ for four specimens with all N3 steel and $5.3 \mu\text{m/yr}$ for specimens with N3 steel in the top layer and MMFX steel in the bottom layer). Straight MMFX steel exhibits significantly lower corrosion rates, with the lowest corrosion rates exhibited by ECR ($0.01 \mu\text{m/yr}$) and MMFX ($0.01 \mu\text{m/yr}$) steel in the specimens in which it is combined with N3 steel in the bottom mat. At 23 weeks, the all-MMFX steel specimens are corroding at $0.6 \mu\text{m/yr}$.

Table 5.11 – Average corrosion rates and corrosion losses as measured in the bench-scale tests**CORROSION RATE AT WEEK 23**

Steel Designation	Heat No.	Specimen						Average	Std. Deviation
		1	2	3	4	5	6		
Southern Exposure Tests									
N3(1) ¹	S44407	3.28	10.64	0.00	5.33	-	-	4.81	4.46
N3(2)	S44420	0.00	2.33	-	-	-	-	1.16	1.65
ECR(1) ^{3, +}	S44407	20.08	0.00	0.00	3.65	-	-	5.93	9.58
ECR(2) ⁺	S44420	0.00	0.00	-	-	-	-	0.00	0.00
ECR(1)*	S44407	0.04	0.00	0.00	0.01	-	-	0.01	0.02
ECR(2)*	S44420	0.00	0.00	-	-	-	-	0.00	0.00
MMFX ²	810737	2.11	0.02	1.03	0.11	0.00	0.03	0.55	0.86
N3/MMFX	S44420/810737	4.73	5.88	5.13	-	-	-	5.25	0.59
MMFX/N3	810737/S44420	0.01	0.01	0.01	-	-	-	0.01	0.00
MMFXb	810737	10.27	3.47	7.48	-	-	-	7.07	3.42
Cracked Beam Tests									
N3(1)	S44407	6.68	6.33	2.17	2.14	-	-	4.33	2.52
N3(2)	S44420	3.21	4.95	-	-	-	-	4.08	1.23
ECR(1) ⁺	S44407	767.55	588.46	858.93	1257.32	-	-	868.06	282.78
ECR(2) ⁺	S44420	25.59	464.19	-	-	-	-	244.89	310.14
ECR(1)*	S44407	0.89	1.30	0.03	0.48	-	-	0.67	0.54
ECR(2)*	S44420	0.03	0.48	-	-	-	-	0.25	0.32
MMFX	810737	3.15	1.25	1.91	3.18	3.23	1.59	2.39	0.90

TOTAL CORROSION LOSS AFTER 23 WEEKS

Steel Designation	Heat No.	Specimen						Average	Std. Deviation
		1	2	3	4	5	6		
Southern Exposure Test									
N3(1)	S44407	0.58	2.09	0.48	1.61	-	-	1.19	0.79
N3(2)	S44420	0.48	0.26	-	-	-	-	0.37	0.16
ECR(1) ⁺	S44407	14.60	2.14	6.77	3.79	-	-	6.83	5.53
ECR(2) ⁺	S44420	5.65	6.39	-	-	-	-	6.02	0.52
ECR(1)*	S44407	0.03	0.00	0.01	0.01	-	-	0.01	0.01
ECR(2)*	S44420	0.01	0.01	-	-	-	-	0.01	0.00
MMFX	810737	0.50	0.00	0.15	0.02	0.06	0.00	0.12	0.19
N3/MMFX	S44420/810737	0.65	1.72	1.26	-	-	-	1.21	0.54
MMFX/N3	810737/S44420	0.01	0.03	0.01	-	-	-	0.02	0.01
MMFXb	810737	1.40	0.40	1.30	-	-	-	1.03	0.55
Cracked Beam Test									
N3(1)	S44407	4.80	4.53	4.95	3.92	-	-	4.55	0.45
N3(2)	S44420	4.20	4.30	-	-	-	-	4.25	0.07
ECR(1) ⁺	S44407	880.93	283.82	315.95	680.11	-	-	540.20	289.65
ECR(2) ⁺	S44420	117.80	113.02	-	-	-	-	115.41	3.38
ECR(1)*	S44407	0.62	0.59	0.21	0.38	-	-	0.45	0.19
ECR(2)*	S44420	0.12	0.12	-	-	-	-	0.12	0.00
MMFX	810737	1.95	1.14	1.66	1.89	1.72	1.59	1.66	0.29

¹ N2 and N3: Conventional, normalized A 615 reinforcing steel² MMFX: MMFX Microcomposite steel³ ECR: Epoxy coated N3 steel⁺ Based on exposed area, four 1/8-in. diameter holes in epoxy * Based on total area of bar exposed to solution

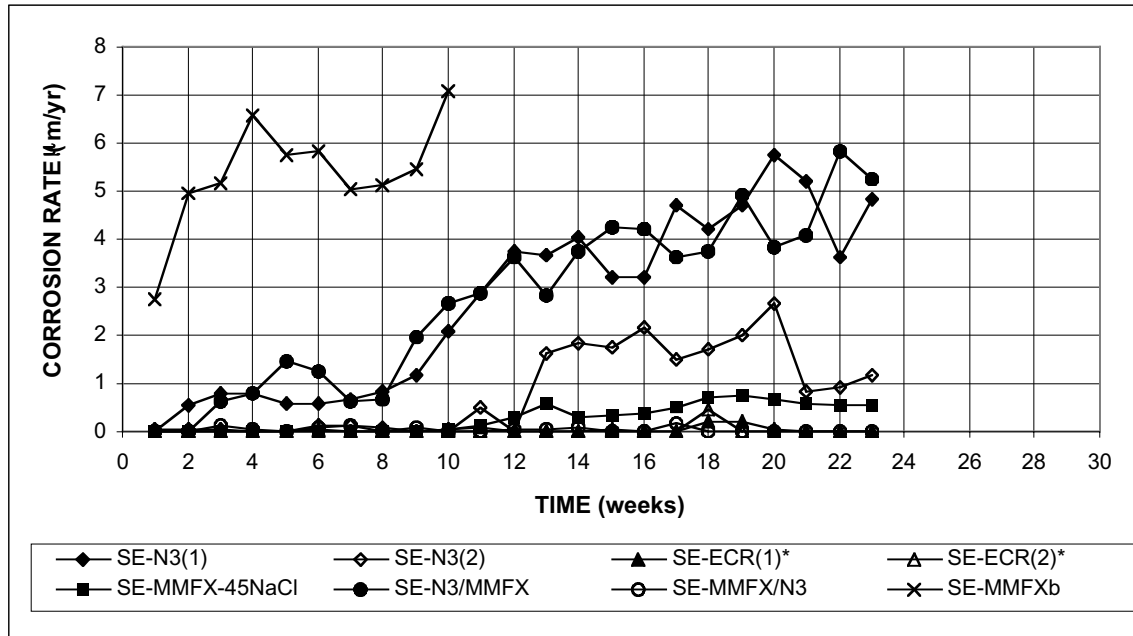


Figure 5.12 - Southern Exposure Test. Average corrosion rate, specimens with w/c=0.45, ponded with a 15% NaCl solution.

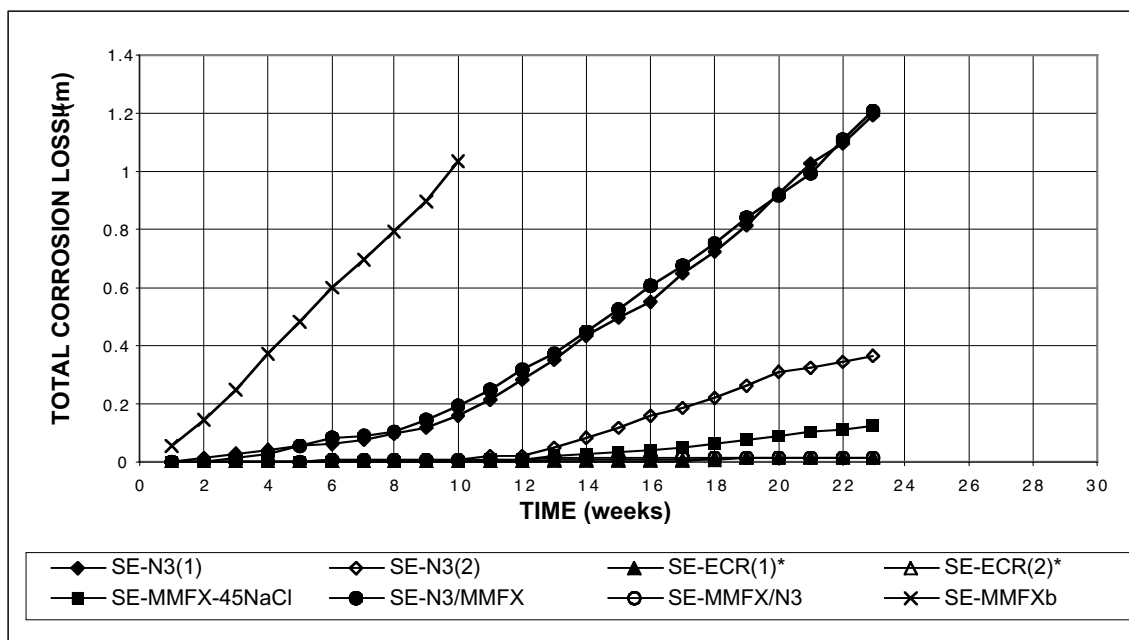


Figure 5.13 - Southern Exposure Test. Average total corrosion loss, specimens with w/c=0.45, ponded with a 15% NaCl solution.

* Based on total area of bar exposed to solution

The N3 bars exhibit corrosion initiation between weeks 2 and 7, while the straight MMFX bars do not exhibit corrosion until week 11. It is surmised that the rapid corrosion rate of the MMFX bent bars may be due to the formation of a void along the bar that formed during fabrication. Bent bars are cantilevered from one side of the form, rather than supported on both sides, as is the case for straight bars. Thus, the bars may have moved slightly during fabrication, resulting in a void. The corrosion of exposed portions of the MMFX specimens in the first series of MMFX macrocell tests [MMFX(1)] provides a clue as to what may be occurring in the MMFX bent bar SE specimen tests. Three additional MMFX bent bar SE tests are planned.

The very low corrosion rate exhibited by the ECR bars based on total bar area can be contrasted with the corrosion rate (as high as $1257 \mu\text{m/yr}$) and total corrosion loss (as high as $881 \mu\text{m}$) at 23 weeks based on the exposed area (four $\frac{1}{8}$ -in. diameter holes in the coating), as shown in Table 5.11 and Figs. 5.14 and 5.15. As for the macrocell specimens, these specimens demonstrate that very high corrosion rates can occur in localized areas, especially when the cathode is unprotected as it is in these tests.

Average corrosion potentials for the top and bottom mats of steel for the Southern Exposure tests are shown in Figs. 5.16a and 5.16b, respectively. In this case, the corrosion potentials are with respect to a copper-copper sulfate electrode (CSE), which gives corrosion potentials about 75 mV more negative than measured with a saturated calomel electrode (SCE). Thus, active corrosion is indicated by corrosion potentials more negative than -350 mV . The results indicate that the average corrosion potential of the MMFX bent bars (MMFXb) drops below -350 mV by the end of the first week. Based on the average corrosion potential, active corrosion began by the end of the eighth week for the N3 steel specimens in which MMFX was used for the bottom mat of steel and for the N3 specimens [except the two specimens in group N3(2)] by nine weeks. The ECR specimens exhibit fluctuating potentials, with some specimens undergoing active corrosion by the end of the 10th week. The specimens with straight MMFX steel on the top layer began active corrosion in the 18th week. Figure 5.16b indicates that the corrosion potential for a number of specimens has dropped below -350 mV for the bottom mat of steel, starting in the 15th week for the N3 and ECR(1) specimens and in the 16th week for the specimens combining MMFX and N3 steel in which the N3 steel is used in the bottom mat. These low corrosion potentials indicate that chlorides have penetrated nearly through the full depth of the specimens.

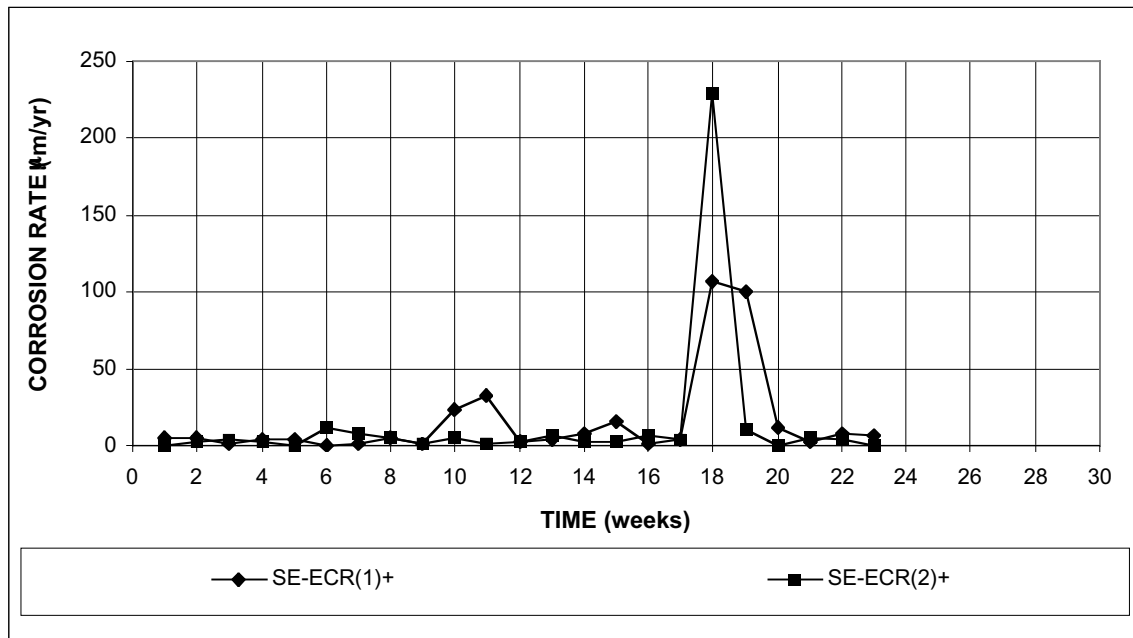


Figure 5.14 - Southern Exposure Test. Average corrosion rate, epoxy-coated bars, specimens with w/c=0.45, ponded with a 15% NaCl solution.

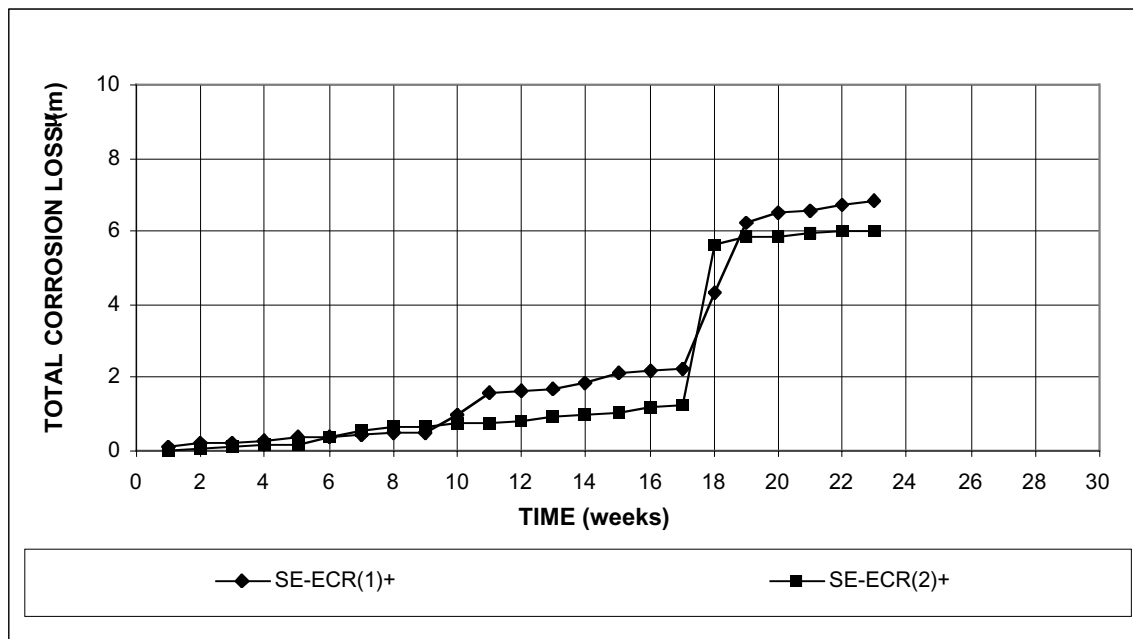


Figure 5.15 - Southern Exposure Test. Average total corrosion loss, epoxy-coated bars, specimens with w/c=0.45, ponded with a 15% NaCl solution.

⁺ Based on exposed area of steel, four $\frac{1}{8}$ -in diameter holes in epoxy

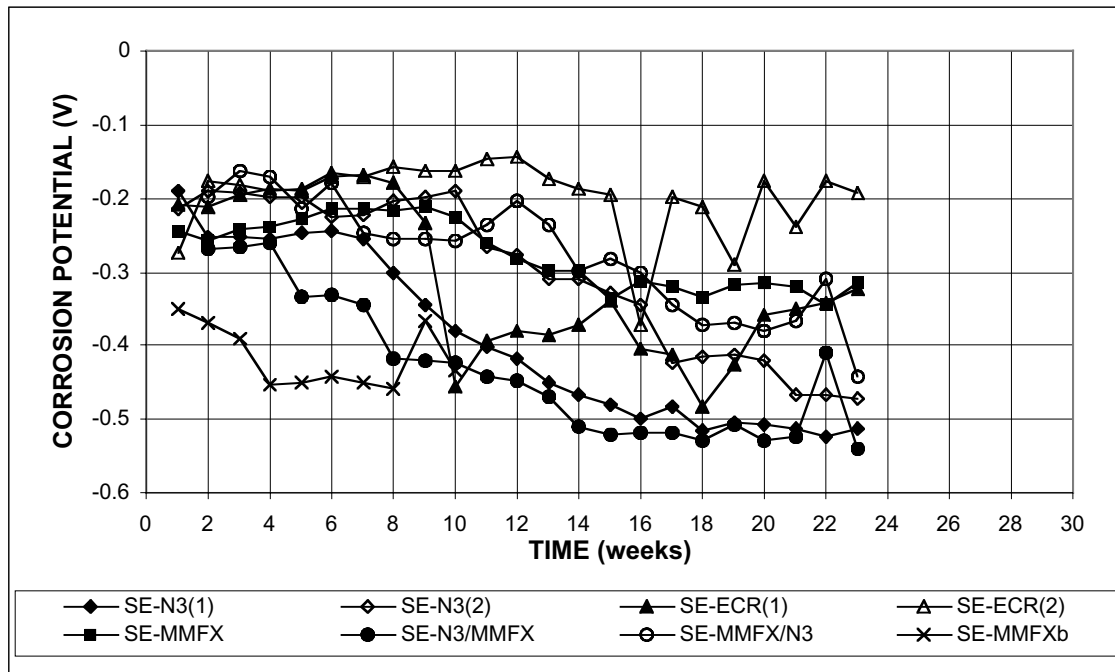


Figure 5.16a - Southern Exposure Test. Average corrosion potential vs. CSE, top mat. Specimens with $w/c=0.45$, ponded with a 15% NaCl solution.

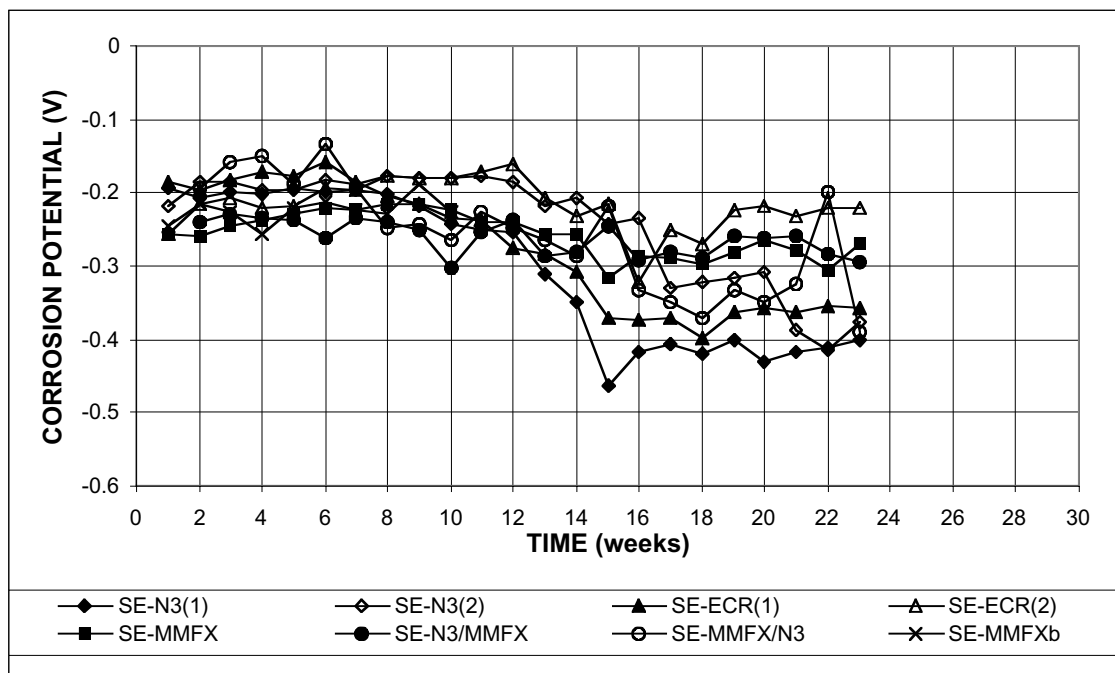


Figure 5.16b - Southern Exposure Test. Average corrosion potential vs. CSE, bottom mat. Specimens with $w/c=0.45$, ponded with a 15% NaCl solution.

The chloride content of the concrete at the initiation of corrosion, the “threshold” value, was determined based on six specimens, five for MMFX steel and one for conventional N3 steel. Chloride content was measured as a percent of concrete weight on both an acid-soluble and water-soluble basis (Procedure C of AASHTO T 260-94 and Procedure A of AASHTO T 260-97). Values for MMFX steel ranged from a low of 0.013% on an acid-soluble basis and 0.011% on a water-soluble basis to a high of 0.274% on an acid-soluble basis and 0.265% on a water-soluble basis. On an acid-soluble basis, the intermediate values were 0.095%, 0.100%, and 0.272%, with corresponding values on a water-soluble basis of 0.085%, 0.091%, and 0.258%. The acid and water-soluble values for conventional steel were 0.030 and 0.025%. Samples were obtained immediately following the first reading in which the corrosion potential had dropped below -350 mV, except that the acid-soluble/water-soluble 0.100%/0.091% reading for MMFX was obtained two weeks following the initial reading below -350 mV. To help select the values that are the most appropriate for use in determining the life expectancy of a reinforced concrete bridge deck, an additional set of tests were performed using simulated concrete pore solution, with various additions of NaCl, to produce NaCl molal ion concentrations of 0.2, 0.4, 0.6, 0.7, 1.0, 1.6, and 6.04. This analysis established that conventional steel is passive in the 0.2 and 0.4 m ion solutions, but not in the 0.6 m ion and higher concentration solutions. MMFX steel lost its passivity for the 1.6 and 6.04 m ion solutions. Based on titration, the Cl^-/OH^- ion ratios for the 0.4 and 1.6 m ion solutions were 0.321 and 1.246, respectively. Thus, the chloride corrosion threshold for MMFX steel appears to be no more than four times higher than it is for conventional steel. Based on the acid and water-soluble values obtained for conventional steel (0.030%/0.025%), the intermediate values, 0.095%/0.085% and 0.100%/0.091%, appear most applicable for MMFX steel. The scatter in the results may be due to a sensitivity of MMFX steel to conditions at the steel surface, as discussed earlier in reference to the bent bar SE tests.

The chloride contents can be converted to weight concentrations on a cubic yard basis using the unit weight of the concrete. For a concrete unit weight of 3777 lb/yd³, threshold chloride contents of 1.04 and 0.94 lb/yd³ are obtained for conventional steel, on an acid and water-soluble basis, respectively. These values match those obtained in earlier studies (1.0 to 1.4 lb/yd³) on an acid-soluble basis. The corresponding values for MMFX steel are 3.60 and 3.32 based on the average of the two intermediate readings. Chloride sampling will continue throughout the duration of the Southern Exposure tests.

Cracked Beam Tests — The cracked beam tests simulate the corrosion behavior of bars in decks in which chlorides have rapid access to the steel due to the formation of cracks in the concrete. These specimens are used to evaluate the corrosion performance of MMFX, conventional, and epoxy-coated reinforcement. Figures 5.17 and 5.18 show the average corrosion rate and average total corrosion loss, respectively, for the three types of steel.

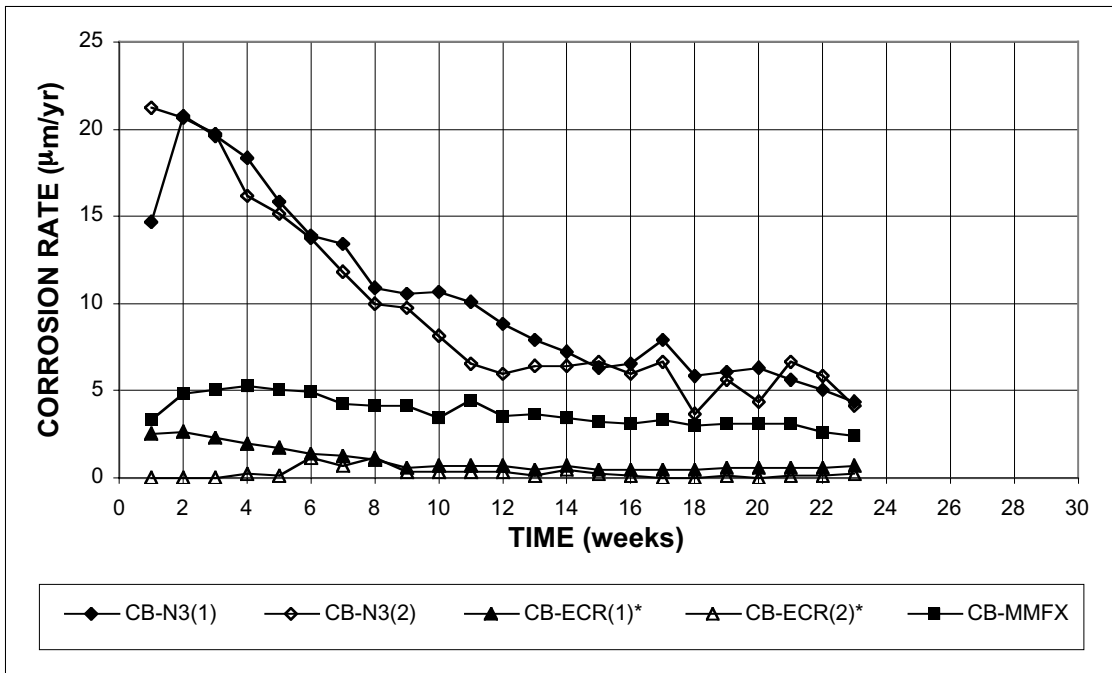


Figure 5.17 - Cracked Beam Test. Average corrosion rate, specimens with $w/c=0.45$, ponded with a 15% NaCl solution.

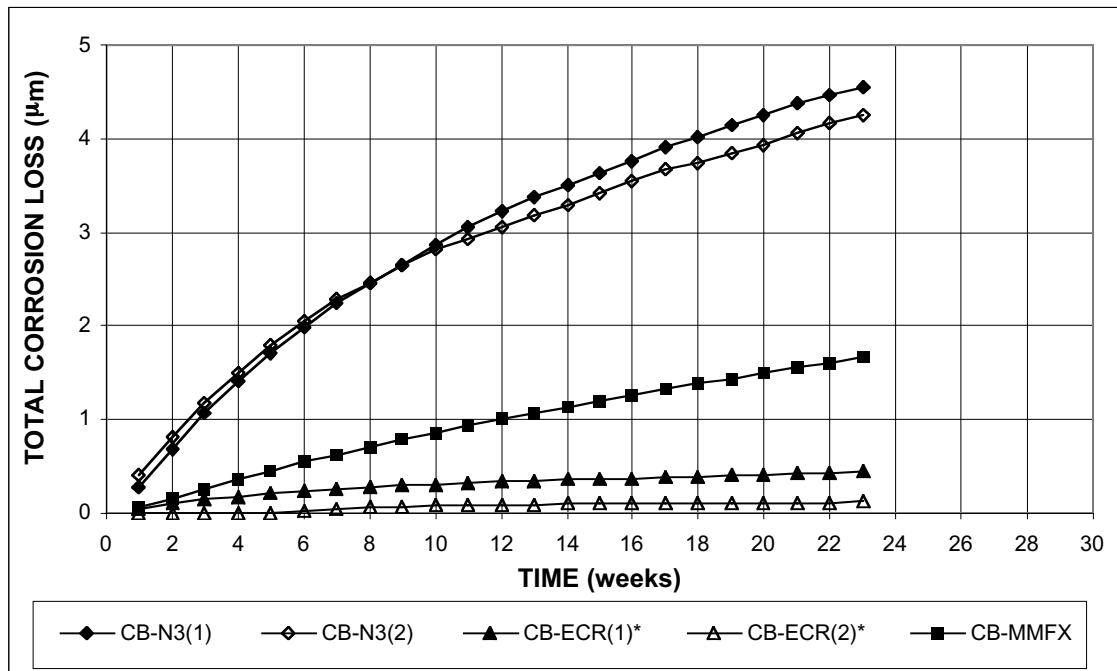


Figure 5.18 - Cracked Beam Test. Average total corrosion loss, specimens with $w/c=0.45$, ponded with a 15% NaCl solution.

* Based on total area of bar exposed to solution

At 23 weeks, the conventional steel exhibits the highest average total corrosion loss, about $4.4\ \mu\text{m}$, at average corrosion rates ranging from a high of $21\ \mu\text{m/yr}$ at one week to a low of $3.5\ \mu\text{m/yr}$ at 18 weeks. This is followed by MMFX steel, with an average total corrosion loss of $1.7\ \mu\text{m}$ at average corrosion rates ranging from a high of $5.5\ \mu\text{m/yr}$ at three weeks to a low of $2.4\ \mu\text{m/yr}$ at 23 weeks. The lowest corrosion, based on full bar area, is exhibited by the ECR specimens, penetrated by four $\frac{1}{8}$ -in. diameter holes in the epoxy. At 23 weeks, the ECR specimens exhibit a total corrosion loss of about $0.3\ \mu\text{m}$ at corrosion rates ranging from a high of $2.5\ \mu\text{m/yr}$ at two weeks to a low of $0.3\ \mu\text{m/yr}$ at 23 weeks. Based on total bar area, the six ECR specimens exhibit a total corrosion loss equal to 7.5% of that exhibited by the conventional reinforcement, while the MMFX steel exhibits a total corrosion loss equal to 37% of that exhibited by the conventional steel. The corrosion rate and total corrosion loss of the ECR bars based on the exposed surface is extremely high, as shown in Figs. 5.19 and 5.20, respectively. The results are similar to that observed for the ECR macrocell specimens. As in the macrocell tests, unprotected bars are used at the cathode. It is expected that, even with the bare cathodes, corrosion rates would have been unmeasurable had the epoxy coating not been damaged in the top bars.

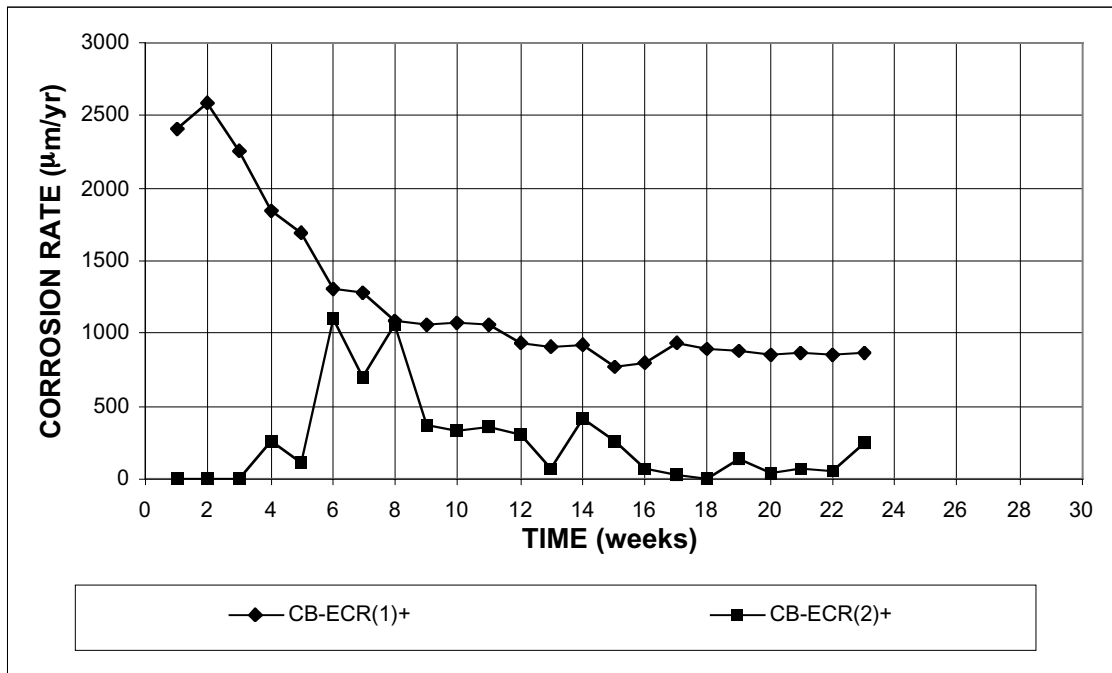


Figure 5.19 - Cracked Beam Test. Average corrosion rate, epoxy-coated bars, specimens with $w/c=0.45$, ponded with a 15% NaCl solution.

The average corrosion potentials for the top and bottom layers of steel are shown in Figs. 5.21a and 5.21b, respectively. The results demonstrate that most of the top bars were undergoing active corrosion by the end of the first week; the corrosion potentials have been nearly constant over 23 weeks; and the range in average potentials is fairly narrow. The specimens with the

damaged epoxy coating in group ECR(1) exhibit the most negative corrosion potentials, with values more negative than -600 mV, while the MMFX specimens exhibit corrosion potentials of about -520 mV. Except for ECR(2), the corrosion potentials of the bottom steel begin to drop by the second week, demonstrating relatively easy access of chlorides to the steel because of the presence of the crack. The bottom layer of the conventional steel specimens, on the average, begins active corrosion in week 8; this occurs for ECR specimens in weeks 15 and 16. At 23 weeks, the MMFX specimens are the only group with bottom bars that have not exhibited an average corrosion potential that is more negative than -350 mV.

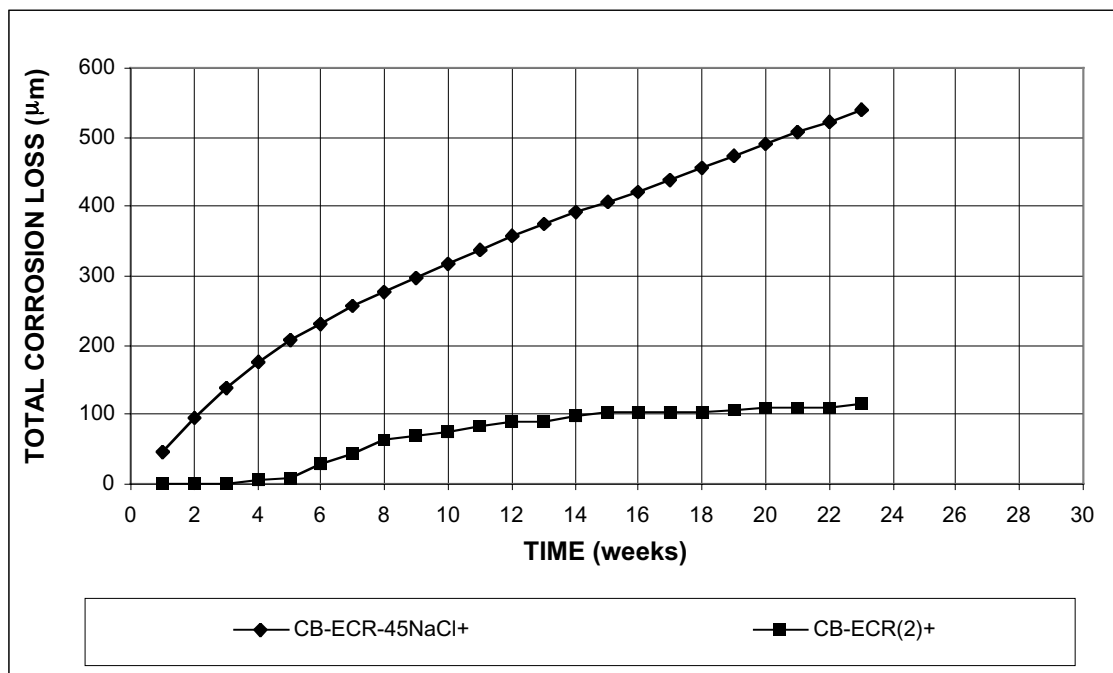


Figure 5.20 - Cracked Beam Test. Average total corrosion loss, epoxy-coated bars, specimens with $w/c=0.45$, ponded with a 15% NaCl solution.

⁺ Based on exposed area of steel, four $\frac{1}{8}$ -in diameter holes in epoxy

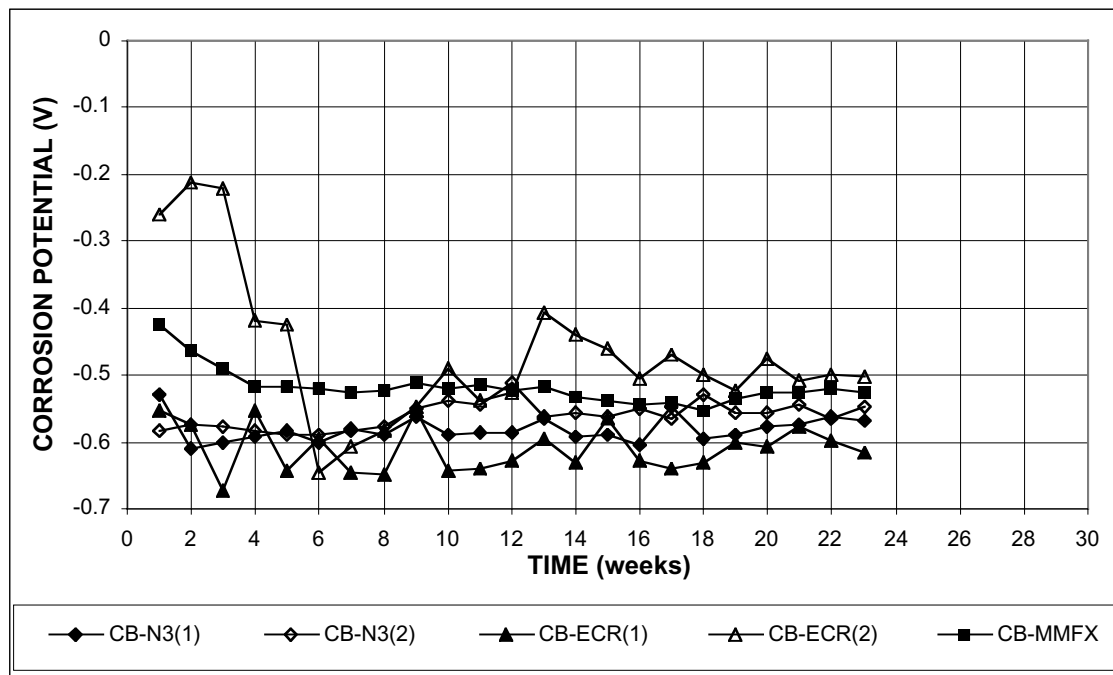


Figure 5.21a - Cracked Beam Test. Average corrosion potential vs. CSE, top mat. Specimens with $w/c=0.45$, ponded with a 15% NaCl solution.

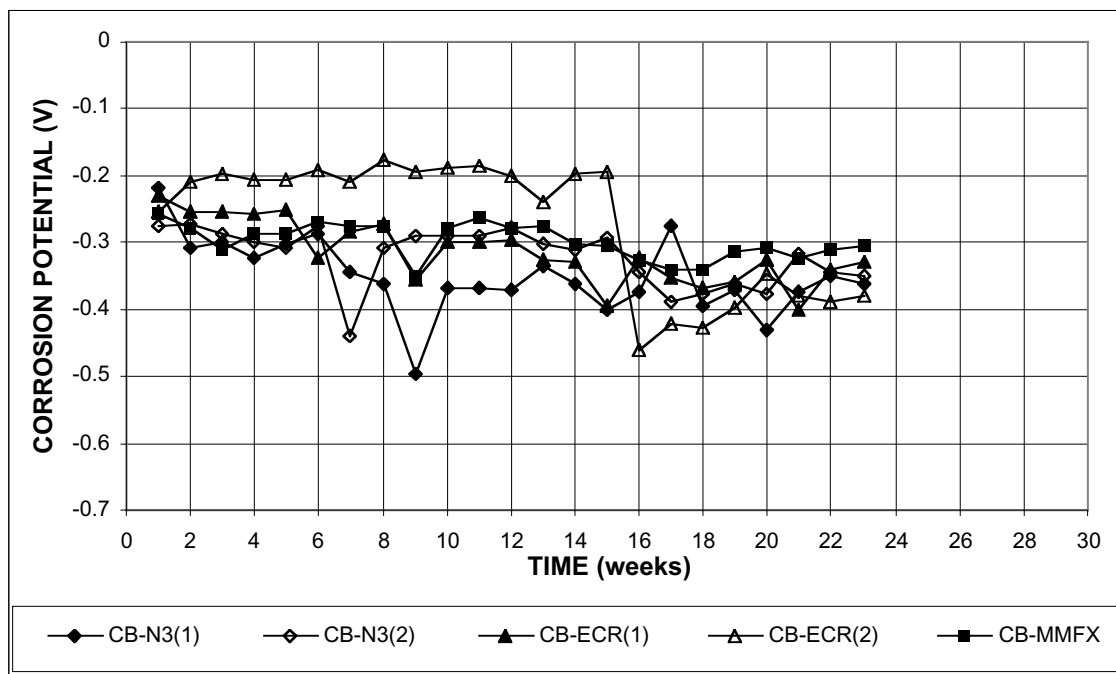


Figure 5.21b - Cracked Beam Test. Average corrosion potential vs. CSE, bottom mat. Specimens with $w/c=0.45$, ponded with a 15% NaCl solution.

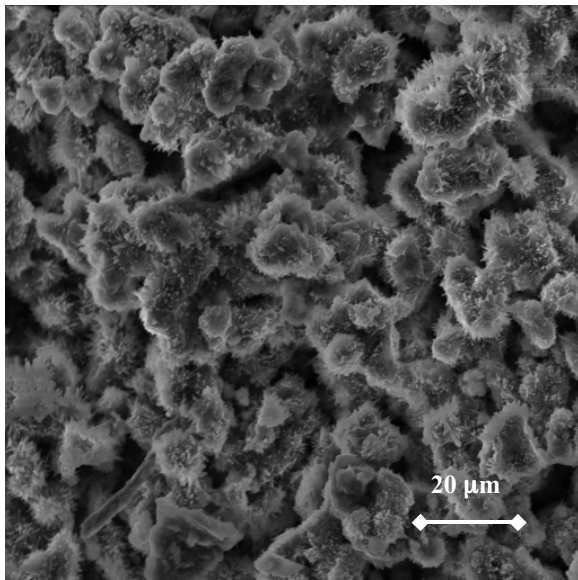
5.4 CORROSION EFFECTS

As discussed in Section 4.4, the scanning electron microscope was used to obtain images of corrosion products on both conventional and MMFX steel. Observations of these corrosion products indicate that they are quite similar for the two materials. Figures 5.22-5.30 present selected images obtained in the study. The images are presented in pairs, with corrosion products for MMFX shown on the left and corrosion products for conventional steel shown on the right. Most images were obtained at a magnification of 680X; a few images were obtained at a magnification of 85X.

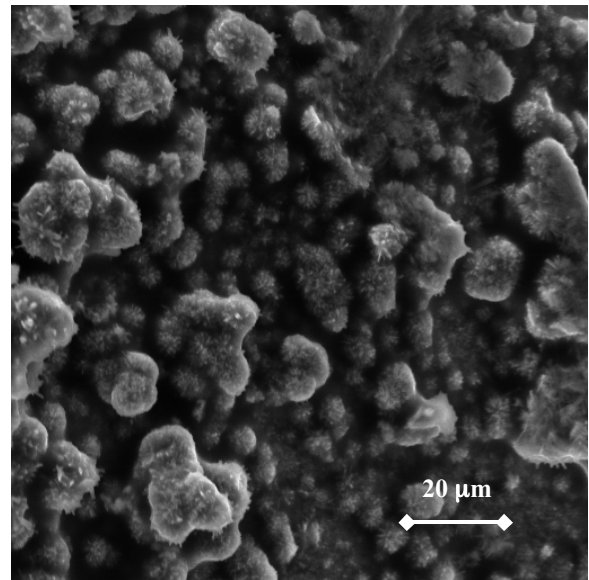
Figures 5.22-5.30 show corrosion products that appear on the anode bars for bare steel macrocell tests. The similarity in some of the images for the two steels is striking. Figure 5.22 shows the corrosion product consisting of nodular structures covered by short fibers. Figures 5.23 and 5.24 show generally smooth, amorphous structures with smaller elements with rather low levels of crystallinity. Figure 5.25 shows a structure similar to that shown in Figs. 5.23 and 5.24, but with rather less angular crystal-like elements. Figure 5.26 shows images, with rather less detail, taken at 85X.

Figures 5.27-5.30 show corrosion products on anodes from mortar-wrapped macrocell tests. Figure 5.27 shows nodular structures similar but somewhat smaller to those seen in Fig. 5.22 for bare steel specimens. Figure 5.27a for MMFX steel shows some of the fibrous structure observed in Fig. 5.22 for both materials. In Fig. 5.27b, the conventional steel corrosion product shown does not appear to be covered with fibers. The images shown in Fig. 5.28 show significant dissimilarity in corrosion products, with the conventional steel (Fig. 5.28b) exhibiting particles with significant levels of crystallinity. Figures 5.29a and b show an amorphous “rock-like” structure that is strikingly similar for the two materials. Finally, Fig. 5.30 shows corrosion products with rather fine structure and low levels of crystallinity. The light regions in Fig. 5.30b are the result of mild charging (build up of negative charge) on the surface of the specimen.

The images shown in this chapter cover only a portion of the range of the corrosion products. However, two key observations can be made. First, the structure of the products can vary widely. Second, products with similar morphology are observed on both metals, suggesting the formation of similar corrosion products.

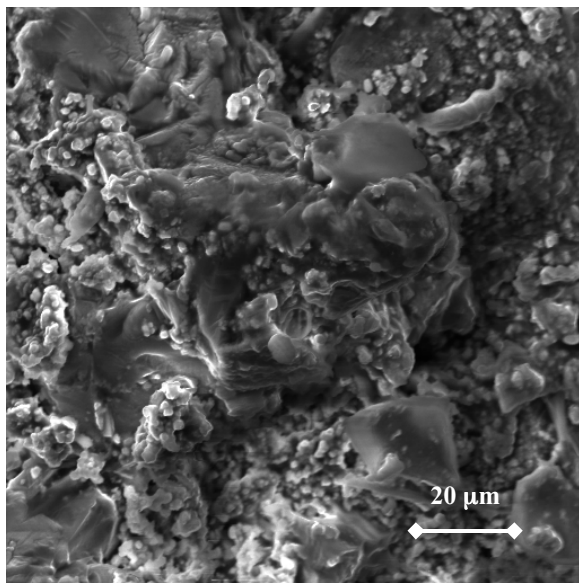


(a)

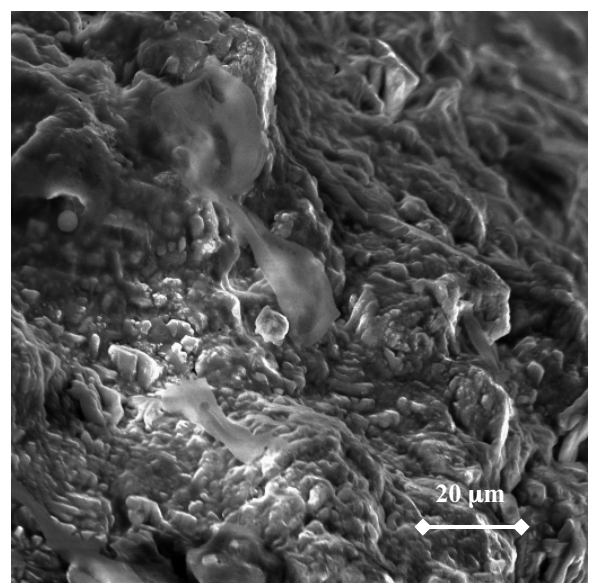


(b)

Figure 5.22 - Nodular corrosion products with fibers on bare bar anodes for (a) MMFX and (b) conventional steel. 680X

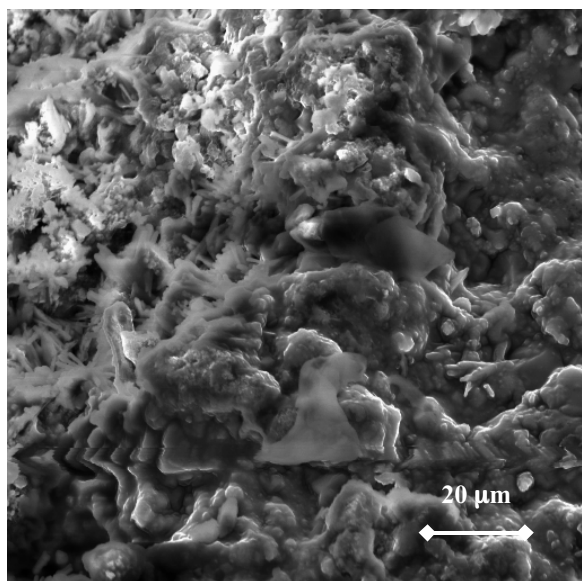


(a)

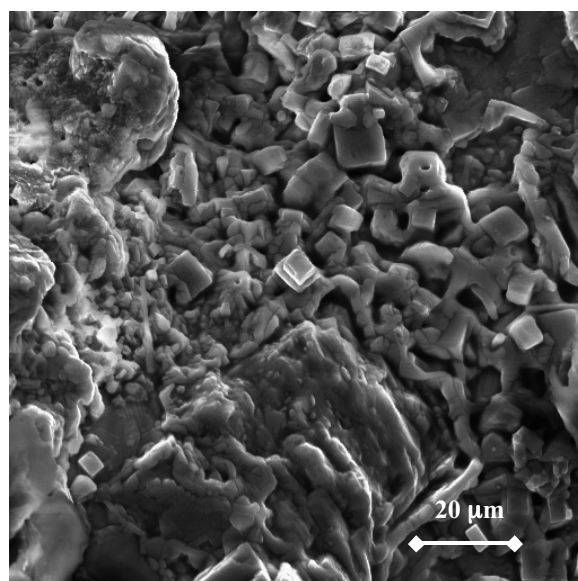


(b)

Figure 5.23 - Amorphous corrosion products with small crystal-like features on bare bar anodes for (a) MMFX and (b) conventional steel. 680X

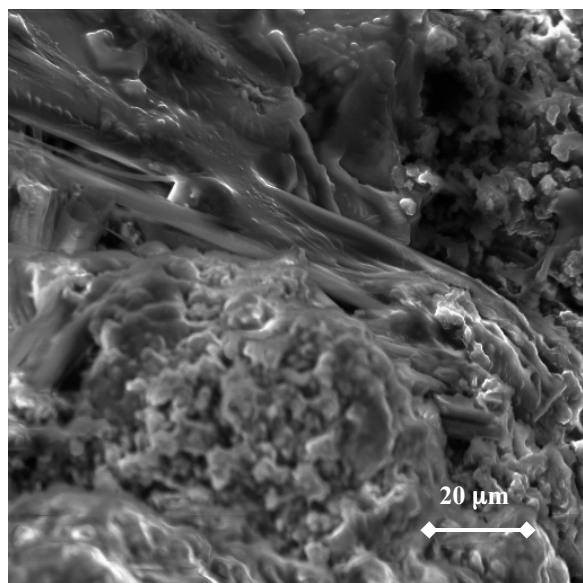


(a)

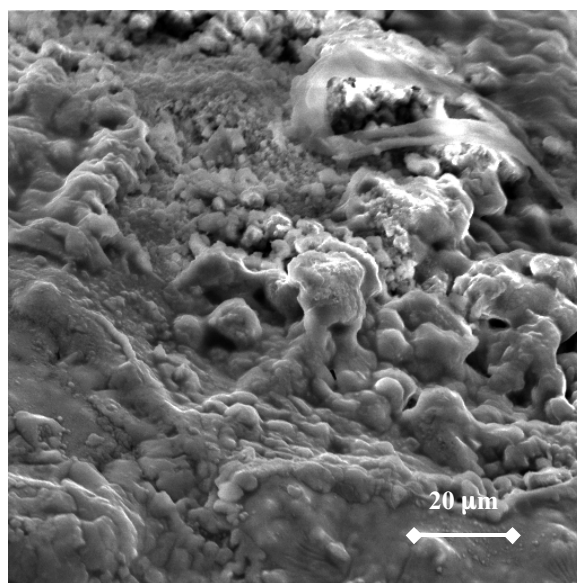


(b)

Figure 5.24 - Amorphous corrosion products with small crystal-like features on bare bar anodes for (a) MMFX and (b) conventional steel. 680X

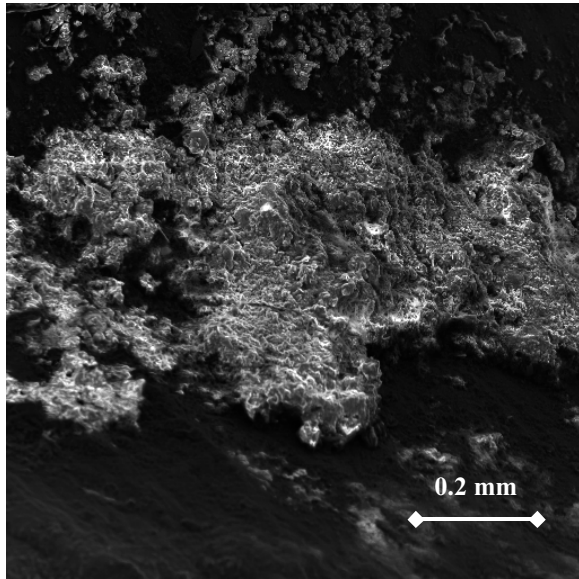


(a)

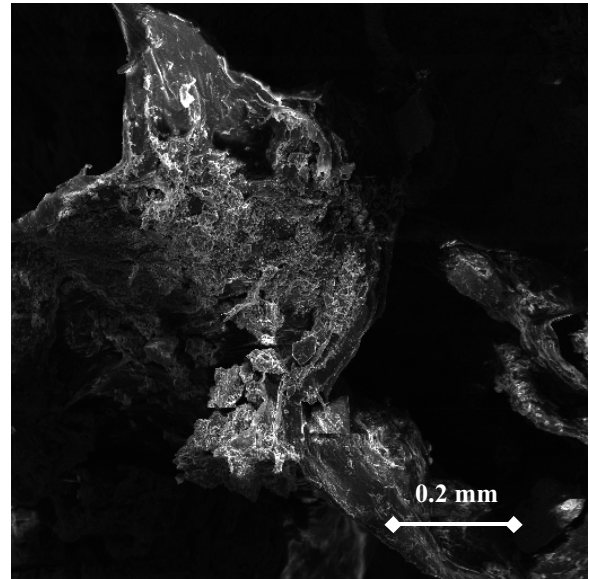


(b)

Figure 5.25 - Amorphous corrosion products on bare bar anodes for (a) MMFX and (b) conventional steel. 680X

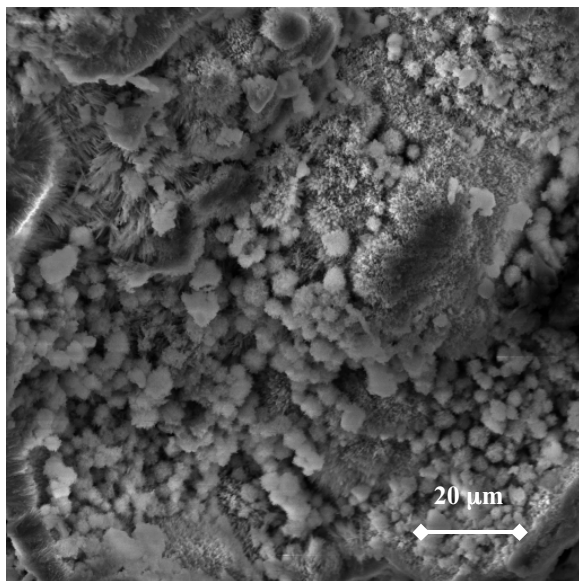


(a)

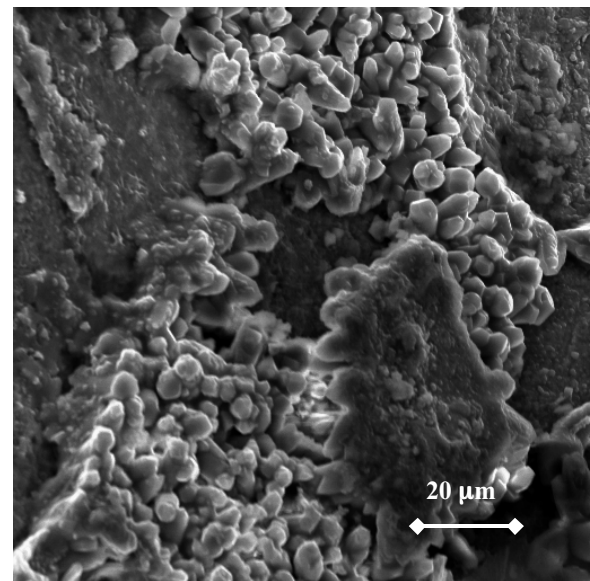


(b)

Figure 5.26 - Corrosion products on bare bar anodes for (a) MMFX and (b) conventional steel. 85X

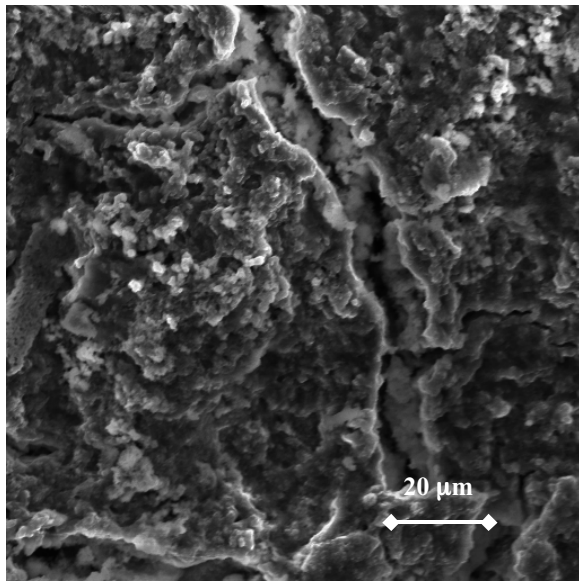


(a)

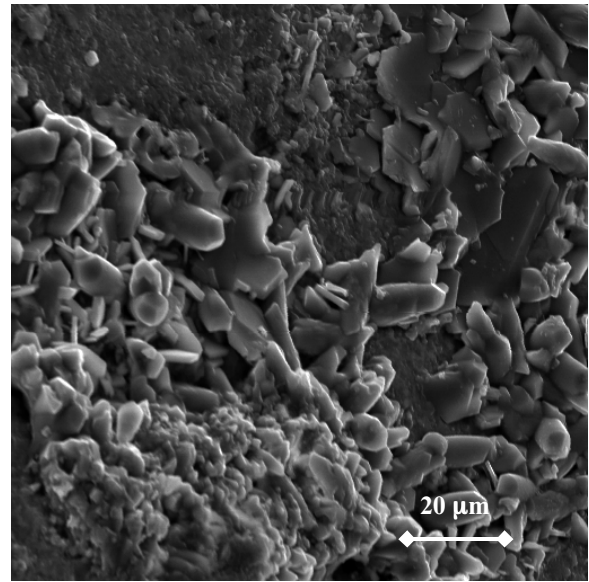


(b)

Figure 5.27 - Nodular corrosion products on anode bars in mortar-wrapped specimens for (a) MMFX and (b) conventional steel. 680X

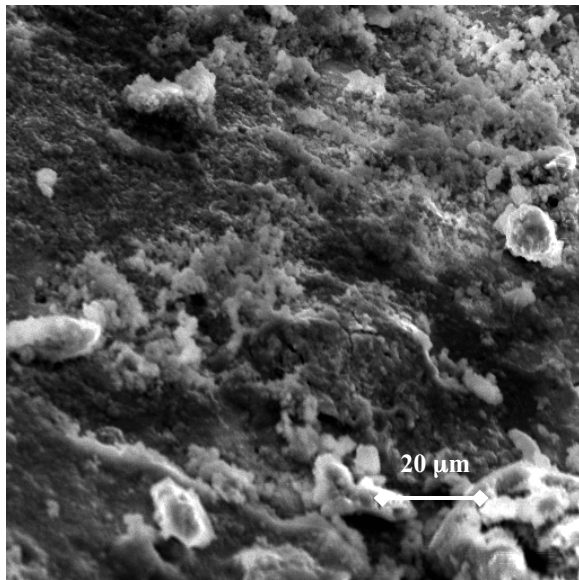


(a)

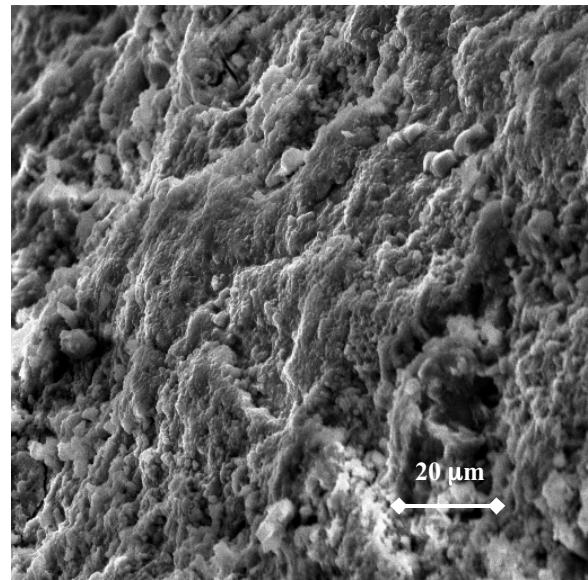


(b)

Figure 5.28 - Corrosion products on anode bars in mortar-wrapped specimens showing differing structure for (a) MMFX and b) conventional steel. 680X



(a)



(b)

Figure 5.29 - Amorphous, rock-like corrosion products for anode bars in mortar-wrapped specimens for (a) MMFX and b) conventional steel. 680X

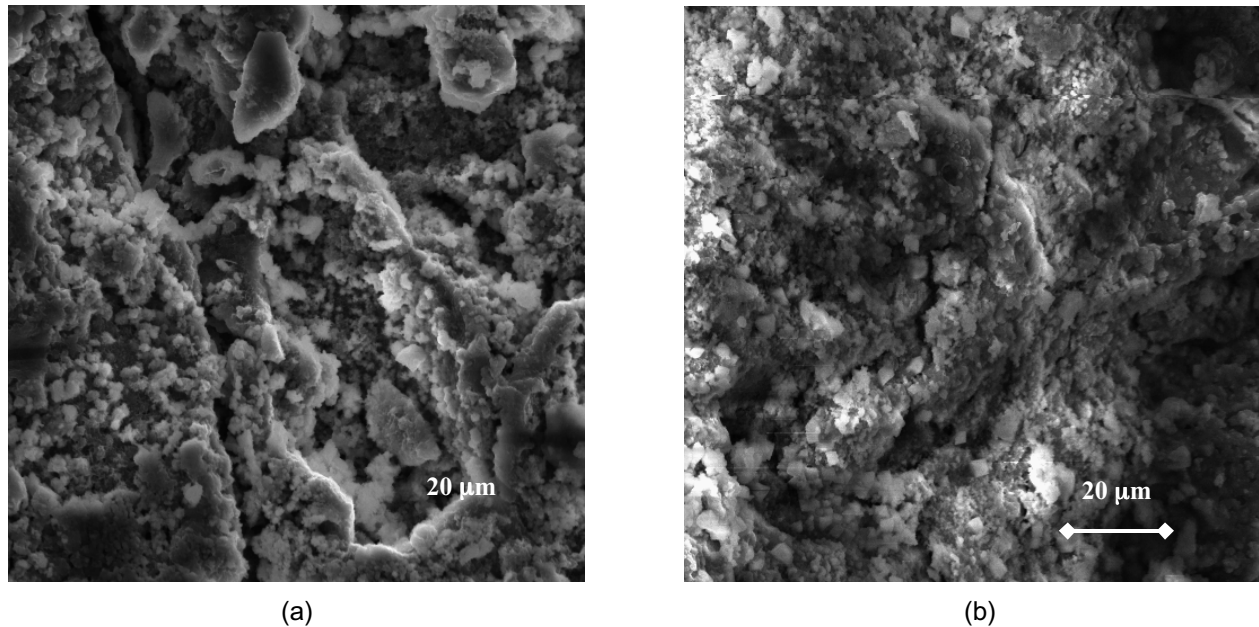


Figure 5.30 - Corrosion products with fine structure for anode bars in mortar-wrapped specimens for (a) MMFX and b) conventional steel. 680X

5.5 LIFE EXPECTANCY AND COST EFFECTIVENESS

The goals of the analyses presented in this section are to estimate the life expectancy and to determine the costs to construct bridge decks using MMFX, conventional, and epoxy-coated reinforcement.

5.5.1 Life Expectancy

As described in Section 4.5.1, the life expectancy of bridge decks is estimated based on both experience and analysis. Estimates are provided for the time to initial repair, or “initial life,” and the time between repairs. Based on experience by SDDOT (Gilsrud 2002), the initial life for bridge decks containing conventional uncoated reinforcement is 10 years under harsh environmental conditions and 25 years in arid conditions. The 25-year period matches that estimated by KDOT (Kepler et al. 2000). For epoxy-coated reinforcement, the SDDOT estimate is 40 years, while the KDOT estimate is 30 years. The estimates for epoxy-coated steel are based on the experience that, over the past 25 years, no bridge decks with epoxy-coated reinforcement required repair due to corrosion damage in either state.

Analysis is required to obtain an estimate for the time to repair of bridges with MMFX steel. The prototype design used for the estimate is a bridge deck with a total deck thickness of 8.5 in. and cover on the top layer of steel of 2.5 in. Time to first repair is estimated based on (1) the chloride content required for corrosion initiation, (2) the time required to reach that chloride concentration at the level of the steel, and (3) the time required for a thickness loss of 0.025 mm (0.00098 in.), which will produce a volume of corrosion products that will crack the concrete (Pfeifer 2000).

Estimates of the chloride concentrations required for corrosion initiation are presented in section 5.2.3. For conventional steel, values of 1.04 and 0.94 lb/yd³ were obtained on an acid and water-soluble basis, respectively. For MMFX steel, values of 3.60 and 3.32 lb/yd³ were obtained. These chloride concentrations can be used in conjunction with data obtained from bridge decks to estimate the time to corrosion initiation.

Miller and Darwin (2000) reported water-soluble chloride concentrations from 40 reinforced concrete bridge decks. Samples were obtained at crack locations (on cracks) and in uncracked concrete (off cracks). The values obtained on cracks are used to estimate the time required to reach specific chloride concentrations. For each concrete placement on the 40 decks, three locations each were sampled on cracks and off cracks. At each location, samples were obtained at $\frac{3}{4}$ in. increments, to a depth of $3\frac{3}{4}$ in. (a total of five samples). To estimate the chloride concentration $2\frac{1}{2}$ in. from the deck surface, a best-fit curve is obtained using four of the samples at each location; the (typically) high chloride value in the upper $\frac{3}{4}$ in. of the deck is discarded for the purpose of this analysis. Background values of chloride concentration (obtained at depth in uncracked concrete) are subtracted from these values and the results are plotted versus age in Fig. 5.31. The data in Fig. 5.31 represents a total of 249 sampling locations. A best-fit line is used to estimate the time required to achieve a specific chloride concentration. The average background chloride concentration for the current data is 0.30 lb/yd³. The best-fit line for net chloride content versus age is

$$\text{net chloride content} = 0.0427 \times \text{age in months} \quad (5.1)$$

Using the corrosion threshold chloride contents for conventional (0.94 lb/yd³) and MMFX steel (3.32 lb/yd³) in conjunction with Eq. (5.1) and an average background chloride concentration of 0.30 lb/yd³ results in estimated times-to-corrosion-initiation of approximately 15 months for conventional steel and 71 months for MMFX Microcomposite steel.

Tables 5.10 and 5.11 summarize the average corrosion rates for the different steels. For conventional and MMFX steel, respectively, these values are 35.6 and 13.3 $\mu\text{m/yr}$ for bare steel macrocell specimens at 15 weeks, 17.6 and 10.5 $\mu\text{m/yr}$ for mortar-wrapped macrocell specimens at 15 weeks, 4.3 and 2.4 $\mu\text{m/yr}$ for cracked beam specimens at 23 weeks, and 3.6 and 0.6 $\mu\text{m/yr}$ for Southern Exposure specimens at 23 weeks. The high corrosion rate of the bent MMFX Southern Exposure specimens (7 $\mu\text{m/yr}$) is not considered. The corrosion rates obtained for the cracked beam specimens are selected as the most realistic, since the chloride contents used for the analysis are based on values obtained at cracks. These values are modified, however. As shown in Fig. 5.12, the corrosion rates of the cracked beam specimens decline steadily after achieving a relatively high value during the first several weeks of the test. Thus, corrosion rates equal to one-half of those measured at 23 weeks are used to determine life expectancy.

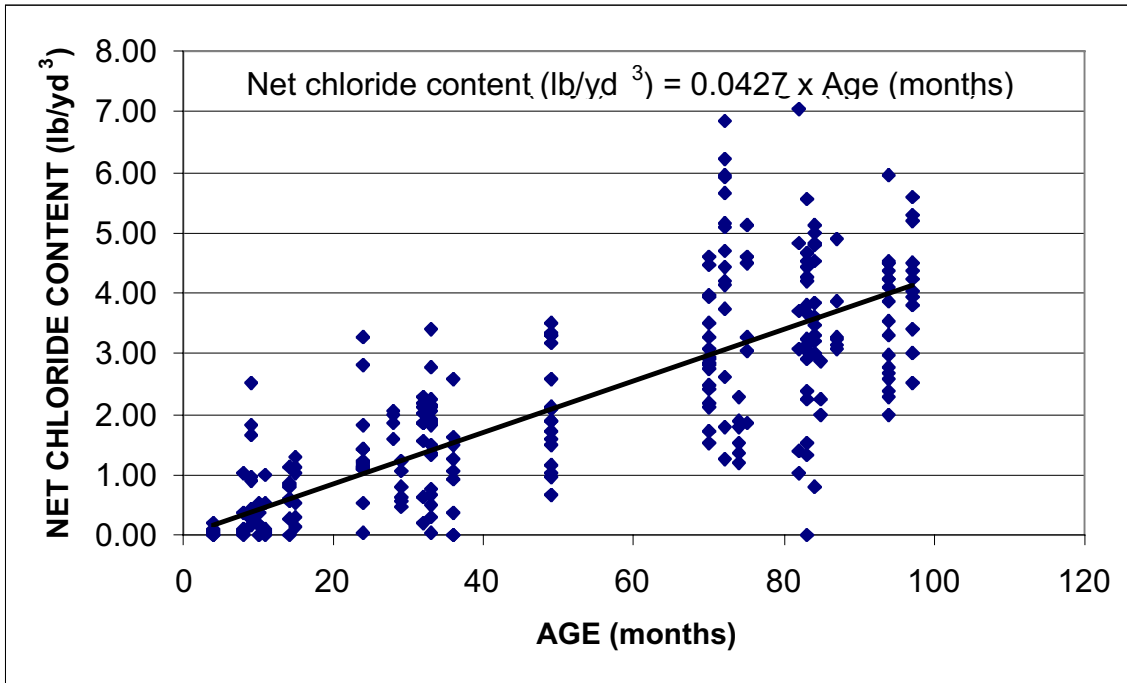


Figure 5.31 - Increase in water-soluble chloride content over background chloride content versus age for 40 bridge decks in Kansas [data from Miller and Darwin (2000)]

Using $0.025 \text{ mm} = 25 \text{ }\mu\text{m}$ as the thickness loss that will result in a volume of corrosion products that will crack concrete (Pfeifer 2000), in conjunction with the calculated times to corrosion initiation, results in periods of approximately 13 years to first repair for conventional steel and 27 years to first repair for MMFX steel. The value for conventional steel matches the experience in many states (Kepler et al. 2000). For completeness, initial values of 27, 30, and 35 years are used in the next section to determine the cost effectiveness of MMFX Microcomposite steel.

Based on experience (Kepler et al. 2000), a value of 25 years is used as the time to second and subsequent repairs for all types of reinforcement.

5.5.2 Cost Effectiveness

Cost effectiveness is evaluated using a typical 8.5 in. bridge deck containing conventional, epoxy-coated, or MMFX reinforcement. The costs and design assumptions are described in Section 4.5.2. Based on the structural evaluations presented in Section 5.2.3, the cost comparisons developed in Section 4.5.2 are based on equal quantities of reinforcement, independent of the reinforcing material used.

As described in Section 5.5.1, for bridge decks containing conventional steel, repair cycles are calculated based on estimates provided by SDDOT (Gilsrud 2002), with a 10-year initial life under harsh environmental conditions and a 25-year initial life under arid conditions. Cost estimates for bridge decks containing epoxy-coated steel are obtained using values of 35 and 40 years for the initial life. The initial life for bridges reinforced with MMFX steel is

calculated using 27, 30, and 35 years. In all cases, additional repairs are based on 25-year cycles for the 75-year economic life used in this analysis.

Comparisons are also included using estimates from an earlier study for the Kansas Department of Transportation (Kepler et al. 2000) for the 8.5 in. bridge deck using conventional and epoxy-coated reinforcement. The initial lives estimated by KDOT officials are 25 and 30 years for bridges containing conventional and epoxy-coated reinforcement, respectively. A 25-year repair cycle is also used for the analyses based on the KDOT estimates.

Cost effectiveness is estimated based on the present value of the costs for each of the bridge decks using discount rates of 2, 4, and 6%. The present value of repair and replacement costs is calculated using Eq. (5.1).

$$P = F \times (1 + i)^{-n} \quad (5.2)$$

where P = present worth, F = cost of repair or replacement, i = discount rate (%/100), and n = time to repair or replacement (in years).

Table 5.12 summarizes the repair schedules and cost estimates for the reinforcement options evaluated. The lowest cost option for all discount rates is the bridge deck containing epoxy-coated reinforcement, based on a 40-year initial life. At a 2% discount rate, the cost is \$261/yd². The next lowest cost option is the deck containing epoxy-coated reinforcement, with a 35-year initial life (\$276/yd² at 2% discount rate). The highest cost option is the deck with conventional steel subjected to harsh exposure. With an initial life of 10 years, the present value of the costs over a 75-year economic life is \$444/yd². Unprotected steel subjected to an arid environment costs \$312/yd² at a 2% discount rate.

Table 5.12 – Cost estimates and repair schedules for bridge decks containing conventional, epoxy-coated and MMFX Microcomposite steel

Reinforcement in deck	New cost (\$/yd ²)	Repair 1 cost (\$/yd ²)	Time to repair 1 (years)	Repair 2 cost (\$/yd ²)	Time to repair 2 (years)	Repair 3 cost (\$/yd ²)	Time to repair 3 (years)	Present value of costs at 2% (\$/yd ²)	Present value of costs at 4% (\$/yd ²)	Present value of costs at 6% (\$/yd ²)
South Dakota Decks										
Conventional- Harsh exposure	112	\$204	10	\$204	35	\$204	60	\$444	\$321	\$259
Conventional - Arid exposure	112	\$204	25	\$204	50			\$312	\$217	\$171
Epoxy-coated	112	\$204	35	\$204	60			\$276	\$183	\$145
	112	\$204	40	\$204	65			\$261	\$170	\$136
MMFX	124	\$204	27	\$204	52			\$316	\$221	\$176
	124	\$204	30	\$204	55			\$305	\$210	\$168
	124	\$204	35	\$204	60			\$288	\$195	\$157
Kansas Decks										
Conventional	110	\$216	25	\$216	50			\$322	\$221	\$172
Epoxy-Coated	114	\$216	30	\$216	55			\$306	\$206	\$160

The cost for MMFX steel ranges from \$316/yd² using a 27-year initial life to \$288/yd² using a 35-year initial life based on a 2% discount rate.

Costs estimated using KDOT figures are similar to those used for the current analysis. The new deck cost is estimated to be \$110/yd² using conventional reinforcement and \$114/yd² using epoxy-coated reinforcement, compared to the cost for SDDOT bridge decks, which is estimated to be \$112/yd² for decks containing either conventional or epoxy-coated steel. The repair cost for the KDOT bridge is estimated to be \$216/yd², compared with \$204/yd² for the SDDOT typical bridge. The present value of the costs for the KDOT bridge decks using conventional and epoxy-coated steel is estimated to be \$322/yd² and \$306/yd², respectively, at a 2% discount rate. The discrepancy between the cost estimates for Kansas and South Dakota bridges using epoxy-coated reinforcement is due to the longer initial life used in the SDDOT analysis.

Overall, the bridge decks containing MMFX Microcomposite steel do not appear to be cost effective when compared to decks containing epoxy-coated reinforcement. To become cost effective, deck design criteria will have to be modified to allow a lower percentage of MMFX steel to be used. In such a case, the effects of increased cracking on deck serviceability and durability will have to be evaluated.

5.6 CONCLUSIONS

The following conclusions are based on the test results and analyses presented in this report.

1. MMFX Microcomposite steel reinforcing bars exhibit yield strengths equal to approximately twice that required of conventional Grade 60 reinforcing steel. Average values range from 110 to 122 ksi, based on the 0.2% offset method and from 128 to 138 ksi, based on 0.7% strain. Tensile strengths range from 161 to 169 ksi. Elongations average approximately 7%, the minimum requirement for ASTM A 615 Grade 75 reinforcement; some individual samples fail to meet this criterion. MMFX reinforcement satisfies ASTM A 615 bend requirements.

2. Most of the MMFX Microcomposite steel bars tested satisfy the mechanical property requirements of high-strength steel bars for prestressing concrete, as specified in ASTM A 722, if the yield strength is based on 0.7% strain.

3. The MMFX Microcomposite steel bars satisfy the requirements for bar geometry specified in ASTM A 615 and provide relative rib areas within or above the normal range in U.S. practice. The bars will provide satisfactory bond strength with concrete.

4. X-ray microanalysis indicates that the chemistry of MMFX steel is consistent for bars within the same heat and very close for the two heats analyzed.

5. Depending on the bridge deck design, use of MMFX Microcomposite steel provides few or no alternative designs that will satisfy all AASHTO bridge design criteria.

6. The corrosion threshold chloride content for MMFX Microcomposite steel is approximately four times higher than the corrosion threshold for conventional reinforcement.

The corrosion rate for MMFX Microcomposite steel is between one-third and two-thirds that of conventional reinforcing steel. In all evaluations, epoxy-coated steel meeting the requirements of ASTM A 775 provides superior corrosion performance to MMFX Microcomposite steel. MMFX Microcomposite steel appears to corrode when the surface is exposed to moist air and chlorides but not in contact with concrete or submerged in water.

7. Similar corrosion products are deposited on the surfaces of MMFX Microcomposite steel and conventional reinforcing steel.

8. Bridge decks containing MMFX Microcomposite reinforcing steel will require repair due to corrosion-induced concrete cracking approximately 30 years after construction, compared to conventional bridge decks which require repair in 10 to 25 years, depending on exposure conditions. Bridge decks containing epoxy-coated reinforcement will require repair 30 to 40 years after construction.

9. Bridge decks containing MMFX Microcomposite steel do not appear to be cost effective when compared to bridge decks containing epoxy-coated reinforcement.

CHAPTER 6

IMPLEMENTATION RECOMMENDATIONS

The evaluations and test results presented in this report lead to the following implementation recommendations.

1. MMFX Microcomposite reinforcing steel should not be used as a direct replacement for epoxy-coated reinforcement without the use of a supplementary corrosion protection system. Use of the material in its current form is not recommended for reinforced concrete bridge decks in South Dakota.

This recommendation is based on the observations that, while MMFX reinforcing steel requires a higher corrosion threshold and corrodes at a lower rate than conventional reinforcement, its corrosion-resistant properties are (1) not superior to that of epoxy-coated reinforcement (Section 5.3) and (2) bridge decks constructed with MMFX Microcomposite steel will have a shorter life expectancy, a higher first cost, and a higher lifetime cost than bridge decks constructed with epoxy-coated reinforcement (Section 5.5). The cost effectiveness of bridges constructed with MMFX reinforcement would be improved if the total reinforcement in the bridge deck were reduced, taking advantage of the material's higher strength. However, concerns of serviceability, especially bridge deck cracking, mitigate against this, as discussed in Section 5.2.3.

2. MMFX Microcomposite steel meets or comes close to meeting the requirements for high-strength steel bars for prestressing concrete as specified in ASTM A 722. Specifications for reinforcing materials should be modified to allow its use in post-tensioned prestressed concrete construction.

As discussed in Section 5.2.1, MMFX Microcomposite steel is a high-strength material with properties similar to those specified under ASTM A 722. With a price of approximately \$0.40/lb (Section 4.5.2), MMFX steel should be competitive with other steels that satisfy this standard. Its high fracture toughness, shown in tests run for the MMFX Steel Corporation of America (Section 5.1.1) indicates that the steel provides other, desirable mechanical properties that are not available in more traditional reinforcing materials.

3. SDDOT should continue to use epoxy-coated reinforcement to provide corrosion protection in bridge decks until such time as a superior corrosion protection system becomes available.

This recommendation is based on superior corrosion performance of epoxy-coated steel compared to MMFX steel (Section 5.3) and the superior life expectancy and cost effectiveness of bridge decks containing epoxy-coated reinforcement compared to the alternatives evaluated in this study.

REFERENCES

AASHTO (1996). *Standard Specifications for Highway Bridges*, American Association of State Highway and Transportation Officials, Washington, DC, 16th edition.

AASHTO T 260-94 (1994). "Standard Test Method for Sampling and Testing for Chloride Ion in Concrete and Concrete Raw Materials," *Standard Specifications for Transportation Materials and Methods of Sampling and Testing*, 17th Edition, Part II Tests, 1995, American Association of State Highway and Transportation Officials, pp. 650-664.

AASHTO T 260-97 (1997). "Standard Test Method for Sampling and Testing for Chloride Ion in Concrete and Concrete Raw Materials," *Standard Specifications for Transportation Materials and Methods of Sampling and Testing*, 19th Edition, Part II Tests, 1998, American Association of State Highway and Transportation Officials, pp. 925-931.

ACI Committee 215 (1992). "Considerations for Design of Concrete Structures Subjected to Fatigue Loading (ACI 215R-74)," *ACI Manual of Concrete Practice 2001*, written 1974, revised 1992, reapproved 1997, American Concrete Institute, Farmington Hills, MI, Part 1.

ACI Committee 408 (2001). *Splice and Development Length of High Relative Rib Area Reinforcing Bars in Tension* (ACI 408.3-01), American Concrete Institute, Farmington Hills, MI, 6 pp.

ASTM A 775/A 775M-00 (2001). "Standard Specification for Epoxy-Coated Steel Reinforcing Bars," *Annual Book of ASTM Standards, 2001*, American Society for Testing and Materials, West Conshohocken, PA, Vol. 01.04, pp. 385-392.

ASTM A 615/A 615M-00 (2001). "Standard Specification for Deformed and Plain Billet-steel Bars for Concrete Reinforcement," *Annual Book of ASTM Standards, 2001*, American Society for Testing and Materials, West Conshohocken, PA, Vol. 01.04, pp. 296-300.

ASTM A 722/A 722M-98 (2001). "Standard Specification for Uncoated High-Strength Steel Bars for Prestressing Concrete," *Annual Book of ASTM Standards, 2001*, American Society for Testing and Materials, West Conshohocken, PA, Vol. 01.04, pp. 344-347.

ASTM C 305-99 (2001). "Standard Practice for Mechanical Mixing of Hydraulic Cement Pastes and Mortars of plastic Consistency," *Annual Book of ASTM Standards, 2001*, American Society for Testing and Materials, West Conshohocken, PA, Vol. 04.01, pp. 220-222.

ASTM C 778-00 (2001). "Standard Specification for Standard Sand," *Annual Book of ASTM Standards, 2001*, American Society for Testing and Materials, West Conshohocken, PA, Vol. 04.01, pp. 368-370.

ASTM E 23-00 (2001). "Standard Test Methods for Notched Bar Impact Testing of Metallic Materials," *Annual Book of ASTM Standards, 2001*, American Society for Testing and Materials, West Conshohocken, PA, Vol. 03.01, pp. 138-162.

ASTM G 109-99a (2001). "Standard Test Method for Determining the Effects of Chemical Admixtures on the Corrosion of Embedded Steel Reinforcement in Concrete Exposed to Chloride Environments," *Annual Book of ASTM Standards, 2001*, Vol. 3.02, American Society for Testing and Materials, West Conshohocken, PA, pp. 482-486

Axelsson, H., Darwin, D., and Locke, C. E., Jr. (1999). "Influence of Adhesion at Steel/Mortar Interface on Corrosion Characteristics of Reinforcing Steel," *SL Report* 99-4, University of Kansas Center for Research, Lawrence, Kansas, 55 pp

Cady, P. D., and Gannon, E. J. (1992). *Condition Evaluation of Concrete Bridges Relative to Reinforcement in Concrete*, Vol. 1, State of the Art of Mixing Methods, SHRP-S/FR-92-103; Strategic Highway Research Program, National Research Council, Washington, D.C., 70 pp.

Cano, O. (2002). MMFX Steel Corporation of America. Personal communication.

Chappelow, C. C., McElroy, A. D., Blackburn, R. R., Darwin, D., deNoyelles, F. G., and Locke, C. E. (1992). *Handbook of Test Methods for Evaluating Chemical Deicers*, Strategic Highway Research Program, Nat. Res. Council, Washington, D.C.

Darwin, D. and Graham, E. K. (1993). "Effect of Deformation Height and Spacing on Bond Strength of Reinforcing Bars," *ACI Structural Journal*, Vol. 90, No. 6, pp. 646-657.

Darwin, D. (1995). "Corrosion-Resistant Steel Reinforcing Bars, Summary Report," *SL Report* 95-2, University of Kansas Center for Research, Lawrence, KS, May, 22 pp.

Darwin, D., Locke, C. E., Senecal, M. R., Schwensen, S. M., Smith, J. L. (1996). "Corrosion Resistant Steel Reinforcing Bars," *Materials for the New Millennium*, K. P. Chong, Ed., ASCE, Reston, VA, pp. 482-491.

Darwin, D., Tholen, M. L., Idun, E. K., and Zuo, J. (1996a). "Splice Strength of High Relative Rib Area Reinforcing Bars," *ACI Structural Journal*, Vol. 93, No. 1, pp. 95-107.

Darwin, D., Zuo, J., Tholen, M. L., and Idun, E. K. (1996b). "Development Length Criteria for Conventional and High Relative Rib Area Reinforcing Bars," *ACI Structural Journal*, Vol. 93, No. 3, pp. 347-359.

Farzammehr, H. (1985). "Pore Solution Analysis of Sodium Chloride and Calcium Chloride Containing Cement Pastes," *Master of Science Thesis*, University of Oklahoma, Norman, OK, 101 pp.

Farzammehr, H., Dehghanian, C., and Locke, C. E. (1987). "Study of the Effects of Cations on Chloride Caused Corrosion of Steel in Concrete," *Revista Técnica de la Facultad de Ingeniería*, Univ. Zulia, Venezuela, Vol. 10, No. 1, pp. 33-40.

Fliz, J., Akshey, S., Li, D., Kyo, Y., Sabol, S., Pickering, H., and Osseo-Asare, K. (1992). "Condition Evaluation of Concrete Bridges Relative to Reinforcement Corrosion – Volume 2 – Method for Measuring the Corrosion Rate of Steel in Concrete," Strategic Highway Research Program.

Gilsrud, T. (2002). South Dakota Department of Transportation. Personal communication.

Kepler, J. L., Darwin, D., and Locke, C. E. (2000). "Evaluation of Corrosion Protection Methods for Reinforced Concrete Highway Structures," *SM Report* No. 58, University of Kansas Center for Research, Lawrence, KS, 221 pp.

Locke, C. E. (1986). "Corrosion of Steel in Portland Cement Concrete: Fundamental Studies," *Corrosion Effects of Stray Currents and the Techniques for Evaluating Corrosion of Rebars in Concrete*, ASTM STP 906, American Society for Testing and Materials, Philadelphia, pp. 5-14.

Manning, D. G. (1996). "Corrosion Performance of Epoxy-Coated Reinforcing Steel: North American Experience," *Construction and Building Materials*, Vol. 10, No. 5, Jul. pp. 349-365.

Martinez, S. L., Darwin, D., McCabe, S. L., and Locke, C. E. (1990). "Rapid Test for Corrosion Effects of Deicing Chemicals in Reinforced Concrete," *SL Report 90-4*, University of Kansas Center for Research, Lawrence, KS, Aug., 61 pp.

McDonald, D. B., Pfeifer, D. W., and Sherman, M. R., 1998, "Corrosion Evaluation of Epoxy-Coated, Metal-Clad and Solid Metallic Reinforcing Bars in Concrete," Publication No. FHWA-RD-98-153, Federal Highway Administration, Dec. 1998, pp. 137.

Miller, G. G. and Darwin, D., (2002). "Performance and Constructability of Silica Fume Bridge Deck Overlays," *SM Report No. 57*, University of Kansas Center for Research, Lawrence, KS, 423 pp.

MMFX Steel Corporation of America website - <http://www.mmfxsteel.com/>

Perenchio, William F. (1992). "Corrosion of Reinforcing Bars in Concrete," Annual Seminar, Master Builders Technology, Cleveland, OH, Dec.

Pfeifer, D. W., and Scali, M. J. (1981). "Concrete Sealers for Protection of Bridge Structures," *NCHRP Report No. 244*, National Cooperative Highway Research Program, Transportation Research Board, Washington, DC, Dec.

Pfeifer, D. W., 2000, "High Performance Concrete and Reinforcing Steel with a 100-Year Service Life," *PCI Journal*, Vol. 45, No. 3, May-June 2000, pp. 46-54.

Sagues, A. A., Powers, R. G., and Kessler, R. (1994). "Corrosion Processes and Field Performance of Epoxy-Coated Reinforcing Steel in Marine Structures," *Corrosion 94*, Paper No. 299, National Association of Corrosion Engineers, Houston, TX.

Senecal, M. R., Darwin, D., and Locke, C. E., Jr. (1995). "Evaluation of Corrosion-Resistant Steel Reinforcing Bars," *SM Report No. 40*, University of Kansas Center for Research, Lawrence, KS, July, 142 pp.

Smith, J. L., Darwin, D., and Locke, C. E., Jr. (1995). "Corrosion-Resistant Steel Reinforcing Bars Initial Tests," *SL Report 95-1*, University of Kansas Center for Research, Lawrence, KS, April, 43 pp

Smith, Jeffery L. and Virmani, Yash Paul (1996). "Performance of Epoxy-Coated Rebars in Bridge Decks," *Report No. FHWA-RD-96-092*, Federal Highway Administration, Washington, DC.

Zuo, J. and Darwin, D. (2000). "Splice Strength of Conventional and High Relative Rib Area Bars in Normal and High Strength Concrete," *ACI Structural Journal*, Vol. 97, pp. 630-641.

APPENDIX A DETAILS OF STRUCTURAL ANALYSES

Table A.1 - Prestressed Girder Bridge - Negative Moment Region

Steel	Spacing (in)	Max. tensile stress in steel (ksi)	Max. compressive stress in concrete (ksi)	Max. allowable spacing (in.)	Minimum Required Steel		Crack-Control Provisions			Maximum Allowable Steel	
					$1.2M_{cr}$ (k-in.)	ΦMn (k-in.)	$f_{s-allowable}$ Eq. (d) (ksi)	$M_{max-service}$ (k-in.)	$f_{s-service}$ (ksi)	ρ_{max}	ρ
Given Design: Grade 60 No.5	6	20.4	1.231	12.375	82	168	32.5	61.4	20.4	0.0241	0.0095
MMFX No.5	6	20.4	1.231	12.375	82	310	32.5	61.4	20.4	0.0085	0.0095
MMFX No.5	7	23.6	1.302	12.375	82	272	30.8	61.4	23.6	0.0085	0.0081
MMFX No.5	8	26.8	1.368	12.375	82	243	29.5	61.4	26.8	0.0085	0.0071
MMFX No.5	9	30.0	1.430	12.375	82	219	28.4	61.4	30.0	0.0085	0.0063
MMFX No.5	10	33.2	1.490	12.375	82	199	27.4	61.4	33.2	0.0085	0.0057
MMFX No.5	11	36.4	1.546	12.375	82	182	26.5	61.4	36.4	0.0085	0.0052
MMFX No.5	12	39.5	1.600	12.375	82	168	25.8	61.4	39.5	0.0085	0.0048
MMFX No.5	13	42.7	1.652	12.375	82	156	25.1	61.4	42.7	0.0085	0.0044
MMFX No.4	6	30.6	1.422	12.375	82	215	33.1	61.4	30.6	0.0085	0.0061
MMFX No.4	7	35.5	1.510	12.375	82	187	31.4	61.4	35.5	0.0085	0.0052
MMFX No.4	8	40.3	1.592	12.375	82	165	30.0	61.4	40.3	0.0085	0.0045
MMFX No.4	9	45.2	1.669	12.375	82	148	28.9	61.4	45.2	0.0085	0.0040
MMFX No.4	10	50.0	1.742	12.375	82	134	27.9	61.4	50.0	0.0085	0.0036
MMFX No.4	11	54.9	1.811	12.375	82	123	27.0	61.4	54.9	0.0085	0.0033
MMFX No.4	12	59.7	1.878	12.375	82	113	26.2	61.4	59.7	0.0085	0.0030
MMFX No.4	13	64.5	1.942	12.375	82	105	25.6	61.4	64.5	0.0085	0.0028
MMFX No.3	6	53.8	1.773	12.375	82	125	33.7	61.4	53.8	0.0085	0.0033
MMFX No.3	7	62.5	1.890	12.375	82	108	32.0	61.4	62.5	0.0085	0.0028
MMFX No.3	8	71.1	2.000	12.375	82	95	30.6	61.4	71.1	0.0085	0.0025
MMFX No.3	9	79.7	2.103	12.375	82	85	29.4	61.4	79.7	0.0085	0.0022
MMFX No.3	10	88.4	2.200	12.375	82	77	28.4	61.4	88.4	0.0085	0.0020
MMFX No.3	11	97.0	2.293	12.375	82	70	27.5	61.4	97.0	0.0085	0.0018
MMFX No.3	12	105.6	2.381	12.375	82	64	26.7	61.4	105.6	0.0085	0.0016
MMFX No.3	13	114.1	2.466	12.375	82	60	26.0	61.4	114.1	0.0085	0.0015

Table A.2 - Prestressed Girder Bridge - Positive Moment Region

Steel	Spacing (in)	Max. tensile stress in steel (ksi)	Max. compressive stress in concrete (ksi)	Max. allowable spacing (in.)	Minimum Required Steel		Crack-Control Provisions			Maximum Allowable Steel	
					1.2*M _{cr} (k-in.)	ΦMn (k-in.)	f _{s-allowable} Eq. (d) (ksi)	M _{max-service} (k-in.)	f _{s-service} (ksi)	ρ _{max}	ρ
Given Design: Gr60 No. 5/ No. 4 alt.											
	6	19.8	0.945	12.375	82	175	36.0	61.4	19.8	0.0241	0.0064
MMFX No.5	6	16.4	0.878	12.375	82	394	61.9	61.4	16.4	0.0085	0.0077
MMFX No.5	7	19.0	0.930	12.375	82	344	58.8	61.4	19.0	0.0085	0.0066
MMFX No.5	8	21.6	0.979	12.375	82	305	56.3	61.4	21.6	0.0085	0.0058
MMFX No.5	9	24.2	1.025	12.375	82	274	54.1	61.4	24.2	0.0085	0.0052
MMFX No.5	10	26.8	1.068	12.375	82	249	52.2	61.4	26.8	0.0085	0.0046
MMFX No.5	11	29.3	1.110	12.375	82	228	50.6	61.4	29.3	0.0085	0.0042
MMFX No.5	12	31.9	1.149	12.375	82	210	49.2	61.4	31.9	0.0085	0.0039
MMFX No.5	13	34.5	1.188	12.375	82	195	47.9	61.4	34.5	0.0085	0.0036
MMFX No.4	6	24.7	1.023	12.375	82	269	64.0	61.4	24.7	0.0085	0.0049
MMFX No.4	7	28.7	1.087	12.375	82	233	60.8	61.4	28.7	0.0085	0.0042
MMFX No.4	8	32.6	1.148	12.375	82	206	58.1	61.4	32.6	0.0085	0.0037
MMFX No.4	9	36.6	1.205	12.375	82	184	55.9	61.4	36.6	0.0085	0.0033
MMFX No.4	10	40.5	1.258	12.375	82	167	54.0	61.4	40.5	0.0085	0.0030
MMFX No.4	11	44.4	1.310	12.375	82	152	52.3	61.4	44.4	0.0085	0.0027
MMFX No.4	12	48.3	1.359	12.375	82	140	50.8	61.4	48.3	0.0085	0.0025
MMFX No.4	13	52.3	1.406	12.375	82	130	49.5	61.4	52.3	0.0085	0.0023
MMFX No.3	6	43.7	1.286	12.375	82	155	66.2	61.4	43.7	0.0085	0.0027
MMFX No.3	7	50.7	1.373	12.375	82	134	62.9	61.4	50.7	0.0085	0.0023
MMFX No.3	8	57.7	1.454	12.375	82	118	60.2	61.4	57.7	0.0085	0.0020
MMFX No.3	9	64.8	1.530	12.375	82	105	57.8	61.4	64.8	0.0085	0.0018
MMFX No.3	10	71.8	1.602	12.375	82	95	55.8	61.4	71.8	0.0085	0.0016
MMFX No.3	11	78.8	1.670	12.375	82	86	54.1	61.4	78.8	0.0085	0.0015
MMFX No.3	12	85.8	1.736	12.375	82	79	52.6	61.4	85.8	0.0085	0.0013
MMFX No.3	13	92.8	1.798	12.375	82	73	51.2	61.4	92.8	0.0085	0.0012

Table A.3 - Continuous Composite (Steel) Girder Bridge - Negative Moment Region

Steel	Spacing (in)	Max. tensile stress in steel (ksi)	Max. compressive stress in concrete (ksi)	Max. allowable spacing (in.)	Minimum		Crack-Control Provisions			Maximum	
					Required Steel					Allowable Steel	
					1.2*M _{cr} (k-in.)	ΦMn (k-in.)	f _{s-allowable} Eq. (d) (ksi)	M _{max-service} (k-in.)	f _{s-service} (ksi)	ρ _{max}	ρ
Given Design: Grade 60 No.5											
	5.5	23.1	1.469	12.375	82	182	33.4	75.6	23.1	0.0241	0.0104
MMFX No.5	5.5	23.1	1.469	12.375	82	333	33.4	75.6	23.1	0.0085	0.0104
MMFX No.5	6	25.1	1.515	12.375	82	310	32.5	75.6	25.1	0.0085	0.0095
MMFX No.5	6.5	27.0	1.560	12.375	82	290	31.6	75.6	27.0	0.0085	0.0088
MMFX No.5	7	29.0	1.602	12.375	82	272	30.8	75.6	29.0	0.0085	0.0081
MMFX No.5	7.5	31.0	1.644	12.375	82	257	30.1	75.6	31.0	0.0085	0.0076
MMFX No.5	8	33.0	1.684	12.375	82	243	29.5	75.6	33.0	0.0085	0.0071
MMFX No.5	8.5	35.0	1.723	12.375	82	230	28.9	75.6	35.0	0.0085	0.0067
MMFX No.5	9	36.9	1.761	12.375	82	219	28.4	75.6	36.9	0.0085	0.0063
MMFX No.5	9.5	38.9	1.798	12.375	82	208	27.9	75.6	38.9	0.0085	0.0060
MMFX No.5	10	40.9	1.834	12.375	82	199	27.4	75.6	40.9	0.0085	0.0057
MMFX No.5	10.5	42.8	1.869	12.375	82	190	26.9	75.6	42.8	0.0085	0.0054
MMFX No.5	11	44.8	1.903	12.375	82	182	26.5	75.6	44.8	0.0085	0.0052
MMFX No.4	5.5	34.6	1.693	12.375	82	232	34.0	75.6	34.6	0.0085	0.0066
MMFX No.4	6	37.7	1.751	12.375	82	215	33.1	75.6	37.7	0.0085	0.0061
MMFX No.4	6.5	40.7	1.806	12.375	82	200	32.2	75.6	40.7	0.0085	0.0056
MMFX No.4	7	43.7	1.859	12.375	82	187	31.4	75.6	43.7	0.0085	0.0052
MMFX No.4	7.5	46.7	1.910	12.375	82	176	30.7	75.6	46.7	0.0085	0.0048
MMFX No.4	8	49.7	1.959	12.375	82	165	30.0	75.6	49.7	0.0085	0.0045
MMFX No.4	8.5	52.6	2.008	12.375	82	156	29.4	75.6	52.6	0.0085	0.0043
MMFX No.4	9	55.6	2.054	12.375	82	148	28.9	75.6	55.6	0.0085	0.0040
MMFX No.3	5.5	60.9	2.106	12.375	82	136	34.7	75.6	60.9	0.0085	0.0036
MMFX No.3	6	66.2	2.183	12.375	82	125	33.7	75.6	66.2	0.0085	0.0033
MMFX No.3	6.5	71.6	2.256	12.375	82	116	32.8	75.6	71.6	0.0085	0.0030
MMFX No.3	7	76.9	2.327	12.375	82	108	32.0	75.6	76.9	0.0085	0.0028
MMFX No.3	7.5	82.2	2.396	12.375	82	101	31.3	75.6	82.2	0.0085	0.0026
MMFX No.3	8	87.5	2.462	12.375	82	95	30.6	75.6	87.5	0.0085	0.0025
MMFX No.3	8.5	92.9	2.526	12.375	82	90	30.0	75.6	92.9	0.0085	0.0023
MMFX No.3	9	98.2	2.588	12.375	82	85	29.4	75.6	98.2	0.0085	0.0022

Table A.4 - Continuous Composite (Steel) Girder Bridge - Positive Moment Region

Steel	Spacing (in)	Max. tensile stress in steel (ksi)	Max. compressive stress in concrete (ksi)	Max. allowable spacing (in.)	Minimum Required Steel		Crack-Control Provisions			Maximum Allowable Steel	
					1.2*M _{cr} (k-in.)	ΦMn (k-in.)	f _s -allowable Eq. (d) (ksi)	M _{max-service} (k-in.)	f _s -service (ksi)	ρ _{max}	ρ
Given Design:											
Gr60 No. 5/	6	22.4	1.125	12.375	82	190	36.0	75.6	22.4	0.0241	0.0069
MMFX No.5	5.5	18.6	1.046	12.375	82	424	63.8	75.6	18.6	0.0085	0.0084
MMFX No.5	6	20.2	1.080	12.375	82	394	61.9	75.6	20.2	0.0085	0.0077
MMFX No.5	6.5	21.8	1.113	12.375	82	367	60.3	75.6	21.8	0.0085	0.0071
MMFX No.5	7	23.4	1.145	12.375	82	344	58.8	75.6	23.4	0.0085	0.0066
MMFX No.5	7.5	25.0	1.175	12.375	82	324	57.5	75.6	25.0	0.0085	0.0062
MMFX No.5	8	26.6	1.205	12.375	82	305	56.3	75.6	26.6	0.0085	0.0058
MMFX No.5	8.5	28.2	1.234	12.375	82	289	55.2	75.6	28.2	0.0085	0.0055
MMFX No.5	9	29.8	1.261	12.375	82	274	54.1	75.6	29.8	0.0085	0.0052
MMFX No.5	9.5	31.4	1.289	12.375	82	261	53.1	75.6	31.4	0.0085	0.0049
MMFX No.5	10	33.0	1.315	12.375	82	249	52.2	75.6	33.0	0.0085	0.0046
MMFX No.5	10.5	34.5	1.341	12.375	82	238	51.4	75.6	34.5	0.0085	0.0044
MMFX No.5	11	36.1	1.366	12.375	82	228	50.6	75.6	36.1	0.0085	0.0042
MMFX No.5	11.5	37.7	1.391	12.375	82	219	49.9	75.6	37.7	0.0085	0.0040
MMFX No.5	12	39.3	1.415	12.375	82	210	49.2	75.6	39.3	0.0085	0.0039
MMFX No.5	12.5	40.9	1.439	12.375	82	202	48.5	75.6	40.9	0.0085	0.0037
MMFX No.4	5.5	28.0	1.217	12.375	82	291	65.9	75.6	28.0	0.0085	0.0054
MMFX No.4	6	30.4	1.259	12.375	82	269	64.0	75.6	30.4	0.0085	0.0049
MMFX No.4	6.5	32.9	1.299	12.375	82	250	62.3	75.6	32.9	0.0085	0.0046
MMFX No.4	7	35.3	1.339	12.375	82	233	60.8	75.6	35.3	0.0085	0.0042
MMFX No.4	7.5	37.7	1.376	12.375	82	219	59.4	75.6	37.7	0.0085	0.0040
MMFX No.4	8	40.2	1.413	12.375	82	206	58.1	75.6	40.2	0.0085	0.0037
MMFX No.4	8.5	42.6	1.448	12.375	82	195	57.0	75.6	42.6	0.0085	0.0035
MMFX No.4	9	45.0	1.483	12.375	82	184	55.9	75.6	45.0	0.0085	0.0033
MMFX No.3	5.5	49.4	1.527	12.375	82	168	68.2	75.6	49.4	0.0085	0.0029
MMFX No.3	6	53.7	1.583	12.375	82	155	66.2	75.6	53.7	0.0085	0.0027
MMFX No.3	6.5	58.1	1.638	12.375	82	144	64.5	75.6	58.1	0.0085	0.0025
MMFX No.3	7	62.4	1.690	12.375	82	134	62.9	75.6	62.4	0.0085	0.0023
MMFX No.3	7.5	66.8	1.741	12.375	82	125	61.5	75.6	66.8	0.0085	0.0022
MMFX No.3	8	71.1	1.790	12.375	82	118	60.2	75.6	71.1	0.0085	0.0020
MMFX No.3	8.5	75.4	1.837	12.375	82	111	59.0	75.6	75.4	0.0085	0.0019
MMFX No.3	9	79.7	1.883	12.375	82	105	57.8	75.6	79.7	0.0085	0.0018

Table A.5 - Continuous Concrete Bridge - Negative Moment Region

Steel	Spacing (in)	Max. allowable spacing (in.)	Minimum Required Steel		Maximum Allowable Steel		Crack-Control Provisions			Fatigue Provisions		
			1.2*M _{cr} (k-in.)	ΦMn (k-in.)	ρ _{max}	ρ	f _{s-allowable} Eq. (d) (ksi)	M _{max-service} (k-in.)	f _{s-service} (ksi)	M _{min-service} (k-in.)	f _{r-allowable}	
											Eq. (e) (ksi)	f _{r-analysis} (ksi)
Given Design:												
Grade 60 No.8	6	18	272	936	0.0241	0.0110	30.8	385.1	22.8	92.5	21.6	17.4
MMFX No.8	6	18	272	1695	0.0085	0.0110	30.8	385.1	22.8	92.5	21.6	17.4
MMFX No.8	7	18	272	1496	0.0085	0.0094	29.3	385.1	26.5	92.5	21.3	20.1
MMFX No.8	8	18	272	1338	0.0085	0.0082	28.0	385.1	30.0	92.5	21.0	22.8
MMFX No.8	9	18	272	1208	0.0085	0.0073	26.9	385.1	33.6	92.5	20.7	25.5
MMFX No.8	10	18	272	1102	0.0085	0.0066	26.0	385.1	37.2	92.5	20.5	28.3
MMFX No.8	11	18	272	1012	0.0085	0.0060	25.2	385.1	40.8	92.5	20.2	31.0
MMFX No.8	12	18	272	936	0.0085	0.0055	24.5	385.1	44.3	92.5	19.9	33.7
MMFX No.8	13	18	272	870	0.0085	0.0051	23.8	385.1	47.9	92.5	19.6	36.4
MMFX No.8	14	18	272	813	0.0085	0.0047	23.2	385.1	51.4	92.5	19.3	39.0
MMFX No.8	15	18	272	763	0.0085	0.0044	22.7	385.1	54.9	92.5	19.0	41.7
MMFX No.8	16	18	272	718	0.0085	0.0041	22.2	385.1	58.5	92.5	18.8	44.4
MMFX No.8	17	18	272	679	0.0085	0.0039	21.8	385.1	62.0	92.5	18.5	47.1
MMFX No.7	6	18	272	1360	0.0085	0.0083	31.4	385.1	29.5	92.5	21.1	22.4
MMFX No.7	7	18	272	1191	0.0085	0.0071	29.8	385.1	34.2	92.5	20.7	26.0
MMFX No.7	8	18	272	1058	0.0085	0.0062	28.5	385.1	38.9	92.5	20.3	29.5
MMFX No.7	9	18	272	952	0.0085	0.0055	27.4	385.1	43.5	92.5	19.9	33.1
MMFX No.7	10	18	272	865	0.0085	0.0050	26.4	385.1	48.2	92.5	19.6	36.6
MMFX No.7	11	18	272	792	0.0085	0.0045	25.6	385.1	52.8	92.5	19.2	40.1
MMFX No.7	12	18	272	731	0.0085	0.0041	24.9	385.1	57.4	92.5	18.8	43.6
MMFX No.7	13	18	272	678	0.0085	0.0038	24.2	385.1	62.1	92.5	18.5	47.1
MMFX No.7	14	18	272	633	0.0085	0.0036	23.6	385.1	66.7	92.5	18.1	50.7
MMFX No.7	15	18	272	593	0.0085	0.0033	23.1	385.1	71.3	92.5	17.7	54.1
MMFX No.7	16	18	272	558	0.0085	0.0031	22.6	385.1	75.9	92.5	17.4	57.6
MMFX No.7	17	18	272	526	0.0085	0.0029	22.2	385.1	80.5	92.5	17.0	61.1
MMFX No.6	6	18	272	1043	0.0085	0.0060	31.9	385.1	39.5	92.5	20.3	30.0
MMFX No.6	7	18	272	907	0.0085	0.0052	30.3	385.1	45.8	92.5	19.8	34.8
MMFX No.6	8	18	272	803	0.0085	0.0045	29.0	385.1	52.1	92.5	19.3	39.6
MMFX No.6	9	18	272	720	0.0085	0.0040	27.9	385.1	58.4	92.5	18.8	44.4
MMFX No.6	10	18	272	652	0.0085	0.0036	26.9	385.1	64.6	92.5	18.3	49.1
MMFX No.6	11	18	272	596	0.0085	0.0033	26.1	385.1	70.9	92.5	17.8	53.9
MMFX No.6	12	18	272	549	0.0085	0.0030	25.3	385.1	77.1	92.5	17.3	58.6
MMFX No.6	13	18	272	509	0.0085	0.0028	24.7	385.1	83.4	92.5	16.8	63.3
MMFX No.6	14	18	272	474	0.0085	0.0026	24.0	385.1	89.6	92.5	16.3	68.1
MMFX No.6	15	18	272	443	0.0085	0.0024	23.5	385.1	95.8	92.5	15.8	72.8
MMFX No.6	16	18	272	417	0.0085	0.0023	23.0	385.1	102.0	92.5	15.3	77.5
MMFX No.6	17	18	272	393	0.0085	0.0021	22.5	385.1	108.2	92.5	14.8	82.2

Table A.6 - Continuous Concrete Bridge - Positive Moment Region

Steel	Spacing (in)	Max. allowable spacing (in.)	Minimum Required Steel		Maximum Allowable Steel		Crack-Control Provisions			Fatigue Provisions		
			1.2*M _{cr} (k-in.)	ΦMn (k-in.)	ρ _{max}	ρ	f _{s-allowable} Eq. (d) (ksi)	M _{max-service} (k-in.)	f _{s-service} (ksi)	M _{min-service} (k-in.)	f _{r-allowable}	
											Eq. (e) (ksi)	f _{r-analysis} (ksi)
Given Design:												
Grade 60 No.8	6	16.5	146	775	0.0241	0.0162	36.0	309.0	21.6	-12.1	23.4	21.7
MMFX No.9	6	16.5	146	1473	0.0085	0.0177	55.1	309.0	18.9	-12.1	23.4	19.0
MMFX No.9	7	16.5	146	1332	0.0085	0.0151	52.3	309.0	21.9	-12.1	23.4	21.9
MMFX No.9	8	16.5	146	1211	0.0085	0.0132	50.1	309.0	24.8	-12.1	23.4	24.9
MMFX No.9	9	16.5	146	1108	0.0085	0.0118	48.1	309.0	27.7	-12.1	23.4	27.8
MMFX No.9	10	16.5	146	1020	0.0085	0.0106	46.5	309.0	30.6	-12.1	23.4	30.7
MMFX No.9	11	16.5	146	944	0.0085	0.0096	45.0	309.0	33.6	-12.1	23.4	33.6
MMFX No.9	12	16.5	146	878	0.0085	0.0088	43.7	309.0	36.5	-12.1	23.4	36.5
MMFX No.9	13	16.5	146	820	0.0085	0.0082	42.6	309.0	39.3	-12.1	23.4	39.4
MMFX No.9	14	16.5	146	770	0.0085	0.0076	41.6	309.0	42.2	-12.1	23.4	42.3
MMFX No.9	15	16.5	146	725	0.0085	0.0071	40.6	309.0	45.1	-12.1	23.4	45.2
MMFX No.9	16	16.5	146	685	0.0085	0.0066	39.7	309.0	48.0	-12.1	23.4	48.1
MMFX No.9	17	16.5	146	649	0.0085	0.0062	38.9	309.0	50.9	-12.1	23.4	51.0
MMFX No.8	6	16.5	146	1269	0.0085	0.0139	56.7	309.0	23.4	-12.1	23.4	23.5
MMFX No.8	7	16.5	146	1131	0.0085	0.0119	53.8	309.0	27.1	-12.1	23.4	27.2
MMFX No.8	8	16.5	146	1018	0.0085	0.0104	51.5	309.0	30.8	-12.1	23.4	30.9
MMFX No.8	9	16.5	146	924	0.0085	0.0092	49.5	309.0	34.4	-12.1	23.4	34.5
MMFX No.8	10	16.5	146	846	0.0085	0.0083	47.8	309.0	38.1	-12.1	23.4	38.2
MMFX No.8	11	16.5	146	779	0.0085	0.0076	46.3	309.0	41.7	-12.1	23.4	41.8
MMFX No.8	12	16.5	146	722	0.0085	0.0069	45.0	309.0	45.3	-12.1	23.4	45.4
MMFX No.8	13	16.5	146	673	0.0085	0.0064	43.8	309.0	49.0	-12.1	23.4	49.0
MMFX No.8	14	16.5	146	630	0.0085	0.0059	42.7	309.0	52.6	-12.1	23.4	52.6
MMFX No.8	15	16.5	146	592	0.0085	0.0055	41.8	309.0	56.2	-12.1	23.4	56.2
MMFX No.8	16	16.5	146	558	0.0085	0.0052	40.9	309.0	59.8	-12.1	23.4	59.8
MMFX No.8	17	16.5	146	528	0.0085	0.0049	40.0	309.0	63.3	-12.1	23.4	63.4
MMFX No.7	6	16.5	146	1036	0.0085	0.0105	58.3	309.0	30.2	-12.1	23.4	30.3
MMFX No.7	7	16.5	146	913	0.0085	0.0090	55.4	309.0	35.0	-12.1	23.4	35.0
MMFX No.7	8	16.5	146	815	0.0085	0.0078	53.0	309.0	39.8	-12.1	23.4	39.8
MMFX No.7	9	16.5	146	736	0.0085	0.0070	50.9	309.0	44.5	-12.1	23.4	44.5
MMFX No.7	10	16.5	146	670	0.0085	0.0063	49.2	309.0	49.2	-12.1	23.4	49.3
MMFX No.7	11	16.5	146	615	0.0085	0.0057	47.6	309.0	53.9	-12.1	23.4	54.0
MMFX No.7	12	16.5	146	569	0.0085	0.0052	46.3	309.0	58.6	-12.1	23.4	58.7
MMFX No.7	13	16.5	146	529	0.0085	0.0048	45.1	309.0	63.3	-12.1	23.4	63.4
MMFX No.7	14	16.5	146	494	0.0085	0.0045	44.0	309.0	68.0	-12.1	23.4	68.1
MMFX No.7	15	16.5	146	463	0.0085	0.0042	43.0	309.0	72.7	-12.1	23.4	72.8
MMFX No.7	16	16.5	146	436	0.0085	0.0039	42.0	309.0	77.4	-12.1	23.4	77.4
MMFX No.7	17	16.5	146	412	0.0085	0.0037	41.2	309.0	82.0	-12.1	23.4	82.1

Table A.6 - Continuous Concrete Bridge - Positive Moment Region (cont)

Steel	Spacing (in)	Max. allowable spacing (in.)	Minimum Required Steel		Maximum Allowable Steel		Crack-Control Provisions			Fatigue Provisions		
			$1.2 \cdot M_{cr}$ (k-in.)	ΦM_n (k-in.)	ρ_{max}	ρ	$f_{s-allowable}$ Eq. (d) (ksi)	$M_{max-service}$ (k-in.)	$f_{s-service}$ (ksi)	$M_{min-service}$ (k-in.)	$f_{r-allowable}$ Eq. (e) (ksi)	$f_{r-analysis}$ (ksi)
MMFX No.6	6	16.5	146	805	0.0085	0.0076	60.1	309.0	40.3	-12.1	23.4	40.4
MMFX No.6	7	16.5	146	704	0.0085	0.0065	57.0	309.0	46.8	-12.1	23.4	46.8
MMFX No.6	8	16.5	146	625	0.0085	0.0057	54.6	309.0	53.1	-12.1	23.4	53.2
MMFX No.6	9	16.5	146	561	0.0085	0.0051	52.5	309.0	59.5	-12.1	23.4	59.5
MMFX No.6	10	16.5	146	509	0.0085	0.0046	50.6	309.0	65.9	-12.1	23.4	65.9
MMFX No.6	11	16.5	146	466	0.0085	0.0042	49.1	309.0	72.2	-12.1	23.4	72.2
MMFX No.6	12	16.5	146	430	0.0085	0.0038	47.7	309.0	78.5	-12.1	23.4	78.6
MMFX No.6	13	16.5	146	399	0.0085	0.0035	46.4	309.0	84.9	-12.1	23.4	84.9
MMFX No.6	14	16.5	146	372	0.0085	0.0033	45.3	309.0	91.2	-12.1	23.4	91.2
MMFX No.6	15	16.5	146	348	0.0085	0.0030	44.2	309.0	97.5	-12.1	23.4	97.5
MMFX No.6	16	16.5	146	328	0.0085	0.0029	43.3	309.0	103.8	-12.1	23.4	103.8
MMFX No.6	17	16.5	146	309	0.0085	0.0027	42.4	309.0	110.1	-12.1	23.4	110.1
MMFX No.5	6	16.5	146	594	0.0085	0.0053	61.9	309.0	56.1	-12.1	23.4	56.1
MMFX No.5	7	16.5	146	516	0.0085	0.0046	58.8	309.0	65.0	-12.1	23.4	65.0
MMFX No.5	8	16.5	146	456	0.0085	0.0040	56.3	309.0	74.0	-12.1	23.4	74.0
MMFX No.5	9	16.5	146	408	0.0085	0.0036	54.1	309.0	82.9	-12.1	23.4	82.9
MMFX No.5	10	16.5	146	370	0.0085	0.0032	52.2	309.0	91.8	-12.1	23.4	91.8
MMFX No.5	11	16.5	146	338	0.0085	0.0029	50.6	309.0	100.7	-12.1	23.4	100.7
MMFX No.5	12	16.5	146	311	0.0085	0.0027	49.2	309.0	109.5	-12.1	23.4	109.5
MMFX No.5	13	16.5	146	288	0.0085	0.0025	47.9	309.0	118.4	-12.1	23.4	118.4
MMFX No.5	14	16.5	146	268	0.0085	0.0023	46.7	309.0	127.2	-12.1	23.4	127.2
MMFX No.5	15	16.5	146	251	0.0085	0.0021	45.6	309.0	136.1	-12.1	23.4	136.1
MMFX No.5	16	16.5	146	236	0.0085	0.0020	44.7	309.0	144.9	-12.1	23.4	144.9
MMFX No.5	17	16.5	146	222	0.0085	0.0019	43.8	309.0	153.7	-12.1	23.4	153.7

APPENDIX B CORROSION TEST RESULTS FOR INDIVIDUAL SPECIMENS

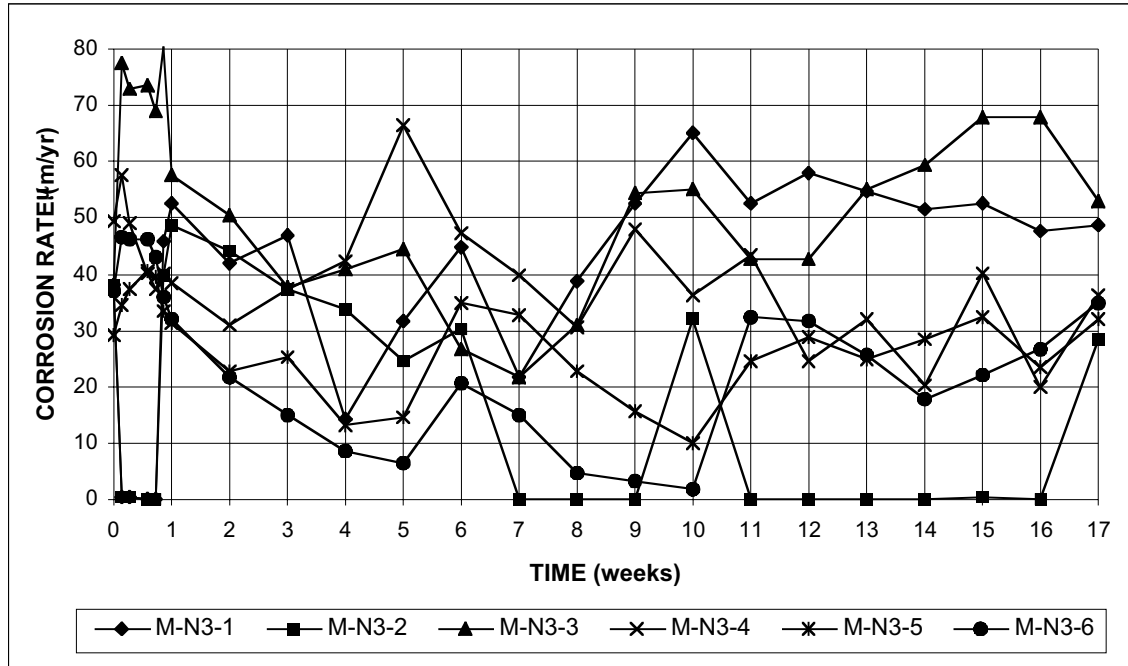


Figure B.1 - Macrocell Test. Corrosion rate. Bare conventional, normalized steel in 1.6 m ion NaCl and simulated concrete pore solution.

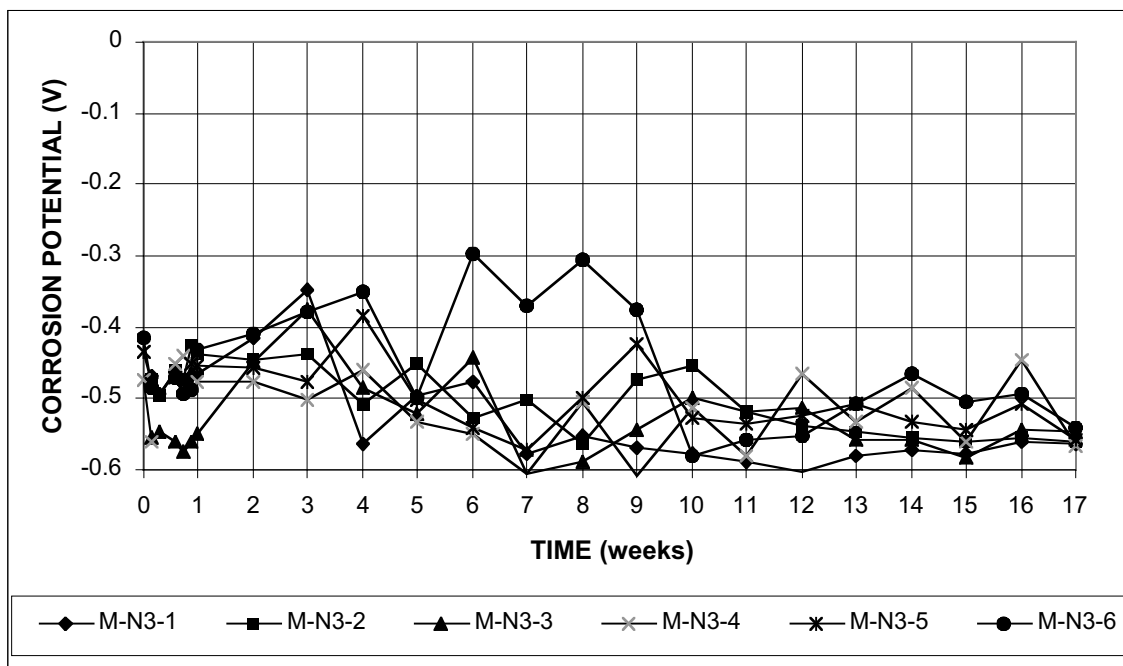


Figure B.2a - Macrocell Test. Corrosion potential vs. saturated calomel electrode, anode. Bare conventional, normalized steel in 1.6 m ion NaCl and simulated concrete pore solution.

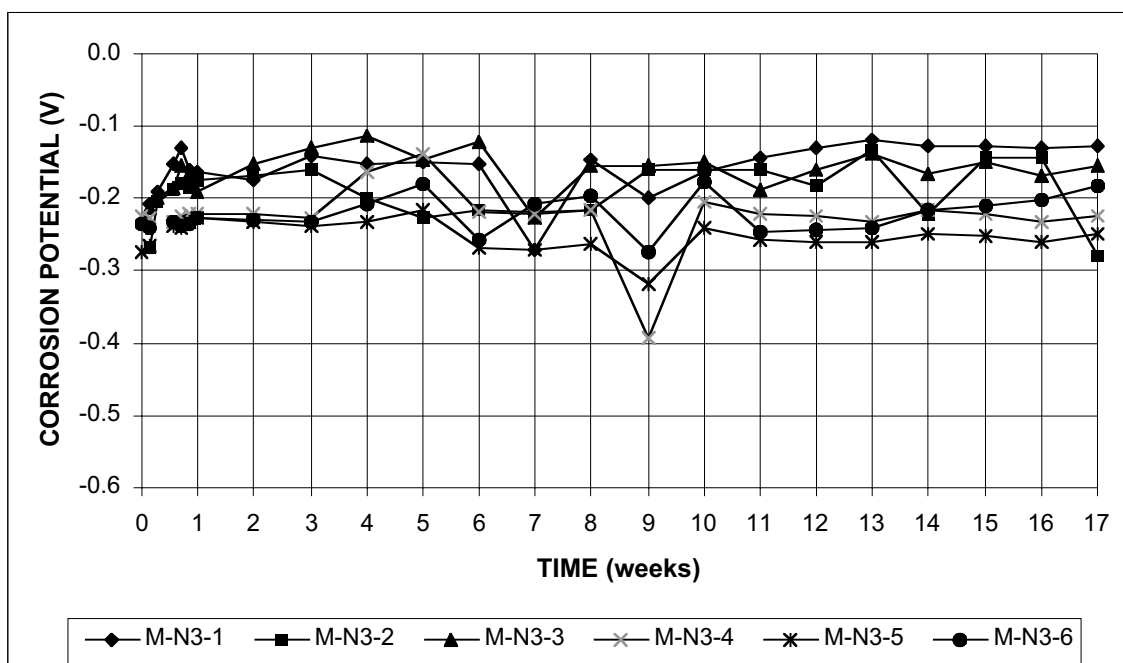


Figure B.2b - Macrocell Test. Corrosion potential vs. saturated calomel electrode, cathode. Bare conventional, normalized steel in 1.6 m ion NaCl and simulated concrete pore solution.

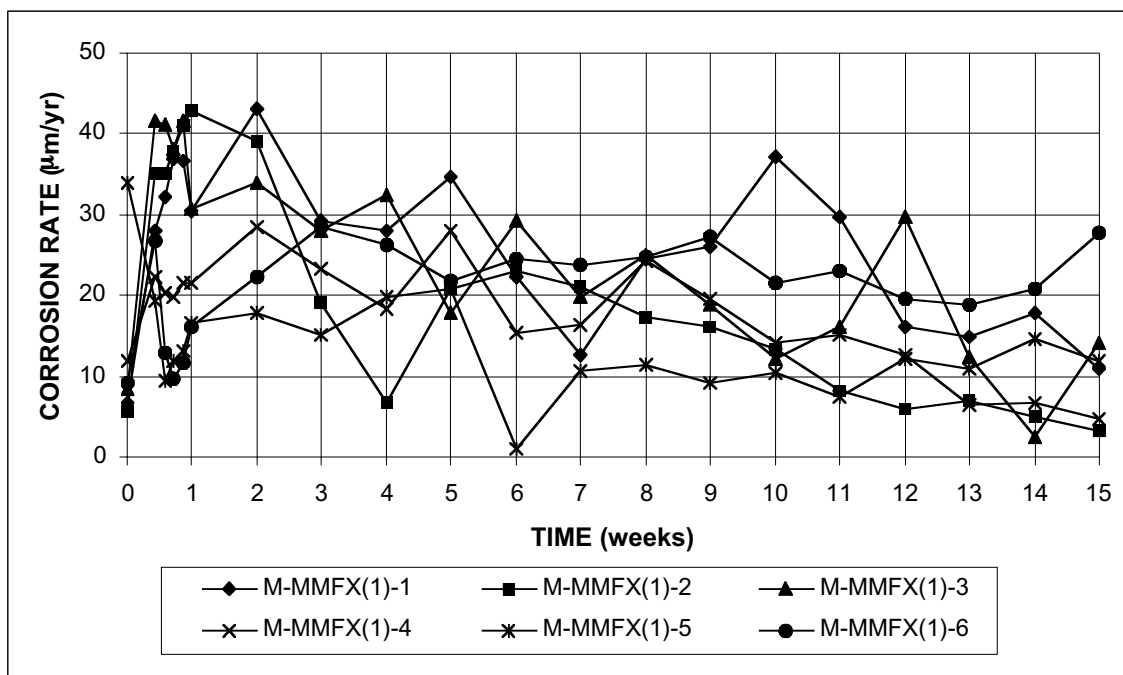


Figure B.3 - Macrocell Test. Corrosion rate. Bare MMFX steel in 1.6 m ion NaCl and simulated concrete pore solution.

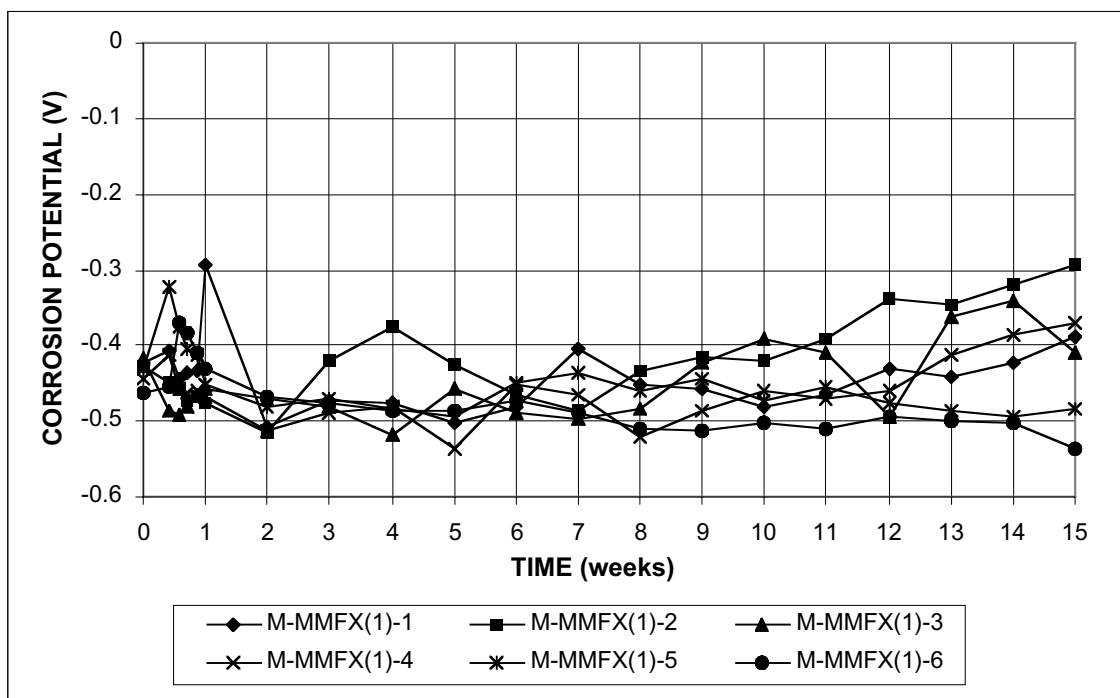


Figure B.4a - Macrocell Test. Corrosion potential vs. saturated calomel electrode, anode. Bare MMFX steel in 1.6 m ion NaCl and simulated concrete pore solution.

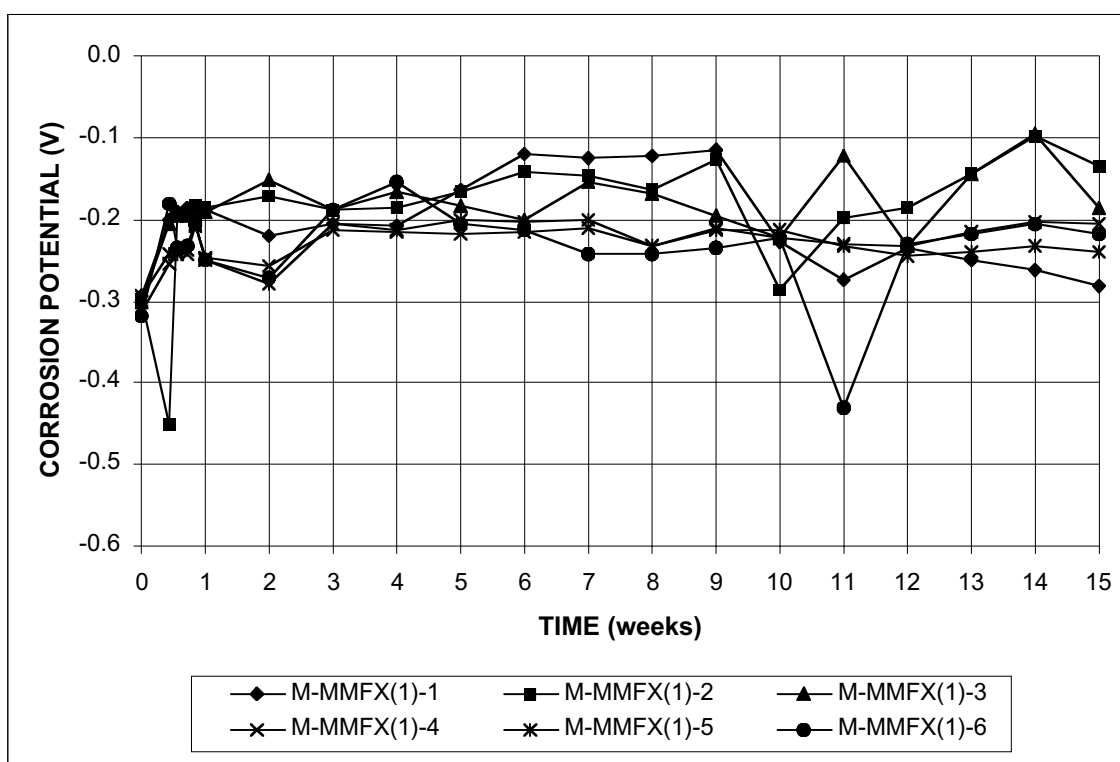


Figure B.4b - Macrocell Test. Corrosion potential vs. saturated calomel electrode, cathode. Bare MMFX steel in 1.6 m ion NaCl and simulated concrete pore solution.

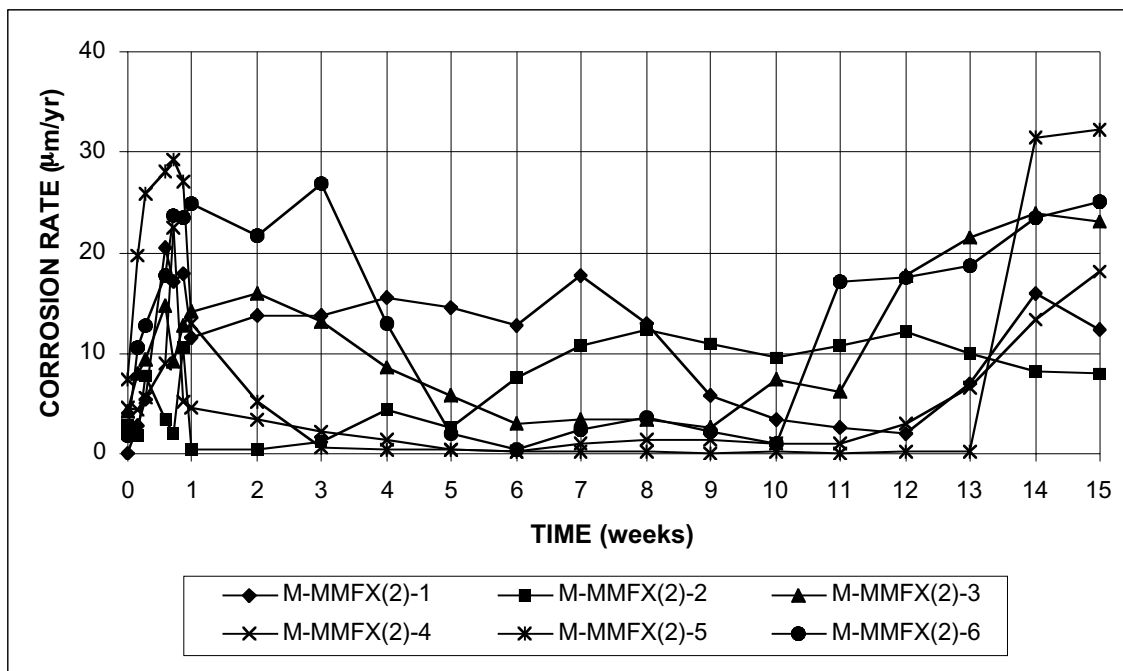


Figure B.5 - Macrocell Test. Corrosion rate. Bare MMFX steel in 1.6 m ion NaCl and simulated concrete pore solution.

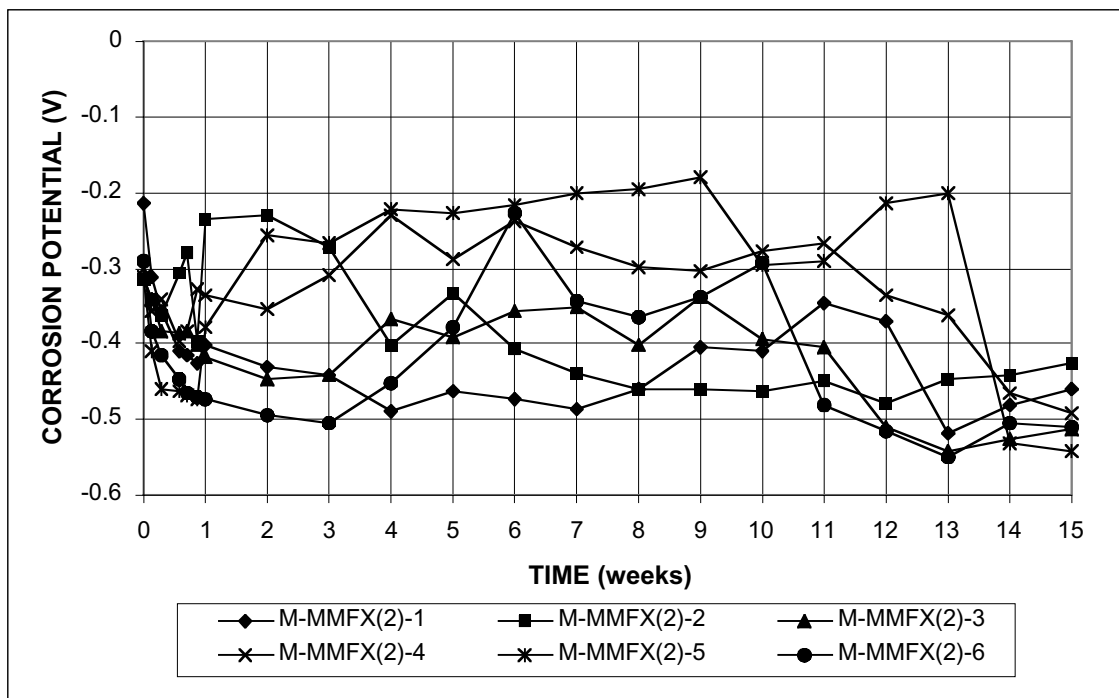


Figure B.6a - Macrocell Test. Corrosion potential vs. saturated calomel electrode, anode. Bare MMFX steel in 1.6 m ion NaCl and simulated concrete pore solution.

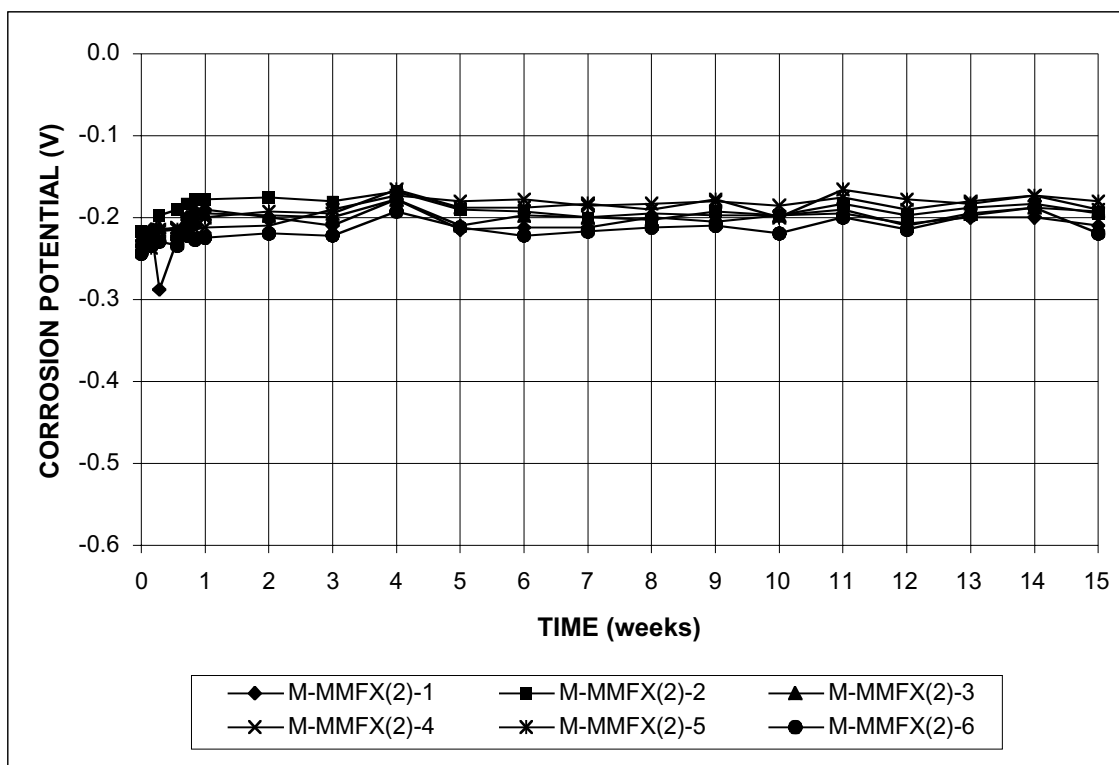


Figure B.6b - Macrocell Test. Corrosion potential vs. saturated calomel electrode, cathode. Bare MMFX steel in 1.6 m ion NaCl and simulated concrete pore solution.

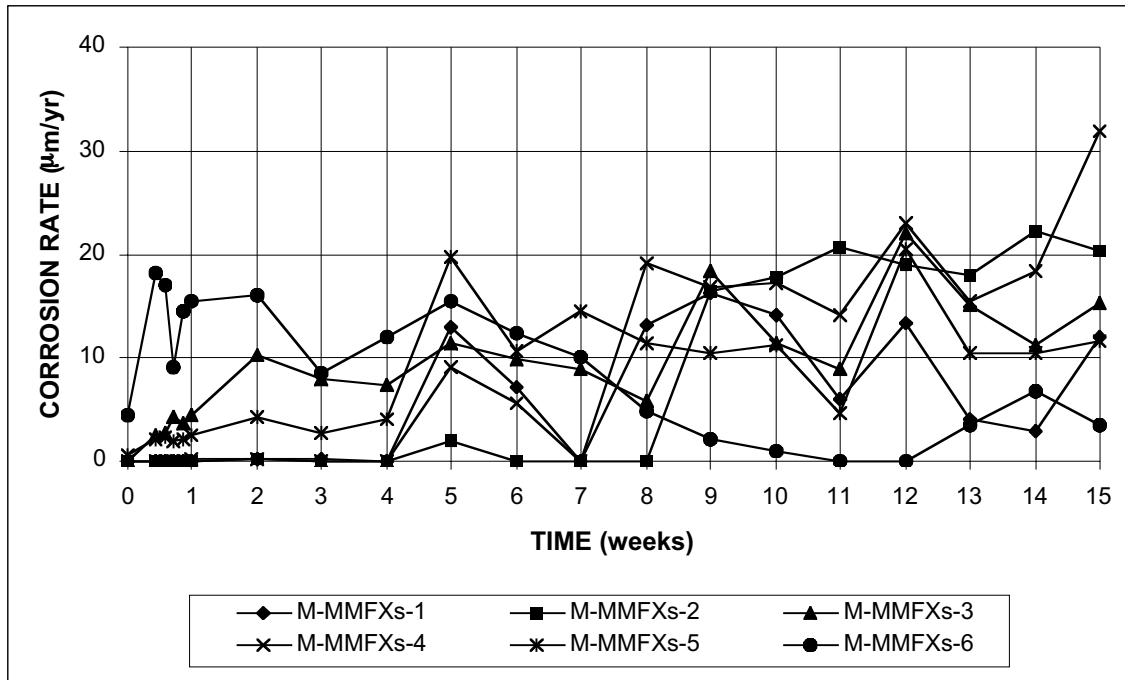


Figure B.7 - Macrocell Test. Corrosion rate. Bare, sandblasted MMFX steel in 1.6 m ion NaCl and simulated concrete pore solution.

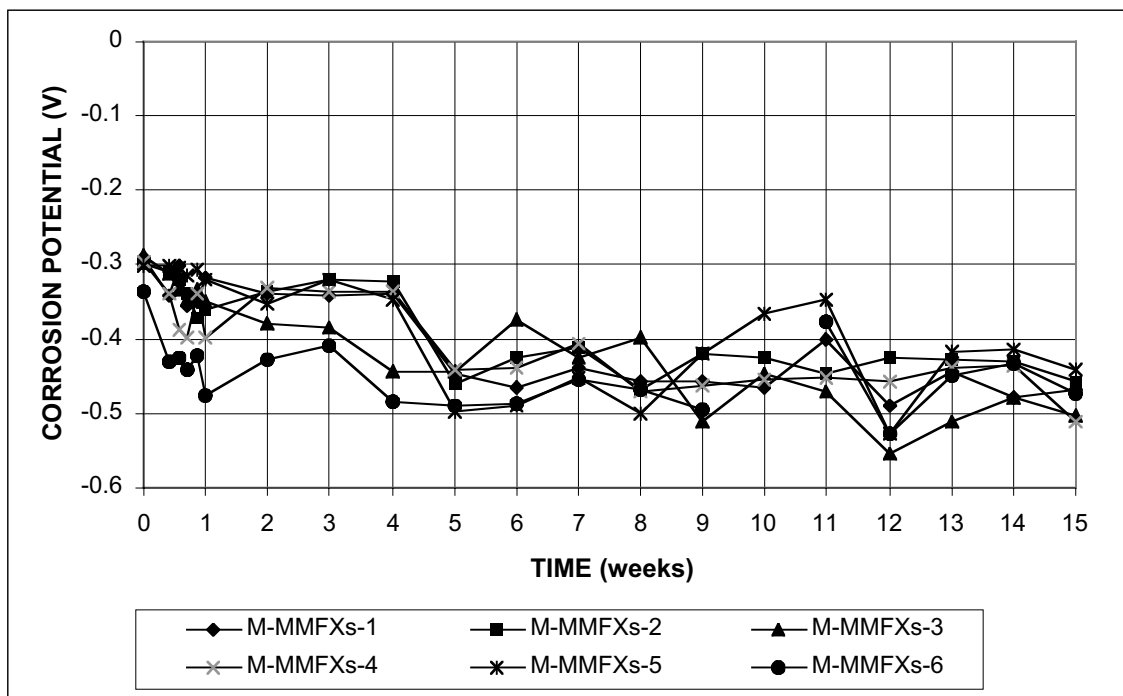


Figure B.8a - Macrocell Test. Corrosion potential vs. saturated calomel electrode, anode. Bare, sandblasted MMFX steel in 1.6 m ion NaCl and simulated concrete pore solution.

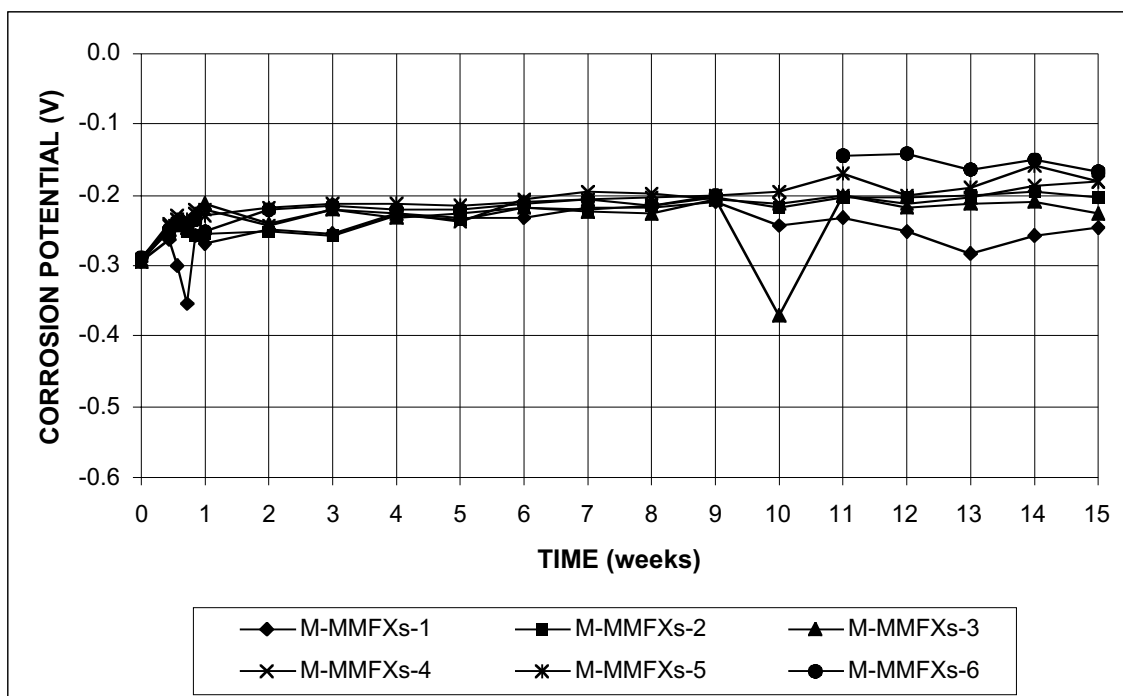


Figure B.8b - Macrocell Test. Corrosion potential vs. saturated calomel electrode, cathode. Bare, sandblasted MMFX steel in 1.6 m ion NaCl and simulated concrete pore solution.

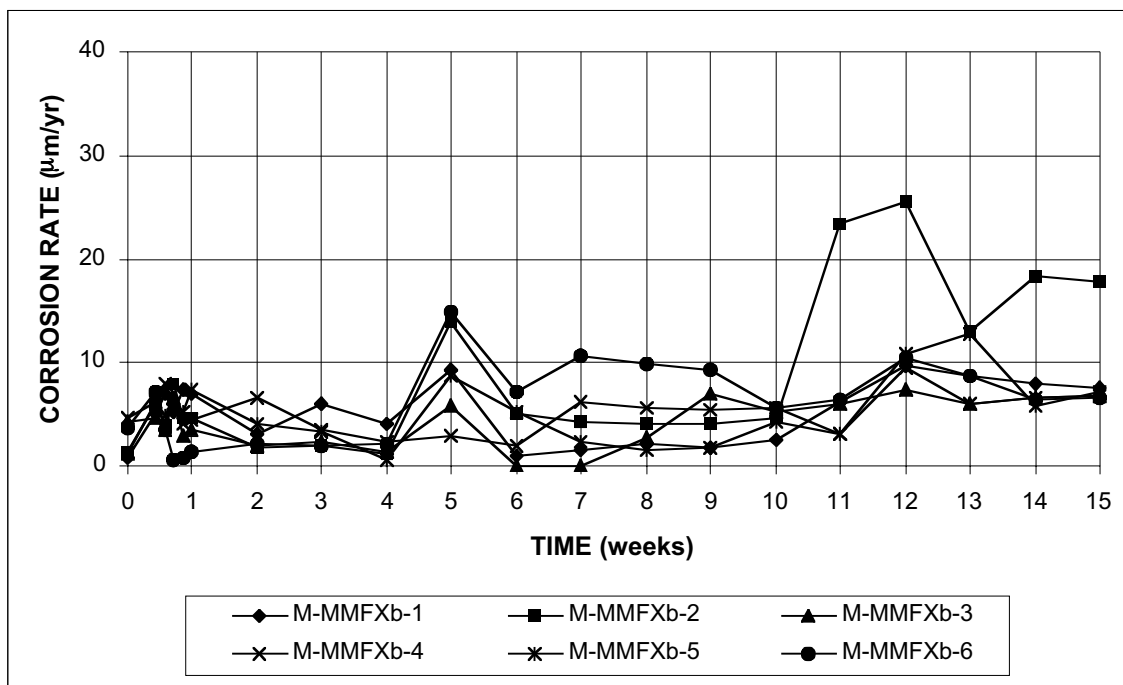


Figure B.9 - Macrocell Test. Corrosion rate. Bare MMFX steel, bent bar at the anode, in 1.6 m ion NaCl and simulated concrete pore solution.

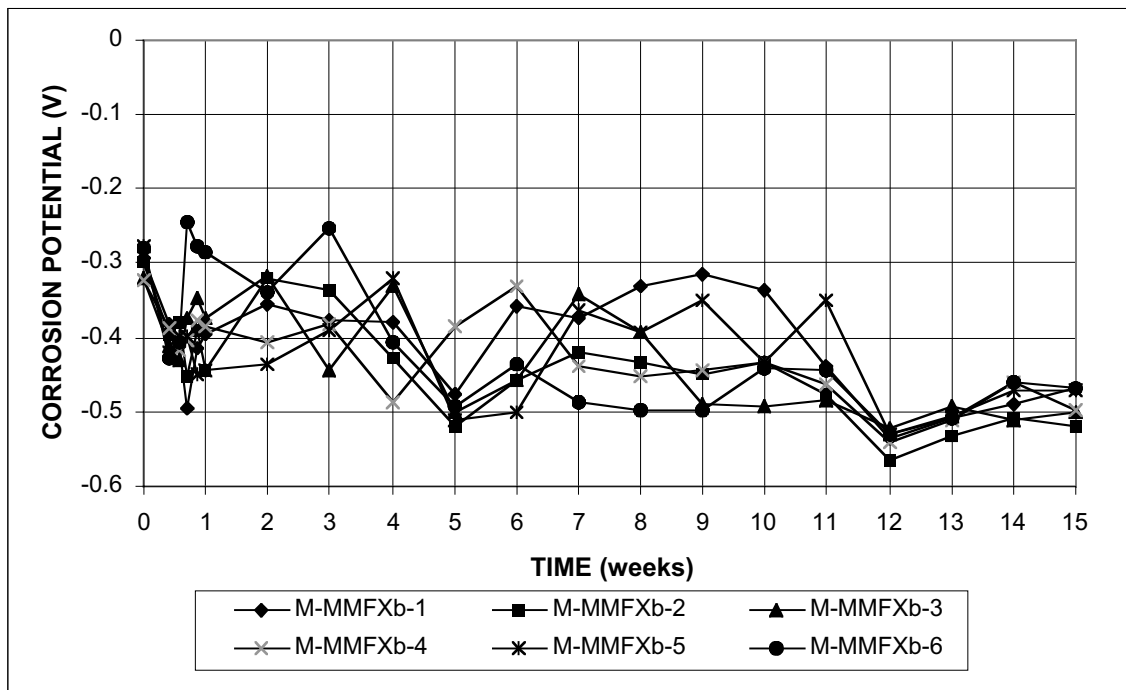


Figure B.10a - Macrocell Test. Corrosion potential vs. saturated calomel electrode, anode. Bare MMFX steel, bent bar at the anode, in 1.6 m ion NaCl and simulated concrete pore solution.

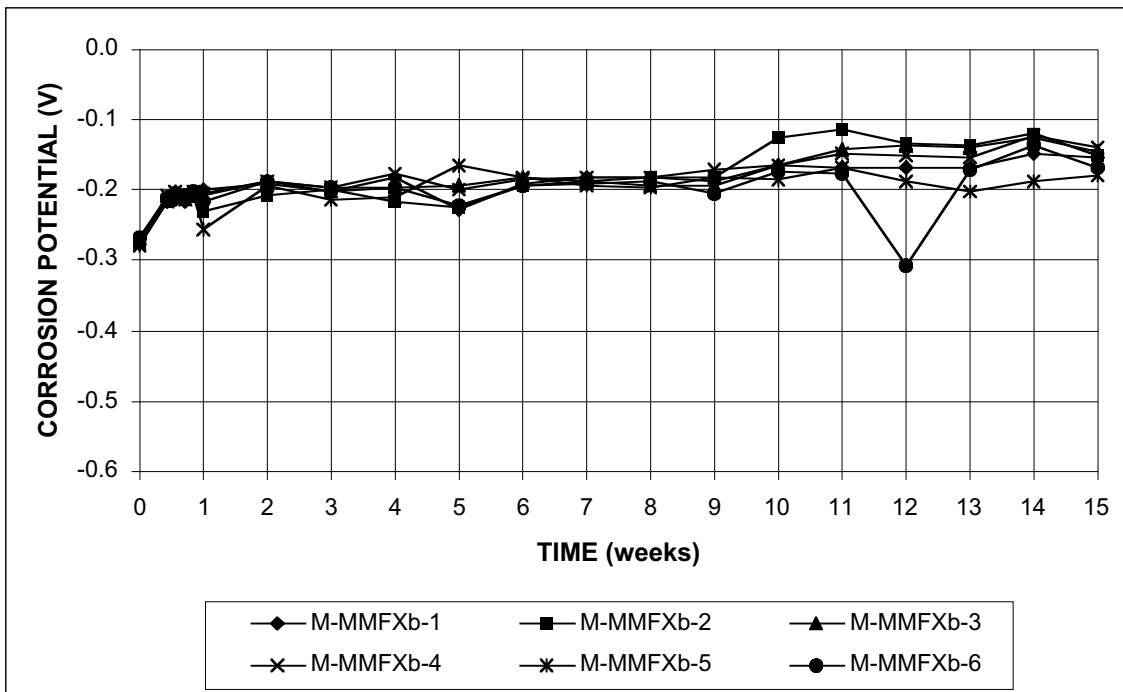


Figure B.10b - Macrocell Test. Corrosion potential vs. saturated calomel electrode, cathode. Bare MMFX steel, bent bar at the anode, in 1.6 m ion NaCl and simulated concrete pore solution.

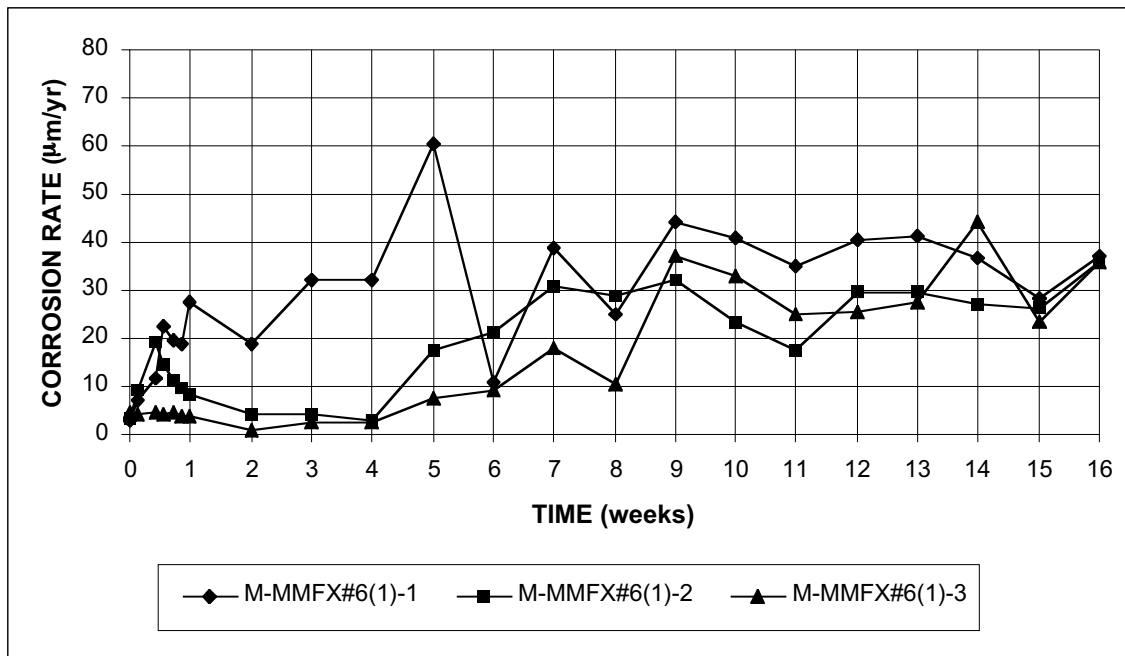


Figure B.11 - Macrocell Test. Corrosion rate. Bare #6 MMFX steel in 1.6 m ion and simulated concrete pore solution.

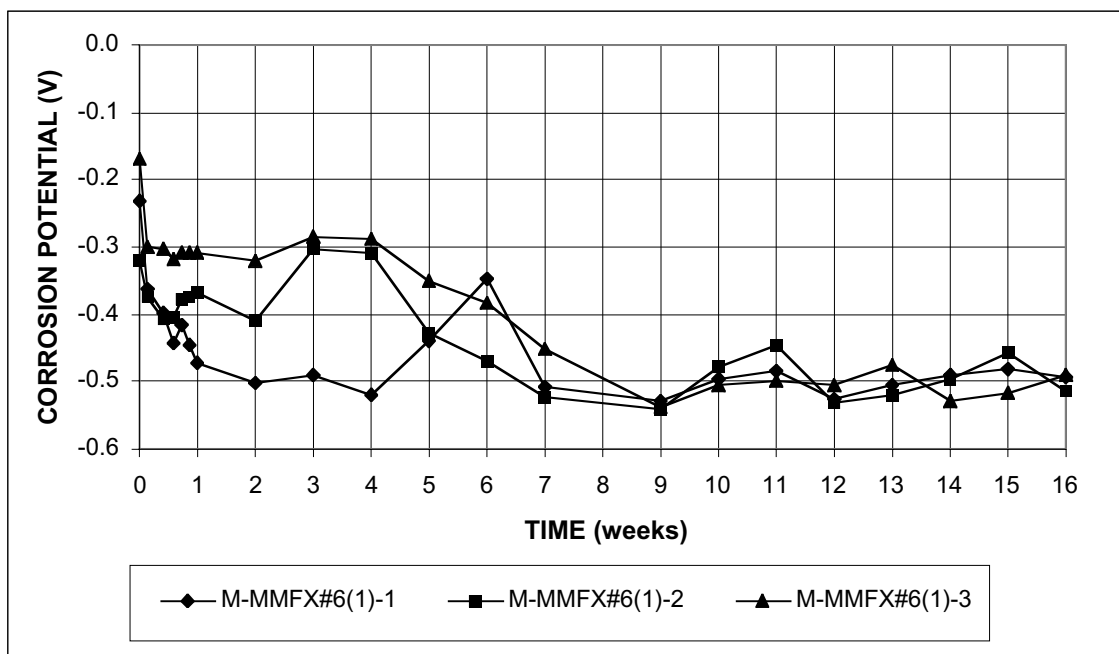


Figure B.12a - Macrocell Test. Corrosion potential vs. saturated calomel electrode, anode. Bare #6 MMFX steel in 1.6 m ion NaCl and simulated concrete pore solution.

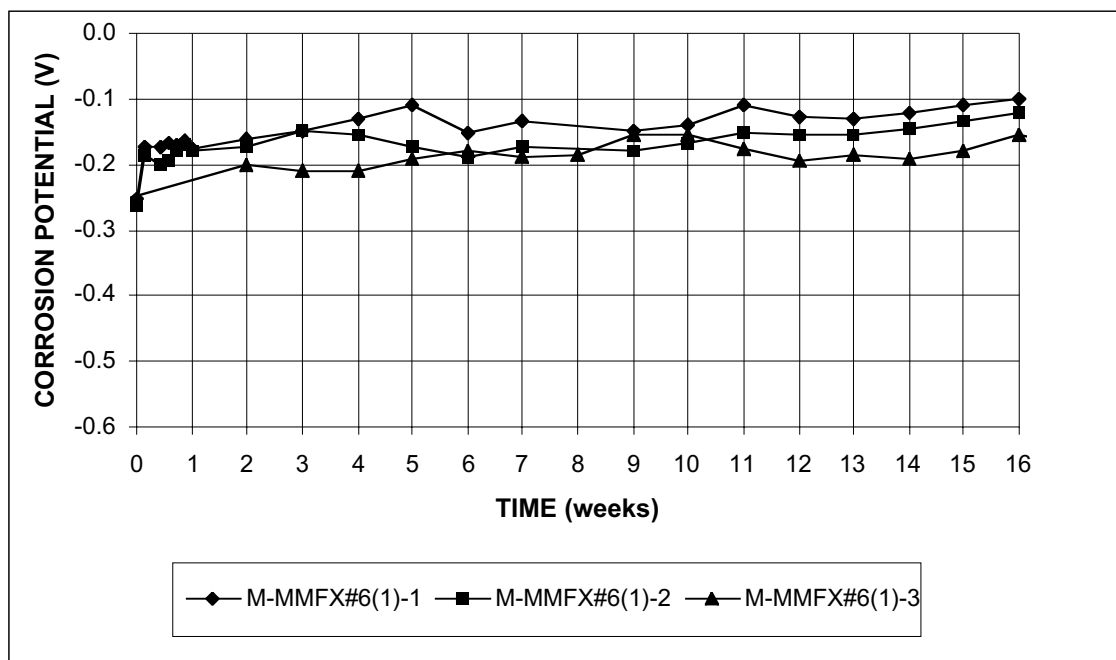


Figure B.12b - Macrocell Test. Corrosion potential vs. saturated calomel electrode, cathode. Bare #6 MMFX steel in 1.6 m ion NaCl and simulated concrete pore solution.

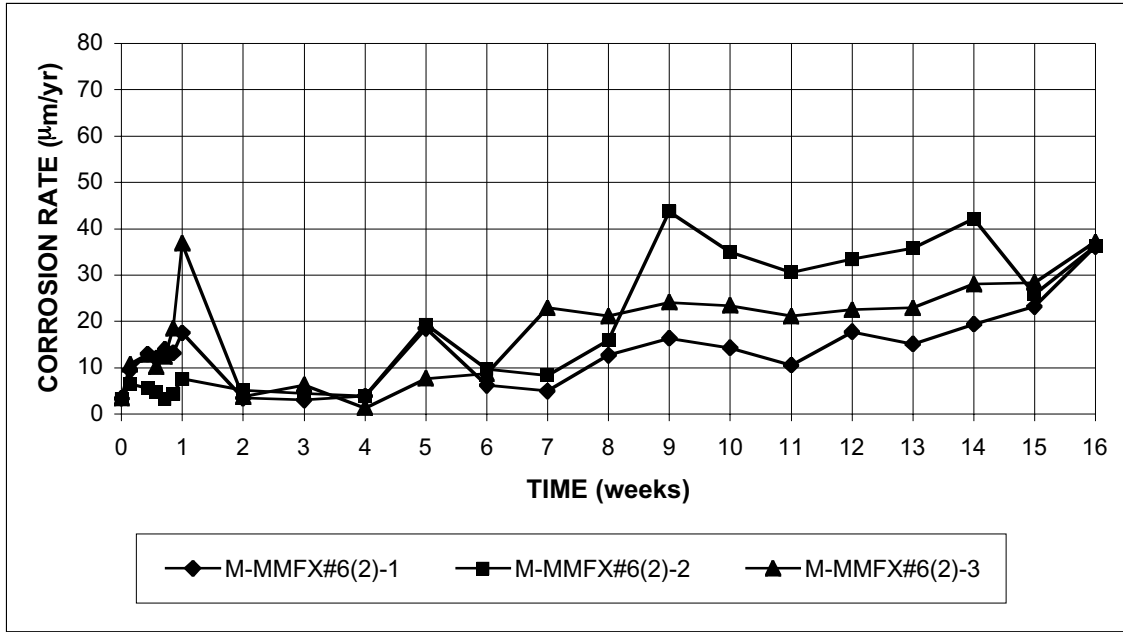


Figure B.13 - Macrocell Test. Corrosion rate. Bare #6 MMFX steel in 1.6 m ion NaCl and simulated concrete pore solution.

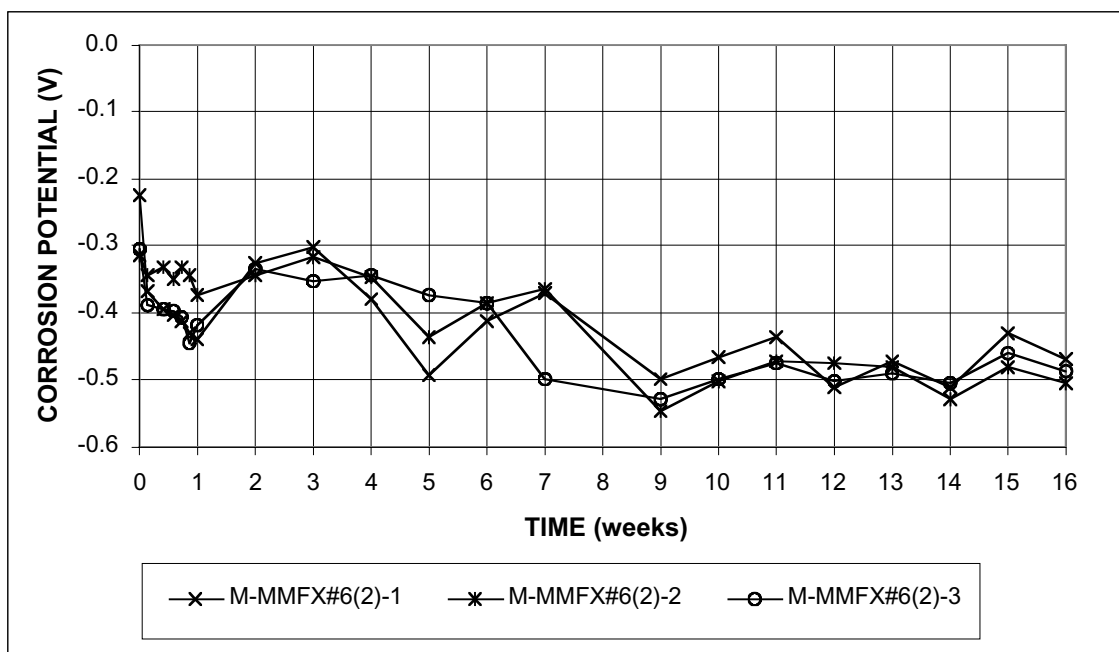


Figure B.14a - Macrocell Test. Corrosion potential vs. saturated calomel electrode, anode. Bare #6 MMFX steel in 1.6 m ion NaCl and simulated concrete pore solution.

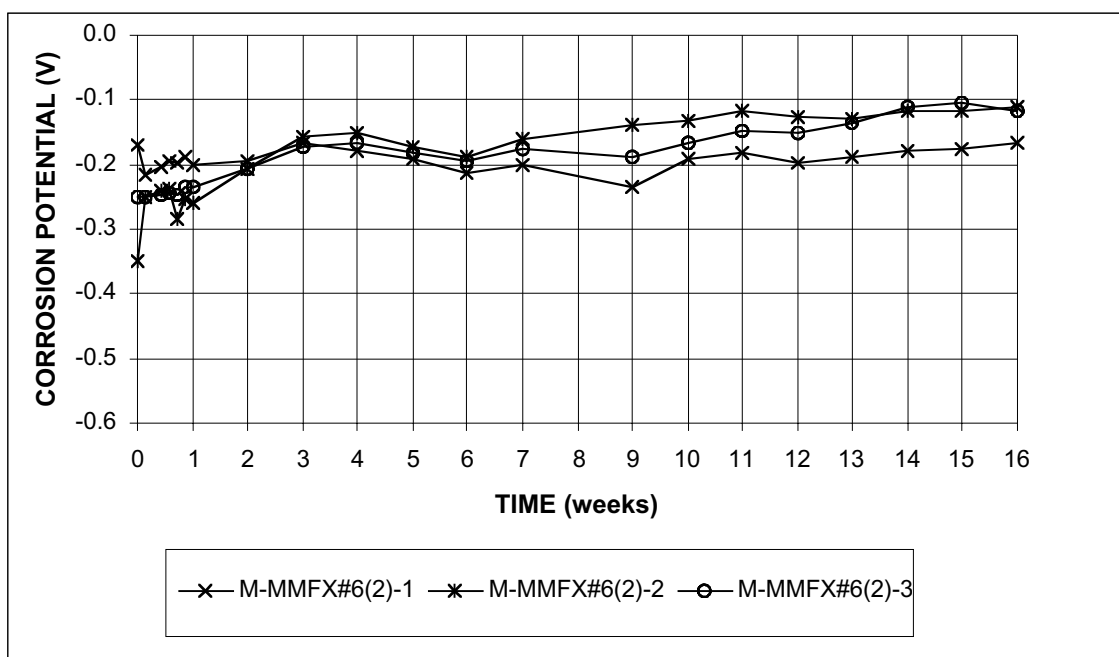


Figure B.14b - Macrocell Test. Corrosion potential vs. saturated calomel electrode, cathode. Bare #6 MMFX steel in 1.6 m ion NaCl and simulated concrete pore solution.

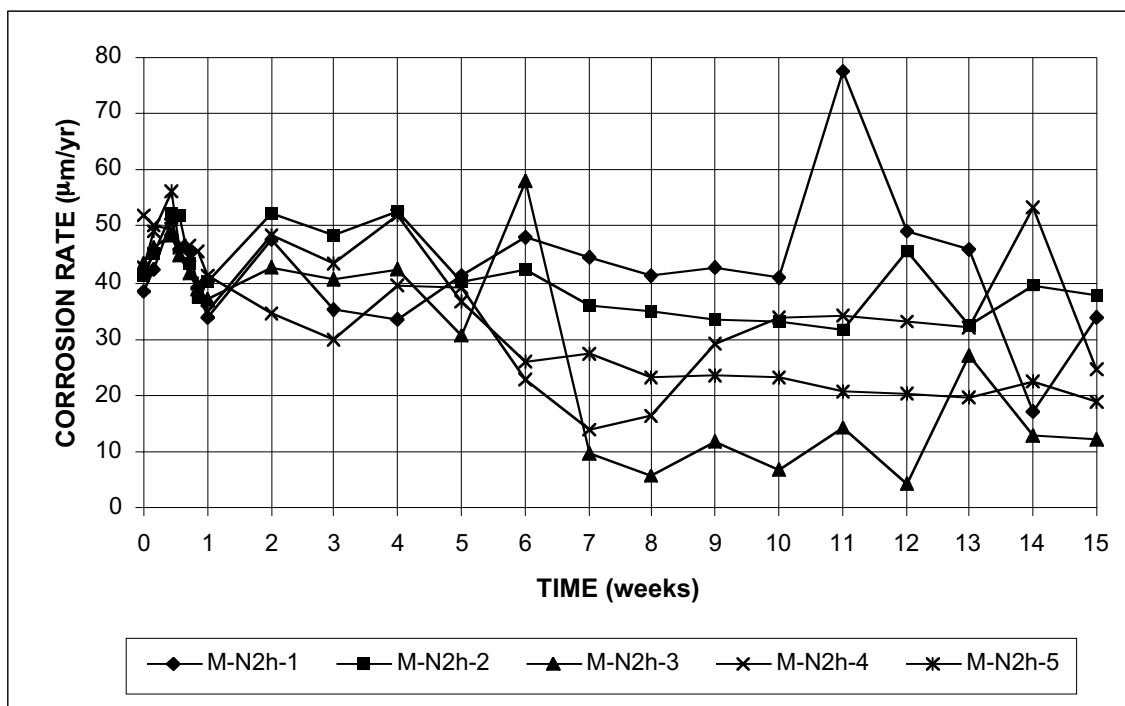


Figure B.15 - Macrocell Test. Corrosion rate. Bare conventional, normalized steel in 6.04 m ion (15%) NaCl and simulated concrete pore solution.

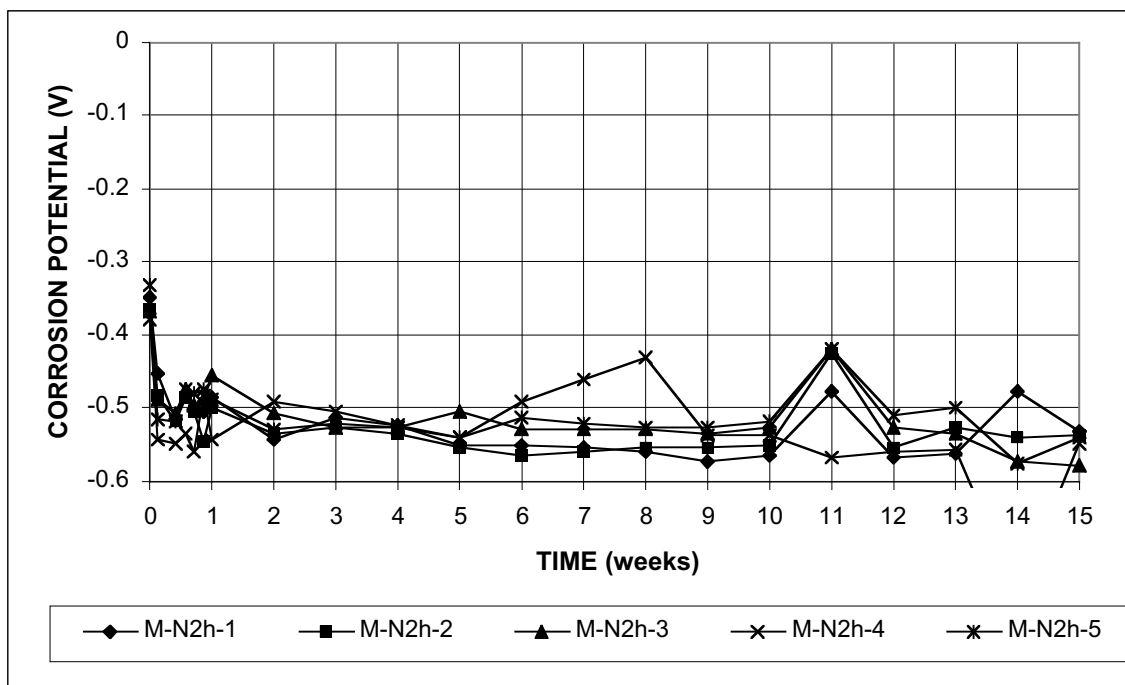


Figure B.16a - Macrocell Test. Corrosion potential vs. saturated calomel electrode, anode. Bare conventional, normalized steel in 6.04m ion (15%) NaCl and simulated concrete pore solution.

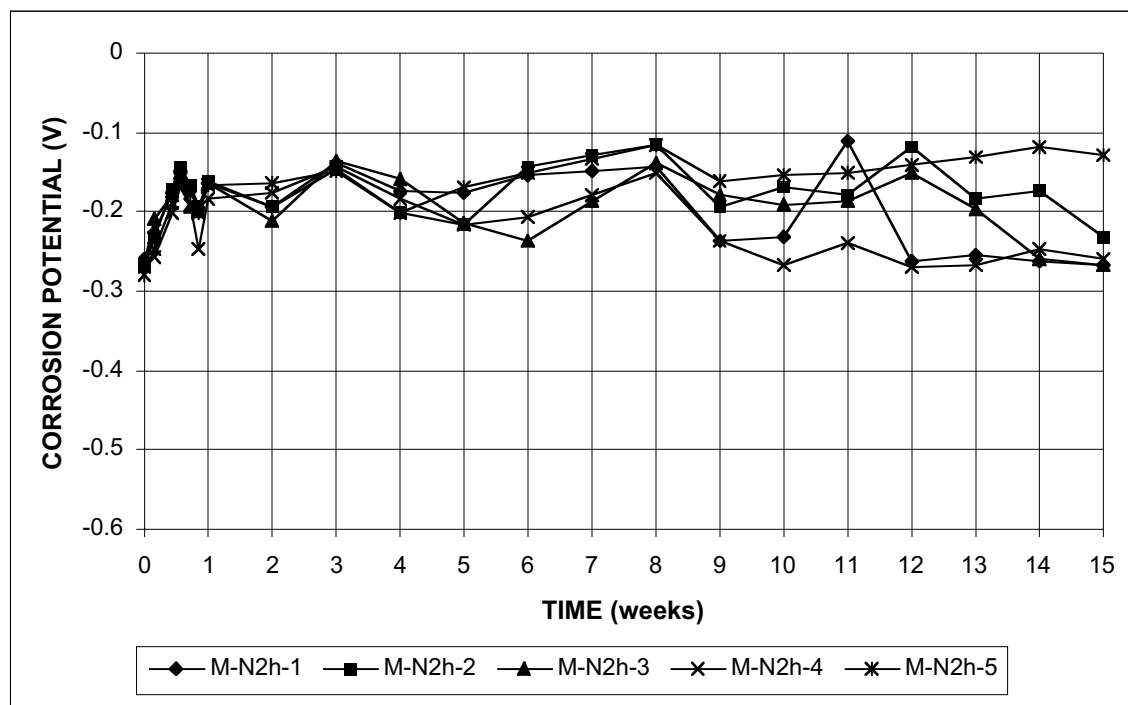


Figure B.16b - Macrocell Test. Corrosion potential vs. saturated calomel electrode, cathode. Bare conventional, normalized steel in 6.04 m ion (15%) NaCl and simulated concrete pore solution.

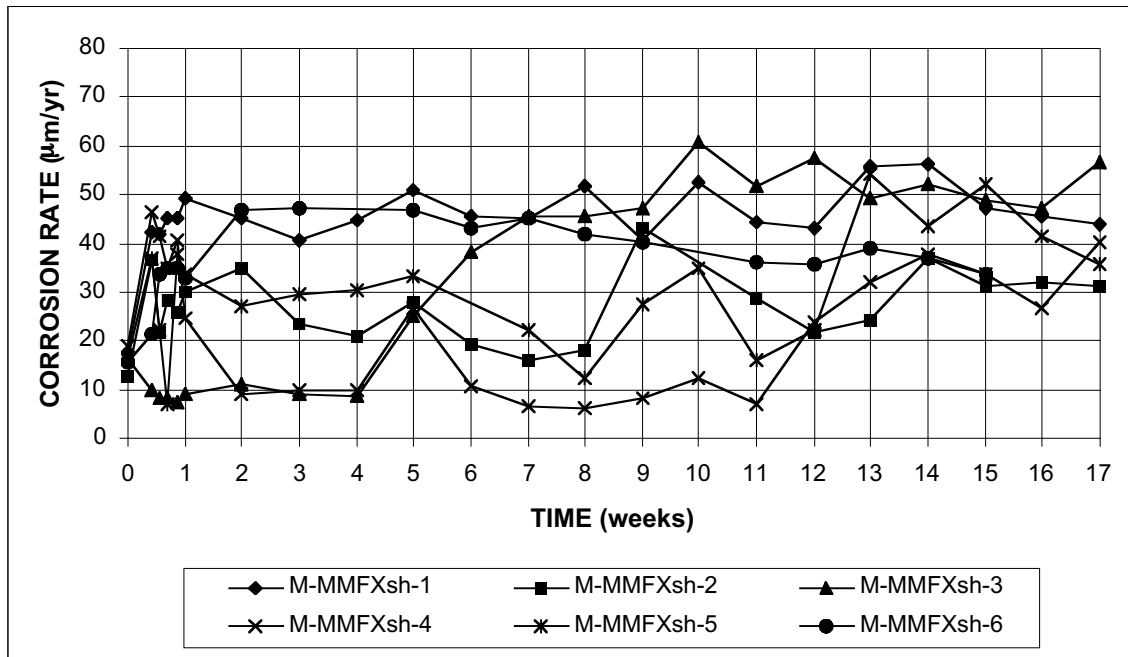


Figure B.17 - Macrocell Test. Corrosion rate. Bare sandblasted MMFX steel in 6.04 m ion (15%) NaCl and simulated concrete pore solution.

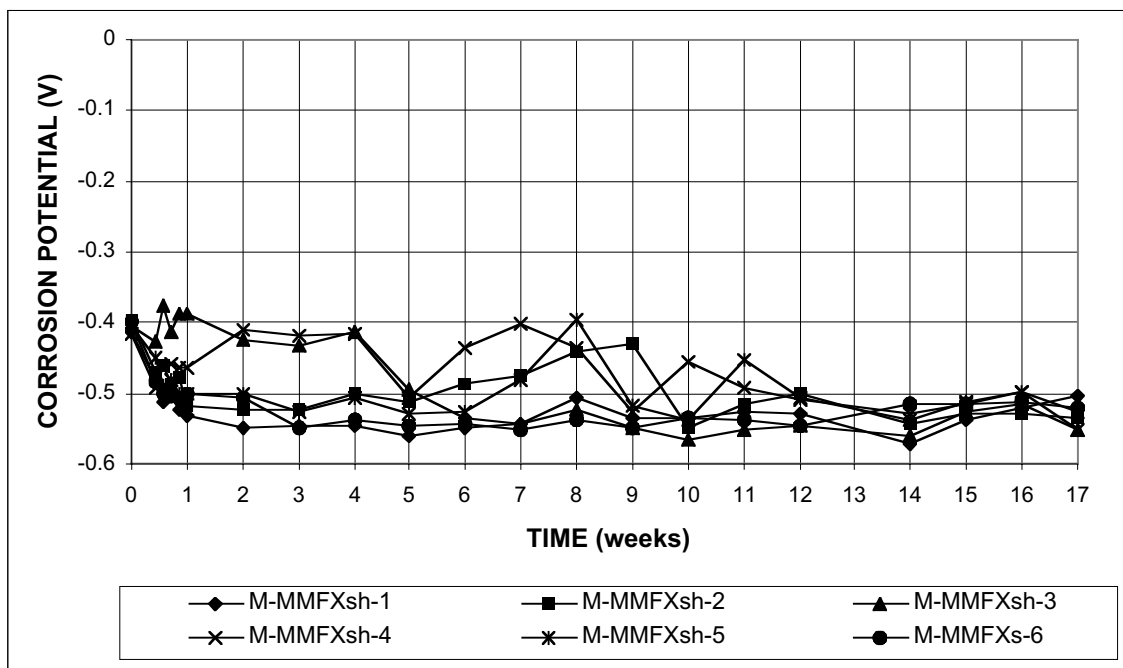


Figure B.18a - Macrocell Test. Corrosion potential vs. saturated calomel electrode, anode. Bare sandblasted MMFX steel in 6.04 m ion (15%) NaCl and simulated concrete pore solution.

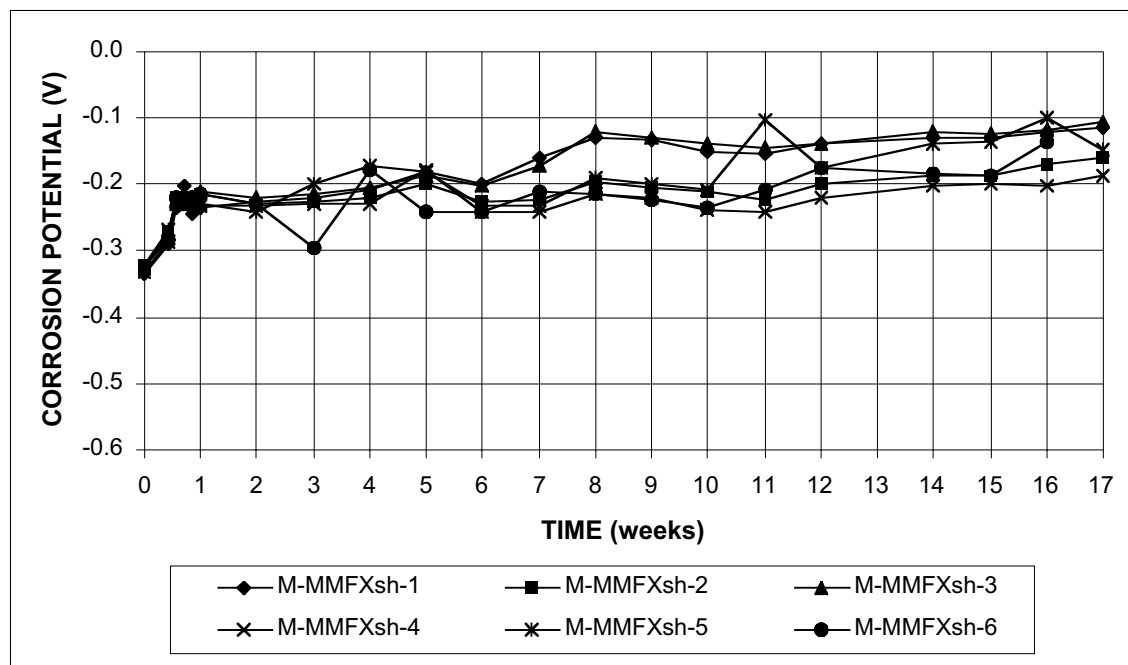


Figure B.18b - Macrocell Test. Corrosion potential vs. saturated calomel electrode, cathode. Bare sandblasted MMFX steel in 6.04 m ion (15%) NaCl and simulated concrete pore solution.

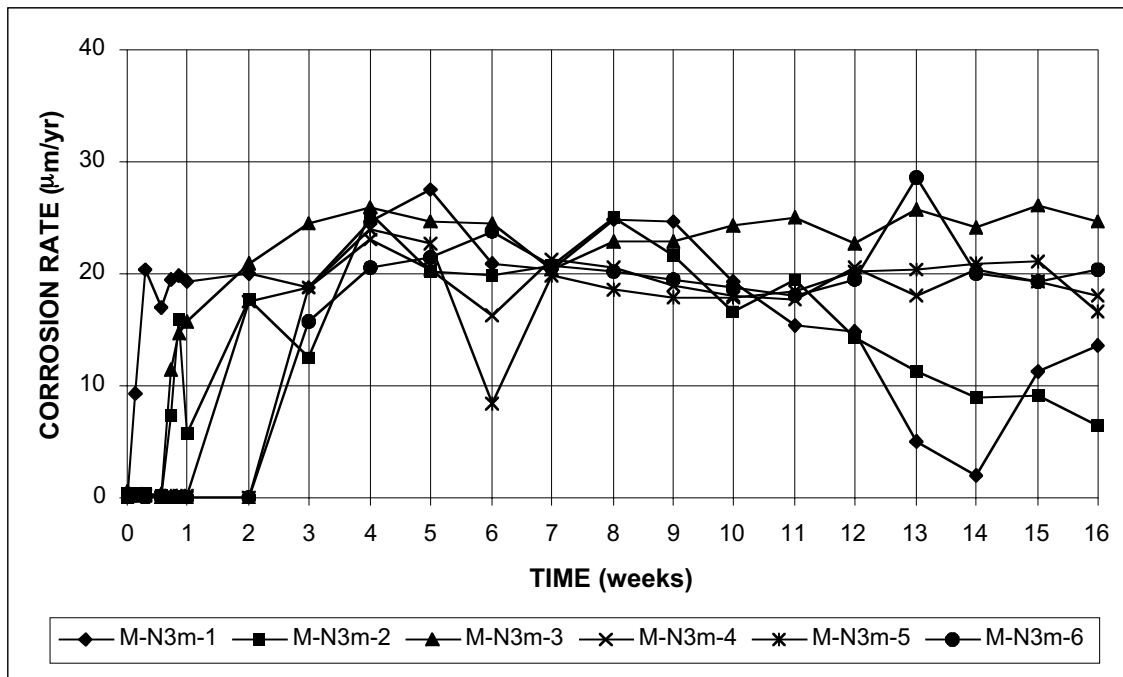


Figure B.19 - Macrocell Test. Corrosion rate. Mortar-wrapped conventional, normalized steel in 1.6 m ion NaCl and simulated concrete pore solution.

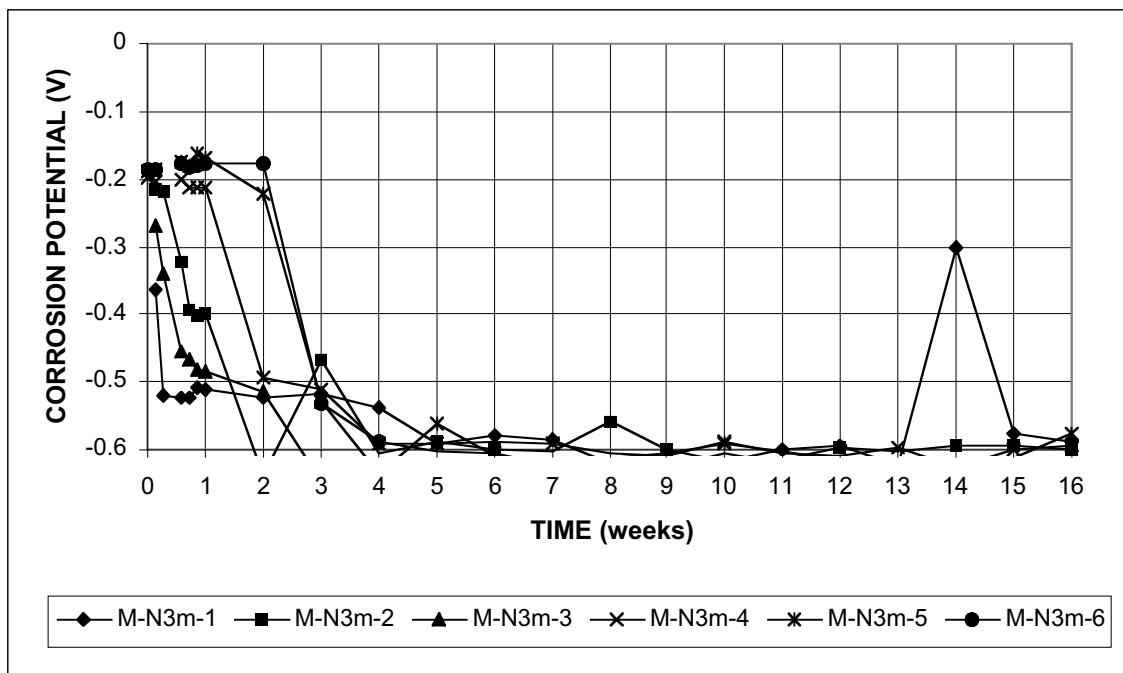


Figure B.20a - Macrocell Test. Corrosion potential vs. saturated calomel electrode, anode. Mortar-wrapped conventional, normalized steel in 1.6 m ion NaCl and simulated concrete pore solution.

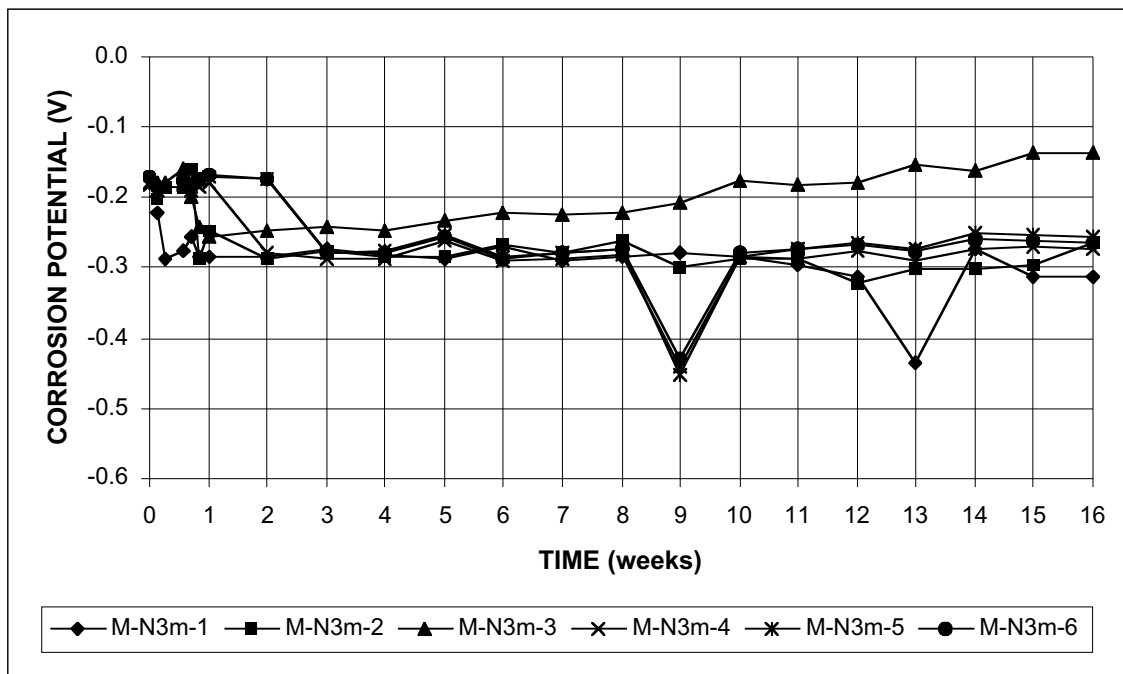


Figure B.20b - Macrocell Test. Corrosion potential vs. saturated calomel electrode, cathode. Mortar-wrapped conventional, normalized steel in 1.6 m ion NaCl and simulated concrete pore solution.

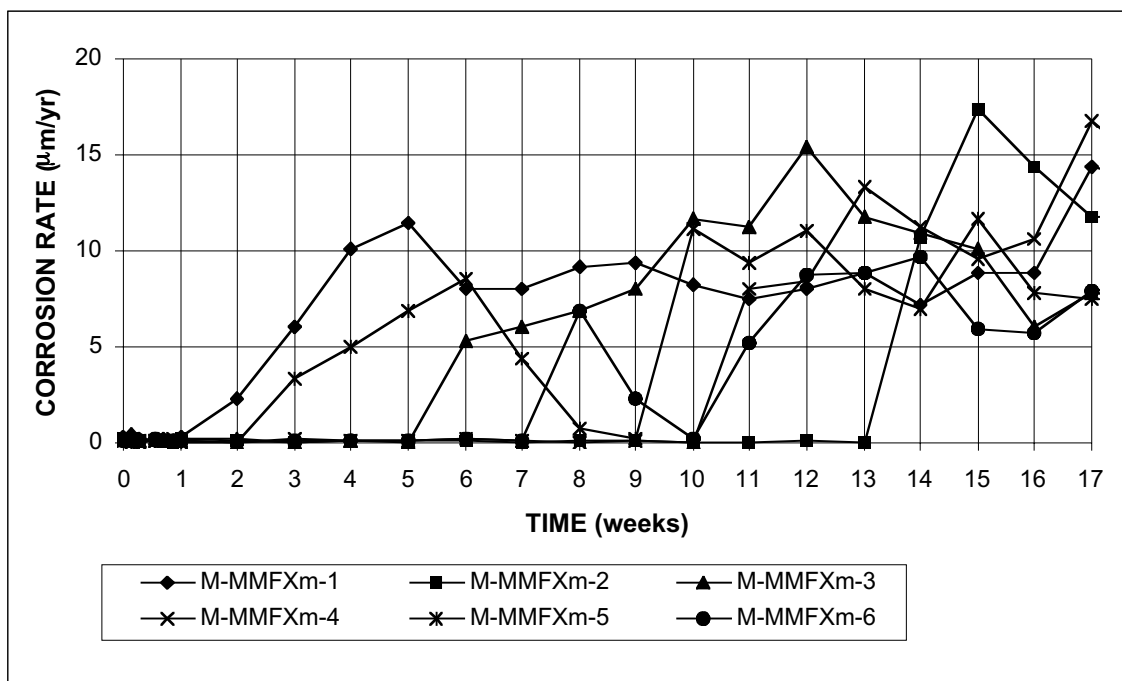


Figure B.21 - Macrocell Test. Corrosion rate. Mortar-wrapped MMFX steel in 1.6 m ion NaCl and simulated concrete pore solution.

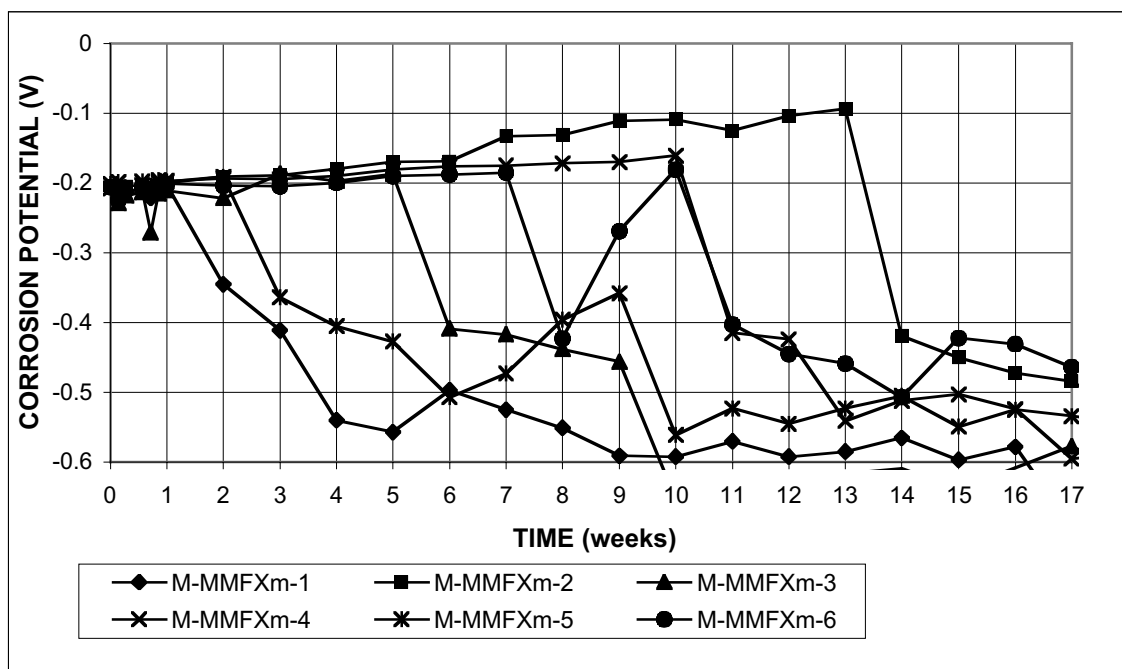


Figure B.22a - Macrocell Test. Corrosion potential vs. saturated calomel electrode, anode. Mortar-wrapped MMFX steel in 1.6 m ion NaCl and simulated concrete pore solution.

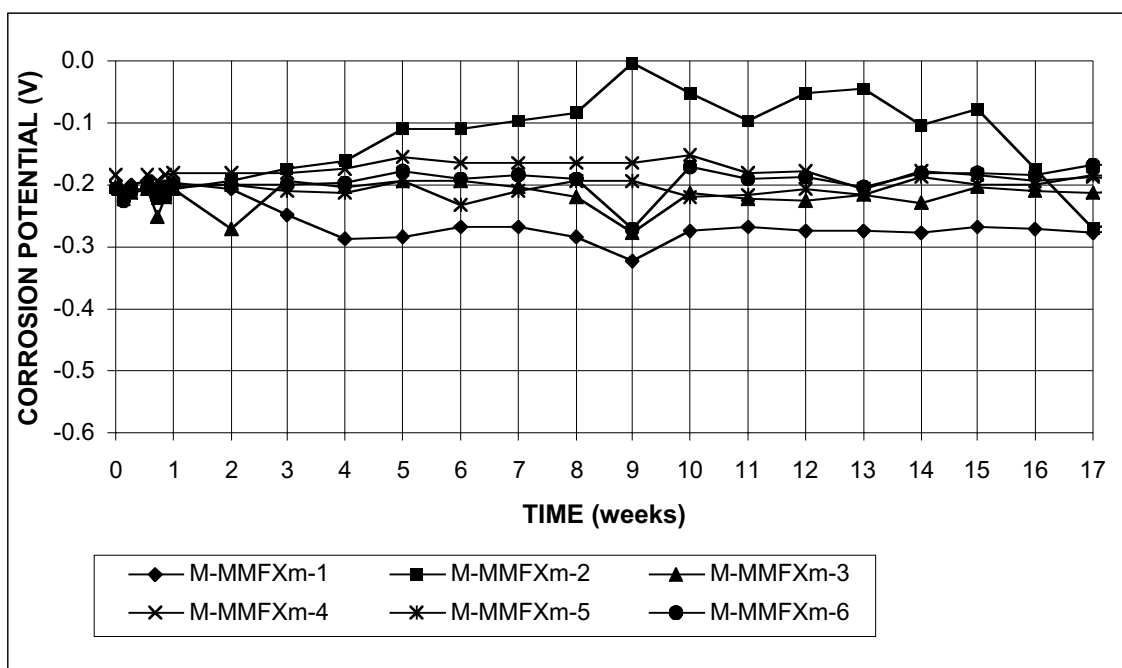


Figure B.22b - Macrocell Test. Corrosion potential vs. saturated calomel electrode, anode. Mortar-wrapped MMFX steel in 1.6 m ion NaCl and simulated concrete pore solution.

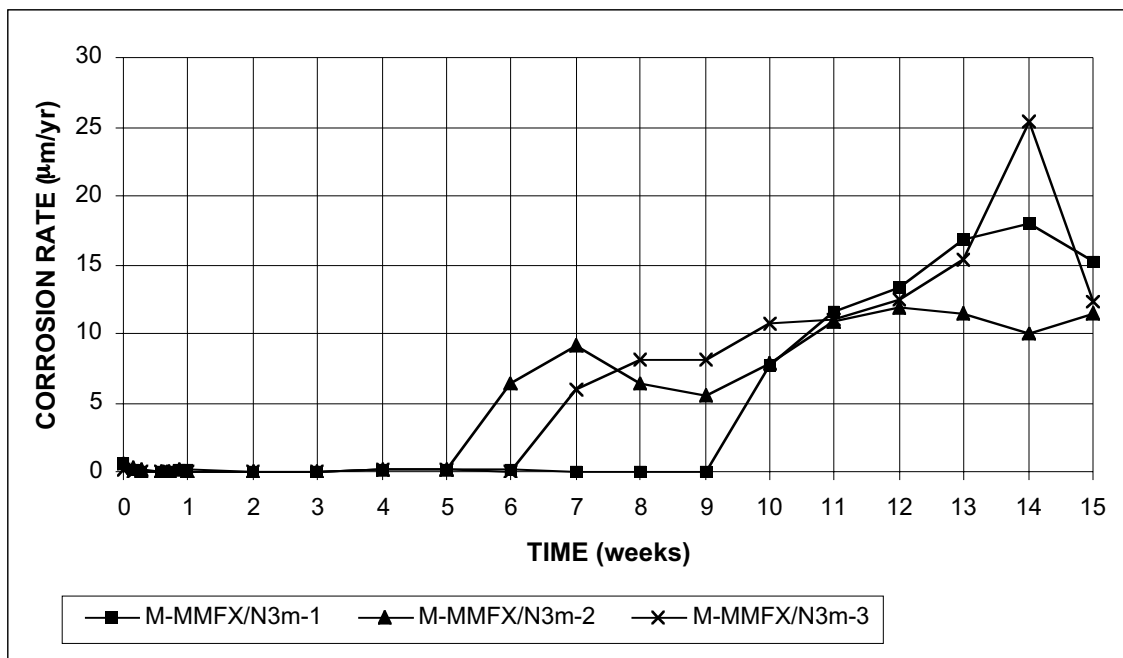


Figure B.23 - Macrocell Test. Corrosion rate. Cathode = mortar-wrapped conventional, normalized steel. Anode = mortar-wrapped MMFX steel in 1.6 m ion NaCl and simulated concrete pore solution.

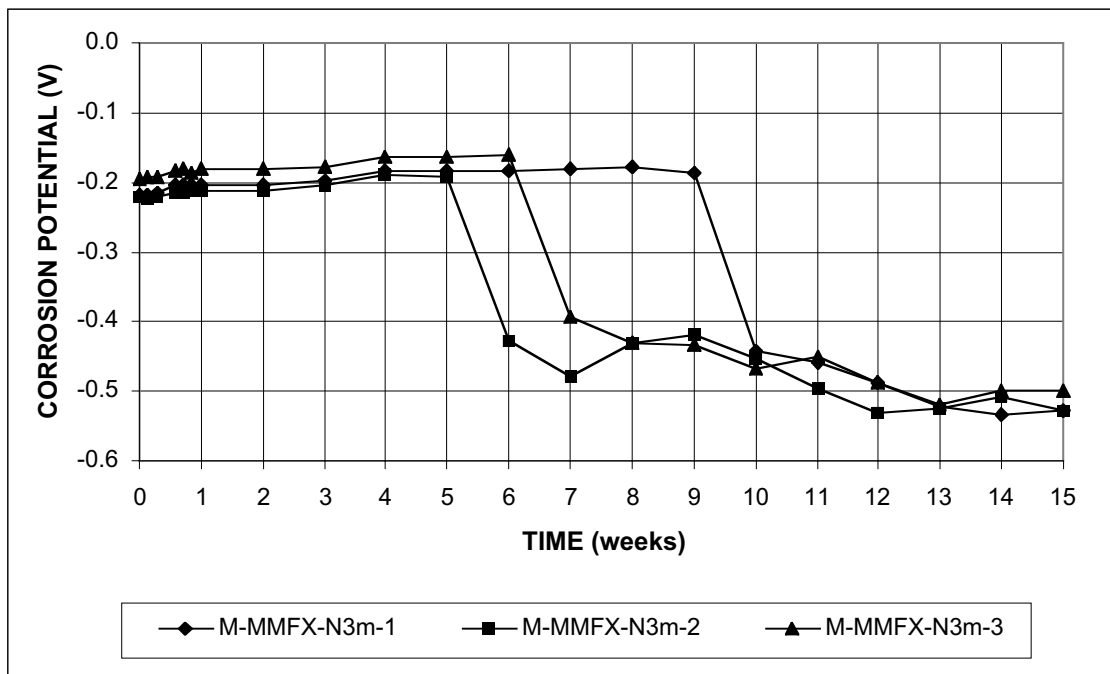


Figure B.24a - Macrocell Test. Corrosion potential vs. saturated calomel electrode, anode. Cathode = mortar-wrapped conventional, normalized steel. Anode = mortar-wrapped MMFX steel in 1.6 m ion NaCl and simulated concrete pore solution.

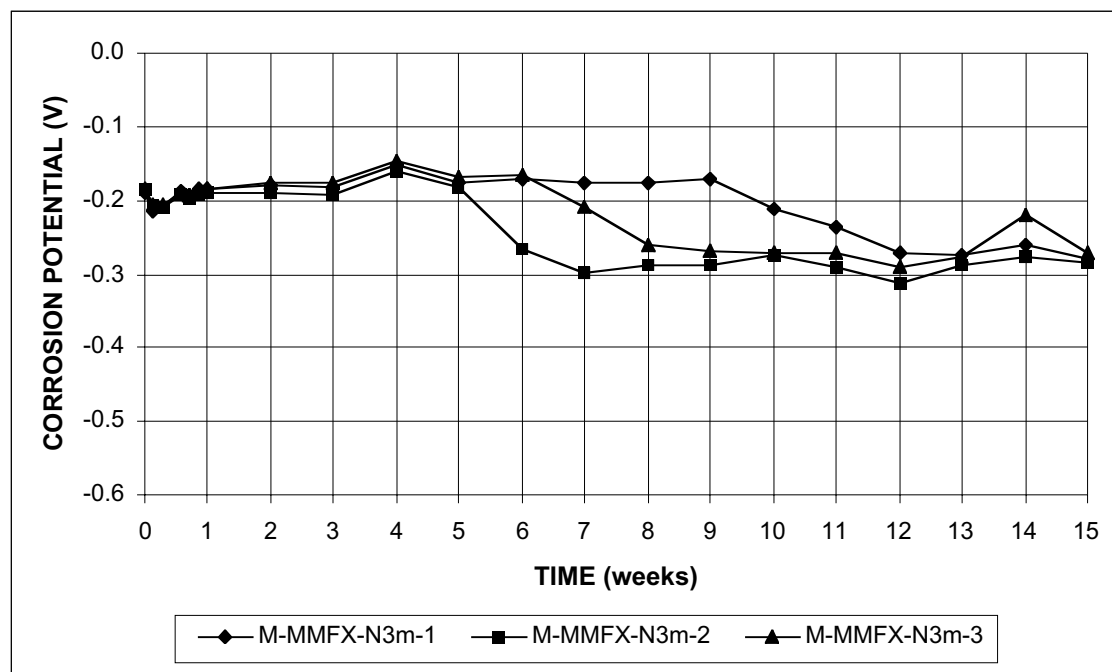


Figure B.24b - Macrocell Test. Corrosion potential vs. saturated calomel electrode, cathode. Cathode = mortar-wrapped conventional, normalized steel. Anode = mortar-wrapped MMFX steel in 1.6 m ion NaCl and simulated concrete pore solution.

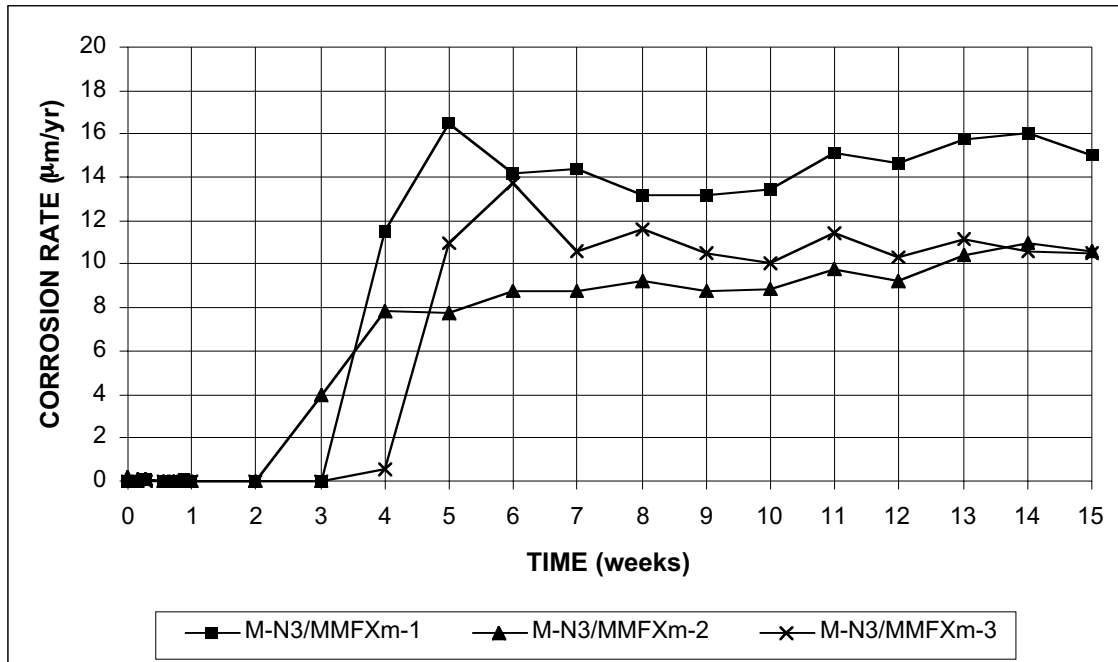


Figure B.25 - Macrocell Test. Corrosion rate. Cathode = mortar-wrapped MMFX steel. Anode = mortar-wrapped conventional, normalized steel in 1.6 m ion NaCl and simulated concrete pore solution.

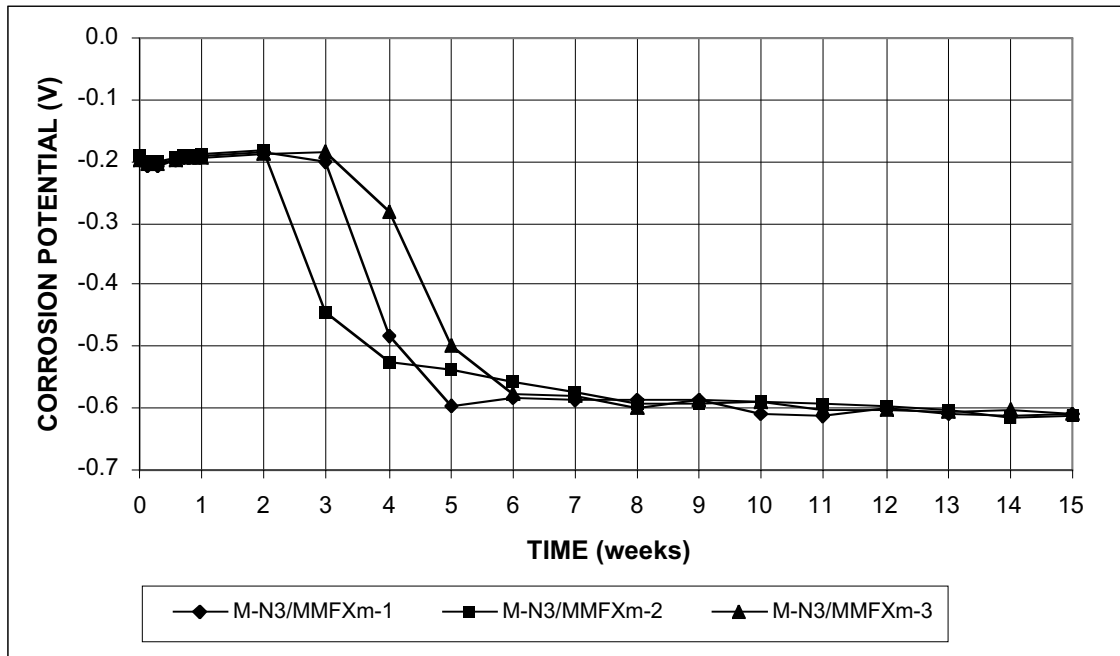


Figure B.26a - Macrocell Test. Corrosion potential vs. saturated calomel electrode, anode. Cathode = mortar-wrapped MMFX steel. Anode = mortar-wrapped conventional, normalized steel in 1.6 m ion NaCl and simulated concrete pore solution

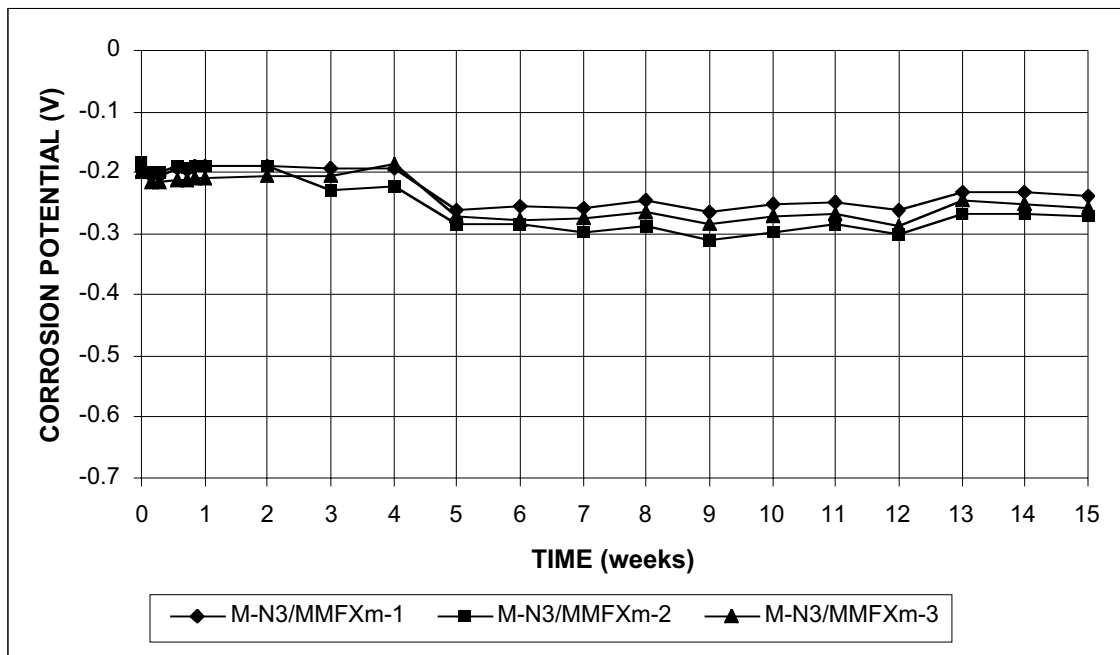


Figure B.26b - Macrocell Test. Corrosion potential vs. saturated calomel electrode, cathode.. Cathode = mortar-wrapped MMFX steel. Anode = mortar-wrapped conventional, normalized steel in 1.6 m ion NaCl and simulated concrete pore solution

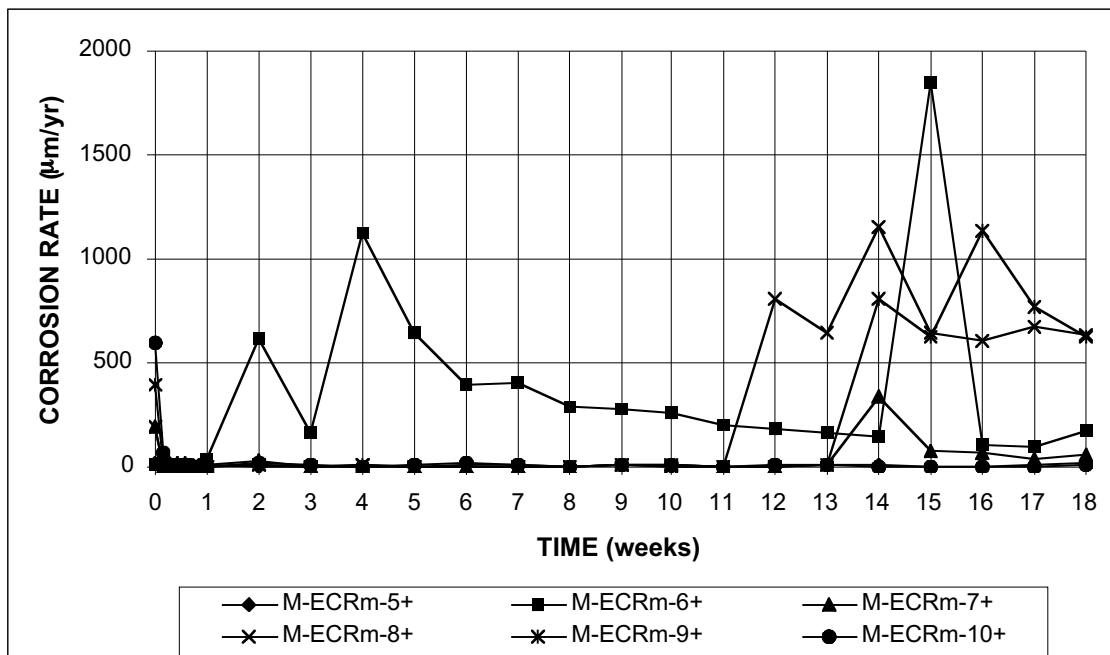


Figure B.27 - Macrocell Test. Corrosion rate based on exposed area of steel (four $\frac{1}{8}$ -in. holes in epoxy). Epoxy-coated steel in 1.6 m ion NaCl and simulated concrete pore solution.

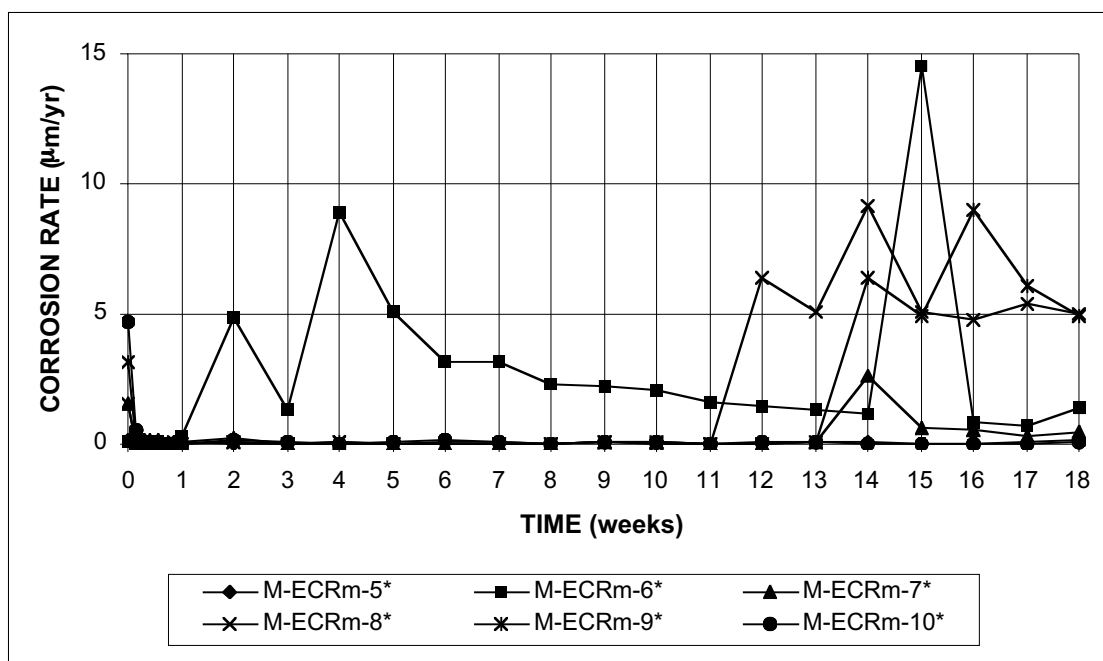


Figure B.28 - Macrocell Test. Corrosion rate based on total area of bar exposed to solution. Epoxy-coated steel in 1.6 m ion NaCl and simulated concrete pore solution.

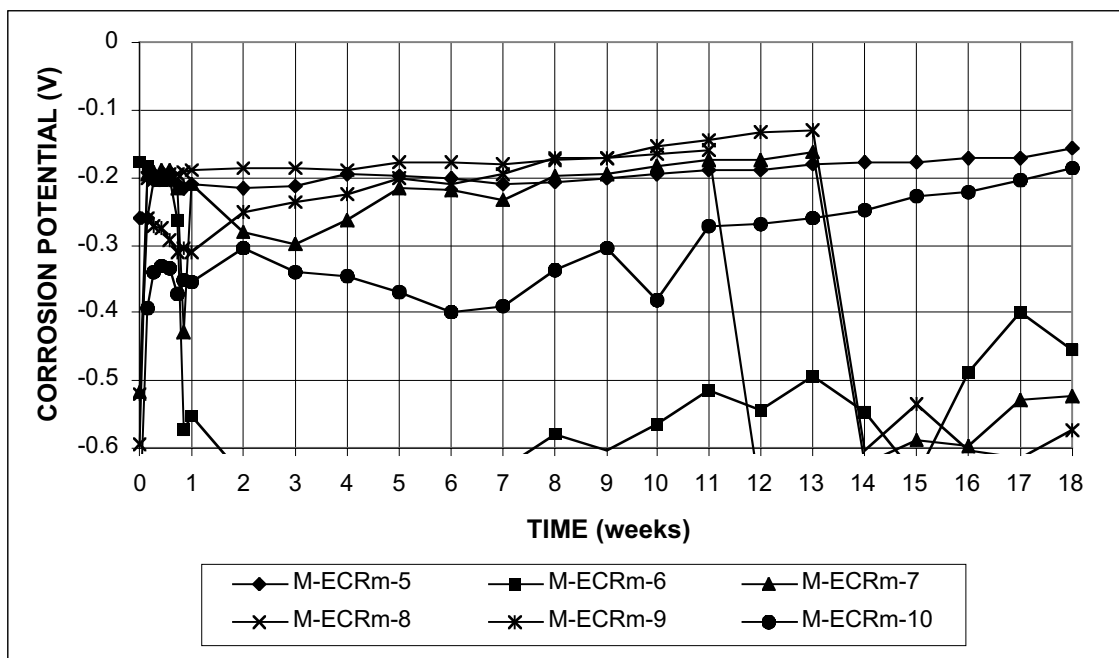


Figure B.29a - Macrocell Test. Corrosion potential vs. saturated calomel electrode, anode. Epoxy-coated steel in 1.6 m ion NaCl and simulated concrete pore solution.

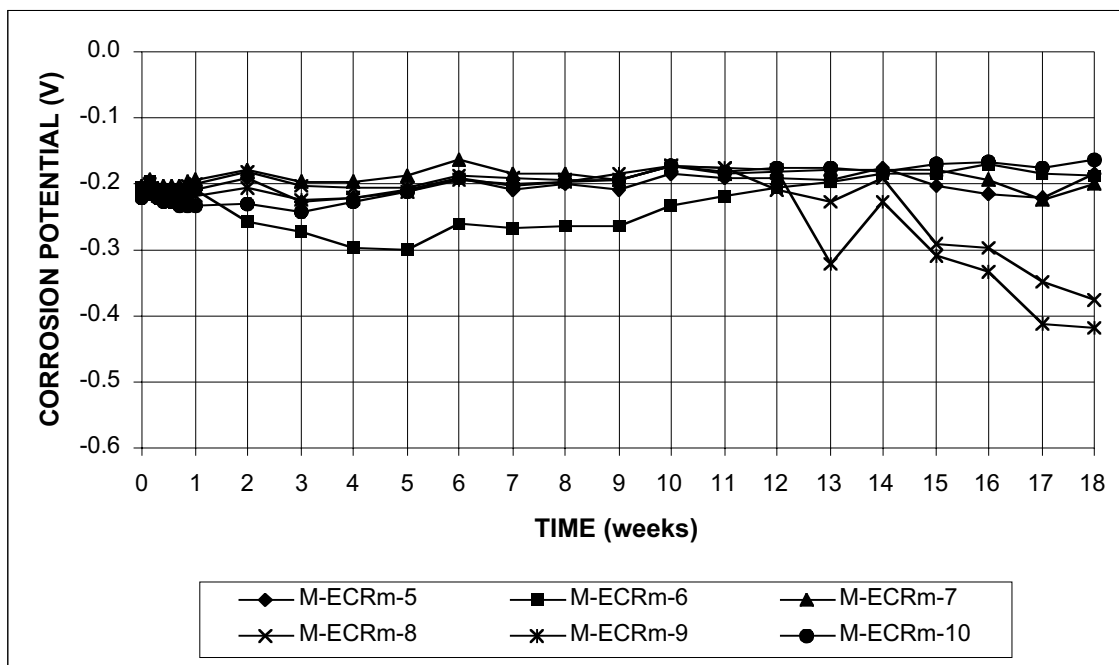


Figure B.29b - Macrocell Test. Corrosion potential vs. saturated calomel electrode, cathode. Epoxy-coated steel in 1.6 m ion NaCl and simulated concrete pore solution

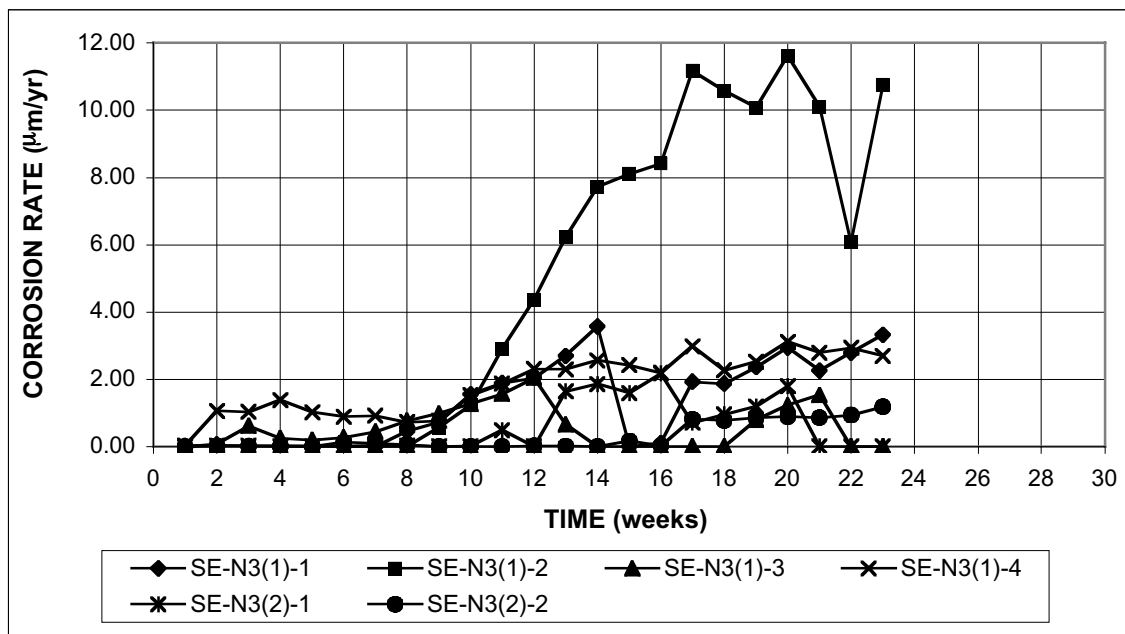


Figure B.30 - Southern Exposure Test. Corrosion rate. Conventional, normalized steel, w/c=0.45, ponded with 15% NaCl solution.

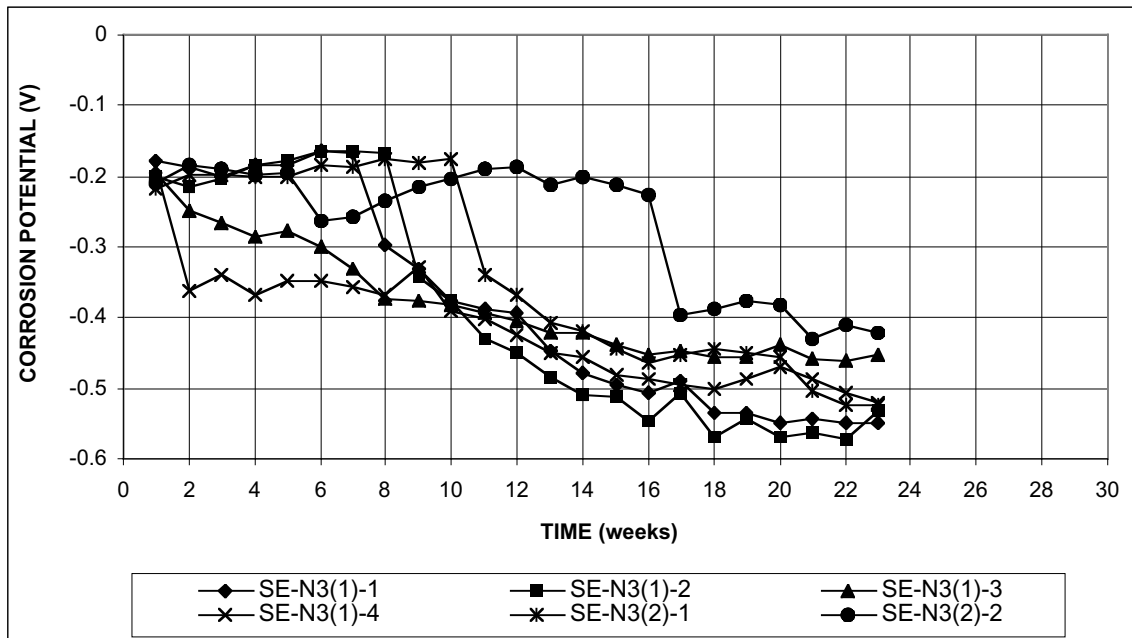


Figure B.31a - Southern Exposure Test. Corrosion potential vs. CSE, top mat. Conventional, normalized steel, w/c=0.45, ponded with 15% NaCl solution.

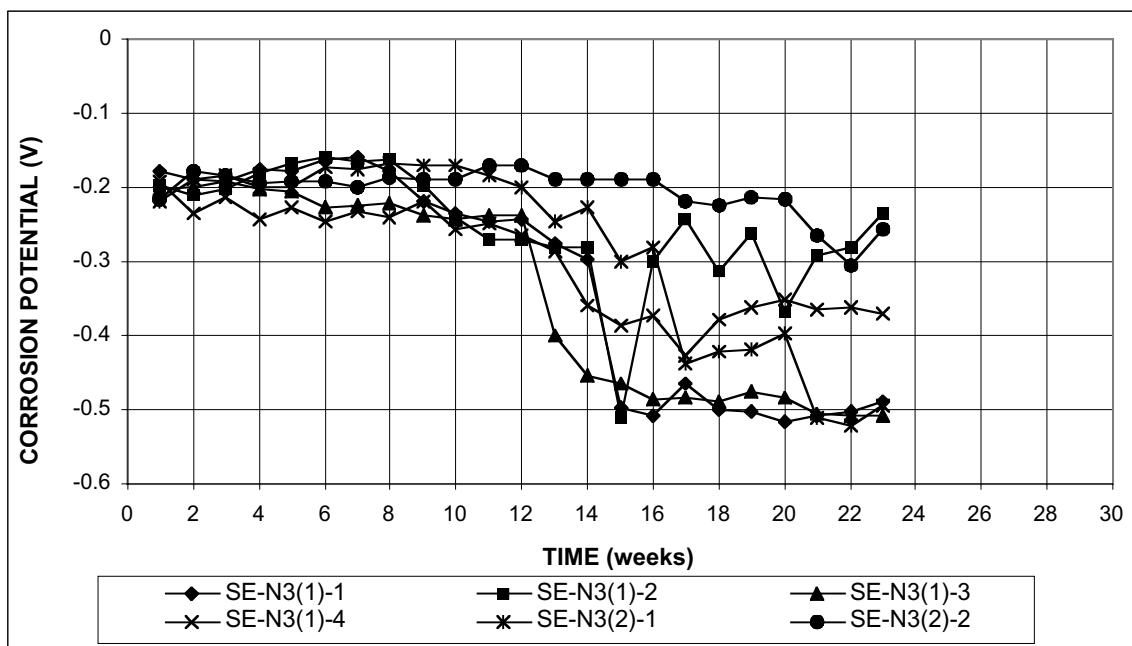


Figure B.31b - Southern Exposure Test. Corrosion potential vs. CSE, bottom mat. Conventional, normalized steel, w/c=0.45, ponded with 15% NaCl solution.

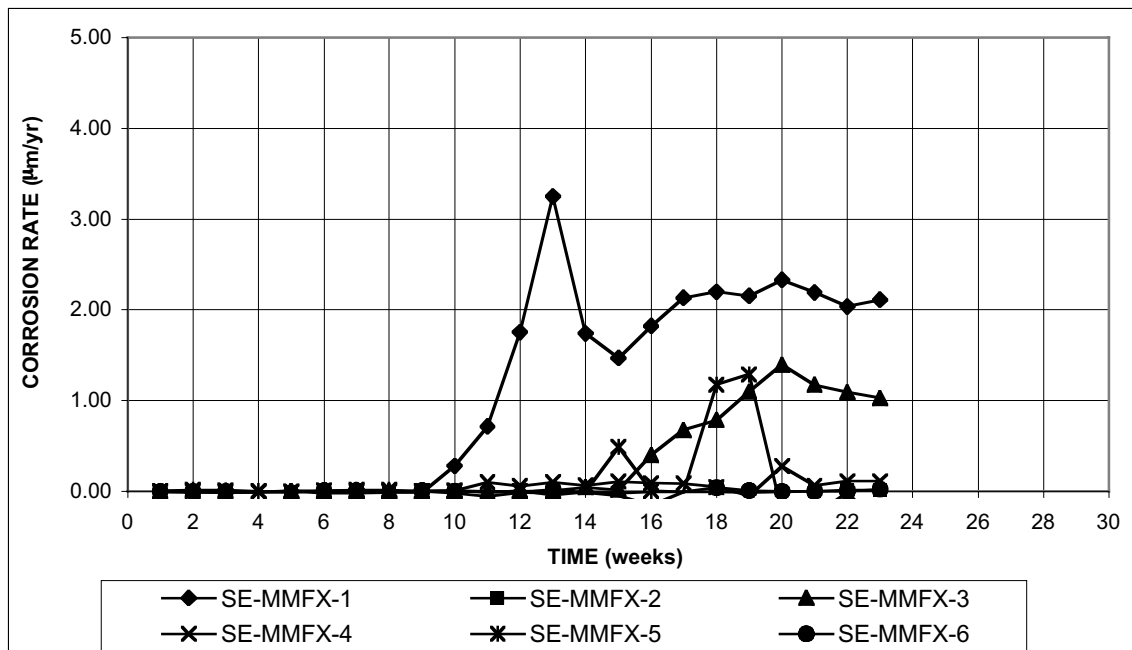


Figure B.32 - Southern Exposure Test. Corrosion rate. MMFX steel, w/c=0.45, ponded with 15% NaCl solution.

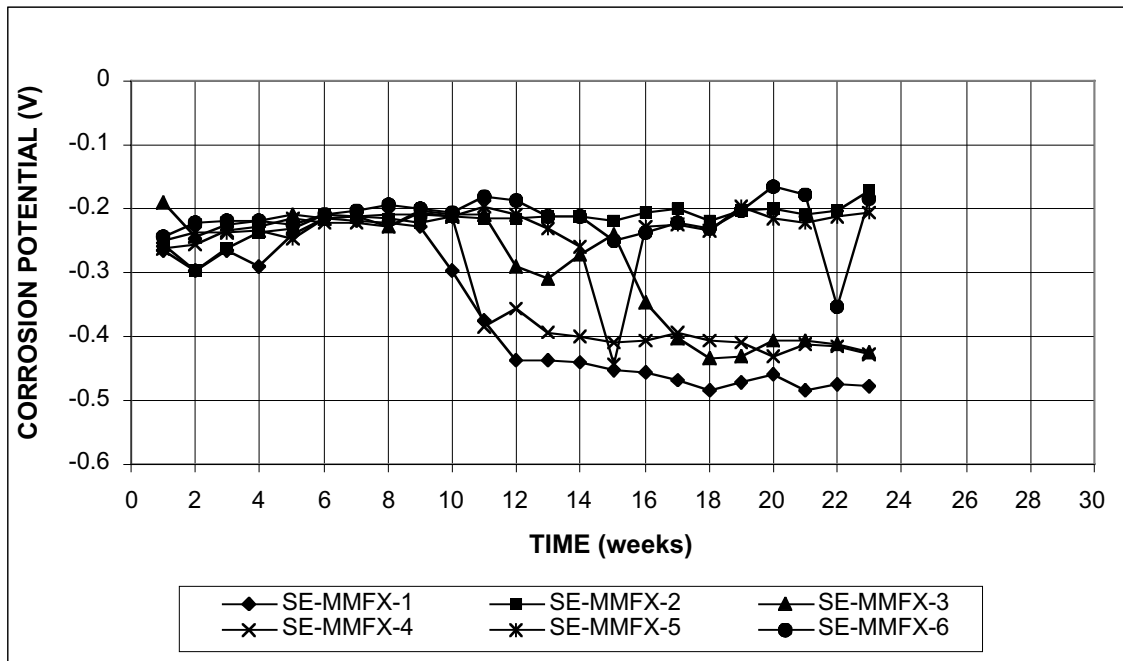


Figure B.33a - Southern Exposure Test. Corrosion potential vs. CSE, top mat. MMFX steel, w/c=0.45, ponded with 15% NaCl solution.

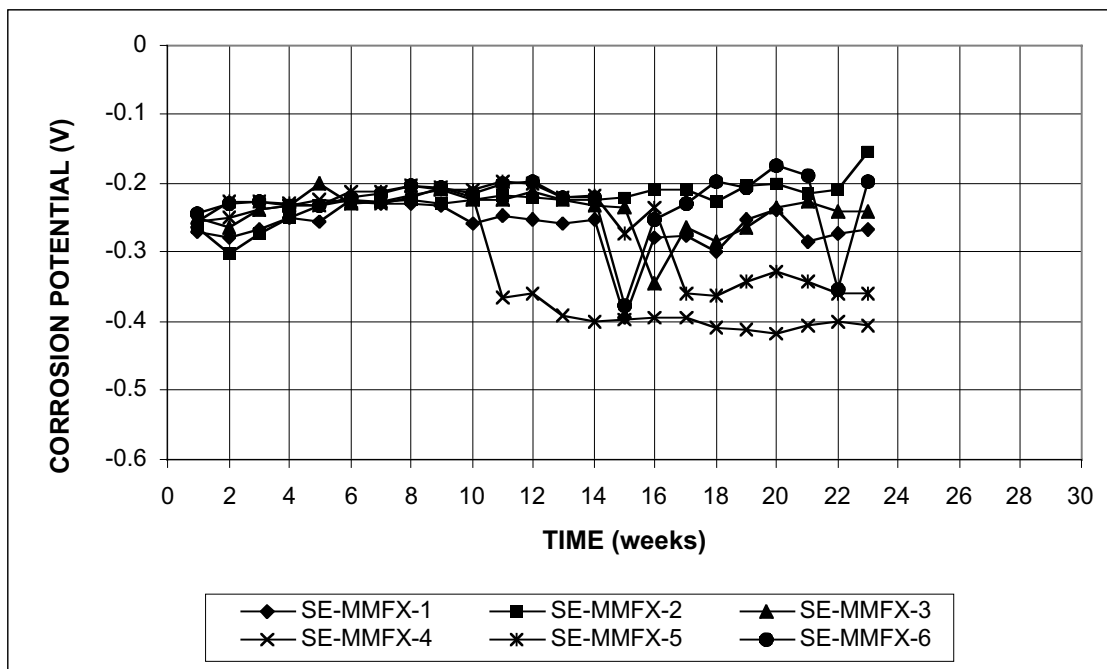


Figure B.33b - Southern Exposure Test. Corrosion potential vs. CSE, bottom mat. MMFX steel, w/c=0.45, ponded with 15% NaCl solution.

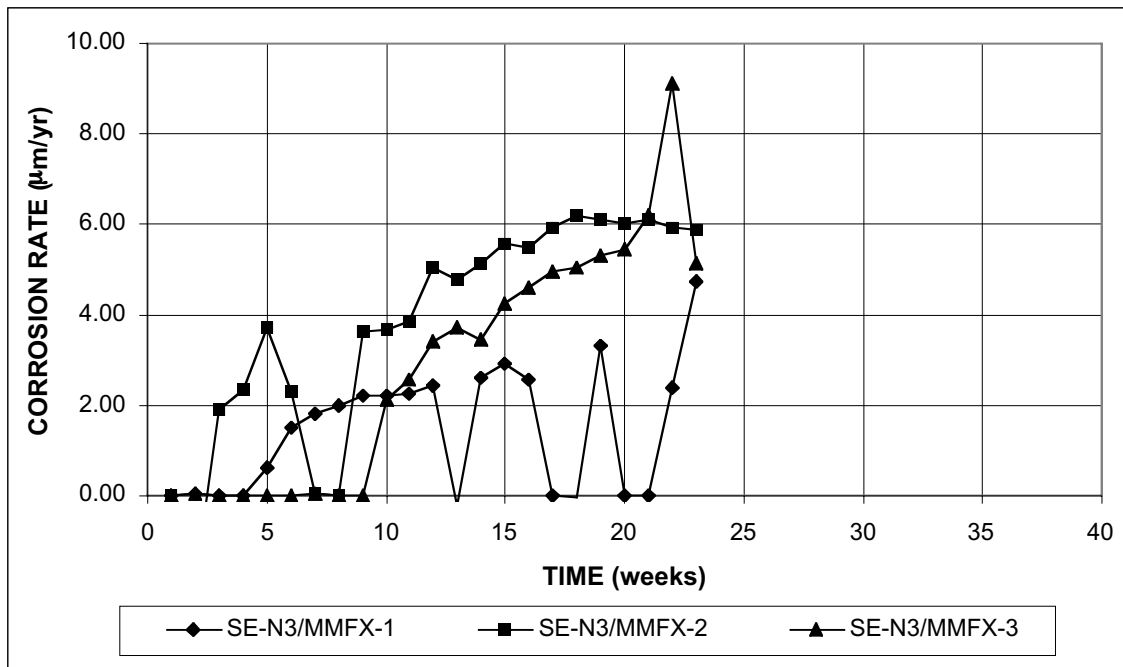


Figure B.34 - Southern Exposure Test. Corrosion rate. Top mat = conventional, normalized steel, bottom mat = MMFX steel, w/c=0.45, ponded with 15% NaCl solution.

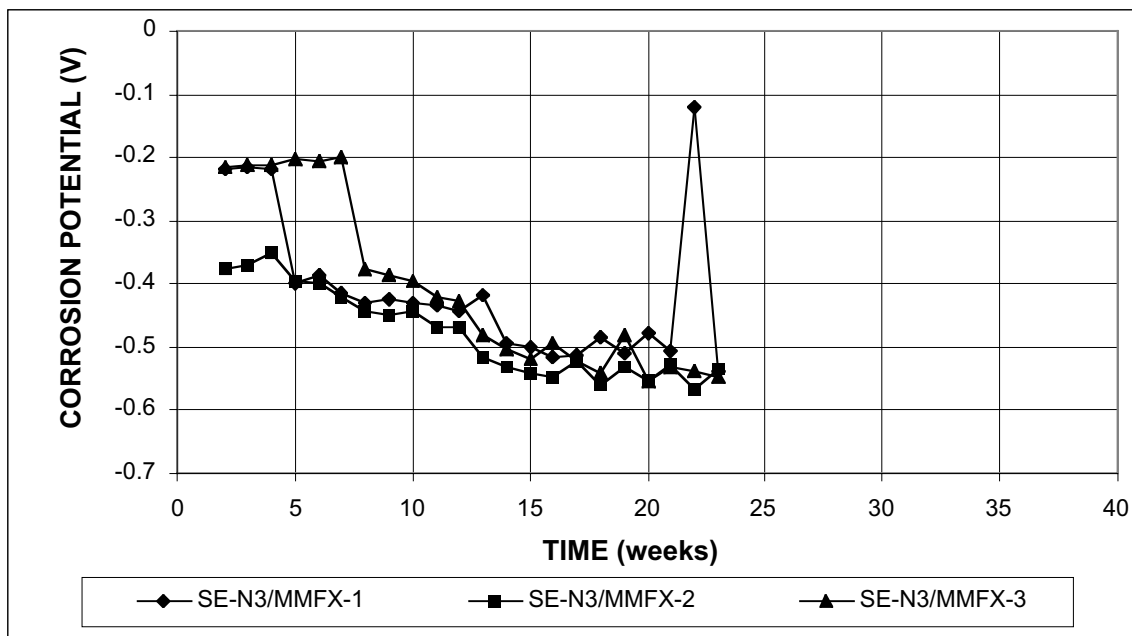


Figure B.35a - Southern Exposure Test. Corrosion potential vs. CSE, top mat. Top mat = conventional, normalized steel, bottom mat = MMFX steel, w/c=0.45, ponded with 15% NaCl solution.

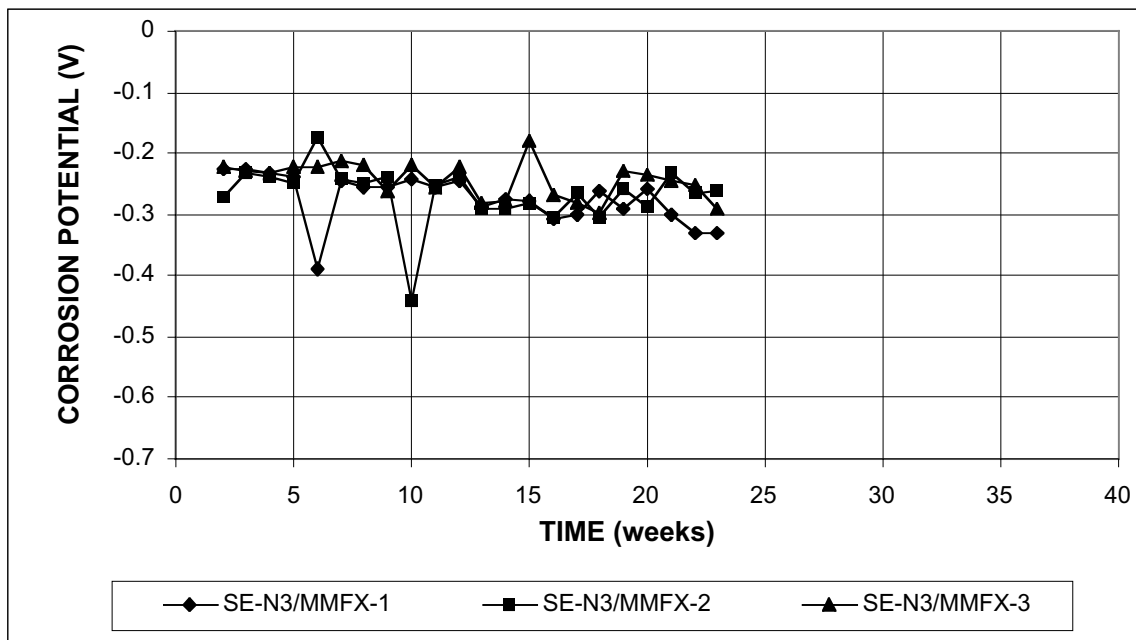


Figure B.35b- Southern Exposure Test. Corrosion potential vs. CSE, bottom mat. Top mat = conventional, normalized steel. Bottom mat = MMFX steel, w/c=0.45, ponded with 15% NaCl solution.

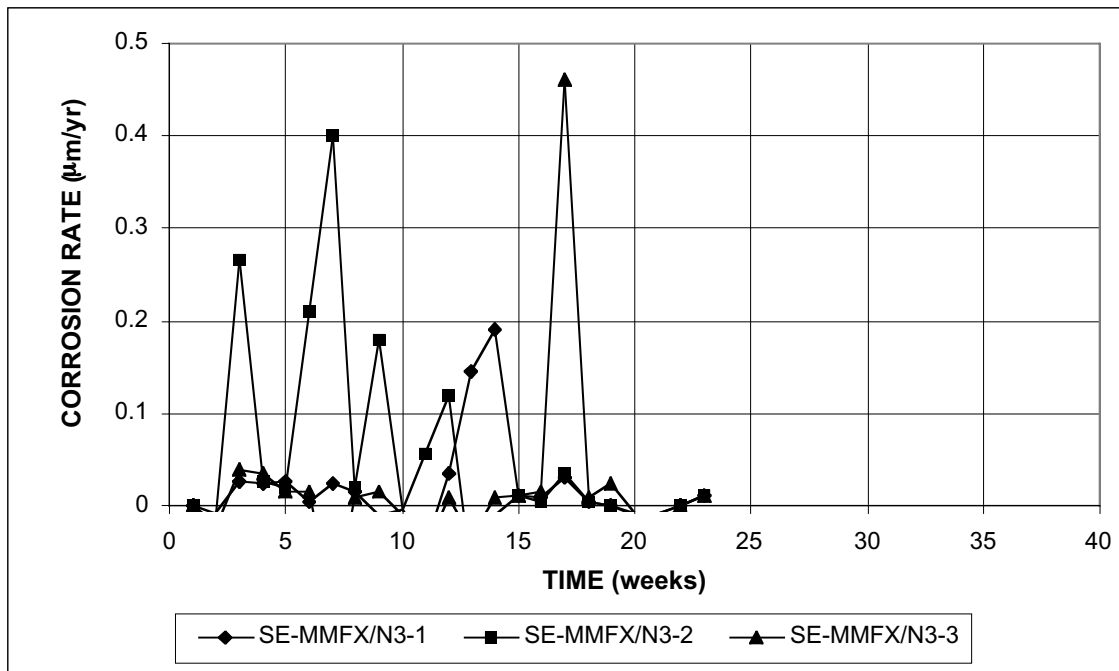


Figure B.36 - Southern Exposure Test. Corrosion rate. Top mat = MMFX steel, bottom mat = conventional steel, normalized, w/c=0.45, ponded with 15% NaCl solution.

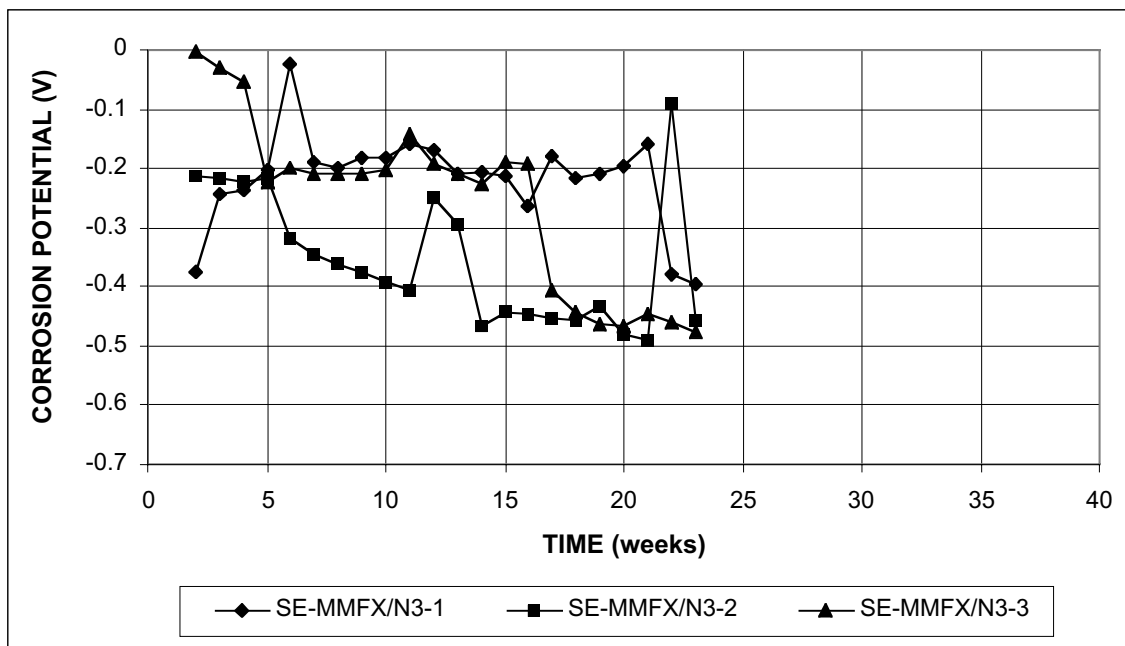


Figure B.37a - Southern Exposure Test. Corrosion potential vs. CSE, top mat. Top mat = MMFX steel, bottom mat = conventional, normalized steel, w/c=0.45, ponded with 15% NaCl solution.

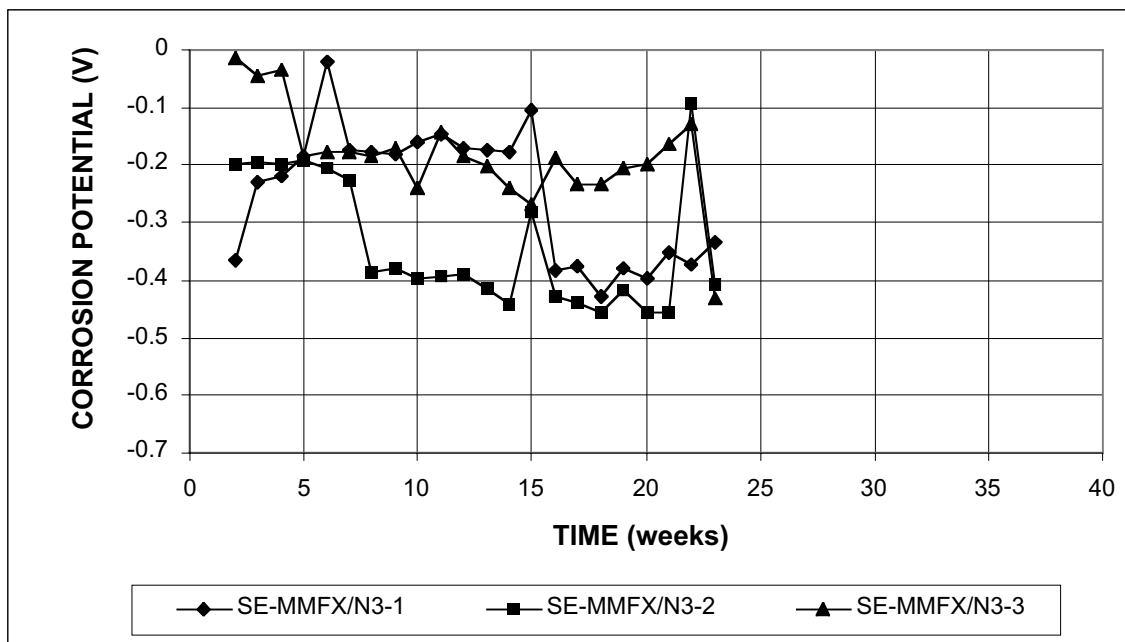


Figure B.37b - Southern Exposure Test – Corrosion potential vs. CSE, bottom mat. Top mat = MMFX steel, bottom mat = conventional, normalized steel, w/c=0.45, ponded with 15% NaCl solution.

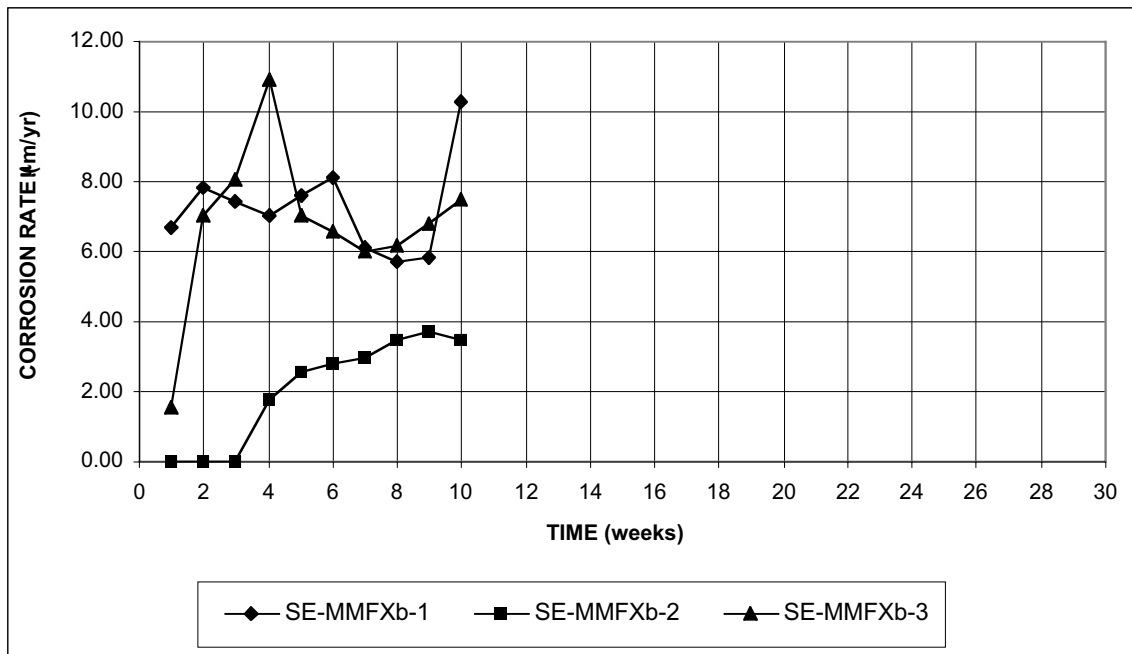


Figure B.38 - Southern Exposure Test. Corrosion rate. MMFX steel, bent bar at anode, w/c=0.45, ponded with 15% NaCl solution.

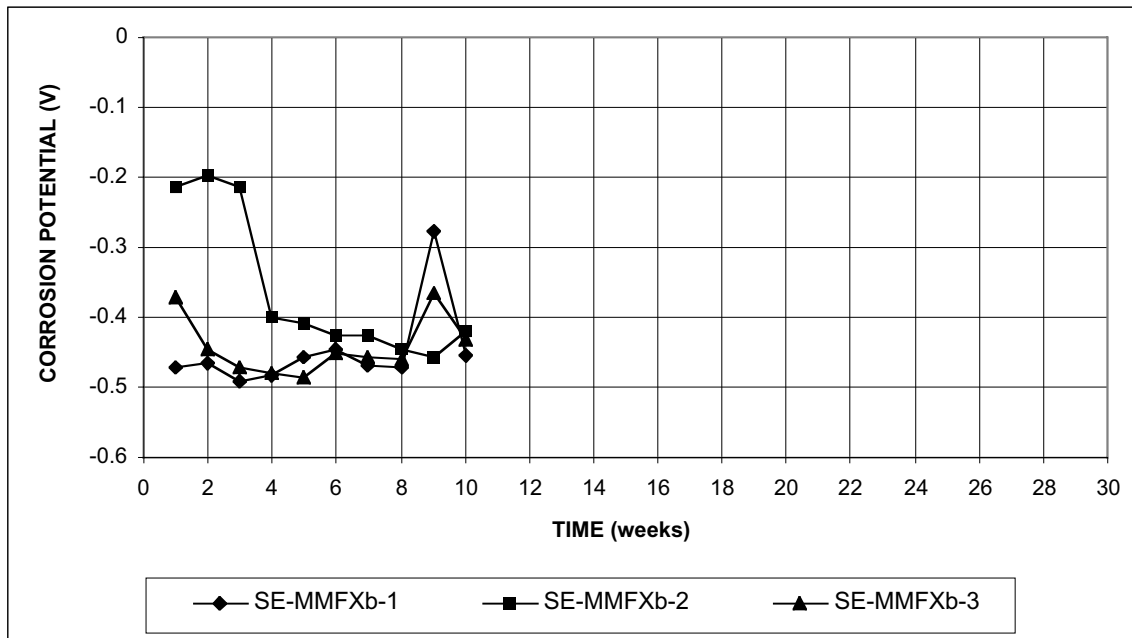


Figure B.39a - Southern Exposure Test – Corrosion potential vs. CSE, top mat. MMFX steel, bent bar at anode, w/c=0.45, ponded with 15% NaCl solution.

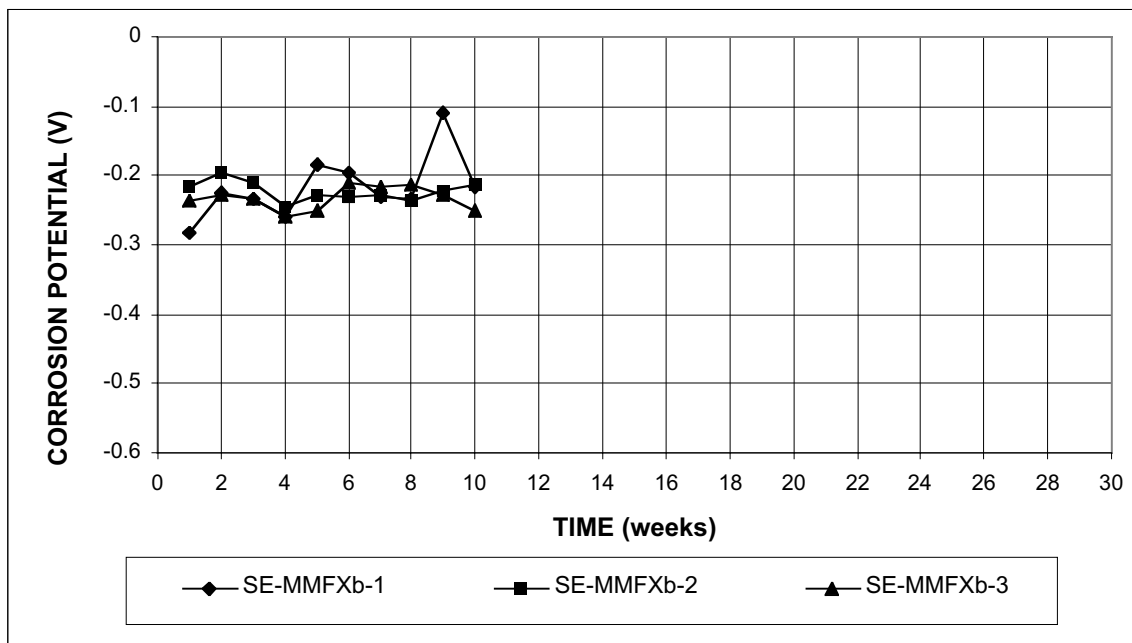


Figure B.39b - Southern Exposure Test – Corrosion potential vs. CSE, bottom mat. MMFX steel, bent bar at anode, w/c=0.45, ponded with 15% NaCl solution.

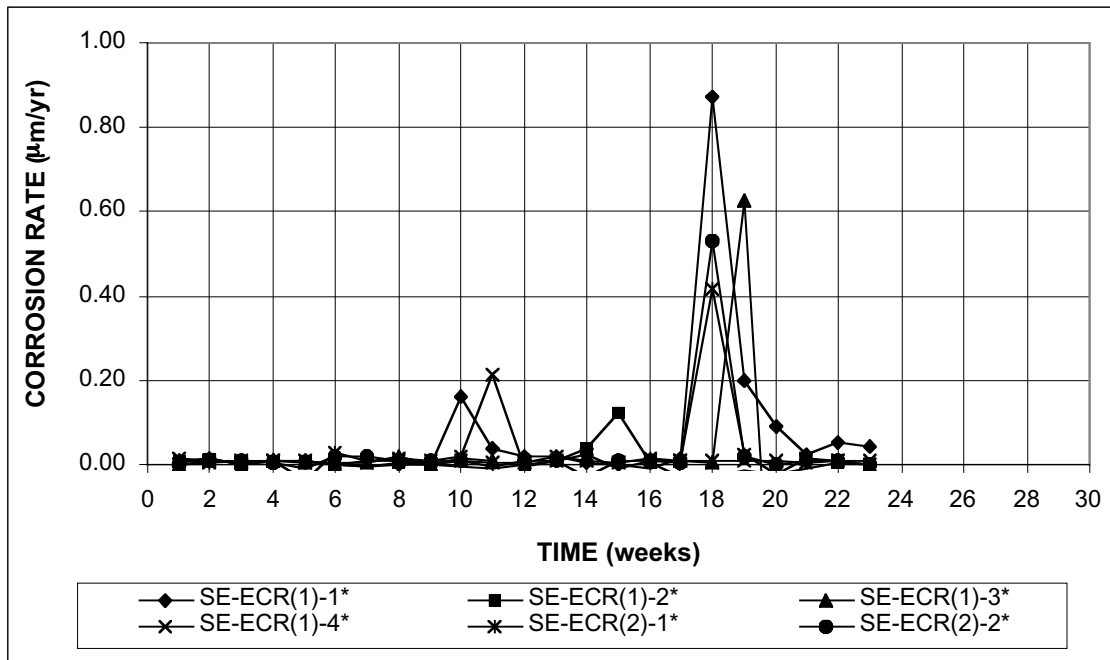


Figure B.40 - Southern Exposure Test. Corrosion rate based on total bar area exposed to solution. Epoxy-coated bars, w/c=0.45, ponded with 15% NaCl solution.

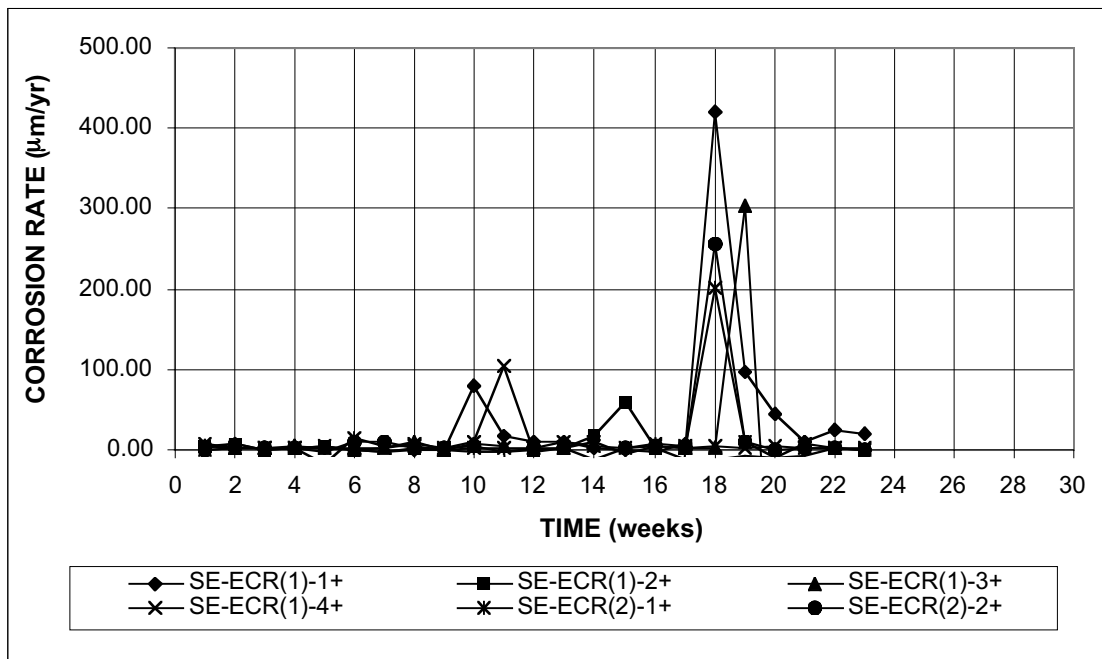


Figure B.41 - Southern Exposure Test. Corrosion rate based on exposed area of steel (four $\frac{1}{8}$ -in. diameter holes in epoxy). Epoxy-coated steel, w/c=0.45, ponded with 15% NaCl solution.

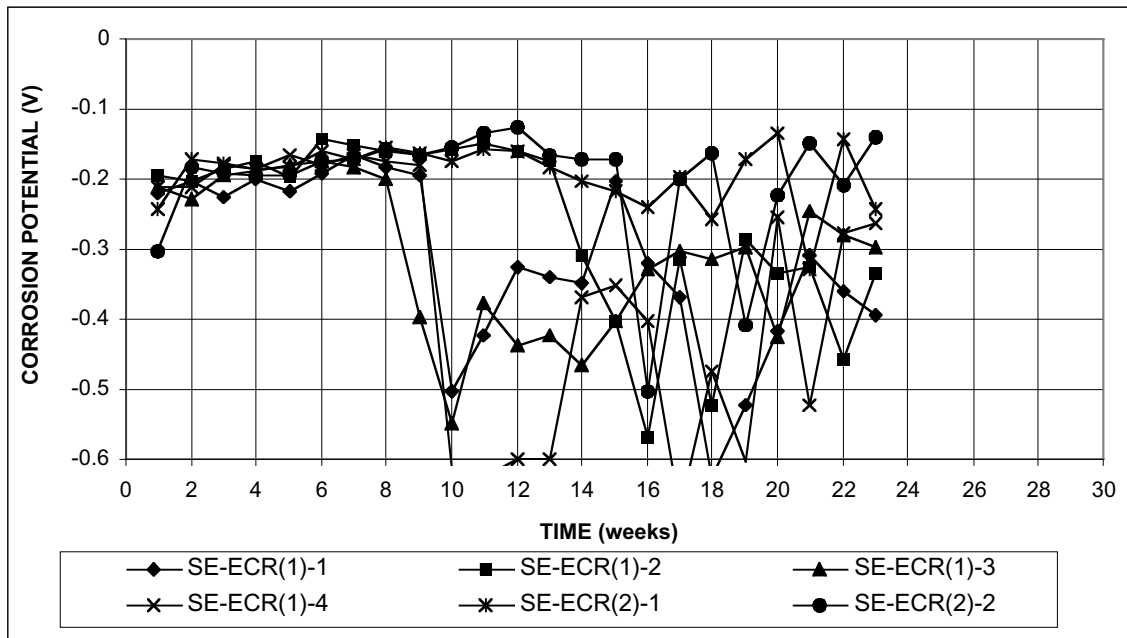


Figure B.42a - Southern Exposure Test. Corrosion potential vs. CSE, top mat. Epoxy-coated steel, w/c=0.45, ponded with 15% NaCl solution.

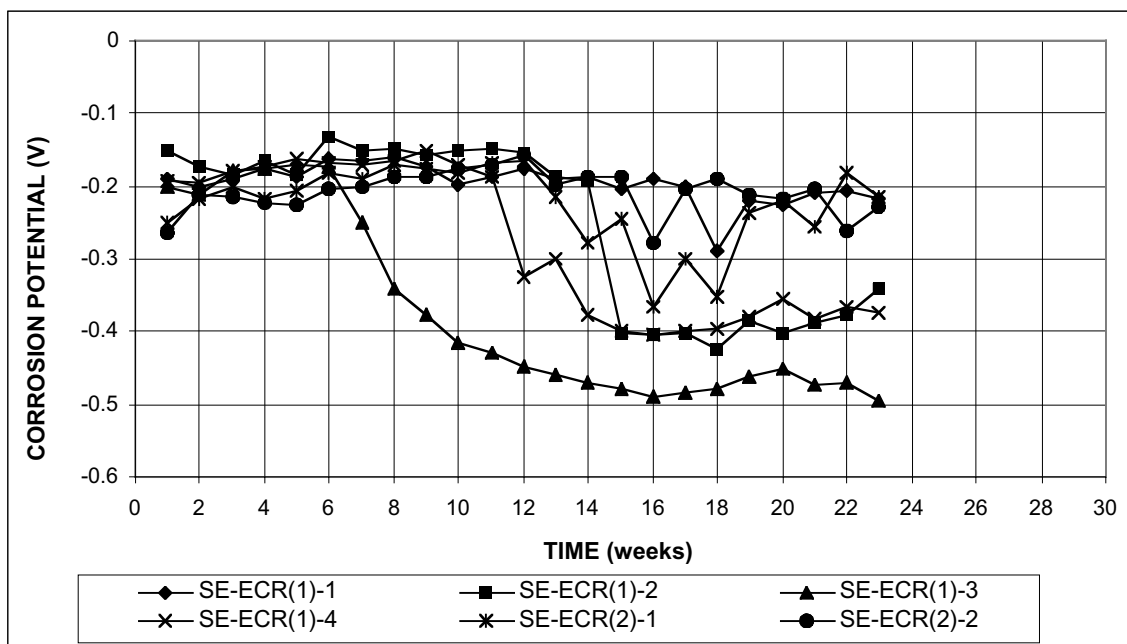


Figure B.42b - Southern Exposure Test. Corrosion potential vs. CSE, bottom mat. Epoxy-coated steel, w/c=0.45, ponded with 15% NaCl solution.

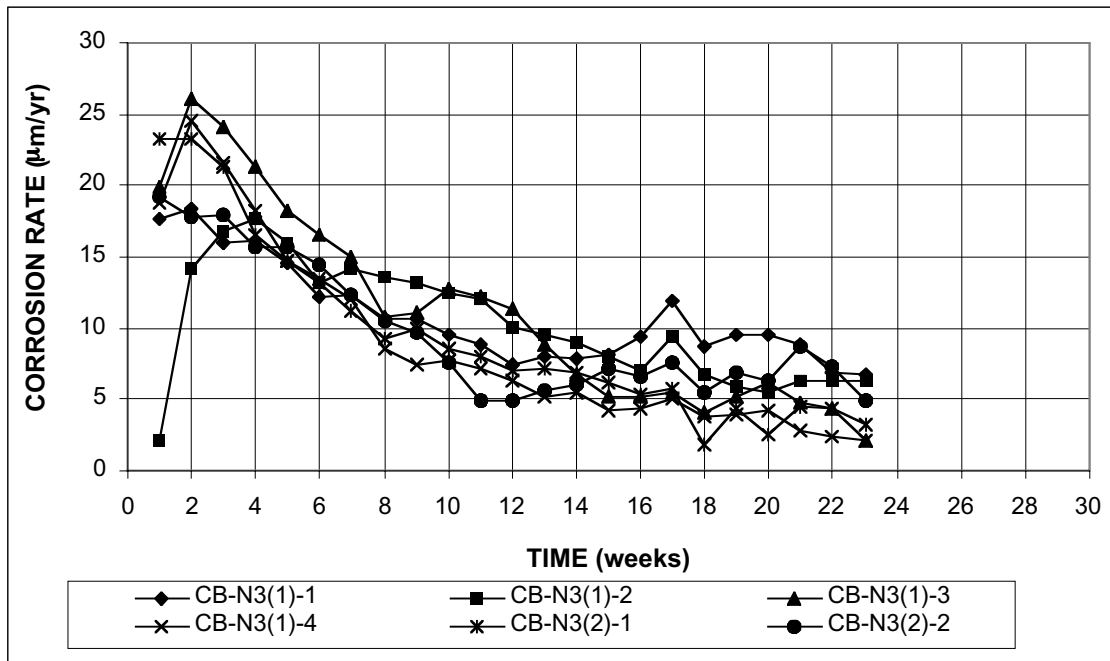


Figure B.43 - Cracked Beam Test. Corrosion rate. Conventional, normalized steel, w/c=0.45, ponded with 15% NaCl solution.

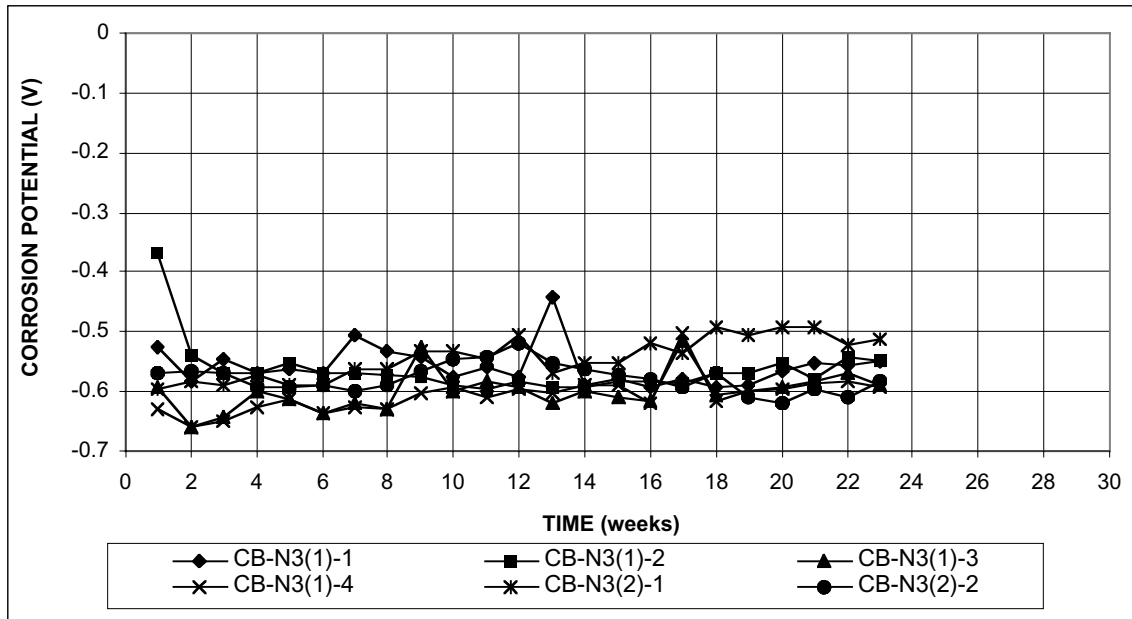


Figure B.44a - Cracked Beam Test. Corrosion potential vs. CSE, top mat. Conventional, normalized steel, w/c=0.45, ponded with 15% NaCl solution.

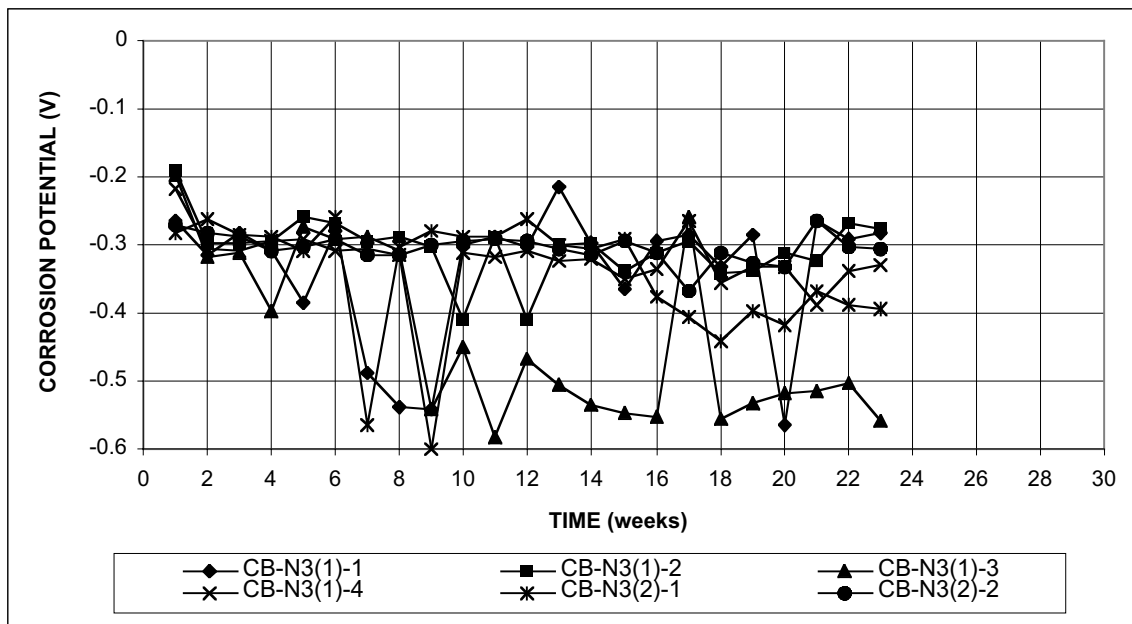


Figure B.44b - Cracked Beam Test. Corrosion potential vs. CSE, top mat. Conventional, normalized steel, w/c=0.45, ponded with 15% NaCl solution.

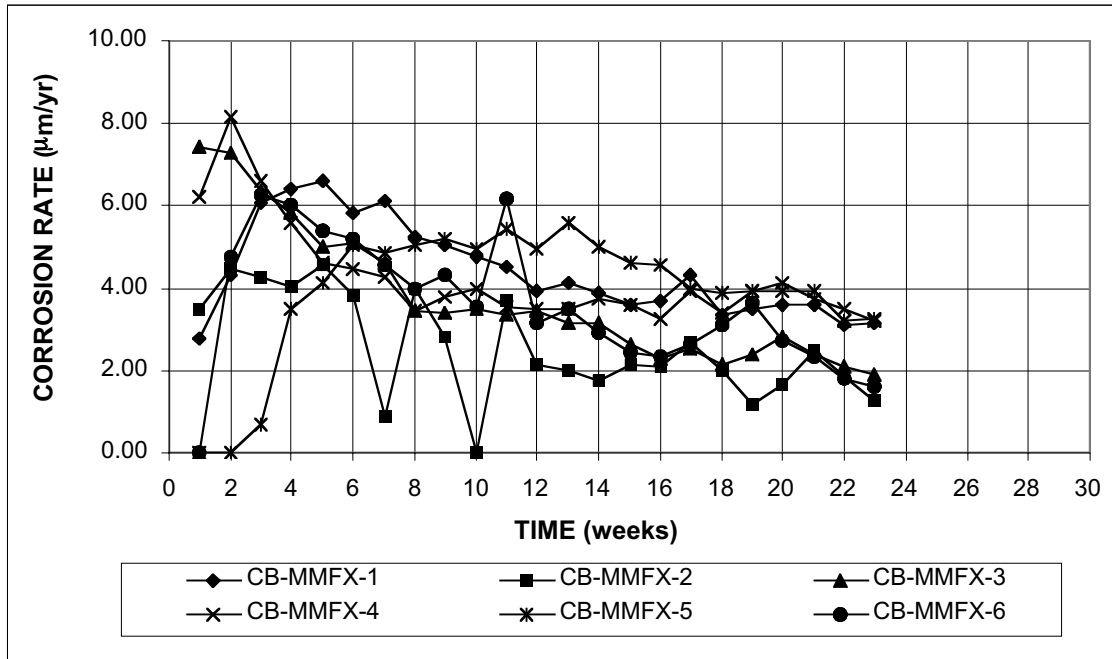


Figure B.45 - Cracked Beam Test. Corrosion rate. MMFX steel, w/c=0.45, ponded with 15% NaCl solution.

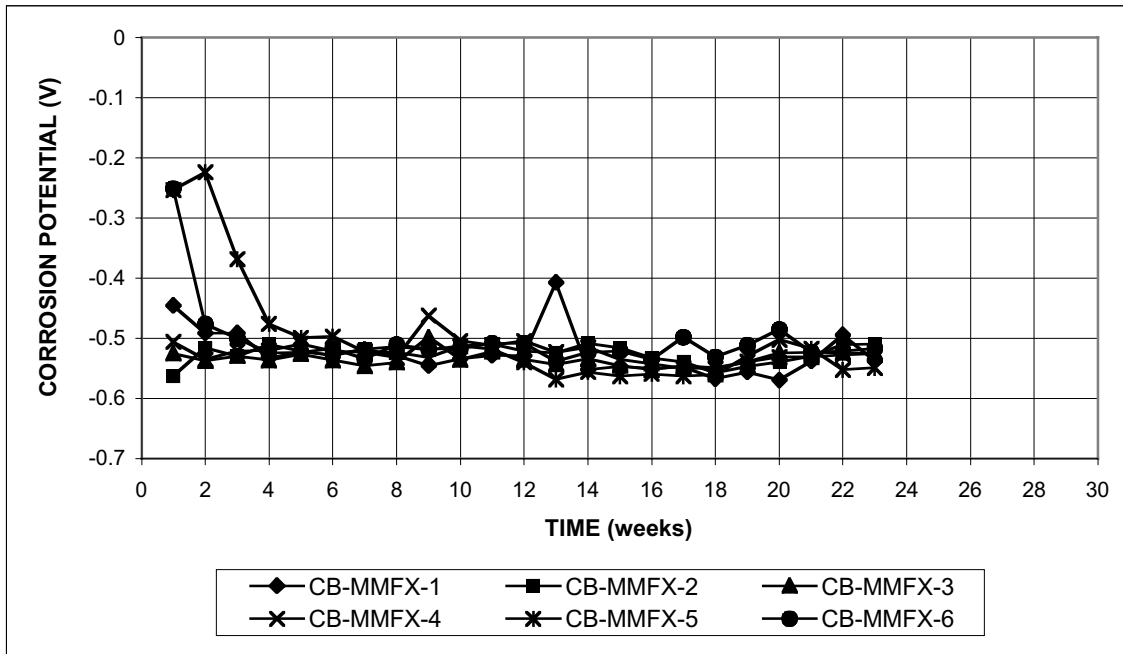


Figure B.46a - Cracked Beam Test. Corrosion potential vs. CSE, top mat. MMFX steel, w/c=0.45, ponded with 15% NaCl solution.

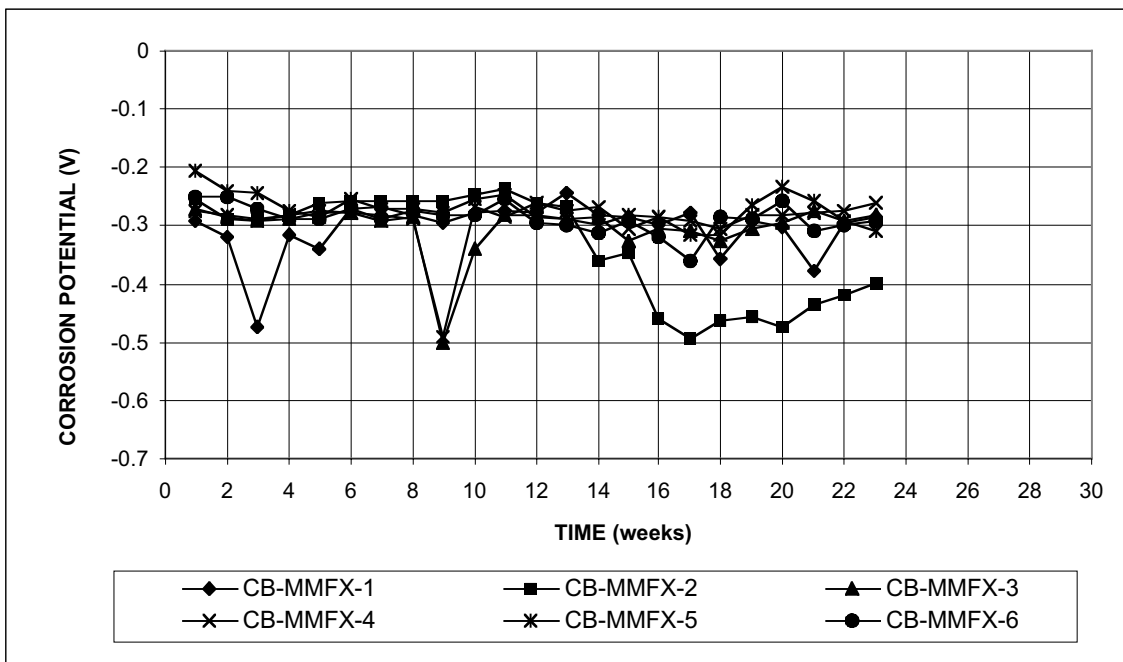


Figure B.46b - Cracked Beam Test. Corrosion potential vs. CSE, bottom mat. MMFX steel, w/c=0.45, ponded with 15% NaCl solution.

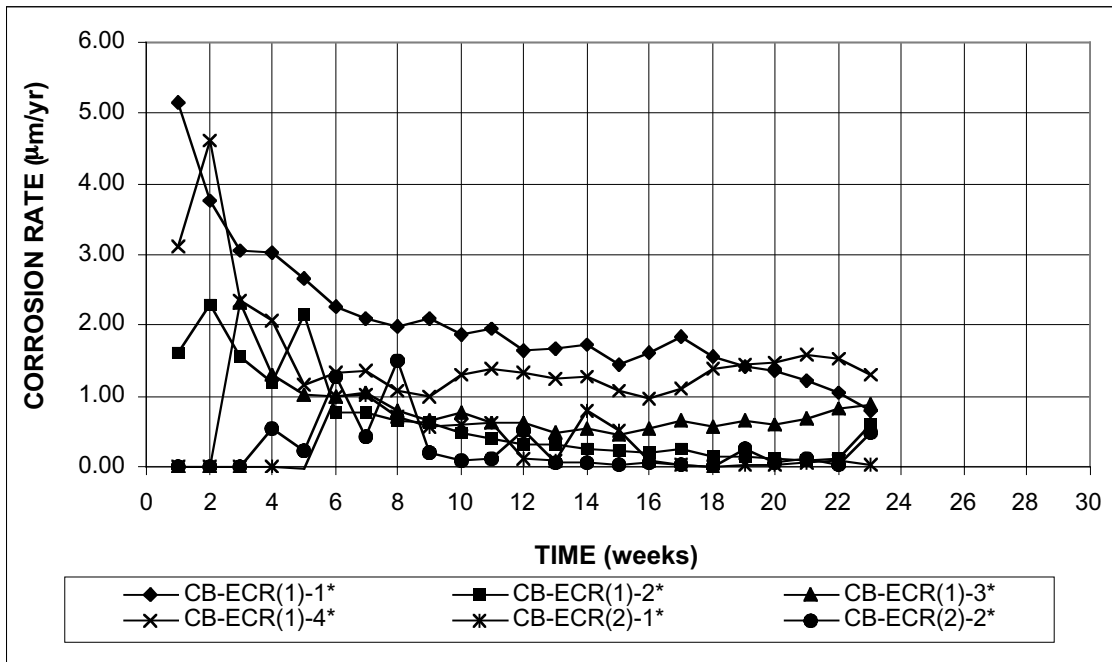


Figure B.47 - Cracked Beam Test. Corrosion rate based on total area of bar exposed to solution. Epoxy-coated steel, w/c=0.45, ponded with 15% NaCl solution.

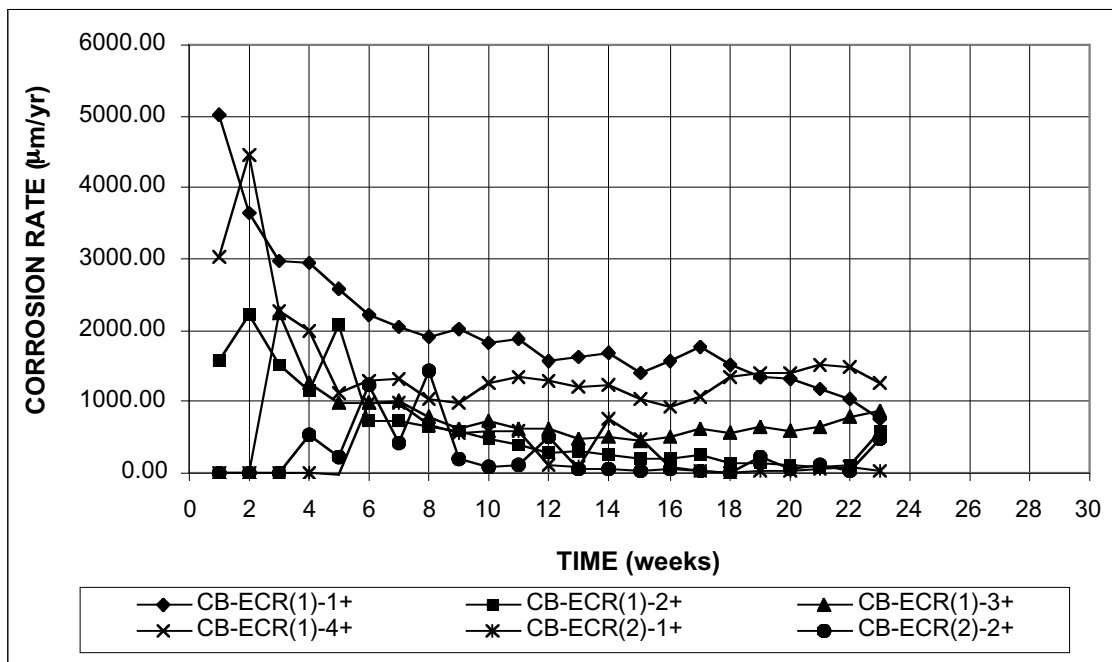


Figure B.48 - Cracked Beam Test. Corrosion rate based on exposed area of steel (four $\frac{1}{8}$ -in. diameter holes in epoxy). Epoxy-coated steel, w/c=0.45, ponded with 15% NaCl solution.

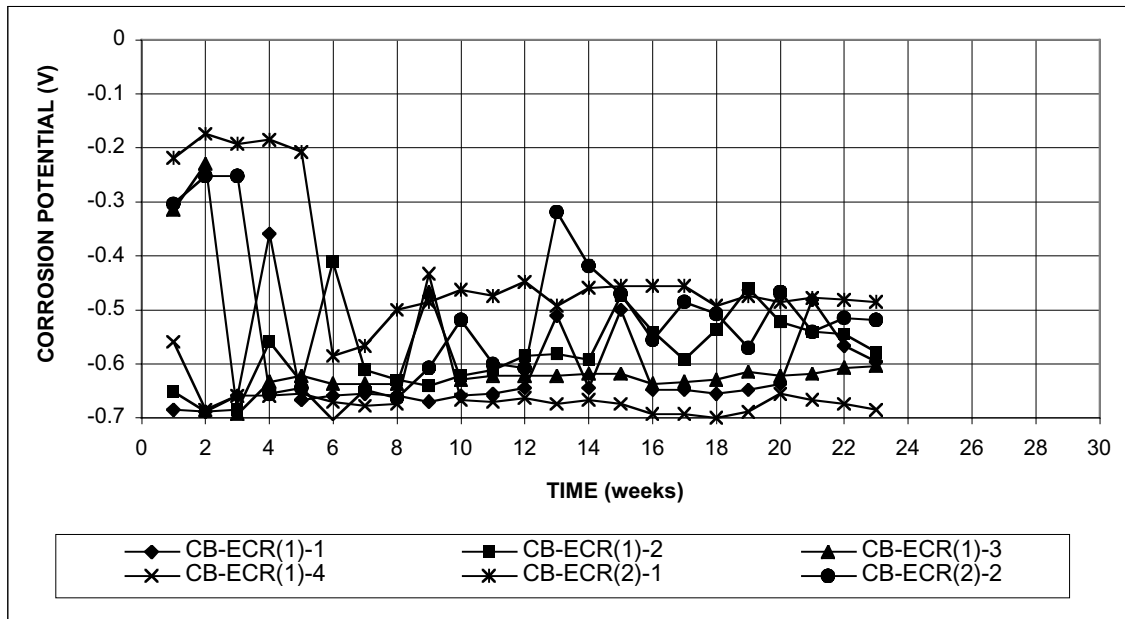


Figure B.49a - Cracked Beam Test. Corrosion potential vs. CSE, top mat. Epoxy-coated steel, w/c=0.45, ponded with 15% NaCl solution.

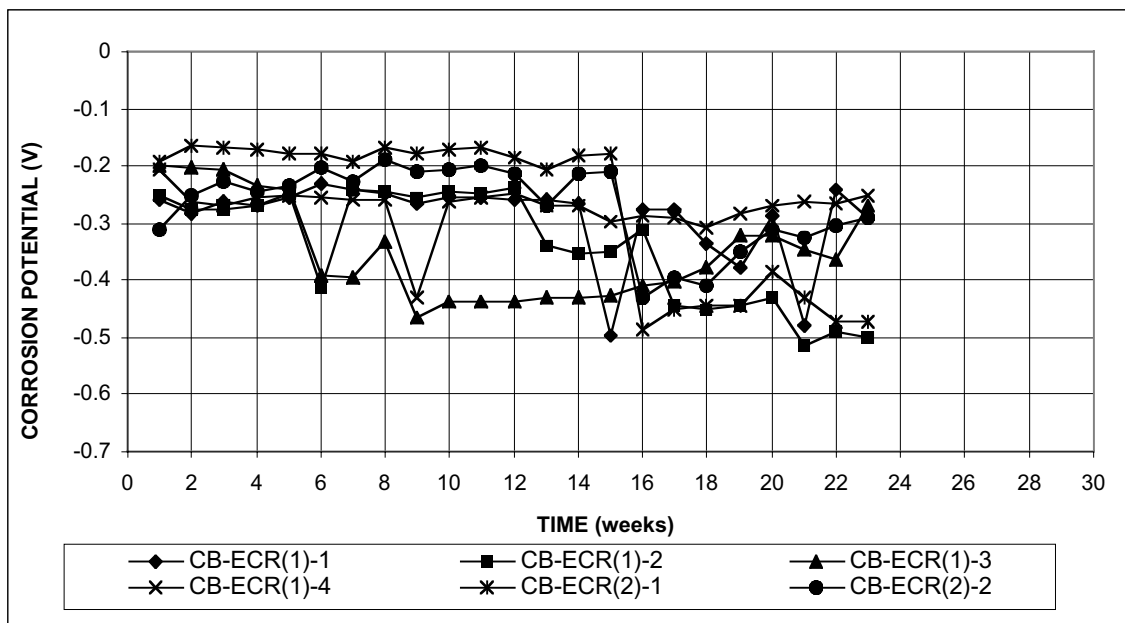


Figure B.49b - Cracked Beam Test. Corrosion potential vs. CSE, bottom mat. Epoxy-coated steel, w/c=0.45, ponded with 15% NaCl solution.